QGeol

JOURNAL OF PETROLOGY

VOLUME 2 · NUMBER 3

OCTOBER 1961

OXFORD · AT THE CLARENDON PRESS

JOURNAL OF PETROLOGY

Editors

T. F. W. BARTH (Oslo); C. E. TILLEY (Cambridge)
L. R. WAGER (Oxford); H. S. YODER (Washington)

Managing Editors

G. M. BROWN (Oxford); S. R. NOCKOLDS (Cambridge)

Honorary Advisory Board

C. R. BURRI (Zürich)
C. W. CORRENS (Göttingen)
H. VON ECKERMANN (Stockholm)
P. ESKOLA (Helsinki)
L. HAWKES (London)
J. E. HAWLEY (Kingston, Ont.)
H. H. HESS (Princeton)
D. S. KORZHINSKY (Moscow)
H. KUNO (Tokyo)
W. T. PECORA (Washington)
E. RAGUIN (Paris)
H. H. READ (London)
A. RITTMANN (Catania)
F. J. TURNER (Berkeley, Calif.)

It is the aim of the editors to provide, in the *Journal of Petrology*, a place for the publication of original researches in the whole range of subjects which fall within a liberal definition of petrology. The subjects will thus include the physics and chemistry of rocks, their mineralogy and textures, and certain aspects of petrology which involve the dating of rocks by natural radioactivity. Quantitative studies of rock-forming minerals, experimental physical chemistry relevant to petrology, and parts of isotope geology, will appropriately find a place. Regional studies, unless they lead to results fundamental to the science of petrology, will not usually be considered suitable to the journal.

The journal is being published at first in 400-page volumes consisting of three numbers per year, in February, June, and October. The subscription price for three consecutive numbers is 80*s*. ($12 in the U.S.A. and Canada), post free. Single numbers cost 30*s*. net. Orders may be placed with any bookseller or sent direct to the publishers.

OXFORD UNIVERSITY PRESS

AMEN HOUSE · LONDON · E.C.4

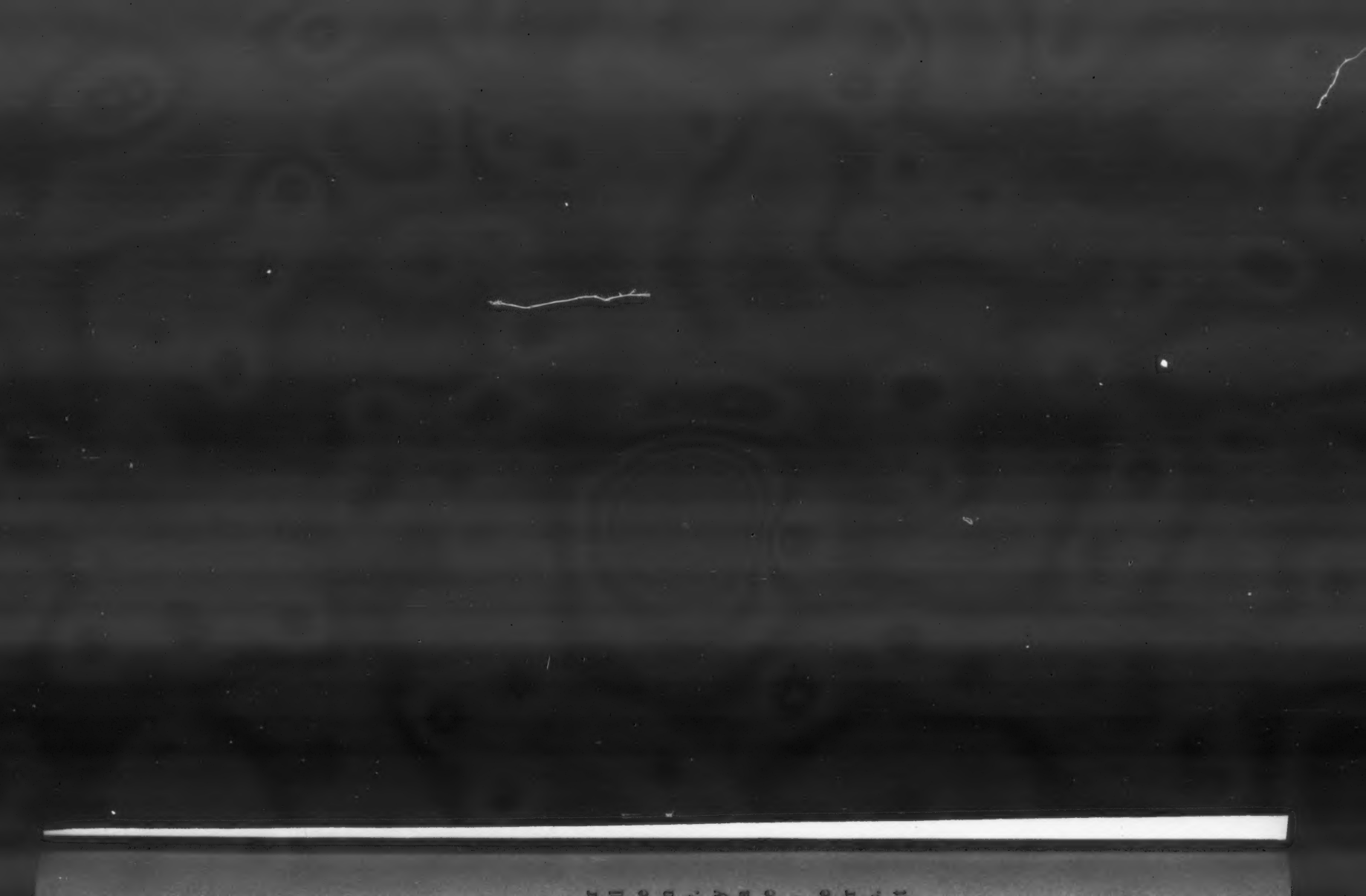

Evolution of Metamorphic Belts

by AKIHO MIYASHIRO

Geological Institute, Faculty of Science, University of Tokyo, Japan

ABSTRACT

Journal of Petrology, Volume 2, *number* 1

ERRATA

p. 50. A footnote to Table 1 should read * See footnote, p. 51.
p. 69. Table 12, 4th column, lines 6, 7, and 8: 0.192_8; 0.170_6; 0.170_6.
p. 75. 1. 5. Simplified. 1. 14. 'and' should read 'the'.
p. 85. Table 19, 3rd tier, 1st column. $2V_Z$.
p. 109. 1. 20. 210 should read 102.
p. 114. 1. 6. D'Achiardi.
p. 117. 1. 6 from bottom. $Fe_6Si_8O_{29}(OH)_4.nH_2O$.
p. 122. 1. 2 from bottom. Insert 'Ka, kaolinite'.

Korzhinskii, 1959). The range of temperature and pressure in a metamorphic terrain and metamorphic belt, however, is usually too wide to be definitive of a single metamorphic facies. Even in a single metamorphic terrain, the variation in temperature would be expressed usually by a series of metamorphic facies. Such a series will be called a *metamorphic facies series* or simply a *facies series*. Thus, from the viewpoint of external conditions, each metamorphic terrain is characterized by a certain metamorphic facies series.

Many authors consider that the mineral facies of regional metamorphism are the greenschist, epidote–amphibolite, amphibolite, and granulite facies. Indeed, this facies series appears to exist in Palaeozoic metamorphic belts of Europe and North America. In many other metamorphic belts, however, different kinds of metamorphic facies series are developed. The series of the greenschist, epidote–amphibolite, amphibolite, and granulite facies is only one of the various possible facies series of regional metamorphism.

A metamorphic facies series can be represented by a curve or a group of

[Journal of Petrology, Vol. 2, Part 3, pp. 277–311, 1961]

Evolution of Metamorphic Belts

by AKIHO MIYASHIRO

Geological Institute, Faculty of Science, University of Tokyo, Japan

ABSTRACT

The metamorphic facies series in regional metamorphism may be classified into the following categories according to an order of increasing rock pressure: (1) andalusite–sillimanite type, (2) low-pressure intermediate group, (3) kyanite–sillimanite type, (4) high-pressure intermediate group, and (5) jadeite–glaucophane type.

In Japan and other parts of the circum-Pacific region, a metamorphic belt of the andalusite–sillimanite type and/or low-pressure intermediate group and another metamorphic belt of the jadeite–glaucophane type and/or high-pressure intermediate group run side by side, forming a pair. The latter belt is always on the Pacific Ocean side. They were probably formed in different phases of the same cycle of orogeny. Their origin is discussed.

Regional metamorphism under higher rock pressures appears to have taken place in later geological times.

The metamorphic facies series of contact metamorphism are briefly discussed.

INTRODUCTION

THIS paper discusses the classification, origin, and historical development of regional metamorphism.

Regional metamorphism takes place in the deeper parts of orogenic belts, while the regional metamorphic rocks are found in what are here called *metamorphic belts*.

Individual metamorphic facies correspond to a certain range of temperature, rock pressure, and other external conditions (Eskola, 1915, 1920, 1939; Korzhinskii, 1959). The range of temperature and pressure in a metamorphic terrain and metamorphic belt, however, is usually too wide to be definitive of a single metamorphic facies. Even in a single metamorphic terrain, the variation in temperature would be expressed usually by a series of metamorphic facies. Such a series will be called a *metamorphic facies series* or simply a *facies series*. Thus, from the viewpoint of external conditions, each metamorphic terrain is characterized by a certain metamorphic facies series.

Many authors consider that the mineral facies of regional metamorphism are the greenschist, epidote–amphibolite, amphibolite, and granulite facies. Indeed, this facies series appears to exist in Palaeozoic metamorphic belts of Europe and North America. In many other metamorphic belts, however, different kinds of metamorphic facies series are developed. The series of the greenschist, epidote–amphibolite, amphibolite, and granulite facies is only one of the various possible facies series of regional metamorphism.

A metamorphic facies series can be represented by a curve or a group of

[Journal of Petrology, Vol. 2, Part 3, pp. 277–311, 1961]

6233.3

curves in a temperature–pressure diagram. According to the location of the curve or curves, the facies series may be classified into various types.

Belts of regional metamorphism are well exposed in Japan. Great progress has been made in the geological and petrological study of these belts in recent years, so that they now afford an important basis for the comparative study of the metamorphic belts of the world.

CLASSIFICATION OF FACIES SERIES OF REGIONAL METAMORPHISM

The classification of metamorphic facies series means a classification of metamorphism and of metamorphic terrains from the viewpoint of certain external conditions. After a survey of the petrographic descriptions of metamorphic rocks from different parts of the world, the writer reached the following conclusion. So far as such a classification is to be based upon easily observable mineralogical differences, the kinds or types of metamorphic facies series in the world are rather limited in number. At the present state of our knowledge, the facies series of regional metamorphism may be most conveniently classified into five categories: three standard types and two intermediate groups. Each of the intermediate groups involves various kinds of metamorphism that are intermediate in character between two of the standard types. As will be discussed later, the present classification is intended to be based on the operating rock pressure. Each standard type of metamorphism is accompanied by characteristic igneous activity in the geosynclinal as well as in the orogenic period.

The systematic classification and nomenclature of subfacies should be based on the veritable classification of facies series. Different parts of one facies belonging to different facies series may well be treated as different subfacies. In this paper, however, a new system of nomenclature of subfacies will not be proposed, the classification and nomenclature of metamorphic facies proposed by Eskola (1939) being adopted.

Kyanite–sillimanite type

This standard type of facies series is characterized by the stability of kyanite in a lower grade and that of sillimanite in a higher grade so far as chemical conditions permit. Andalusite and glaucophane are absent. The type metamorphic terrain is in the main part of the Grampian Highlands of Scotland, as studied by Barrow (1893, 1912), Tilley (1925), Harker (1932), Wiseman (1934), Snelling (1957), Chinner (1960), and others.

The facies series of this type is composed of the greenschist, epidote–amphibolite, and amphibolite facies, in order of increasing temperature. In this type, almandine garnet occurs commonly in the middle and high grades, not only in pelitic but also in basic metamorphic rocks. Staurolite is also common, while cordierite is absent. The metamorphic belt is usually divided into progressive metamorphic zones characterized by the following minerals: chlorite, biotite, almandine, kyanite, and sillimanite. The zone of staurolite may be delineated

as an independent zone between those of almandine and kyanite. The progressive mineralogical variations are summarized in Fig. 1.

This type of regional metamorphism or mineral zoning was sometimes called the Dalradian or Barrovian one. The main part of the Caledonian metamorphic belt in Norway and that of the Appalachian metamorphic belt in North America appear to belong to this type. In the highest grade of this facies series, the

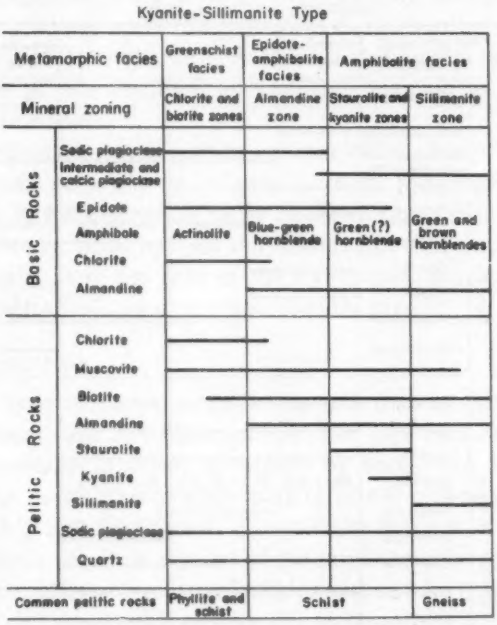

FIG. 1. Progressive mineralogical variations in regional metamorphism in the main part of the Grampian Highlands of Scotland (Harker, 1932; Wiseman, 1934; &c.).

granulite facies may occur (Chapman, 1952). If all the world is considered, this type may not be more abundant than the other two standard types. It is not justified to regard this type as being 'normal' or ordinary in comparison with the other two, as was done by many authors.

This type of regional metamorphism appears to be always accompanied by the emplacement of a large amount of granitic rocks. Synkinematic granites are usually abundant in the high-grade parts of the metamorphic terrain. Much smaller amounts of gabbroic and ultrabasic rocks are also usually present.

Andalusite–sillimanite type

This standard type of facies series is characterized by the stability of andalusite in a lower grade and of sillimanite in a higher grade, so far as the chemical conditions permit. Kyanite, staurolite, and glaucophane are absent. The type

metamorphic terrain is in the central part of the Abukuma Plateau in Japan, as studied by Miyashiro (1953, 1958), Shido (1958), and Shido & Miyashiro (1959).

The facies series of this type is composed of the greenschist and amphibolite facies. The epidote–amphibolite facies is practically absent. In this type, almandine occurs in some pelitic metamorphic rocks of high grades, and does not occur in ordinary basic metamorphic rocks. In the low and middle grades,

Andalusite-Sillimanite Type

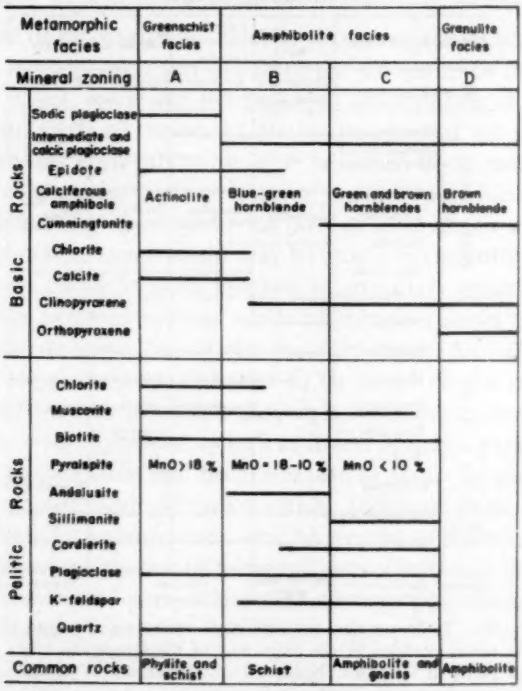

FIG. 2. Progressive mineralogical variations in regional metamorphism in the central Abukuma Plateau, Japan (Miyashiro, 1953, 1958; Shido, 1958; Shido & Miyashiro, 1959).

pyralspite garnet is rare and, when it occurs, is manganiferous (Miyashiro, 1953). Cordierite occurs commonly. The progressive mineralogical variations are summarized in Fig. 2.

The highest grade of regional metamorphism in the type metamorphic terrain is in the amphibolite facies, as stated above. The contact metamorphism by synkinematic intrusions in the terrain produced the same type of metamorphic facies series, though the highest grade of the contact metamorphism reached what may be regarded as a part of the granulite facies, since orthopyroxene was formed there. This highest-grade part is also shown in Fig. 2.

Formerly, this type of regional metamorphism was called the central Abukuma

type (Miyashiro, 1958). The Buchan type of Read (1952) is not the same as this, but belongs to the low-pressure intermediate group to be mentioned later. The Ryoke metamorphic belt of Japan and some metamorphic belts formed in Early Palaeozoic time in New South Wales, Australia, appear to belong to this type.

Many geologists regarded the regional metamorphism of this type as contact metamorphism only, because of the occurrence of andalusite and cordierite. The occurrence of such minerals, however, depends upon the operating temperature and pressure, and not upon the geological distinction between the contact and regional types. Metamorphism is to be regarded as regional providing the thermal structure of the resultant metamorphic terrain is independent of individual plutonic masses.

This type of regional metamorphism appears to be always accompanied by the emplacement of a large amount of granitic rocks. Synkinematic granites are usually abundant in the high-grade parts of the metamorphic terrain. Granite may occur abundantly, however, not only inside but also outside the regional metamorphic terrain, as in the case of the Ryoke belt. Much smaller amounts of gabbroic and ultrabasic rocks are also usually present.

Jadeite–glaucophane type

This standard type of facies series is characterized by the stability of the jadeite–quartz assemblage and glaucophane. The type metamorphic terrain is in the Kanto Mountains in Japan, as studied by Seki (1958, 1960 *b*, *c*, 1961*b*).

The facies series in the type metamorphic terrain is composed of the glaucophane–schist and greenschist facies. This terrain belongs to the Sanbagawa metamorphic belt. In the Bessi district of the same metamorphic belt, not only rocks of the glaucophane–schist facies but also rocks of the epidote–amphibolite facies and even eclogite are exposed, as will be described later (p. 295). These rocks may represent higher-grade parts of the present type of facies series. It is not certain, however, whether the metamorphic terrain of the Bessi district is of the jadeite–glaucophane type or of the high-pressure intermediate group to be mentioned later.

Lawsonite and pumpellyite usually occur in the metamorphic terrains of this type. The stable form of Al_2SiO_5 is probably kyanite, as was found in the Bessi district (Banno, 1957). Pyralspite garnet occurs commonly, and is almandine in some cases and more manganiferous in others. Andalusite, sillimanite, and cordierite do not occur. Note that jadeite in quartz-free rocks would not be characteristic of this type. The progressive mineralogical variations in the type metamorphic terrain are summarized in Fig. 3.

The regional metamorphism of this type and of similar nature, producing glaucophane, was called glaucophanitic metamorphism in some cases. At least some parts of the Kamuikotan metamorphic belt of Hokkaido and of the Franciscan metamorphic terrain of California appear to belong to this type.

This type of regional metamorphism is usually accompanied by the emplace-

ment of a large volume of ultrabasic rocks (mostly serpentinite). Gabbroic rocks are also present, but granitic rocks are absent.

Formerly, many authors stated that the formation of glaucophane schists is due to a special kind of metasomatism, and Turner (1948) and others denied the existence of the glaucophane–schist facies. On the other hand, the glaucophane-schist facies was advocated by de Roever (1955*a*) and Miyashiro & Banno (1958).

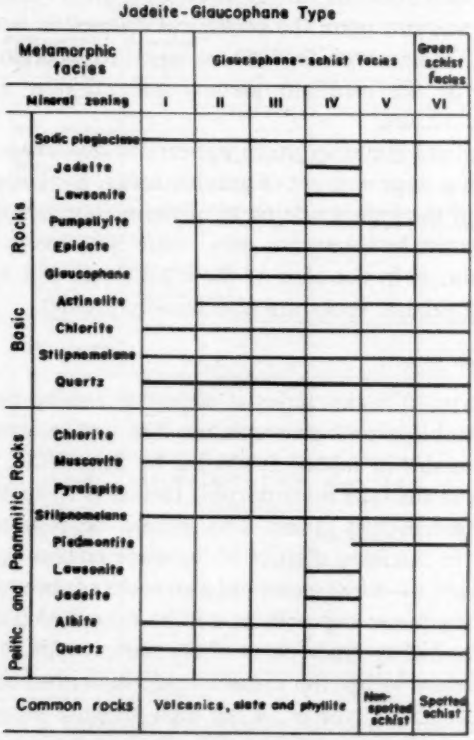

FIG. 3. Progressive mineralogical variations in regional metamorphism in the Kanto Mountains, Japan (Seki, 1958, 1960 *b*, *c*, 1961*b*). Recrystallization is very incomplete in zone I.

It appears, however, that the existence of the glaucophane–schist facies has now become widely accepted and need not be advocated further.

It is surprising that no one had dealt with the glaucophanitic metamorphism as a progressive one having zones not only of the glaucophane–schist facies but also of some other facies, before Banno (1958*a*) and Seki (1958) succeeded in clarifying the mineral zoning of glaucophanitic terrains in Japan.

Low-pressure and high-pressure intermediate groups

As will be discussed later (p. 284), the prevailing rock pressure for the

andalusite-sillimanite type is lower than that for the kyanite–sillimanite type, which latter is, in turn, probably lower than that for the jadeite–glaucophane type. There are many cases of regional metamorphism that may be regarded as being intermediate in character between the andalusite–sillimanite and kyanite–sillimanite types. Probably the prevailing rock pressure in these cases was intermediate between the pressures for the two standard types concerned. These cases of metamorphism will be said to belong to the *low-pressure intermediate group*.

As an example of the low-pressure intermediate group, the metamorphic terrain in the north-eastern Grampian Highlands (Aberdeenshire and Banffshire) of Scotland may be cited. In this area, andalusite and cordierite occur in pelitic metamorphic rocks, just as in the andalusite–sillimanite type, but staurolite also occurs just as in the kyanite-sillimanite type. Read (1952) called such a metamorphism the Buchan type. The association of andalusite and staurolite is not rare in the world. Many of the Precambrian metamorphic terrains in the Baltic and Canadian shields have this mineral association, and appear to belong to the low-pressure intermediate group. The coexistence of andalusite, staurolite, and kyanite as reported by Yamaguchi (1951) from Korea, as well as the coexistence of andalusite, kyanite, and sillimanite as reported by Hietanen (1956) from Idaho, indicates that the terrains belong to the low-pressure intermediate group.

There are other cases of regional metamorphism that may be regarded as being intermediate in character between the kyanite–sillimanite and jadeite–glaucophane types. Probably the prevailing rock pressure in these cases was intermediate between the pressures of the two standard types concerned. These cases of metamorphism will be said to belong to the *high-pressure intermediate group*.

For example, there exist many glaucophanitic metamorphic terrains where the jadeite–quartz assemblage is not found. If we consider that the jadeite–quartz assemblage was not produced in any grades of these terrains, then the metamorphism belongs to the high-pressure intermediate group. In this case, however, conclusive determination would be rather difficult, because jadeite is apt to be overlooked in many cases and the jadeite-bearing part may have been lost by some later events. Metamorphic terrains that resemble those of the kyanite–sillimanite type, except for the rare, sporadic occurrence of glaucophanic amphibole, probably belong to the high-pressure intermediate group.

Discrimination between types of metamorphism with the aid of minerals of solid-solution series

When some minerals characteristic of a type of metamorphism occur in a metamorphic terrain, one can readily identify the type. In many cases, however, appropriate characteristic minerals do not occur owing to the limited range in chemical composition of the metamorphic rocks developed. Even in such cases,

one may be able to recognize the type through investigation of the solid-solution relations of some metamorphic minerals, as exemplified below.

Pyralspite garnet may occur in pelitic metamorphic rocks in any types of regional metamorphism, but the Mn content of pyralspite is much higher in the andalusite–sillimanite type than in the kyanite–sillimanite type (Miyashiro, 1953, 1958). The Na content of common hornblende in ordinary basic metamorphic rocks is high in the jadeite–glaucophane type and low in the kyanite–sillimanite type, and is still lower in the andalusite–sillimanite type (Shido, 1958; Shido & Miyashiro, 1959). Plagioclase becomes more calcic with rising temperature in any types of metamorphism, but the rate of increase of the Ca content is greater in the andalusite–sillimanite type than in the kyanite–sillimanite type (Miyashiro, 1958; Shido, 1958). In the jadeite–glaucophane type, intermediate and calcic plagioclases could not be formed.

Temperature, rock pressure, and other external conditions

The temperature and rock pressure corresponding to the three standard types of metamorphic facies series can be inferred from the experimentally determined stability relations of characteristic minerals.

The kyanite–sillimanite equilibrium curve was experimentally determined by Clark, Robertson, & Birch (1957) and by Clark (1960), as shown by line (*k*) in Fig. 4. Though the stability relations of andalusite have not been determined, they are probably approximately as shown in the same figure (Miyashiro, 1953; Thompson, 1955; Clark *et al.*, 1957; Miyashiro, 1960*a*).

The equilibrium curve for the reaction: jadeite+quartz = albite was experimentally determined by Birch & LeComte (1960), as shown in Fig. 4.

Typical temperature/rock-pressure curves corresponding to the three standard types of regional metamorphism are shown by arrows (1), (2), and (3) in Fig. 4. It is clear that the prevailing rock pressure in the andalusite–sillimanite type is lower than that in the kyanite–sillimanite type, which latter in turn is lower than that in the jadeite–glaucophane type. If it be assumed that the pressures shown in this figure were produced lithostatically by the weight of the overlying rocks, the depth of regional metamorphism is much greater than that so far inferred from geological studies. As our geological studies are not generally complete, such a great depth may have been actually reached in a locally and temporarily thickened crust during orogeny. It is also possible that orogenic compression played an important part in producing such pressures, at least in some cases.

The upper and lower limits of metamorphic temperature would differ in different types. It is only rarely that the metamorphism of the jadeite–glaucophane type reaches so high a temperature as to produce biotite, whereas that of the kyanite–sillimanite type commonly produces biotite in the middle- and high-grade parts. In the metamorphism of the andalusite–sillimanite type, most of the metamorphic rocks are higher in grade than the biotite isograd, and on the lower-temperature side of the biotite isograd recrystallization is usually very

incomplete. Although the lowest temperature for the formation of biotite should vary to some extent with rock and water pressures, the above relations might well be considered as suggestive that the metamorphic temperature in the jadeite–glaucophane type is generally lower than that in the kyanite–sillimanite

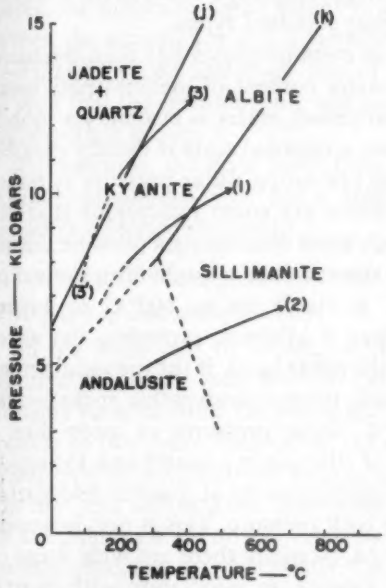

FIG. 4. Stability relations of andalusite, kyanite, and sillimanite and of the jadeite–quartz assemblage and albite. The solid lines (*k*) and (*j*) represent the experimentally determined equilibrium curves for the kyanite–sillimanite transformation, and for the reaction jadeite + quartz = albite, respectively. The arrows (1), (2), and (3) represent typical temperature/rock-pressure relations in regional metamorphism of the kyanite–sillimanite type, andalusite–sillimanite type, and jadeite–glaucophane type, respectively.

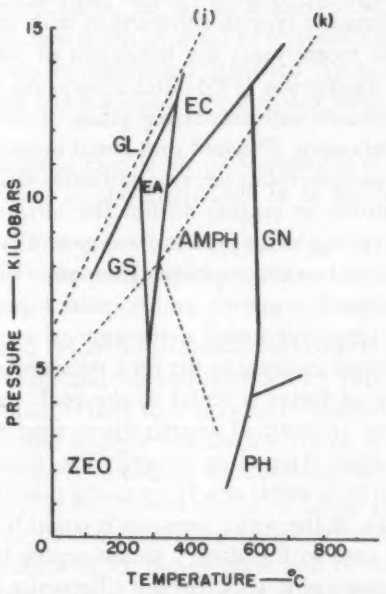

FIG. 5. Estimated temperatures and rock pressures of metamorphic facies. The solid lines (*k*) and (*j*) correspond to those of Fig. 4. GL, glaucophane–schist facies; EC, eclogite facies; GS, greenschist facies; EA, epidote–amphibolite facies; AMPH, amphibolite facies; GN, granulite facies; PH, pyroxene–hornfels facies; ZEO, zeolite facies.

type, which latter, in turn, tends to be lower than that in the andalusite–sillimanite type, as shown in Fig. 4.

In a high grade of the andalusite–sillimanite and kyanite–sillimanite types of regional metamorphism, where sillimanite is stable, muscovite decomposes by reaction with quartz to produce sillimanite, potassium feldspar, and water. The equilibrium temperature of the reaction was thermodynamically calculated for a wide range of rock and water pressures (Miyashiro, 1960*b*). The result is 450°–590° C. The decomposition of biotite by reaction with quartz takes place in the highest grade (granulite facies), probably of the andalusite–sillimanite and

kyanite–sillimanite types. This temperature was estimated at 700°–800° C. (Miyashiro, 1960*c*).

The temperatures and rock pressures of metamorphic facies are roughly shown in Fig. 5. Note that there is a fundamental difference between this figure and fig. 2 of Francis (1956), who attached too great an importance to the kyanite–sillimanite type in comparison with the other standard types.

In recent years the behaviour of water in metamorphism has been discussed by Thompson (1955) and others. As the water content of metamorphic rocks decreases with increasing grade of metamorphism, water is evidently a mobile component. The fact that zonal mapping on a regional scale is usually possible in metamorphic terrains indicates that the prevailing water pressure is rather uniform or regular within the terrains. There are some indications that the prevailing water pressure was generally much lower than the rock pressure during regional metamorphism. Kennedy (1960) showed that pyrophyllite, instead of sillimanite+quartz and kyanite+quartz, is stable up to 600° C or higher temperatures under a pressure of more than 4 kilobars, providing the water pressure is equal to the rock pressure. On the other hand, if the prevailing pressure of water is equal to the rock pressure, quartzo-feldspathic rocks would begin to melt at temperatures near 600° C under pressures of more than 4 kilobars. Therefore, pyrophyllite, instead of sillimanite+quartz and kyanite+quartz, is stable nearly up to the minimum melting-point of quartzo-feldspathic rocks, if the water pressure is equal to the rock pressure. This is not, however, the case with ordinary metamorphic terrains. Actually there are wide areas of metamorphic rocks where sillimanite and kyanite, in association with quartz, are stable at temperatures much lower than the melting-point of quartzo-feldspathic rocks. For this reason the prevailing water pressure is considered to be generally much lower than the rock pressure during metamorphism.

Shaw (1956) showed that, generally, the iron in metamorphic rocks tends to be progressively reduced with increasing metamorphism. In the central Abukuma Plateau, not only the water content but also the oxygen content of metamorphic rocks decreases with increasing metamorphism, whereas in the Grampian Highlands the water content decreases but the oxygen content does not decrease (Miyashiro, 1958, pp. 267–8). These facts suggest that the mobility of oxygen would differ in different metamorphic terrains. In the central Abukuma Plateau, a recent investigation of oxide minerals in metamorphic rocks did not reveal the existence of local difference in the chemical potential of oxygen (Banno & Kanehira, 1961). Many authors showed from studies of mineral parageneses, however, that metamorphic rocks are closed with regard to oxygen. This conclusion was reached by Eugster (1959) in considering the metamorphosed iron formation of Michingan (low-pressure intermediate group), by Thompson (1957) in the northern Appalachians (kyanite–sillimanite type), by Chinner (1960) in the Grampian Highlands (kyanite–sillimanite type), and by Banno & Kanehira (1961) in glaucophanitic metamorphic rocks of the Bessi district,

Japan. It is now clear that the partial pressure of oxygen in metamorphic rocks is generally independent of that of water.

Variation of metamorphic facies series within a metamorphic belt

In many metamorphic belts, the character of the metamorphic facies series produced differs to some extent in different parts. So far as is known to the writer, the variation within a metamorphic belt is not so great as to result in the metamorphic belt including two of the above-mentioned standard types, but is such that the metamorphic belt involves one standard type and one adjacent intermediate group.

For example, the main part of the Grampian Highlands of Scotland is of the kyanite–sillimanite type, but a smaller part of the Highlands is of the low-pressure intermediate group.

PAIRED METAMORPHIC BELTS IN THE MAIN PART OF JAPAN

Two pairs of metamorphic belts

In the main part of Japan, i.e. Honsyu (Honshu), Sikoku (Shikoku), and Kyusyu (Kyushu), there are four belts of regional metamorphic rocks, running roughly parallel along the island arc of Japan. These four may be considered to belong to two pairs, here called the *older* and *younger*. As shown in Fig. 6, the older pair of metamorphic belts is composed of the *Hida metamorphic belt* on the northern side and the *Sangun metamorphic belt* on the southern. Large parts of the older pair are now covered by the Japan Sea, and the original structure is greatly obscured by later events. On the other hand, the younger pair of metamorphic belts is to the south of the older pair, and is composed of the *Ryoke–Abukuma metamorphic belt* on the northern, and the *Sanbagawa* (*Sambagawa*) *metamorphic belt* on the southern side. The original structure of this pair is relatively well preserved.

Each pair of metamorphic belts probably represents deeper parts of an orogenic belt in geological time. The ages of the orogenies and metamorphisms have been a subject of hot dispute amongst Japanese geologists in recent years. The geological evidence was not, in most cases, conclusive. For an historical review of this problem see Minato (1960), although the old radiometric dating which he quoted is quite unreliable. New isotopic dating is now giving important evidence relevant to this problem (Kuno *et al.*, 1960; Miller *et al.*, 1961; Banno & Miller, 1961). At the present state of our knowledge, it is most probable that the age of orogeny and regional metamorphism in the older pair is Late Palaeozoic and/or Early Mesozoic, whereas that in the younger pair is Late Mesozoic. The former would correspond to the Akiyosi (Akiyoshi) cycle of orogeny proposed by Kobayashi (1941), and the latter to his Sakawa cycle. The K–A ages so far obtained may be summarized as follows:

Hida metamorphic belt	180–90 million years (Triassic)
Ryoke–Abukuma metamorphic belt	91–102 million years (Cretaceous)
Sanbagawa metamorphic belt	84–93 million years (Cretaceous)

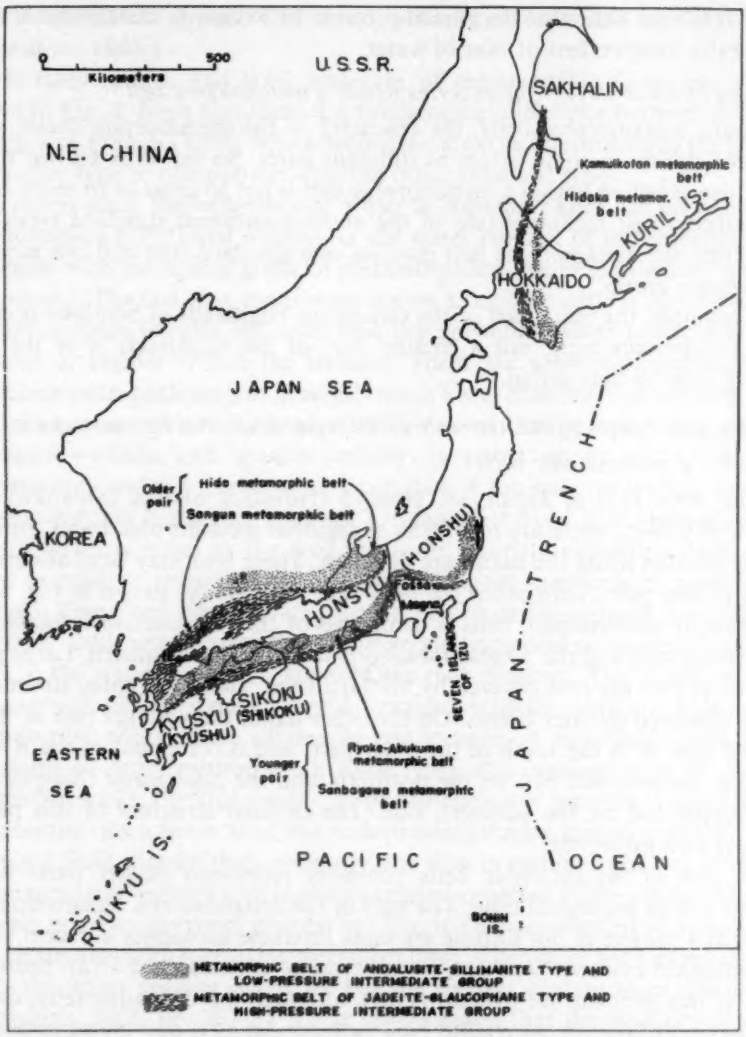

FIG. 6. Metamorphic belts of Japan, restored to the original state.

The regional metamorphism of the Sangun belts has not been dated, but some metamorphic terrains of the belt are covered by unmetamorphosed Middle Triassic sediments.

The tectonic development of Japan may be outlined as follows: From Early Palaeozoic time (at least Silurian), there was a large geosyncline roughly along the present site of the island arc of Japan. Thick sediments, especially of Late Palaeozoic time, were deposited there. The geosynclinal pile was subjected to orogeny and regional metamorphism first in Late Palaeozoic and/or Early

Mesozoic time, and secondly in Late Mesozoic time. Thus, two pairs of metamorphic belts were formed, and constituted the backbone of the Japan arc. Afterwards, in the Tertiary period, the main site of active tectonic movement shifted to the zone along the Japan Trench, which itself was formed probably by this tectonic movement. Thus, the Japan Trench and the adjacent zone to the west (Kuril Islands, north-eastern Honsyu, Seven Islands of Izu, and Bonin Islands) are a Cenozoic and present-day orogenic belt (Sugimura, 1960). The western part of Japan became a more stable region in Cenozoic time.

In each of the two pairs, the metamorphic belt on the northern side (i.e. continental side) is of the andalusite–sillimanite type and/or low-pressure intermediate group accompanied by abundant granitic rocks, whereas that on the southern side (i.e. Pacific Ocean side) is of the jadeite–glaucophane type and/or high-pressure intermediate group accompanied by abundant ultrabasic rocks. As will be shown on later pages, the occurrence of such paired metamorphic belts is a common feature not only in Japan but also in other parts of the circum-Pacific region. I have always called such paired metamorphic belts *metamorphic belts of the Japan type*, because they are most typically developed and most thoroughly investigated in Japan (Miyashiro, 1959).

There follows a rather detailed review of our knowledge of the metamorphic belts of the younger pair, which will help in understanding similar relations that are less completely preserved or less sufficiently investigated in other parts of the circum-Pacific region.

Ryoke–Abukuma metamorphic belt

As shown in Figs. 6 and 7, the Ryoke–Abukuma metamorphic belt is composed of two wings, each of which is convex towards the south-east (i.e. towards the Pacific Ocean). The western wing is called the *Ryoke metamorphic belt*, and runs from Takato in central Honsyu to central Kyusyu. On the other hand, the eastern wing is now divided into three areas: (1) a small area north of the Kanto Mountains, (2) Tukuba (Tsukuba) district, and (3) Abukuma Plateau. The metamorphic terrains of the Abukuma Plateau are divided into two main masses by granitic intrusions, i.e. a central part (Gosaisyo, Takanuki, and Nakoso districts) and a southern part (Hitati district).

The two wings meet in an area of later tectonic disturbance, usually called the *Fossa Magna*, in central Honsyu. This area is at the intersection of the Japan arc with the Izu–Marianas arc, which latter runs southward from the Seven Islands of Izu through the Bonin (Ogasawara) Islands to the Marianas Islands (Fig. 6). It is conceivable that the Ryoke–Abukuma metamorphic belt was originally in a single arcuate form and afterwards deformed into the present form, composed of two wings, by later events related to crustal disturbances of the Izu–Marianas arc.

Fig. 8 shows a provisional classification of granitic rocks (in a broad sense) in the main part of Japan according to the geological ages of their emplacement.

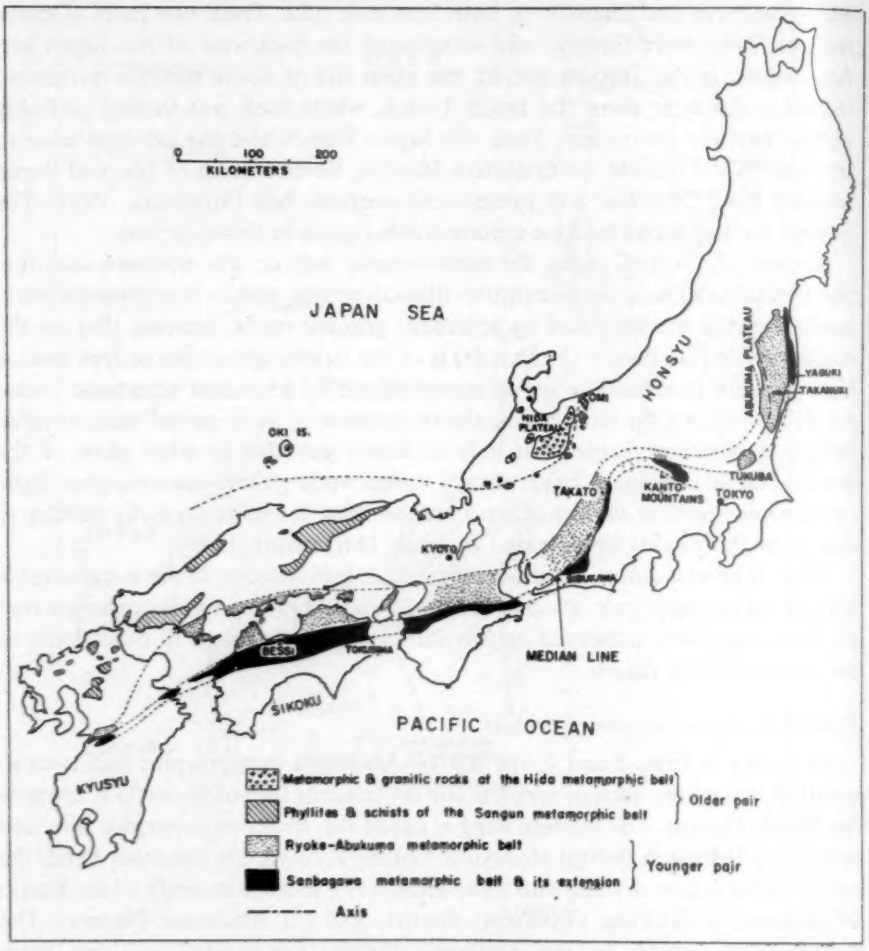

FIG. 7. Metamorphic belts in the main part of Japan.

It is clear that most of the granitic rocks now exposed widely in Japan, both inside and outside the Ryoke–Abukuma metamorphic belt, were formed by the Late Mesozoic orogeny that caused the Ryoke–Abukuma metamorphism.

The granitic rocks inside the Ryoke–Abukuma metamorphic belt may be classified into synkinematic and post-kinematic. The facies series of regional metamorphism in the belt is practically identical with that formed through contact metamorphism by the synkinematic granites, whereas it differs from that formed through contact metamorphism by the post-kinematic granites. A much smaller volume of gabbroic rocks is also present. Usually, the intrusion of gabbroic rocks was earlier than that of granitic rocks. The thermal structure of

this metamorphic belt was controlled mainly by the regional uprise of isogeothermal surfaces through the geosynclinal pile and was partly modified by the distribution of synkinematic intrusions. Synkinematic granites tend to be more abundant in high-grade parts of the thermal structure.

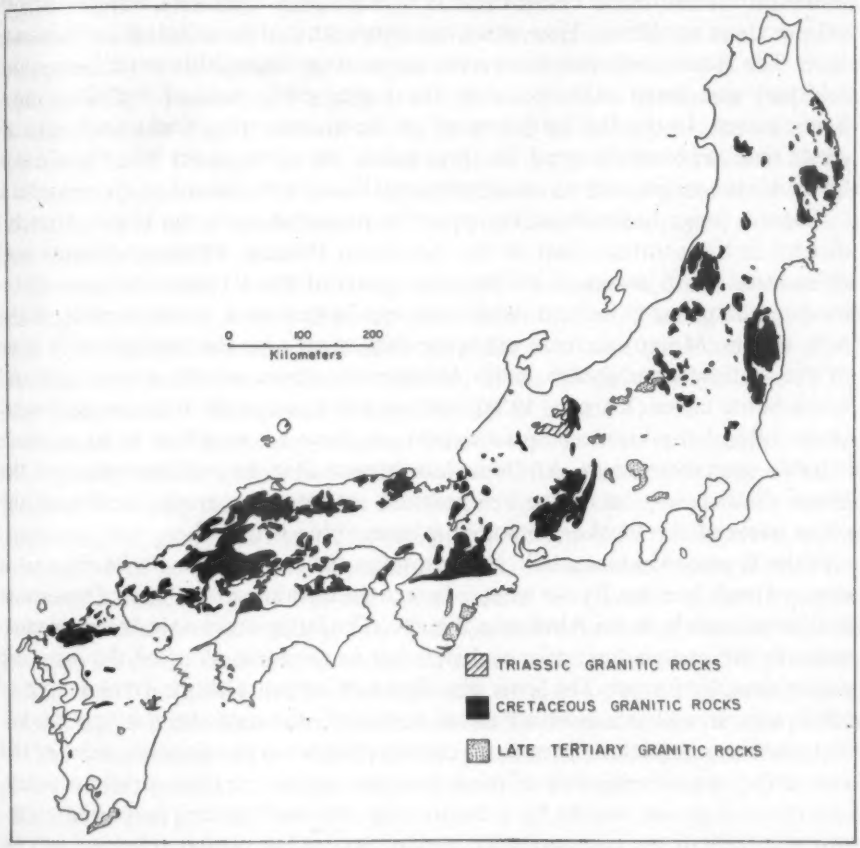

FIG. 8. Provisional classification of granitic rocks in the main part of Japan, according to the geological ages of their emplacement. Note that Cretaceous granitic rocks are widely distributed not only inside, but also outside, the Ryoke–Abukuma metamorphic belt.

The metamorphic terrain of the Abukuma Plateau has an axis towards which the metamorphic grade increases from both sides, as shown in Fig. 7. The axis runs, near its western margin, roughly parallel to the elongation of the metamorphic belt. It appears that certain parts of the Ryoke metamorphic belt also has an axis of the highest metamorphic grade, which in the eastern part is situated near the south-eastern margin of the belt. In the Ryoke belt, the metamorphic rocks were derived mostly from pelitic and psammitic sediments of Palaeozoic formations and only rarely from basic volcanics, whereas in the Abukuma

Plateau, metamorphic rocks of basic as well as psammitic and pelitic compositions are abundant.

Pelitic metamorphic rocks in low grades are slates and phyllites, both with recrystallized biotite, and those in middle grades are schists, sometimes with andalusite or cordierite. Pelitic rocks in high grades are gneisses, sometimes with sillimanite or cordierite. Thus, this metamorphism is of the andalusite–sillimanite type. The reaction of muscovite with quartz to produce sillimanite, potassium feldspar, and water takes place in the higher-grade part of the sillimanite-bearing area. In the Ryoke belt most of the metamorphic rocks are higher in grade than the biotite isograd. In other words, the rocks on the lower-grade side of the biotite isograd are too poorly recrystallized to be classed as metamorphic.

There is some doubt about the type of metamorphism in the Hitati (Hitachi) district in the southern part of the Abukuma Plateau. There, andalusite and sillimanite occur just as in all the other parts of the Ryoke–Abukuma metamorphic belt, but chloritoid, which has not been found in other parts of the belt, occurs. Moreover, there are some data suggesting the presence of a zone of the epidote–amphibolite facies between the zones of the greenschist and amphibolite facies (Kuroda, 1959), and recrystallization of rocks on the lower-grade side of the biotite isograd appears to have advanced so as to produce chlorite–muscovite slates. All these data suggest that the metamorphism of the Hitati district may be of the low-pressure intermediate group, unlike all the other parts of the Ryoke–Abukuma metamorphic belt.

In the Ryoke–Abukuma belt, the terrain on the continental side of the axis is exposed mainly in the Ryoke wing, whereas the terrain on the Pacific Ocean side is exposed mainly in the Abukuma Plateau. The latter is richer in basic volcanic rocks in the geosynclinal pile, and is richer in gabbroic rocks of the orogenic phase, than the former. The latter also shows more conspicuous development of schistosity, as well as a more advanced degree of recrystallization in low grades, than the former. Such differences in character between the opposite sides of the axis of the metamorphic belt of the andalusite–sillimanite type, or low-pressure intermediate group, would be a commonly observed feature in paired metamorphic belts of the circum-Pacific region. Somewhat similar relations will be mentioned later (pp. 298 & 302) in the cases of the paired metamorphic belts of Hokkaido and California.

Detailed investigations of the metamorphic facies series in this belt were made in the central part of the Abukuma Plateau (Gosaisyo, Takanuki, and Nakoso districts) by Miyashiro (1953, 1958), Shido (1958), and Shido & Miyashiro (1959). Hence, this region was taken as the type metamorphic terrain of the andalusite–sillimanite type, as shown in Fig. 2. In this region pelitic rocks are in subordinate amount and basic rocks are much more abundant. The metamorphic terrain was divided into three progressive metamorphic zones, A, B, and C, on the basis of the progressive variation in calciferous amphiboles in the basic metamorphic rocks. Zone A is characterized by actinolite, and belongs to

the greenschist facies. Zone B is characterized by common hornblende with Z = blue-green, whereas zone C is characterized by common hornblende with Z = green or brown (without a bluish tinge). Zones B and C belong to the amphibolite facies. As mentioned before, the contact metamorphism by synkinematic intrusions produced a metamorphic facies series practically identical to the facies series of the regional metamorphism. In the contact metamorphism by synkinematic gabbros, however, not only zones A, B, and C but also zone D, representing a higher grade than zone C, is produced. This zone is also shown in Fig. 2. Zone D is characterized by the appearance of orthopyroxene, and belongs to the lower-pressure part of the granulite facies. (Whether this zone belongs to the granulite facies or to the pyroxene–hornfels facies depends upon the definition of the two facies. In this paper, this zone is put into the granulite facies.)

The compositional variation from actinolite to common hornblende in the passage from zones A to B is abrupt and discontinuous. Throughout zones B and C, hornblendes in the basic metamorphic rocks have large contents of Al in four- and sixfold co-ordination (Shido, 1958; Shido & Miyashiro, 1959). Cummingtonite is widespread in amphibolites of zone C.

In zones A and B, pyralspite garnet does not occur in common pelitic rocks, but is confined to somewhat more manganiferous metasediments. When it occurs, it is highly manganiferous, and the Mn content decreases with increasing metamorphic grade. In zone C, pyralspite is common in pelitic rocks and is almandine in composition (Miyashiro, 1953). Biotite also shows a tendency towards a decrease in the Mn content as well as an increase in the Ti content with increasing metamorphic grade. The crystal structure of potassium feldspar changes gradually from the microcline structure to the orthoclase with increasing metamorphism (Shido, 1958). The high–low inversion point of quartz is lower in the higher-grade metamorphics than in the lower-grade ones (Iiyama, 1954).

The opaque minerals are mainly pyrite, pyrrhotite, magnetite, and ilmenite in zone A, and pyrrhotite, magnetite, and ilmenite in zones B and C (Banno & Kanehira, 1961).

Sanbagawa metamorphic belt

The Sanbagawa (Sambagawa) metamorphic belt was called the Sanbagawa–Mikabu or Nagatoro metamorphic belt by some authors. The main part of this belt runs along the eastern and southern sides (i.e. Pacific Ocean side) of the Ryoke metamorphic belt. Between the Ryoke and Sanbagawa metamorphic belts there is a long fault, called the *median line* or *median tectonic line*, as shown in Fig. 7. This fault cuts off granitic and metamorphic rocks of the Ryoke belt from metamorphic rocks of the Sanbagawa belt. Mylonite was formed along this fault. It would have originated at a later stage or immediately after the Late Mesozoic orogeny. The eastern extension of the Sanbagawa metamorphic belt outcrops in the Kanto Mountains and probably farther in the north-eastern

margin of the Abukuma Plateau (Yaguku and Yamagami districts). Thus, the Sanbagawa metamorphic belt and its extension lie on the Pacific Ocean side of the full length of the Ryoke–Abukuma metamorphic belt. The tectonic features of this belt were analysed by Nakayama (1959) and others.

The Sanbagawa metamorphic belt is accompanied by abundant ultrabasic rocks (serpentinite, dunite, &c.) and gabbros. Granitic rocks are absent. A fault comparable to the median line is not clear in the Abukuma Plateau, where the easternmost extension of the Sanbagawa metamorphic belt is intruded by post-kinematic granites of the Ryoke–Abukuma belt.

In most of the main part of the Sanbagawa metamorphic belt as well as in the Kanto Mountains, the grade of metamorphism increases towards the median line. In the opposite direction the Sanbagawa metamorphic terrain grades into unmetamorphosed Palaeozoic formations. At some places in Sikoku a marked tectonic zone was found near the southern margin of the metamorphic terrain (Kojima & Suzuki, 1958). The grade of metamorphism appears to be related to the geographical position within the metamorphic belt, but not to the stratigraphical position in the geosynclinal pile. At some places the grade increases towards the lower stratigraphical horizon, and at others it increases towards the higher. Generally, the increase of metamorphic grade is not related to the distribution of igneous masses. An exceptional situation appears to exist in the Bessi district, where the metamorphic grade becomes highest in the vicinity of large basic and ultrabasic masses, which are situated about 6 km to the south of the northern margin of the Sanbagawa metamorphic belt.

The metamorphic rocks of this belt were derived mostly from pelitic, psammitic, and basic volcanic rocks of Middle and Upper Palaeozoic formations. The metamorphism is of the jadeite–glaucophane type at least in some parts, and may be of the high-pressure intermediate group in others. Glaucophane occurs in many parts of the belt, and the distribution of glaucophane is related to the metamorphic grades of the terrains but not to the distribution of ultrabasic and gabbroic masses. Jadeite associated with quartz was found in a certain part of the Kanto Mountains and Sibukawa district (Seki, 1960 *b*, *c*). The jadeite–quartz–albite assemblage was found, in which probably the solid solutions of jadeite and albite play an essential role. In most of the metamorphic belt, the metamorphic temperature was too low to produce biotite, and only in and near the Bessi district was biotite formed in pelitic rocks.

The lower-grade part of the metamorphic facies series was elaborately investigated in the Kanto Mountains by Seki (1958, 1960 *b*, *c*, 1961 *b*). Hence this region was taken as the type metamorphic terrain of the jadeite–glaucophane type. Here Seki showed that the area of almost unmetamorphosed Palaeozoic formations grades with increasing metamorphism into the zone of crystalline schists without albite porphyroblasts (called non-spotted schists), and further into the zone of crystalline schists with conspicuous albite porphyroblasts (called spotted schists). The zone of non-spotted schists and lower grades belongs

to the glaucophane–schist facies, whereas the zone of spotted schists belongs to the greenschist facies, as shown in Fig. 3. Pumpellyite tends to occur in lower grades, whereas piemontite tends to occur in higher grades. Probably, piemontite can have a large content of Mn only at relatively high temperatures (Miyashiro & Seki, 1958*a*). Seki divided the metamorphic region into six zones on the basis of progressive mineralogical changes (Fig. 3). It is interesting that lawsonite and jadeite (associated with quartz) are confined to a middle-grade part (zone IV) of the region. It is conceivable that the temperature–pressure curve corresponding to this metamorphism grazes the stability field of the jadeite–quartz assemblage, as is exemplified by a line (3)–(3′) in Fig. 4. It is also conceivable that the production of lawsonite in this part made the associated albite become more sodic, and hence promoted the formation of jadeite.

The metamorphic facies series in the higher-grade part of the Sanbagawa belt was investigated in the Bessi district by Banno (Banno, 1959; Miyashiro & Banno, 1958). Here, the metamorphic terrain was divided into four zones: I*a*, I*b*, II, and III, in the order of increasing metamorphism. Zone I*a* is characterized by the occurrence of actinolite and pumpellyite, and zone I*b* by the occurrence of actinolite (and not pumpellyite). Zone II is characterized by the occurrence of common hornblende with Z = blue-green. Glaucophane occurs in zones I*a*, I*b*, and the lower-grade part of zone II. Zone III is characterized by the occurrence of biotite in pelitic metamorphic rocks. In the higher-grade part of zone III, diopside and kyanite were found in some basic rocks. Zones I*a* and I*b* belong to the glaucophane–schist facies, and zone III belongs to the epidote–amphibolite facies. Jadeite has not been found in the Bessi and surrounding districts, and it is conceivable that the metamorphism here belongs to the high-pressure intermediate group. The opaque minerals contained in the metamorphic rocks of this district are mainly pyrite, pyrrhotite, haematite, and magnetite, and only in zone III does ilmenite also occur (Banno & Kanehira, 1961).

The mineralogy of the Sanbagawa metamorphic belt is greatly diversified. Not only glaucophane (Seki, 1958; Iwasaki, 1960*b*), jadeite (Seki & Shido, 1959; Seki, 1960 *a*, *b*, *c*, 1961*a*), lawsonite (Seki, 1957, 1958), pumpellyite (Seki, 1958), piemontite (Miyashiro & Seki, 1958*a*; Hashimoto, 1959), kyanite (Banno, 1957), and stilpnomelane (Kozima, 1944), but also magnesio–riebeckite (Miyashiro & Iwasaki, 1957), magnesio–arfvedsonite (Banno, 1958*b*), aegirine–augite (Banno, 1959), aegirine–jadeite (Iwasaki, 1960*a*; Kanehira & Banno, 1960), paragonite (Banno, 1960), and ferriphengite (Kanehira & Banno, 1960) were found. Jadeite occurs not only in quartz-bearing metamorphic rocks but also in quartz-free veins associated with ultrabasic intrusives.

In the Bessi district a large mass of dunite occurs within the highest-grade metamorphic zone. This mass is probably an intrusive emplaced almost simultaneously with the regional metamorphism. In parts of the dunite mass, many sub-parallel bands of eclogite, up to 1 m thick, are interlayered with bands of

dunite and harzburgite. Some parts of the eclogite are composed of diopside and pyrope with a small amount of common hornblende, whereas other parts are composed of almandine–pyrope, omphacite (Na_2O = 2·84 per cent), common hornblende, and epidote (Miyashiro & Seki, 1958*b*; Shido, 1959). This dunite–eclogite complex would represent the highest-temperature member belonging to the same pressure group as the metamorphic rocks of the Bessi district.

Older pair of metamorphic belts

As stated before, the older pair is composed of the Hida and Sangun metamorphic belts.

The Hida metamorphic belt is exposed mainly in the Hida Plateau of central Honsyu (Fig. 7). The western extension of the belt is mostly beneath the Japan Sea, and only a small part is exposed in the Oki Islands. The exposed terrain of the belt is mainly composed of quartzo-feldspathic gneisses, amphibolites, and crystalline limestones, closely associated with numerous small granitic masses. Large granitic masses, collectively called the Hunatu granite, intruded these rocks and probably represent late- or post-kinematic intrusion of this belt.

The petrographic study of the Hida metamorphic belt has been made, but not yet in sufficient detail. In the largest exposed metamorphic area, about 20–40 km south of Toyama, the grade of metamorphism appears to increase southward, judging from the southward increase in grain size of limestones and graphite deposits (Nozawa, 1959). Sillimanite occurs in many parts of the area, whereas andalusite was found only from near its northern margin. The north-eastern end of the Hida belt (Kurobe-gawa district) shows somewhat different characters, where kyanite, andalusite, sillimanite, and staurolite were found by Ishioka and others (e.g. Ishioka & Suwa, 1956). These features suggest that the Hida metamorphic belt belongs to the andalusite–sillimanite type and low-pressure intermediate group.

The eastern part of the Sangun metamorphic belt is an arcuate belt lying on the eastern and southern sides of the Hida Plateau. In this part, metamorphic rocks are exposed in small separate areas, such as Omi, Gamata, and Naradani, all arranged within the belt. Between the Hida and Sangun metamorphic belts, there appears to exist a median fault, although its exact location has become obscured by later granitic, sedimentary, and volcanic rocks. The Sangun metamorphic belt is accompanied by abundant ultrabasic rocks (mostly serpentinite).

The metamorphic terrain of the Omi district at the north-eastern end of the Sangun belt was studied by Banno (Banno, 1958*a*; Miyashiro & Banno, 1958). The metamorphic rocks developed there were derived most from sedimentary and basic igneous rocks. The metamorphic terrain was divided into two progressive metamorphic zones, i.e. a zone of chlorite and one of biotite in order of increasing temperature. The metamorphic grade increases from both sides towards the axial zone, where a large mass of serpentinite is exposed. Glauco-

phane is confined to the chlorite zone. The jadeite–quartz assemblage was not found, although jadeite occurs abundantly in quartz-free albitite masses within serpentinites associated with the metamorphic rocks. Common hornblende occurs in the biotite zone. At least the lower-grade part of the chlorite zone belongs to the glaucophane–schist facies, whereas the biotite zone belongs to the epidote–amphibolite facies.

In the Gamata and Naradani districts of the Sangun belt, the metamorphic rocks belong to the greenschist facies with actinolite, and neither glaucophane nor common hornblende occurs (Seki, 1959).

In most of the Sangun metamorphic terrains in western Honsyu, the metamorphic grade is so low that biotite is not formed and recrystallization is incomplete. The metamorphic rocks are mostly slates and phyllites. Glaucophane was found extremely rarely. In northern Kyusyu, however, the Sangun metamorphic terrain is intruded and highly metamorphosed by many granitic masses. Probably these granites are not genetically related to the Sangun metamorphism but are the northern extension of granitic areas genetically related to the Ryoke metamorphism.

Probably the Sangun metamorphic belts are of the high-pressure intermediate group.

PAIRED METAMORPHIC BELTS IN THE CIRCUM-PACIFIC REGION

The metamorphic belts in various countries around the Pacific Ocean are now to be considered briefly. It will be shown that metamorphic belts of contrasted characters occur in pairs, just as in the main part of Japan.

Hokkaido

Paired metamorphic belts are exposed, running in a north–south direction, in the central part of Hokkaido, the northernmost island of Japan. They are shown in Figs. 6 and 9. The metamorphism of these belts took place during the orogeny in Late Mesozoic time.

The eastern metamorphic belt of the pair is called the *Hidaka metamorphic belt*, which was geologically studied in detail by Hunahashi and his collaborators (Hunahashi, 1957). Here, metamorphic rocks derived from psammitic and pelitic sediments are widely developed, and andalusite and sillimanite occur in rocks of appropriate compositions and grades. Cordierite also occurs, but neither kyanite nor staurolite is present. This metamorphic belt belongs to the andalusite–sillimanite type.

This metamorphic belt has an axis of the highest metamorphic grade, along which so-called migmatite is exposed. On both sides of the axis, rocks of decreasing grades (i.e. gneisses and then schists) are exposed successively in parallel zones. At the western margin of the belt, the zone of schists is in thrust-contact with unmetamorphosed sedimentary terrain, whereas on the eastern side, the zone of schists grades outward into that of hornfelses, which latter

grades into unmetamorphosed sediments. The development of schistosity is more pronounced on the western side of the axis than on the eastern. Plutonic rocks, both granitic and gabbroic, are abundant in the belt, and gabbroic rocks are more abundant on the western side of the axis. Peridotite is also present in the westernmost part. These asymmetrical features on the opposite sides of the axis are similar to relations in the Ryoke–Abukuma metamorphic belt.

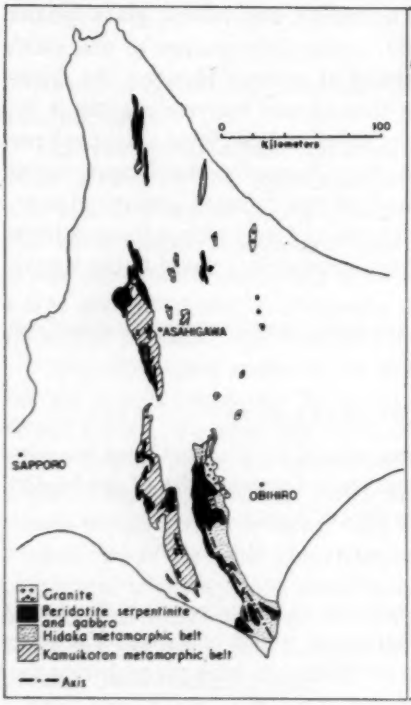

FIG. 9. Metamorphic and associated plutonic rocks of the Hidaka and Kamuikotan metamorphic belts in Hokkaido.

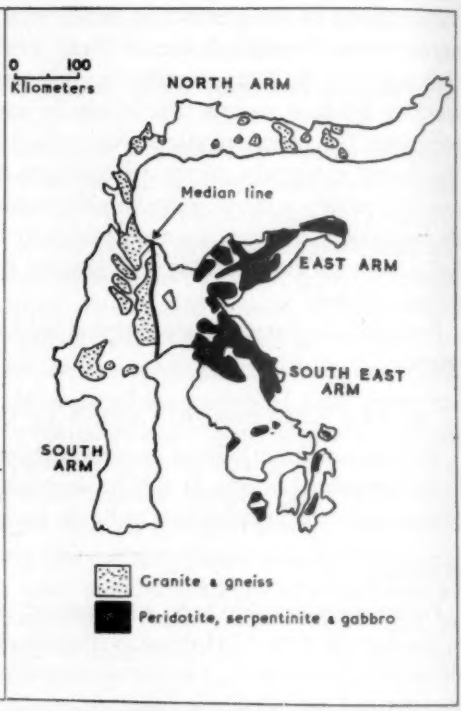

FIG. 10. Distribution of granite and gneiss, as contrasted with that of peridotite, serpentinite, and gabbro, in Celebes.

The western metamorphic belt of the pair is called the *Kamuikotan metamorphic belt*. The metamorphic rocks developed there were derived from basic volcanic and sedimentary rocks of Mesozoic age. Glaucophane is widespread, and jadeite occurs in association with quartz in a wide area (Shido & Seki, 1959). Most or all of the belt belongs to the jadeite–glaucophane type. Lawsonite and pumpellyite are also widespread.

The Kamuikotan metamorphic belt is accompanied by abundant ultrabasic rocks (mostly serpentinite), as described by Suzuki (1952). Formerly, many authors stated that glaucophane occurs in the contact zone around ultrabasic masses. Recent investigations, however, showed that the distribution of glauco-

phane has no definite relationship to ultrabasic masses, although in some contact zones recrystallization is so advanced that the metamorphic rocks are coarser-grained there than in other parts of the terrain, and the presence of coarse-grained glaucophane schists is very impressive.

A large part of the terrain belongs to the glaucophane–schist facies. In a certain part of the belt, however, Shido & Seki (1959) found epidote–hornblende schist, probably belonging to the epidote–amphibolite facies.

In an area to the north-west of Asahigawa, M. Hatano (personal communication) carried out zonal mapping of the Kamuikotan metamorphic terrain, and showed that there is an axis of the highest metamorphic grade that trends, roughly, in a north-north-east direction near the western margin of the exposed metamorphic terrain.

In geological structure the western part of Hokkaido is a northern extension of the main part of Japan, whereas the central and eastern parts of Hokkaido belong to a different geological province. The paired metamorphic belts in Hokkaido were formed probably along the western margin of the latter province. In south Sakhalin, a belt of metamorphic rocks similar to those of the Kamuikotan belt lies in a north–south direction. It is probably the northern extension of the Kamuikotan metamorphic belt, as shown in Fig. 6.

Celebes

The island of Celebes belongs to an orogenic belt of Late Mesozoic to Cenozoic age. The island shows a remarkable four-armed morphology, which is due to a connected double arc with its concave side towards the Pacific Ocean (Fig. 10). The north arm, the western part of central Celebes, and the south arm together constitute the inner arc, where Late Mesozoic and Tertiary granitic rocks are widespread, in association with biotite-rich schists (Bemmelen, 1949).

The granitic masses of the inner arc are cut abruptly on the eastern side by a great fault, called the *median line*, trending north–south. Mylonite was formed along the median line. The east arm, the central and eastern parts of central Celebes, and the south-east arm, which all lie to the east of the median line, together constitute the outer arc. In this arc basic and ultrabasic plutonic rocks of Mesozoic and Cenozoic ages are widely exposed, together with glaucophanitic metamorphic rocks. Basic volcanic rocks are abundant in the geosynclinal pile (Kündig, 1956). In some parts jadeite was found in association with quartz (de Roever, 1955*b*). It is claimed that metamorphic rocks of an older orogenic cycle remain (de Roever, 1947), but the evidence for it is not conclusive.

Thus, the inner and outer arcs constitute paired metamorphic belts. There are many pairs of double arcs in the circum-Pacific region. The structure of Celebes suggests that paired metamorphic belts may underlie the sedimentary and volcanic cover of the double arcs. In the double arc of Ryukyu (Riukiu), glaucophanitic metamorphic rocks are exposed in parts of the outer arc (Hanzawa, 1935; Yossii, 1935).

New Zealand

In New Zealand orogeny took place in Jurassic times, and geosynclinal sediments and volcanic rocks of Palaeozoic to Jurassic age were metamorphosed into schists. The schists are widely exposed in the South Island, and the southern, central, and northern parts of the schist belt are called the *Otago*, *Alpine*, and *Marlborough schists*, respectively (Grindley *et al.*, 1959), as shown in Fig. 11.

The axis of this metamorphic belt trends north-east in the northern part of

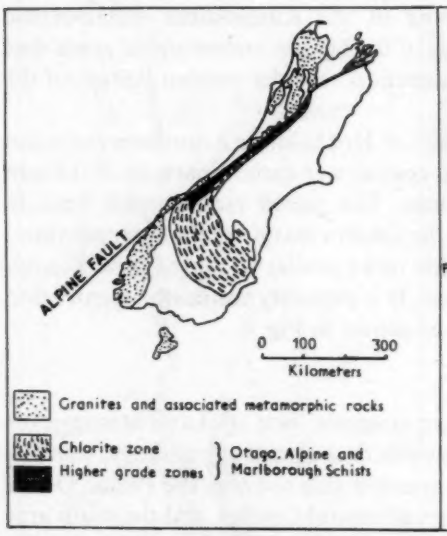

FIG. 11. Plutonic and metamorphic rocks of Palaeozoic and Mesozoic ages in the South Island of New Zealand.

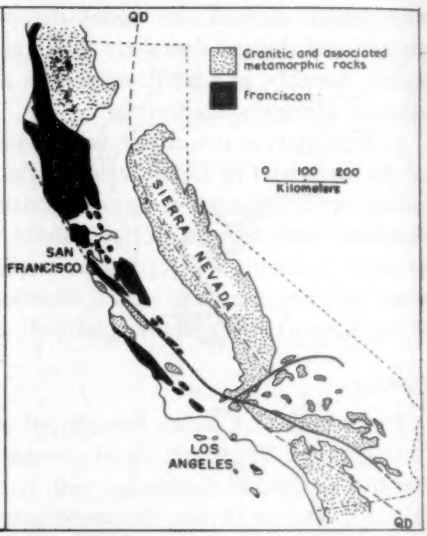

FIG. 12. Distribution of basement rocks in California. The line *QD–QD* represents the 'quartz diorite boundary line' of Moore (1959).

the island, and turns to the south-east in the southern part. The belt is cut by a later fault, called the *Alpine fault*. In the southern and northern parts, the metamorphic grade increases from both sides towards the axis, whereas in the central part the grade increases westwards only, because there the western half of the metamorphic belt is lost by the Alpine fault.

The progressive metamorphism in this belt was studied by Turner (1938), Hutton (1940), Reed (1958), and others. Most of the metamorphic terrain is low in metamorphic grade, belonging to the chlorite zone (greenschist facies). Narrow zones of higher metamorphic grades, characterized by biotite, by almandine, and by oligoclase (greenschist to amphibolite facies), are present in the Alpine schists in the vicinity of the Alpine fault. Recently, Coombs *et al.* (1959) established the zeolite facies, which is lower in metamorphic grade than the greenschist facies.

Hutton (1940) found a crossite core in some actinolite crystals of this meta-

morphic belt, which probably belongs to the high-pressure intermediate group. Like the glaucophanitic metamorphic belts, it includes a wide, well-recrystallized, low-grade area. Pumpellyite, piedmontite, stilpnomelane, and kyanite were found. This metamorphic belt is accompanied neither by granitic nor by gabbroic and ultrabasic rocks.

To the west of this metamorphic belt, there is another belt of granitic and associated metamorphic rocks. The plutonism and metamorphism in this region appear to have taken place in Late Palaeozoic times. The metamorphic rocks are generally high in grade, and contain andalusite, sillimanite, and cordierite. Probably this metamorphism is of the andalusite–sillimanite type and/or low-pressure intermediate group. Granitic and gneissic rocks of probable Precambrian age occur at certain places within this metamorphic belt. Probably they represent the basement for Palaeozoic metamorphic rocks of this belt.

Thus, these two metamorphic belts in the South Island may be regarded as being in a pair, just as in Japan and Celebes. Although the ages of their metamorphism differ, the difference is not great.

California

The Sierra Nevada and the coast ranges of California belong to the Late Mesozoic to Early Tertiary orogenic belt along the west coast of North America. The metamorphic belt of the Sierra Nevada and that of the coast ranges appear to constitute a pair, as in many other parts of the circum-Pacific region (Fig. 12).

In the Sierra Nevada and adjacent areas, gigantic masses of granitic rocks are exposed in association with various metamorphic rocks. Much smaller amounts of gabbroic and ultrabasic rocks are also present. Generally the grade of regional metamorphism is not high, and only the contact aureoles around plutonic masses reach a high grade, producing andalusite. The granites are post-kinematic. High-grade regional metamorphic rocks and synkinematic granites would be still hidden under the ground.

The coast ranges are underlain by the Franciscan formation. Recent investigations have revealed that metamorphism of the jadeite–glaucophane type took place, in the Franciscan, on a regional scale. Glaucophane, lawsonite, and jadeite (associated with quartz) were produced widely in poorly recrystallized greywackes (Bloxam, 1956; McKee, 1958). Well-recrystallized glaucophane schists occur in more limited areas. Basic volcanic rocks are abundant in the geosynclinal pile. Large amounts of gabbroic and ultrabasic rocks are associated with the Franciscan.

Two fault blocks, called *Salina* and *Anacapia*, composed of granitic and high-grade metamorphic rocks, occur within the area of the coast ranges. Probably they were originally in the southern extension of the Sierra Nevada, and were afterwards transported westward by movements along strike-slip faults (King, 1959). Radiometrically dated Precambrian plutonic rocks occur in Anacapia

and areas to the south-east of the Sierra Nevada. The geosynclinal pile of the Sierra Nevada probably has a Precambrian crystalline basement.

Exposed plutonic rocks of the coast ranges, the Sierra Nevada, and adjacent regions, tend to become more acidic and more potassic towards the east. Moore (1959) showed that in the western part of the regions now under consideration quartz–diorite is the dominant 'granitic' rock, whereas in the eastern part granodiorite and quartz–monzonite are the dominant 'granitic' rocks, and that a boundary line, called the *quartz–diorite boundary line*, can be drawn between the two parts, as shown in Fig. 12. It is somewhat similar to relations in the Ryoke–Abukuma and Hidaka metamorphic belts.

ORIGIN AND DEVELOPMENT OF METAMORPHIC BELTS

Origin of paired metamorphic belts

Most of the younger orogenic belts in the circum-Pacific region have a pair of metamorphic belts, as described above. The characters of the paired metamorphic belts may be summarized as follows:

The metamorphic belt on the continental side will be called the *inner metamorphic belt*. It is of the andalusite–sillimanite type and/or low-pressure intermediate group. It has an axis of the highest metamorphic grade, if the original structure is preserved. The metamorphic rocks were usually derived mostly from sediments, which were probably deposited on the sialic basement. The basement may be of Precambrian age in some cases. Basic volcanic rocks are abundant in the geosynclinal pile in certain cases, but not so in many others. The inner metamorphic belt is always accompanied by the intrusion of a large amount of granitic rocks (in a wide sense), usually together with a much smaller volume of gabbroic types. A small volume of ultrabasic rocks may also be present.

The metamorphic belt on the Pacific Ocean side will be called the *outer metamorphic belt*. It is of the jadeite–glaucophane type and/or high-pressure intermediate group. It also has an axis of the highest metamorphic grade, if the original structure is preserved. The metamorphic rocks were usually derived largely from basic volcanic rocks as well as from sediments. The basement of their deposition is not known, and may be the basic ocean floor. The outer metamorphic belt is usually accompanied by the intrusion of a large volume of gabbroic and ultrabasic (mostly serpentinitic) rocks. Granitic rocks are absent.

In the younger pair of the main part of Japan and in Celebes, the two associated metamorphic belts are in direct contact with each other, having a fault between them. On the other hand, in Hokkaido and in New Zealand there is a zone of practically unmetamorphosed rocks between the two belts.

We may consider that the inner metamorphic belt was formed in the geosynclinal pile deposited on the sialic basement at the margin of the continental crust, whereas the outer metamorphic belt was formed in the geosynclinal pile deposited on the ocean floor outside the continental crust. Granitic rocks in the

inner metamorphic belt would have formed by remelting or mobilization of the basement and geosynclinal sediments. On the other hand, in the outer metamorphic belt there would be no sialic basement to form granitic rocks by remelting, and basic volcanic and plutonic rocks, together with ultrabasic rocks, would be formed in abundance by uprise from the basic and/or ultrabasic layer below. It is also possible that some outer metamorphic belts have a sialic basement that is too thin to produce granitic intrusions.

The regional metamorphism of the jadeite–glaucophane type and high-pressure intermediate group in the outer metamorphic belt represents higher rock pressures, and generally lower temperatures, than that of the andalusite–sillimanite type and low-pressure intermediate group in the inner metamorphic belt. On the lithostatic assumption, the higher rock pressure is due to the greater depth of down-buckling and/or underthrusting in the outer metamorphic belt than in the inner, during orogeny. The down-buckling of the outer metamorphic belt would not be generally simultaneous with that of the inner metamorphic belt. The two metamorphic belts were formed, probably, at different phases of the same cycle of orogeny. Probably, the outer metamorphic belt represents the site of the main down-buckle, and would be comparable with the present-day trench, whereas the inner metamorphic belt would represent a subordinate down-buckle of shorter duration. The commonly observed, very weak recrystallization in the lower-grade part of the inner metamorphic belt would be due mainly to the shorter duration of this episode.

The cause of lower temperature in the outer metamorphic belt is not clear. The absence of a sialic basement may be an important factor in this respect, because sialic rocks would produce a large amount of radiogenic heat and would transfer heat by intrusive movements. Recent measurements of heat flow on the ocean bottom have revealed that the amount of heat flow is much smaller in the trench than in other parts of the earth's surface. Whatever the cause of this low value may be, it would be related to the low temperature deduced for the outer metamorphic belt.

Historical development of metamorphic belts

The writer made a survey of petrographic descriptions of metamorphic rocks in the Canadian and Baltic shields, and was greatly impressed by the fact that andalusite, sillimanite, and cordierite are widespread, and staurolite and almandine are also rather common, whereas kyanite is rare, and jadeite and glaucophane are absent. This fact strongly suggests that the metamorphism in these Precambrian shields is mainly of the andalusite–sillimanite type and low-pressure intermediate group.

In the so-called Svecofennides of the Baltic shield, pelitic rocks of middle grades are characterized by the occurrence of andalusite and cordierite, whereas those of high grades are characterized by the occurrence of sillimanite, cordierite, and almandine (Eskola, 1914; Simonen, 1953; Magnusson *et al.*, 1960). Stauro-

lite occurs in some parts (Seitsaari, 1951). In the so-called Karelides, pelitic rocks contain andalusite, cordierite, staurolite, and almandine (Eskola, 1927; Magnusson *et al.*, 1960). In the Baltic shield, kyanite occurs in a few localities in Sweden (Magnusson *et al.*, 1960; Bergström, 1960), but is associated with manganiferous andalusite in some of them. In a locality in Finnish Lapland, kyanite occurs in association with staurolite (Eskola, 1952). All these facts being taken into consideration, andalusite is much more widespread than kyanite in the metamorphic rocks of the Baltic shield.

In the Canadian shield, andalusite, sillimanite, and staurolite occur in the Grenville province as well as in northern Michigan of the Superior province (Engel & Engel, 1953; James, 1955). Cordierite also occurs in the Grenville province. In the vicinity of Great Slave Lake, andalusite, sillimanite, cordierite, and staurolite were described by a few authors. Heinrich and Corey (1959) found kyanite associated with manganiferous andalusite in some Precambrian rocks of New Mexico.

There is a wide area of radiometrically dated Precambrian metamorphic rocks in the southern part of the north-eastern provinces (Manchuria) in China and in the northern part of Korea. These rocks contain andalusite, sillimanite, and staurolite, and are devoid of kyanite, as in the above two shields. In central and southern Korea, kyanite, commonly in association with andalusite and staurolite, occurs in so-called Precambrian metamorphic rocks, although the evidence for a Precambrian age is not certain (e.g. Yamaguchi, 1951).

These Precambrian metamorphic terrains are in the northern region of the earth, where 'continental growth' with geological time is rather evident. The Precambrian shields in the southern region, such as those of India and Africa, where 'continental growth' is not so evident, appear to be somewhat different in character. In Precambrian metamorphic rocks in India, kyanite is widespread, and in those in Africa both kyanite and andalusite are widespread.

Some Palaeozoic metamorphic terrains belong to the andalusite–sillimanite type and low-pressure intermediate group, whereas others belong to the kyanite–sillimanite type. For example, Early Palaeozoic metamorphic belts of New South Wales in Australia (Joplin, 1942, 1943; Vallance, 1953 *a*, *b*) are of the andalusite–sillimanite type. The Palaeozoic metamorphic belt in the Scottish Highlands and Norway is mainly of the kyanite–sillimanite type, but contains some areas of the low-pressure intermediate group (Harker, 1932; Wiseman, 1934; Read, 1952; Clifford, 1958; Goldschmidt, 1915; Vogt, 1927). The Middle Palaeozoic metamorphic belt in the Appalachians is very similar (Barth, 1936; Billings *et al.*, 1952). The Late Palaeozoic metamorphic terrain of the Pyrenees appears to belong to the low-pressure intermediate group (Zwart, 1959; Allaart, 1959).

Most of the paired metamorphic belts in the circum-Pacific region were formed in Mesozoic time. They are composed of a belt of the andalusite–sillimanite type and/or low-pressure intermediate group and another belt of the

jadeite–glaucophane type and/or high-pressure intermediate group, as stated before. The metamorphism in the Pennine nappes of the Alps would belong to the high-pressure intermediate group (Plas, 1959).

The great serpentine belt in eastern Australia is associated with the Brisbane metamorphic complex which contains some glaucophane-like amphiboles. If these rocks may be regarded as being in a pair with the granitic and metamorphic rocks to the west, they would represent the incipient formation of paired metamorphic belts in Palaeozoic time in the circum-Pacific region. The glaucophane schists in this case, however, are probably of the high-pressure intermediate group, and the metamorphism of the jadeite–glaucophane type appears to be confined to Mesozoic time. As regards the Cenozoic regional metamorphism, we have hardly any data with which to discuss it.

Thus, we may conclude that regional metamorphism of the andalusite–sillimanite type and low-pressure intermediate group took place widely from Precambrian through Mesozoic time, whereas that of the kyanite–sillimanite type was common in Palaeozoic time, and that of the jadeite–glaucophane type became common in Mesozoic time. The dominant types of regional metamorphism changed with geological age. It may be considered that regional metamorphism under lower rock pressures (that is, probably at shallower depths) appears to have taken place in all ages, whereas regional metamorphism under higher rock pressures (that is, probably at greater depths) appears to have taken place only in later geological times.

Working hypothesis

The rarity of glaucophane and lawsonite in early geological ages has already been noticed by Eskola (1939), de Roever (1956), and Plas (1959). de Roever claimed that it is a result of the secular decrease of geothermal gradient in the earth's crust through geological time. Metamorphic belts of the jadeite–glaucophane type, however, are commonly associated with those of the andalusite–sillimanite type. This fact is contradictory to de Roever's hypothesis.

For the cause of variation in types of regional metamorphism with geological ages, no definite answer can be given at present. A working hypothesis for it is, however, proposed below.

It is generally believed that the earth was formed about 4,500 million years ago, and the oldest rocks exposed on the earth are about 3,000 million years old. It may be assumed that the primitive sialic crust was formed during the period from 4,500 to 3,000 million years ago through partial melting and differentiation of the basic and/or ultrabasic layer of the earth. The outlines of the primitive crusts would have been somewhat similar to the shapes of the present-day continents, and the primitive crust would have been thicker in the central part of each mass than in the margins. The change of dominant types of regional metamorphism with geological time would be a result of a change in the spatial relationship between the sialic crust and orogenic belts.

In Precambrian time orogenic movements would have taken place mainly (but not exclusively) in the central part of the primitive sialic mass. The sialic crust there would have been relatively thick and strong and, consequently, would have resulted in relatively shallow down-buckles that caused metamorphism of the andalusite–sillimanite type and low-pressure intermediate group. In Palaeozoic time orogenic belts would have moved outward into the more marginal part of the sialic mass, where the crust was partly thick and partly thin. Orogenic movements would have produced down-buckles of greater depths in the thin parts of the crust, with the resultant formation of metamorphic belts of the kyanite–sillimanite type. In Mesozoic time orogenic belts would have moved still farther outward, to the margin of the sialic mass, and the main site of the orogenic down-buckle would have been in the geosynclinal pile that was deposited on a very thin sialic basement or directly on the basic ocean floor. Thus, the down-buckle in this case would have reached a great depth with resultant formation of metamorphic belts of the high-pressure intermediate group and jadeite–glaucophane type. On the other hand, on the nearby continental margin a smaller degree of down-buckling would have taken place to produce metamorphic belts of the andalusite–sillimanite type and low-pressure intermediate group.

In this hypothesis the 'continental growth' by orogenies during the period from Precambrian to Palaeozoic time was only apparent. Actually, it meant a gradual progress of recrystallization and hardening of the pre-existing primitive sialic crust from the centre towards the margin. The true growth of continents began in Mesozoic time, when the main site of orogeny passed over the margin of the primitive sialic masses into the oceanic regions.

FACIES SERIES OF CONTACT METAMORPHISM

The classification of metamorphism into regional and contact types is based on the geological relations. This classification, then, does not necessarily correspond to the classification of metamorphism based on the metamorphic facies series. Contact metamorphism appears to produce different facies series in different cases. In this respect, however, our knowledge is very incomplete, and only a cursory survey will be given below.

In the central Abukuma Plateau the metamorphic facies series developed in the contact aureoles of synkinematic granites is practically identical to that developed through regional metamorphism of the same region (i.e. of the andalusite–sillimanite type), whereas the facies series developed in the contact aureoles of the post-kinematic granites is different. Shido (1958) made a detailed investigation of the contact aureole around the post-kinematic Iritono granite in the central Abukuma Plateau.

In the Iritono contact aureole the low-grade zone is characterized by basic hornfelses with the actinolite–labradorite (or andesine)–quartz assemblage with, or without, chlorite. It is remarkable that epidote and zoisite are absent, and

that the plagioclase is calcic despite the stable presence of actinolite. It may be that calcic plagioclase becomes stable at a lower grade than common hornblende in this aureole, owing to the very low rock pressure operating there. This assemblage does not belong to any metamorphic facies so far known. It is a new facies or subfacies, which might well be called the *actinolite–calcic plagioclase hornfels facies*. The associated hornfelses of sedimentary origin are biotite–plagioclase–quartz hornfelses, sometimes with muscovite or pyralspite.

The middle-grade zone of the Iritono contact aureole is characterized by basic hornfelses with the common hornblende–plagioclase assemblage with or without cummingtonite, clinopyroxene, and biotite. The colour (Z) of the common hornblende is brownish-green or brown. Blue-green common hornblende, such as is widespread in the middle grade of the associated regional metamorphism, is almost absent. The high-grade zone of the contact aureole is characterized by the appearance of orthopyroxene, producing the orthopyroxene–hornblende–plagioclase assemblage sometimes together with cummingtonite, clinopyroxene, and biotite. Almandine is stable in pelitic rocks of the middle grade, but the stability of almandine in the high-grade zone is not clearly established, because pelitic rocks are absent there. Conceivably, almandine is stable in the high-grade zone as well, should the chemical conditions permit.

Thus, the contact aureole of the Iritono district shows a metamorphic facies series that is different from any of the above-mentioned regional-metamorphic facies series. This facies series probably represents a rock pressure lower than that found in any type of regional metamorphism.

Some contact aureoles, such as those of the Kristiania district (Goldschmidt, 1911) and of the Comrie district (Tilley, 1924), contain andalusite and cordierite, and are devoid of almandine. Sillimanite may be present. Such aureoles would represent a still lower rock pressure than that in the Iritono contact aureole.

On the other hand, Compton (1960) described a contact aureole with staurolite together with andalusite, sillimanite, and cordierite. It would be of the low-pressure intermediate group.

The sanidinite facies is probably the highest-temperature member in some contact metamorphic facies series. This facies may well be divided into certain subfacies representing different temperatures and pressures. For example, pigeonite is stable only in a high-temperature part of the facies. Some acidic volcanic rocks of Japan contain pyralspite garnet and sillimanite (not mullite, according to an investigation by S. Aramaki). A lower-temperature part of the sanidinite facies is probably characterized by the stability of almandine, spessartine, sillimanite, cordierite with a large distortion index (Miyashiro *et al.*, 1955; Miyashiro, 1957), and osumilite (Miyashiro, 1956). On the other hand, a higher-temperature part of the facies is probably characterized by the stability of pigeonite, mullite, and cordierite with smaller distortion indices. Though the petrographic evidence is not available, spessartine is probably stable in the higher-temperature part as well, should the chemical conditions permit.

ACKNOWLEDGEMENTS

This paper is the result of my collaboration with some colleagues and students in the University of Tokyo during the last six years. I am greatly indebted to my collaborators, especially to Yotaro Seki, Fumiko Shido, and Shohei Banno, who inspired me with their many important discoveries. We enjoyed lively discussions with, and helpful advice from, one another. Naturally, I am solely responsible for possible mistakes in this paper.

Professor Hisashi Kuno, of the same university, read the manuscript with friendly criticism. I am also grateful to M. Gorai, R. S. Fiske, and many other friends for much advice.

REFERENCES

ALLAART, J. H., 1959. The geology and petrology of the Trois Seigneurs Massif, Pyrenees, France. *Leid. geol. Meded.* **22**, 97–214.

BANNO, S., 1957. Kyanite from the Bessi mining district (in Japanese). *J. geol. Soc. Japan*, **63**, 598.

—— 1958*a*. Glaucophane schists and associated rocks in the Omi district, Japan. *Jap. J. Geol. Geog.* **29**, 29–44.

—— 1958*b*. Notes on rock-forming minerals. (1) Magnesioarfvedsonite from the Bessi district. *J. geol. Soc. Japan*, **64**, 386–7.

—— 1959. Aegirinaugites from crystalline schists in Sikoku. Ibid. **65**, 652–7.

—— 1960. Notes on rock-forming minerals. (12) Finding of paragonite from the Bessi district, Sikoku, and its paragenesis. Ibid. **66**, 123–30.

—— & KANEHIRA, K., 1961. Sulfides and oxides in schists of the Sanbagawa and central Abukuma metamorphic terranes. *Jap. J. Geol. Geog.* **32**, 331–48.

—— & MILLER, J., 1961. New data on the age of the Ryoke and Sanbagawa metamorphism (in Japanese). *Kagaku*, **31**, 144.

BARROW, G., 1893. On an intrusion of muscovite–biotite–gneiss in the south-eastern Highlands of Scotland, and its accompanying metamorphism. *Quart. J. geol. Soc. Lond.* **49**, 330–58.

—— 1912. On the geology of Lower Dee-side and the southern Highland border. *Proc. geol. Ass. Lond.* **23**, 274–90.

BARTH, TOM F. W., 1936. Structural and petrologic studies in Dutchess County, New York. Part II. Petrology and metamorphism of the Paleozoic rocks. *Bull. geol. Soc. Amer.* **47**, 775–850.

BEMMELEN, R. W. VAN, 1949. *The geology of Indonesia.* The Hague: Government Printing Office.

BERGSTRÖM, L., 1960. An occurrence of kyanite in a pegmatite in western Sweden. *Geol. Fören. Stockh. Förh.* **82**, 270–2.

BILLINGS, M. P., THOMPSON, J. B., JR., & ROGERS, J., 1952. Geology of the Appalachian Highlands of east-central New York, southern Vermont, and southern New Hampshire. *Guidebook for field trips in New England*, 1–71. Geologists of Greater Boston, Boston.

BIRCH, F., & LECOMTE, P., 1960. Temperature-pressure plane for albite composition. *Amer. J. Sci.* **258**, 209–17.

BLOXAM, T. W., 1956. Jadeite-bearing metagraywackes in California. *Amer. Min.* **41**, 488–96.

CHAPMAN, C. A., 1952. Structure and petrology of the Sunapee quadrangle, New Hampshire. *Bull. geol. Soc. Amer.* **63**, 381–425.

CHINNER, G. A., 1960. Pelitic gneisses with varying ferrous/ferric ratios from Glen Clova, Angus, Scotland. *J. Petrol.* **1**, 178–217.

CLARK, S. P., JR., 1960. Kyanite revised. *J. geophys. Res.* **65**, 2482.

—— ROBERTSON, E. C., & BIRCH, F., 1957. Experimental determination of kyanite–sillimanite equilibrium relations at high temperatures and pressures. *Amer. J. Sci.* **255**, 628–40.

CLIFFORD, T. N., 1958. A note on kyanite in the Moine series of southern Ross-shire, and a review of related rocks in the Northern Highlands of Scotland. *Geol. Mag. Lond.* **95**, 333–46.

COMPTON, R. R., 1960. Contact metamorphism in Santa Rosa range, Nevada. *Bull. geol. Soc. Amer.* **71**, 1383–1416.

COOMBS, D. S., ELLIS, A. J., FYFE, W. S., & TAYLOR, A. M., 1959. The zeolite facies, with comments on the interpretation of hydrothermal synthesis. *Geochim. et Cosmoch. Acta*, **17**, 53–107.

ENGEL, A. E. J., & ENGEL, C. G., 1953. Grenville series in the northwest Adirondack Mountains, New York. Part I. General features of the Grenville series. *Bull. geol. Soc. Amer.* **64,** 1013–47.

ESKOLA, P., 1914. On the petrology of the Orijärvi region in south-western Finland. *Bull. Comm. géol. Finl.* **40.**

—— 1915. On the relations between the chemical and mineralogical composition in the metamorphic rocks of the Orijärvi region. Ibid. **44.**

—— 1920. The mineral facies of rocks. *Norsk. geol. Tidsskr.* **6,** 143–94.

—— 1927. Petrographische Charakteristik der kristallinen Gesteine von Finland. *Fortschr. Min.* **11,** 57–112.

—— 1939. Die metamorphen Gesteine, in *Die Entstehung der Gesteine*, by Tom. F. W. Barth, C. W. Correns, & P. Eskola, 263–407. Berlin: Julius Springer.

—— 1952. On the granulites of Lapland. *Amer. J. Sci.*, Bowen vol., 133–71.

EUGSTER, H. P., 1959. Reduction and oxidation in metamorphism, in *Researches in geochemistry*, 397–426. New York: Wiley & Sons.

FRANCIS, G. H., 1956. Facies boundaries in pelites at the middle grades of regional metamorphism. *Geol. Mag. Lond.* **93,** 353–68.

GOLDSCHMIDT, V. M., 1911. Die Kontaktmetamorphose im Kristianiagebiet. *Videnskaps Skrifter.* I, Mat.-Naturv. Kl. **11.**

—— 1915. Geologisch-petrographische Studien im Hochgebirge des südlichen Norwegens: III. Die Kalksilikatgneise und Kalksilikatglimmerschiefer im Trondhjem-Gebiete. Ibid. **10.**

GRINDLEY, G. W., HARRINGTON, H. J., & WOOD, B. L., 1959. The geological map of New Zealand, 1:2,000,000. *Bull. geol. Surv. N.Z.*, N.S., **66.**

HANZAWA, S., 1935. Topography and geology of the Riukiu Islands. *Sci. Rep. Tôhoku Univ.*, ser. II, **17,** 1–61.

HARKER, A., 1932. *Metamorphism.* London: Methuen & Co.

HASHIMOTO, M., 1959. Piedmontite from piedmontite-bearing muscovite–quartz schist from Inasato, Nagano Prefecture. *Bull. nat. Sci. Mus. Tokyo*, **4,** 183–7.

HEINRICH, E. WM., & COREY, A. F., 1959. Manganian andalusite from Kiawa Mountain, Rio Arriba County, New Mexico. *Amer. Min.* **44,** 1261–71.

HIETANEN, A., 1956. Kyanite, andalusite, and sillimanite in the schist in Boehls Butte quadrangle, Idaho. Ibid. **41,** 1–27.

HUNAHASHI, M., 1957. Alpine orogenic movement in Hokkaido, Japan. *J. Fac. Sci. Hokkaido Univ.*, ser. IV, **9,** 415–69.

HUTTON, C. O., 1940. Metamorphism in the Lake Wakatipu region, western Otago, New Zealand. *Mem. Dep. sci. industr. Res. N.Z.* **5.**

IIYAMA, T., 1954. High–low inversion point of quartz in metamorphic rocks. *J. Fac. Sci. Tokyo Univ.*, sec. II, **9,** 193–200.

ISHIOKA, K., & SUWA, K., 1956. Metasomatic development of staurolite schist from rhyolite in the Kurobe-gawa area, central Japan (a preliminary report). *J. Earth Sci. Nagoya Univ.* **4,** 123–40.

IWASAKI, M., 1960*a*. Clinopyroxene intermediate between jadeite and aegirine from Suberi-dani, Tokusima Prefecture. *J. geol. Soc. Japan*, **66,** 334–40.

—— 1960*b*. Colorless glaucophane and associated minerals in quartzose schists from eastern Sikoku, Japan. Ibid. 566–74.

JAMES, H. L., 1955. Zones of regional metamorphism in the Precambrian of northern Michigan. *Bull. geol. Soc. Amer.* **66,** 1455–88.

JOPLIN, G. A., 1942. Petrological studies in the Ordovician of New South Wales. I. The Cooma complex. *Proc. Linn. Soc. N.S.W.* **67,** 156–96.

—— 1943. Petrological studies in the Ordovician of New South Wales. II. The northern extension of the Cooma complex. Ibid. **68,** 159–83.

KANEHIRA, K., & BANNO, S., 1960. Ferriphengite and aegirinjadeite in a crystalline schist of the Iimori district, Kii Peninsula. *J. geol. Soc. Japan*, **66,** 654–9.

KENNEDY, G. C., 1960. Phase relations of some rocks and minerals at high temperatures and high pressures. *Trans. Amer. geophys. Un.*, **41,** 283–6.

KING, P. B., 1959. *The evolution of North America.* Princeton: Princeton Univ. Press.

KOBAYASHI, T., 1941. The Sakawa orogenic cycle and its bearing on the origin of the Japanese Islands. *J. Fac. Sci. Tokyo Univ.*, sec. II, **5,** 219–578.

KOJIMA, G., & SUZUKI, T., 1958. Rock structure and quartz fabric in a thrusting shear zone: the Kiyomizu tectonic zone in Shikoku, Japan. *J. Sci. Hiroshima Univ.*, ser. C, **2,** 173–93.

KORZHINSKII, D. S., 1959. *Physico-chemical basis of the analysis of the paragenesis of minerals.* New York: Consultant Bureau.

KOZIMA, Z., 1944. On stilpnomelane in green-schists in Japan. *Proc. imp. Acad. Japan*, **20,** 322–8.

KÜNDIG, E., 1956. Geology and ophiolite problems of East Celebes. *Kon. Ned. Geol. Mijnb. Genoot. Geol. Ser.* **16** (Gedenkboek H. A. Brouwer), 210–35.

KUNO, H., BAADSGAARD, H., GOLDICH, S., & SHIOBARA, K., 1960. Potassium–argon dating of the Hida metamorphic complex, Japan. *Jap. J. Geol. Geog.* **31**, 273–8.

KURODA, Y., 1959. Petrological study on the metamorphic rocks of the Hitachi district, north-eastern Japan. *Sci. Rep. Tokyo Kyoiku Daig.*, sec. C, **58.**

MCKEE, B., 1958. Jadeite alteration of sedimentary and igneous rocks. *Program, 1958 Annual Meetings, Geol. Soc. Amer.*, 108.

MAGNUSSON, N. H., THORSLUND, P., BROTZEN, F., ASKLUND, B., & KULLING, O., 1960. Description to accompany the map of the pre-Quaternary rocks of Sweden. *Sverig. geol. Unders. Afh.*, ser. Ba, **16.**

MILLER, J., SHIDO, F., BANNO, S., & UYEDA, S., 1961. New data on the age of orogeny and metamorphism in Japan. *Jap. J. Geol. Geog.* **32**, 145–51.

MINATO, M., 1960. On the age of metamorphism in the Japanese Islands. *Int. geol. Rev.* **2**, 901–11.

MIYASHIRO, A., 1953. Calcium-poor garnet in relation to metamorphism. *Geochim. et Cosmoch. Act*, **4**, 179–208.

—— 1956. Osumilite, a new silicate mineral, and its crystal structure. *Amer. Min.* **41**, 104–16.

—— 1957. Cordierite–indialite relations. *Amer. J. Sci.* **255**, 43–62.

—— 1958. Regional metamorphism of the Gosaisyo–Takanuki district in the central Abukuma Plateau. *J. Fac. Sci. Toyko Univ.*, sec. II, **11**, 219–72.

—— 1959. Abukuma, Ryoke, and Sanbagawa metamorphic belts (in Japanese). *J. geol. Soc. Japan*, **65**, 624–37.

—— 1960*a*. Thermodynamics of reactions of rock-forming minerals with silica. Part III. Andalusite, kyanite, sillimanite, and corundum. *Jap. J. Geol. Geog.* **31**, 107–11.

—— 1960*b*. Thermodynamics of reactions of rock-forming minerals with silica. Part IV. Decomposition reactions of muscovite. Ibid. 113–20.

—— 1960*c*. Thermodynamics of reactions of rock-forming minerals with silica. Part V. Decomposition reactions of phlogopite. Ibid. 241–6.

—— & BANNO, S., 1958. Nature of glaucophanitic metamorphism. *Amer. J. Sci.* **256**, 97–110.

—— IIYAMA, T., YAMASAKI, M., & MIYASHIRO, T., 1955. The polymorphism of cordierite and indialite. Ibid. **253**, 185–208.

—— & IWASAKI, M., 1957. Magnesioriebeckite in crystalline schists of Bizan in Sikoku, Japan. *J. geol. Soc. Japan*, **63**, 698–703.

—— & SEKI, Y., 1958*a*. Enlargement of the composition field of epidote and piedmontite with rising temperature. *Amer. J. Sci.* **256**, 423–30.

—— —— 1958*b*. Mineral assemblages and subfacies of the glaucophane schist facies. *Jap. J. Geol. Geog.* **29**, 199–208.

MOORE, J. G., 1959. The quartz–diorite boundary line in the western United States. *J. Geol.* **67**, 198–210.

NAKAYAMA, I., 1959. Tectonic features of the Sambagawa metamorphic zone, Japan. *Mem. Coll. Sci. Kyoto*, ser. B, **26**, 103–10.

NOZAWA, T., 1959. On the age of Hida metamorphic rocks (a preliminary note) (in Japanese). *J. geol. Soc. Japan*, **65**, 463–9.

PLAS, L. VAN DER, 1959. Petrology of the northern Adula region, Switzerland. *Leid. géol. Meded.* **24**, 411–602.

READ, H. H., 1952. Metamorphism and migmatization in the Ythan Valley, Aberdeenshire. *Trans. Edinb. geol. Soc.* **15**, 265–79.

REED, J. J., 1958. Regional metamorphism in southeast Nelson. *Bull. geol. Surv. N.Z.*, N.S., **60.**

ROEVER, W. P. DE, 1947. Igneous and metamorphic rocks in eastern Central Celebes, in *Geological explorations in the island of Celebes under the leadership of H. A. Brouwer*, 65–173. Amsterdam: North-Holland Publishing Co.

—— 1955*a*. Some remarks concerning the origin of glaucophane in the North Berkeley Hills, California. *Amer. J. Sci.* **253**, 240–4.

—— 1955*b*. Genesis of jadeite by low-grade metamorphism. Ibid. **253**, 283–98.

—— 1956. Some differences between post-Paleozoic and older regional metamorphism. *Geol. en Mijnb.* (NW ser.), **18**, 123–7.

SEITSAARI, J., 1951. The schist belt northeast of Tampere in Finland. *Bull. Comm. géol. Finl.* **153.**

SEKI, Y., 1957. Lawsonite from the eastern part of the Kanto Mountains. *Sci. Rep. Saitama Univ.*, ser. B, **2**, 363–73.

—— 1958. Glaucophanitic regional metamorphism in the Kanto Mountains, central Japan. *Jap. J. Geol. Geog.* **29**, 233–58.

SEKI, Y., 1959. Petrological studies on the circum-Hida crystalline schists. I. *Sci. Rep. Saitama Univ.*, ser. B, **3**, 209–20.
—— 1960*a*. Jadeite and associated minerals of meta-gabbroic rocks in the Sibukawa district, central Japan. *Amer. Min.* **45**, 668–79.
—— 1960*b*. Distribution and mineral assemblages of jadeite-bearing metamorphic rocks in Sanbagawa metamorphic terrains of central Japan. *Sci. Rep. Saitama Univ.*, ser. B, **3**, 313–20.
—— 1960*c*. Jadeite in Sanbagawa crystalline schists of central Japan. *Amer. J. Sci.* **258**, 705–15.
—— 1961*a*. Notes on rock-forming minerals. (17) Jadeite from Kanasaki of the Kanto Mountains, central Japan. *J. geol. Soc. Japan*, **67**, 101–4.
—— 1961*b*. Pumpellyite in low-grade regional metamorphism. *J. Petrol.* **2**, 407–23.
—— & SHIDO, F., 1959. Finding of jadeite from the Sanbagawa and Kamuikotan metamorphic belts, Japan. *Proc. Japan Acad.* **35**, 137–8.
SHAW, D. M., 1956. Geochemistry of pelitic rocks. Part III. Major elements and general geochemistry. *Bull. geol. Soc. Amer.* **67**, 919–34.
SHIDO, F., 1958. Plutonic and metamorphic rocks of the Nakoso and Iritono districts in the central Abukuma Plateau. *J. Fac. Sci. Tokyo Univ.*, sec. II, **11**, 131–217.
—— 1959. Notes on rock-forming minerals. (9) Hornblende-bearing eclogite from Gongen-yama of Higasi-Akaisi in the Bessi district, Sikoku. *J. geol. Soc. Japan*, **65**, 701–3.
—— & MIYASHIRO, A., 1959. Hornblendes of basic metamorphic rocks. *J. Fac. Sci. Tokyo Univ.*, sec. II, **12**, 85–102.
—— & SEKI, Y., 1959. Notes on rock-forming minerals. (11) Jadeite and hornblende from the Kamuikotan metamorphic belt. *J. geol. Soc. Japan*, **65**, 673–7.
SIMONEN, A., 1953. Stratigraphy and sedimentation of the Svecofennidic, early Archean supracrustal rocks in southwestern Finland. *Bull. Comm. géol. Finl.* **160.**
SNELLING, N. J., 1957. Notes on the petrology and mineralogy of the Barrovian metamorphic zones. *Geol. Mag. Lond.* **94**, 297–304.
SUGIMURA, A., 1960. Zonal arrangement of some geophysical and petrological features in Japan and its environs. *J. Fac. Sci. Tokyo Univ.*, sec. II, **12**, 133–53.
SUZUKI, J., 1952. Ultrabasic rocks and associated ore deposits of Hokkaido, Japan. *J. Fac. Sci. Hokkaido Univ.*, ser. IV, **8**, 175–210.
THOMPSON, J. B., JR., 1955. The thermodynamic basis for the mineral facies concept. *Amer. J. Sci.* **253**, 65–103.
—— 1957. The graphical analysis of mineral assemblages in pelitic schists. *Amer. Min.* **42**, 842–58.
TILLEY, C. E., 1924. Contact metamorphism in the Comrie area of the Perthshire Highlands. *Quart. J. geol. Soc. Lond.* **80**, 22–70.
—— 1925. A preliminary survey of metamorphic zones in the southern Highlands of Scotland. Ibid. **81**, 100–12.
TURNER, F. J., 1938. Progressive regional metamorphism in southern New Zealand. *Geol. Mag. Lond.* **75**, 160–74.
—— 1948. Mineralogical and structural evolution of the metamorphic rocks. *Mem. geol. Soc. Amer.* **30.**
VALLANCE, T. G., 1953*a*. Studies in the metamorphic and plutonic geology of the Wantabadgery–Adelong–Tumbarumba district, N.S.W. I. Introduction and metamorphism of the sedimentary rocks. *Proc. Linn. Soc. N.S.W.* **78**, 90–121.
—— 1953*b*. Studies in the metamorphic and plutonic geology of the Wantabadgery–Adelong–Tumbarumba district, N.S.W. II. Intermediate-basic rocks. Ibid. **78**, 181–96.
VOGT, TH., 1927. Sulitelmafeltets geologi og petrografi. *Norg. geol. Unders.* **121.**
WISEMAN, J. D. H., 1934. The central and south-west Highland epidiorites: a study in progressive metamorphism. *Quart. J. geol. Soc. Lond.* **90**, 354–417.
YAMAGUCHI, T., 1951. On the so-called Yonchon system and its regional metamorphism (in Japanese). *J. geol. Soc. Japan*, **57**, 419–38.
YOSSII, M., 1935. On some glaucophane-rocks from the Ryukyu Archipelago. *Sci. Rep. Tôhoku Univ.*, ser. II, **16**, 225–48.
ZWART, H. J., 1959. Metamorphic history of the central Pyrenees. Part I. *Leid. geol. Meded.* **22**, 419–90.

The Origin of Sillimanite in Glen Clova, Angus

by G. A. CHINNER

Department of Mineralogy and Petrology, Cambridge

WITH ONE PLATE

ABSTRACT

At the sillimanite isograd in Glen Clova, sillimanite appears to have formed within biotite, rather than in kyanite. Biotite is thought to have been a nucleating agent, the trigonally arranged oxygen octahedra and tetrahedra in the alternate mica layers acting as nuclei for the growth of the octahedral Al–O and the tetrahedral (Al, Si)–O chains that constitute the sillimanite structure. Nucleation seems to have been dominantly epitaxial; no permanent breakdown of biotite was involved, and it is suggested that Al and Si for sillimanite growth was mainly derived from the solution of unstable kyanite.

INTRODUCTION

In his original formulation of the concept of mineral zoning in the Scottish Dalradian metamorphic rocks, Barrow (1893) did not discuss in detail the relationship between the two highest grade zones (those characterized by kyanite and sillimanite) although on the basis of Vernadsky's supposed experimental transformation of kyanite to sillimanite, he did suggest that sillimanite arose from kyanite as the result of temperature increase.

More recent work, both in Barrow's type-area, and in other regionally metamorphosed terrains, has suggested that the development of sillimanite is a more complex phenomenon, often involving growth in micas and rarely showing any clear connexion with kyanite. This paper presents observations and an interpretation on the growth of sillimanite in the vicinity of the sillimanite isograd in Glen Clova, Angus.

Recrystallization history of the Glen Clova Pelitic gneisses

Two papers on the petrology of Glen Clova have been recently published: one by Harry (1958), dealing mainly with the quartzo-feldspathic gneisses (Barrow's 'older granites') whose formation broadly concurred with regional metamorphism, and the other (Chinner, 1960) dealing with the pelitic gneisses. The latter rocks, essentially quartz–oligoclase–biotite–muscovite–garnet–kyanite gneisses, with or without sillimanite, are divided broadly into two groups on the basis of their iron oxide mineral content: the haematite-free gneisses, and the haematite-bearing gneisses. As a reflection of their varying oxygen contents, the haematite-free gneisses contain manganese-poor almandine garnets and brown, iron-rich biotites, in contrast to the more manganiferous garnets and generally green, magnesium-rich biotites of the haematite-bearing gneisses.

In contrast to the relative homogeneity and medium grain size of pelitic schists in the lower-grade zones of the Scottish Dalradian, the sillimanite zone

[Journal of Petrology, Vol. 2, Part 3, pp. 312–23, 1961]

pelites are inhomogeneous, coarsely grained, and show an abundance of disequilibrium textures, features which presumably result from the successive stages of 'older granite' formation, metasomatism, and possibly even partial melting (Tuttle & Bowen, 1958, p. 125) to which they have been subjected.

The general fabric of the pelitic gneisses appears to date from the earliest recognizable stage of metamorphism. Kyanite forms an integral part of this fabric. It occurs as regularly distributed prisms of a grain size generally commensurate with that of associated micas and garnets, and often shows a high degree of preferred orientation, with [001] lying parallel to the rock lineation and (100) parallel to the foliation; in thin section, the (100) and (010) cleavages are thus consistently seen. Simple twinning giving a reflection of the (010) cleavages across the composition plane (100) is very common, and the crystals are often considerably bent. Kyanite may include grains of garnet, mica, quartz, or tourmaline, or be included by any of these minerals (Chinner, 1960, figs. 2 and 3; Barrow, 1893, plate XVI). A finer-grained 'needle' kyanite which occurs in small amount along grain-boundaries appears to belong to a later stage of crystallization, and will be described subsequently.

In contrast to the regularity of kyanite development, the occurrence of sillimanite is irregular in the extreme, and appears to have dated from a stage later than that of the formation of the main, kyanite-bearing rock fabric. In the field, sillimanite is often conspicuous as creamy-white, fibrous lenticles varying in width from a few millimetres to several centimetres, as veinlets or faserkiesel parallel to the foliation of the more micaceous beds, and as knot-like extensions of these penetrating the interbedded, more siliceous, kyanite-free semipelitic gneisses (Fig. 1).

In thin section, these veins are resolved into coarse mats of fine, fibrolitic sillimanite, often meandering in sinuous waves through the micaceous foliae of the rock; this sillimanite is usually intimately intergrown with, and apparently replacing, biotite, the *c*-axes of the sillimanite lying parallel to the mica cleavages. Such sillimanite is well illustrated in the delicate lithograph of Barrow's (1893) fig. 2, plate XVI; it is also shown in Harry's (1958) fig. 1, plate I, and in the Plate, fig. A, of this paper. Where biotite flakes have been cut parallel to the mica cleavage, the sillimanite fibrelets may often be seen to be oriented parallel to the zone axis [010], and to the two pressure-figure directions at 60° to this, forming a triangular pattern (Plate, fig. B).

The coarser fibrolite felts are seamed with cracks perpendicular to their length, due to the incipient development of a basal cleavage; when a section has been cut normal to the length of a felt, a finely granular aggregate is seen, giving a uniaxial positive figure due to the parallelism of the *c*-axes and a random distribution of the *a*- and *b*-axes of the individual fibrelets. The amount of biotite intergrown with the fibrolite is extremely variable; in some felts it shows as only a trace of faint brown pleochroism, while in many biotite-rich areas sillimanite is completely lacking. Fibrolite rarely occurs with the green magnesian biotites,

so the haematite-bearing gneisses are generally sillimanite-poor. Similarly, the association of sillimanite and muscovite is uncommon: where it does occur, there is no regularity of orientation, with schools of tiny, discrete sillimanite rodlets traversing muscovite flakes at varying angles to the cleavage. It appears

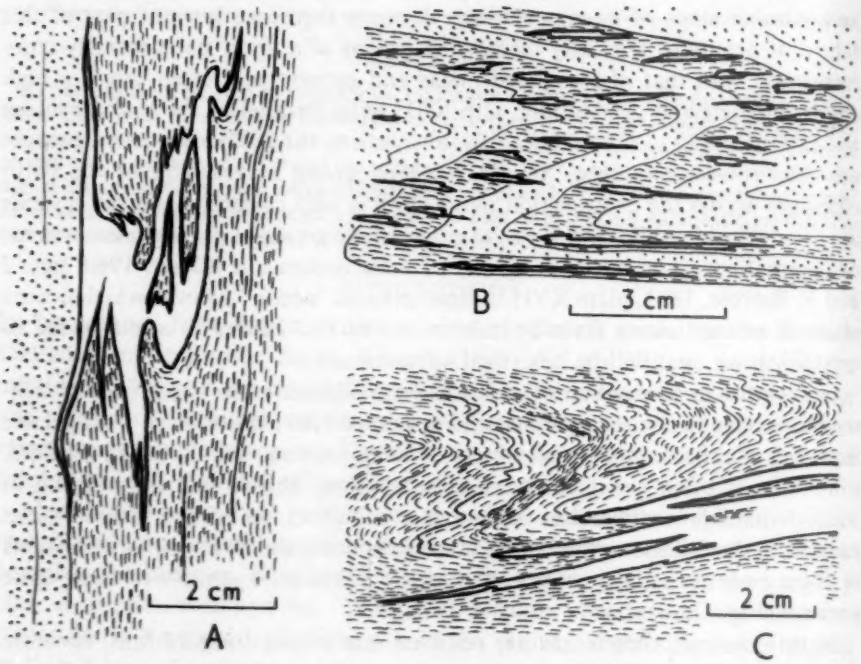

FIG. 1. Field-sketches of sillimanite veining. Stipple ornament: semipelitic (quartz–feldspar–biotite–muscovite–garnet) gneiss. Dashed ornament: pelitic (quartz–feldspar–biotite–muscovite–garnet–kyanite) gneiss. Heavily outlined, left blank: sillimanite-rich veins. A, Craig Maud, Glen Doll. B, The Lunkard, Glen Doll. C, Bassies, Glen Clova.

likely that if sillimanite–muscovite textures originally existed, they have been destroyed by extensive recrystallization and growth of muscovite during the later phases of metamorphism.

The fine, fibrous, and felted fibrolite appears to be the sillimanite of earliest formation; various slides show progressive stages of recrystallization, from the simple resolution of the felts into discrete rods, to the coarse growth of sillimanite prisms several millimetres in length, often as stellate aggregates enclosed in biotite and tourmaline, clusters about the edges of garnet porphyroblasts, or running in swarms and trails through mosaics of quartz (Barrow, 1893, plate XVII, fig. 1; Harry, 1958, plate I, fig. 2). Two generations of quartz may often be distinguished here: the coarse, strained quartzes belonging to the fabric of the original kyanite gneisses, and finer mosaics of granulated, recrystallized quartz containing sillimanite (Plate, fig. D).

Obvious textural relationships between sillimanite and pre-existing kyanite are difficult to find. The veinlets which contain the greatest concentrations of early formed fibrolite enclose volumes of rock with thicknesses of the order of centimetres to tens of centimetres in which little or no sillimanite can be found and in which the original kyanite-bearing gneiss is preserved almost untouched. Harry (1958, p. 408) has observed veins of sillimanite sharply cutting kyanite crystals with no sign of the inversion of the latter to the former; if pseudomorphs of sillimanite after kyanite do exist in the regional gneisses in Glen Clova, they are undoubtedly rare. In general, however, kyanite appears to be absent from those rocks in which sillimanite is abundant (i.e. greater than 15 per cent by volume) and most coarsely recrystallized.

The preservation of sillimanite in all stages of formation and recrystallization suggests that the myriad localized processes presumably trending to the end-product of a homogeneous sillimanite-bearing gneiss were incompletely synchronized; while fibrolite was just forming in one portion of a rock, earlier-formed fibrolite was recrystallizing in another. Simultaneously, no doubt, the associated minerals were also recrystallizing; textures in which coarse sillimanite is enclosed within biotite (Plate, fig. C), garnet, tourmaline, and quartz may be taken to indicate growth of these minerals either contemporaneously with, or subsequent to, the recrystallization of the sillimanite. Some rocks, however, show textures involving staurolite, kyanite, and muscovite which I consider to indicate growth of these minerals after the main period of sillimanite development—implying that recrystallization of coarse sillimanite was followed by retrogression to staurolite–kyanite zone conditions. Although this paper is mainly concerned with the origin of the sillimanite, the subjective nature of this interpretation requires that a brief description of the 'retrogressive' textures be given here.

The main evidence for post-sillimanite growth is taken to be the occurrence of euhedral staurolite prisms within both fibrolite felts and sillimanite swarms, in part apparently replacing sillimanite, in part including it (Fig. 2 A–C). Billings (1937, p. 552) has described an apparently similar case from New Hampshire in which porphyroblasts of sillimanite have been replaced by aggregates of staurolite, and has suggested that the iron required for the replacement has been provided by biotite, muscovite being formed in the process, but there is no textural evidence for such a source of iron in the Glen Clova examples. However, since the total content of staurolite in any thin section seen does not exceed some 3 per cent, the amount of iron and magnesium required would not be great, and could probably be derived from slight redistribution of elements within the individual rocks.

Associated with the retrogressive staurolite are small amounts of oriented intergrowths and outgrowths of kyanite (Fig. 2); secondary kyanite rarely occurs without staurolite, although, of course, when alone it is difficult to distinguish from early formed kyanite which persisted through the sillimanite-forming period.

Growth of retrogressive kyanite and staurolite appears to have been followed by the recrystallization of muscovite at the partial expense of the aluminium silicates. Typical of the textures taken as evidence for this stage of crystallization are the small 'corroded' relicts and droplets of kyanite and staurolite, and

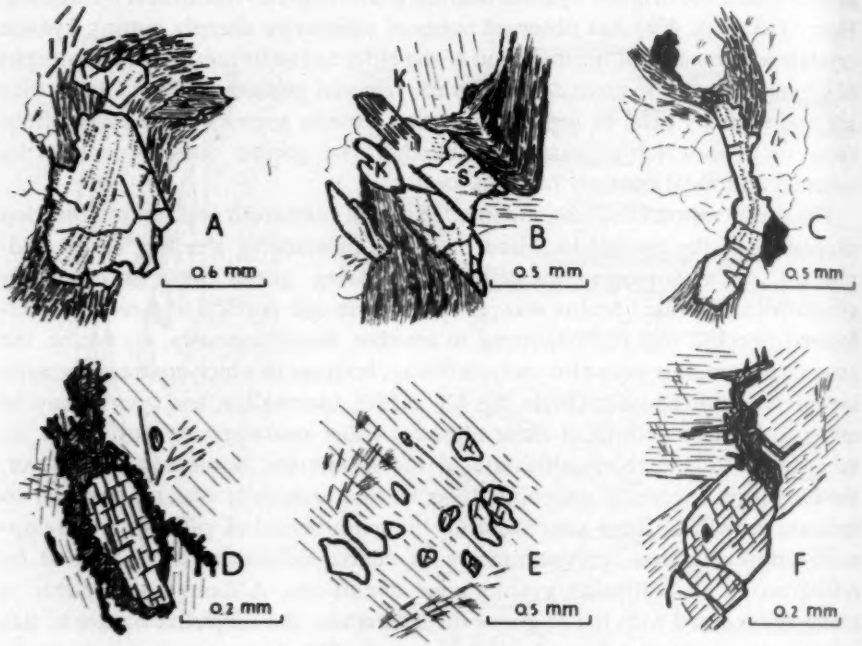

FIG. 2. Textures suggestive of post-sillimanite growth. A, staurolite (heavily outlined) in a sillimanite swarm, with trails of inclusions of sillimanite. 83039, Corrie Carlowie. B, staurolite (*S*) prisms with sharp boundaries against a fibrolite felt, and with oriented outgrowths of kyanite (*K*); (100) kyanite parallels (010) staurolite. 83014, Ben Reid. C, staurolite grain as a 'pseudomorph' of a sillimanite vein confined between areas of quartz and magnetite. Staurolite contains trails of fine inclusions; quartz grains include fine sillimanite needles. 83039, Corrie Carlowie. D, kyanite crystal surrounded by an aggregate of fine kyanite, staurolite (and sillimanite?). Enclosing muscovite flakes include needles of sillimanite. 83062, Bassies. E, droplets of kyanite (heavily outlined) and fine needles of sillimanite within a coarse flake of muscovite. 83060, Bassies. F, coarse kyanite grain from which a finer aggregate of kyanite and staurolite has grown along the boundaries between the enclosing muscovite flakes. 83062, Bassies.

the remnants of sillimanite swarms, found enclosed in muscovite plates. This growth of muscovite appears to have been related to a high activity of water and potassium in the fluid phase at the staurolite–kyanite grade, for the staurolite and kyanite relicts frequently show evidence of a third, post-muscovite regeneration: trails of fine, stubby kyanite and staurolite prisms grow from the edges of the relicts and may be traced for several millimetres along the cleavages or grain-boundaries of the enclosing muscovite (Fig. 2). Such fine 'needle' kyanite is quite abundant in some rocks, forming thorny sheaths about kyanite, sillimanite, or garnet grains, or occurring along the boundaries between quartz and

feldspar, mica, or garnet. This growth of needle kyanite and staurolite probably resulted from the migration of aluminium, silicon, and divalent ions along grain-boundaries at a stage when coarse recrystallization was no longer possible. The final mineralogical reconstructions evident in the Glen Clova gneisses are those more usually referred to as retrograde metamorphism—sporadic pseudomorphing of biotite and garnet by chlorite, and the replacement of plagioclase and aluminium silicates by fine-grained aggregates of sericitic mica, processes related to the activity of water and potassium at a very late stage of metamorphism.

THE ORIGIN OF SILLIMANITE

From the preceding description it will be apparent that the sillimanite occurrences in Glen Clova are very similar to those described from many other areas of regional metamorphism (see discussions in Tozer, 1955; Francis, 1956). The sillimanite of earliest formation occurs as haphazardly distributed fibrolite associated with biotite, and dates from a stage following the development of the main rock fabric; it shows no obvious relationship to pre-existing kyanite.

This mode of occurrence immediately raises the possibility that the sillimanite formed as a metastable phase. However, in view of the development of sillimanite in the Scottish Dalradian in a zone of regional extent as the high-grade culmination of a well-displayed sequence of progressive metamorphism, I consider this possibility to be unlikely. The superimposition of sillimanite on the fabric of a kyanite-bearing gneiss will therefore be taken as evidence that such a rock was initially metamorphosed under physical conditions within the kyanite stability field, and subsequently under conditions within the sillimanite stability field.

The phase rule dictates that two polymorphs can coexist stably only along the curve of univariant equilibrium that separates their respective stability fields. However, the presence of a foreign element which distributes itself unequally between the polymorphs introduces another component into the system and hence expands the univariant curve into a divariant band. It is well known that the structures of the aluminium silicates vary widely in their ability to accommodate trivalent ions substituting for aluminium: andalusite, for example, can accommodate more trivalent iron and manganese than can either kyanite or sillimanite. The difficulties in separating kyanite from associated sillimanite have so far prevented any study of the distribution of iron and manganese between them, although analyses in the literature suggest that ferric iron can substitute more readily in kyanite than in sillimanite. The analysis of Table 1 shows that, at least in the haematite-bearing rocks, kyanite may contain a relatively high amount of ferric iron; the possibility must therefore be kept in mind that there existed in Glen Clova a zone, of width dependent upon the oxidation ratios of the rocks concerned, within which an iron-rich kyanite was in equilibrium with an iron-poor sillimanite. However, since such a zone would be

expected to attain a significant width only in rocks of high oxidation ratio, it seems more reasonable at the present time to assume that the association of sillimanite and kyanite in Glen Clova is an unstable one.

TABLE 1

Analysis of kyanite from haematite-bearing gneiss no. 11

(Chinner, 1960, p. 187)

	Weight per cent	*Metals to 5 (O)*
SiO_2	36·56	0·99
Al_2O_3	61·80	1·96
Fe_2O_3	1·51	0·03
Na_2O	0·08	
K_2O	0·58	
	100·53	

TiO_2, MgO, CaO sought but not found. $N\gamma = 1{\cdot}732$. Included haematite was removed by grinding to a fine powder and boiling in HCl.

Certainly, the reluctance of kyanite to invert to sillimanite has been noted elsewhere (cf. Clark *et al.*, 1957), and is hardly surprising in view of the small free-energy difference between the two polymorphs [$\Delta G^\circ = 0{\cdot}3$ KCals/mole (data from Fyfe, *et al.*, 1958)]. In the vicinity of the sillimanite isograd the physical conditions, though fluctuating, can hardly have been far from the curve, or band, that separates their fields of stability; the rocks under consideration were thus probably within the zone of indifference within which the temperature overstep was insufficient to allow nucleation of sillimanite within kyanite.

The question is thus why sillimanite forms in mica. Since the muscovite–sillimanite relations are somewhat equivocal, only the growth of sillimanite in biotite will be considered here.

The triangular arrangement of early formed fibrolite within biotite flakes closely resembles that found when pyrophyllite or muscovite breaks down to mullite or diaspore (Comeforo *et al.*, 1948; Holser, 1956), or phlogopite to chlorite (Roy & Mumpton, 1958), and suggests some sort of structural control. The main features of the structure of sillimanite (Hey & Taylor, 1931) are chains of Al–O octahedra paralleling the *c*-axis, and linked together by chains of slightly distorted oxygen tetrahedra which also parallel *c*, the tetrahedrally co-ordinated cations being alternately Si and Al. In mica, the alternate sheets of Al–O octahedra and Si–O tetrahedra normal to the *c*-axis are composed of hexagonal arrays, the 'sides' of each hexagon (each composed of a pair of octahedra or a pair of tetrahedra) being oriented parallel to [010] and to the two pressure-figure directions at 60° to this. Nucleation and growth of sillimanite on these trigonally arranged octahedra or tetrahedra could thus lead to a

triangular arrangement with the same orientation in the host biotite, as is actually found (Plate, fig. B).

TABLE 2

Composition of a Glen Clova biotite calculated to 24 (O, OH)

(Chinner, 1960, table 5, no. 1)

Si	5·25	Fe^{3+}	0·15	Ca	0·00
Al (4)	2·75	Fe^{2+}	2·34	Na	0·14
Al (6)	0·87	Mn	0·01	K	1·66
Ti	0·34	Mg	2·00	OH	3·83

The Glen Clova biotites are not, of course, ideal micas. The analysis in Table 2 indicates that aluminium occurs in less than one-sixth of the octahedral sites, although one in three of the tetrahedral sites is aluminium-bearing. The question thus arises as to whether the nucleation process was one involving breakdown of the mica, the silicon and aluminium rearranging themselves within the chains of octahedra and tetrahedra, or whether it was a case of oriented growth (epitaxis), the silicon and aluminium being derived from outside the mica. Cases of epitaxial growth on mica of substances so chemically different as magnetite, staurolite, garnet, and even ammonium iodide are very well known (cf. Buckley, 1951). On the other hand, instability of biotite is suggested by observations not only in Glen Clova, but from many other similar occurrences (Watson, 1948; Tozer, 1955) where sillimanite appears to have been in the process of replacing the mica, although in Glen Clova the apparent recrystallization of coarse sillimanite with biotite (Plate, fig. C) suggests that any such instability was only temporary.

From the chemical viewpoint, the derivation of sillimanite wholly from biotite seems rather unlikely. Assuming, in the first instance, that sillimanite could arise by the complete breakdown of an iron-rich biotite in the haematite-free Glen Clova gneisses, an equation is obtained:

$$\underset{\text{biotite: 600 c.c.}}{(OH)_8K_4Mg_4Fe_5Al_8Si_{10}O_{40}} \rightarrow \underset{\substack{\text{sillimanite}\\ 200\text{ c.c.}}}{4Al_2SiO_5} + \underset{\substack{\text{quartz}\\ 226\text{ c.c.}}}{10SiO_2} + (H_8K_4Mg_4Fe_5O_8)$$

It is very difficult to tell whether quartz is associated with the earlier-formed fibrolite, but the more recrystallized sillimanites do occur with considerable quantities of mosaic quartz. The relative quantities of the two minerals cannot be accurately determined in thin section since the sillimanite with its high refractive index will be normally grossly over-estimated against the lowly refracting quartz; nevertheless, the association could suggest that an equation of this type was operative. The most serious problem, however, is the fate of the elements K, Na, Mg, and Fe which would be liberated if biotite were to break down to sillimanite in this manner. Francis (1956), in discussing the same problem, suggested that the iron molecule of the biotite breaks down first,

leaving a biotite enriched in magnesium, and precipitating iron as magnetite and potassium as microcline. While, however, iron ores appear to be a common associate of the fibrolite of Kildonan, Scotland (Watson, 1948) and in the Glen district of Donegal (Tozer, 1955), their abundance in Glen Clova is controlled by the pre-existing oxygen content of the rocks, and potash-feldspar is absent from the aluminium silicate-bearing assemblages. A series of four biotites analysed from haematite-free rocks containing sillimanite in varying stages of recrystallization (Table 3) shows no significant change in MgO/FeO ratio: the 'decolorization' of biotites associated with fibrolite which was noted by Tozer and interpreted by Francis as evidence of magnesium enrichment is probably due to superimposition, in thin section, of fibrolite mats on the mica, reducing the effective thickness of the section of biotite and hence the intensity of its pleochroism.

TABLE 3

Molecular $(MgO \times 100)/(MgO+FeO)$ *ratios of biotites from haematite-free gneisses*

(Complete analytical data in Chinner, 1960, table 5)

Rock no.	*Sillimanite content*	*mol.* $\frac{(MgO \times 100)}{(MgO+FeO)}$ *of biotite*
3	no sillimanite	48
1	12 per cent incipient fibrolite	46
5	17 per cent, mainly matted fibrolite, some coarse sillimanite	48
4	31 per cent, coarse sillimanite	45
2	32 per cent coarse sillimanite, recrystallized with quartz and biotite	45

The sole alternative, if one is to regard the sillimanite as being wholly derived from biotite, is to postulate the complete removal of magnesium, iron, and alkalis from the system, suggesting, in fact, alumina metasomatism by subtraction. This postulate involves metasomatic losses of a high order. Thus, if a rock contains 20 per cent by weight of sillimanite derived from biotite, the original rock (since the amount of sillimanite formed in the equation is only one-third that of the parent biotite, and a decrease in volume of the rock is involved) must have contained at least 40 per cent of biotite; since the biotites of the haematite-free rocks contain some 20 per cent of FeO and 10 per cent of MgO, the metasomatic removal of these constituents would involve a loss of the order of 8 per cent FeO and 4 per cent MgO of the total rock composition. Analyses of rocks no. 2, 4, and 5 (Chinner, 1960, table 1), all of which contain more than 20 per cent by weight of sillimanite, are not at all unusual for pelitic rocks, and give no suggestion that any such spectacular metasomatism was involved in their formation. Sillimanite is thus unlikely to have arisen from the breakdown of

biotite alone; the impression that sillimanite replaces biotite may therefore be illusory.

This, of course, does not preclude the possibility that nucleation and growth of sillimanite was aided by some form of temporary instability in the mica. In addition to the parameters of temperature and total pressure, iron-bearing biotites are very sensitive to changes in the partial pressures of water and oxygen (Wones & Eugster, 1959). Small changes in the activity of oxygen and water during metamorphism might well produce instability of particular biotite compositions (without producing instability of biotite in general) which would be relieved by a change in the composition of the biotite, or by a reversion of μO_2 and μH_2O to approximately their original values. During the period of 'temporary' instability thus produced, the activated state of the biotite concerned would provide very favourable conditions for the nucleation of sillimanite. That such an effect may have been operative is suggested by the observation that sillimanite is less frequently associated with the magnesian biotites of the haematite-bearing gneisses than with the more iron-rich biotites of the haematite-free gneisses. Both types of biotite are of the same structural variety, 1M, so the difference in their behaviour may be accounted for by the greater sensitivity of the iron-rich biotites to minor fluctuations of μO_2 during metamorphism.

None the less, it seems likely that the nucleation effect was dominantly epitaxial, and that the greater bulk of the alumina and silica required for sillimanite growth must be sought from outside the biotite. The vein-like nature of many sillimanite occurrences of this type has suggested to some authors (cf. Watson, 1948) the possibility of the introduction of alumina derived from granitic magma or from migmatitic processes. In Glen Clova, the concept of alumina introduction for a rock containing, say, 20 per cent sillimanite, encounters the same chemical difficulties involved in the 'subtraction' theory outlined above. It would, in effect, suggest the introduction of silica and alumina into a rock of unusual composition to produce a rock of quite normal pelitic composition.

These difficulties, however, would be minimized if it were possible for aluminium and silicon dissolved from unstable kyanite to be transferred through the medium of the fluid phase out to sillimanite nuclei forming in nearby flakes of mica (cf. Francis, 1956, p. 358). Such a process, being dependent upon rates of diffusion or of movement in the fluid phase, would be localized in its efficacy, and would account for the limited extent and haphazard nature of sillimanite veining; it would also account for the general rarity of kyanite in those rocks where sillimanite is more abundant, evenly developed, and more coarsely crystallized. Since presumably any biotite would be capable of forming sillimanite nuclei by epitaxis, whether or not its host rock was originally aluminous enough to develop kyanite, the movement of an aluminium-bearing fluid phase from pelitic beds in which kyanite was dissolving could give rise to the growth of sillimanite in the kyanite-free, less pelitic gneisses interbedded with them.

The generally vein-like distribution of sillimanite in both pelitic and semipelitic gneisses certainly suggests the existence during metamorphism of channelways, possibly representing the loci of shearing movements during deformation, along which the fluid phase could move with relative ease. Along such channelways fluctuations in μO_2 and μH_2O might be greater, thus providing the optimum conditions for the nucleation of sillimanite in biotite. The small rock volumes in which kyanite has remained apparently unaltered since the early stages of metamorphism, and in which little or no sillimanite has formed within biotite, may thus represent volumes which had no effective connexion with the channelways of fluid movement. Their preservation would thus suggest that diffusion of aluminium and silicon within the intergranular fluid was of limited importance. This suggestion is in harmony with previous conclusions (Chinner, 1960, p. 211) that the preservation, or partial preservation, of original differences in the ferrous/ferric ratios in the Glen Clova gneisses was the result of the limited capacity of the intergranular fluid phase for transfer of hydrogen and oxygen.

It must be emphasized here that in many areas where sillimanite has apparently formed in a manner similar to that in Glen Clova, and where potash feldspar is likewise absent from pelitic compositions, there is no evidence that the rocks concerned ever contained kyanite (cf. Watson, 1948; Tozer, 1955). The possibility arises that in such cases sillimanite represents the alumina excess which would result from the partial fusion of quartz, plagioclase, and muscovite aggregates in the formation of low melting-point liquids within the migmatite zones (cf. Tuttle & Bowen, 1958). In the absence of quantitative data however, the question remains largely conjectural.

CONCLUSIONS

The role of biotite in the development of sillimanite at the sillimanite isograd in Glen Clova appears to have been that of a nucleating agent, the trigonally arranged chains of oxygen tetrahedra and octahedra in the alternate mica sheets acting as nuclei for growth of the octahedral and tetrahedral chains that constitute the sillimanite structure. Nucleation was probably dominantly epitaxial, the alumina and silica for sillimanite growth being mainly derived from unstable kyanite and transferred to the sillimanite nuclei through the medium of the fluid phase. Although temporary instability of particular biotite compositions may have aided the nucleation, it seems unlikely that much sillimanite was formed by actual replacement of the mica, or that any extensive breakdown of biotite was involved. Whether or not additional alumina may be derived by the fusion of muscovite will no doubt become clearer when more is known of the origin of the migmatitic gneisses in the high-grade zones of the Scottish Highlands.

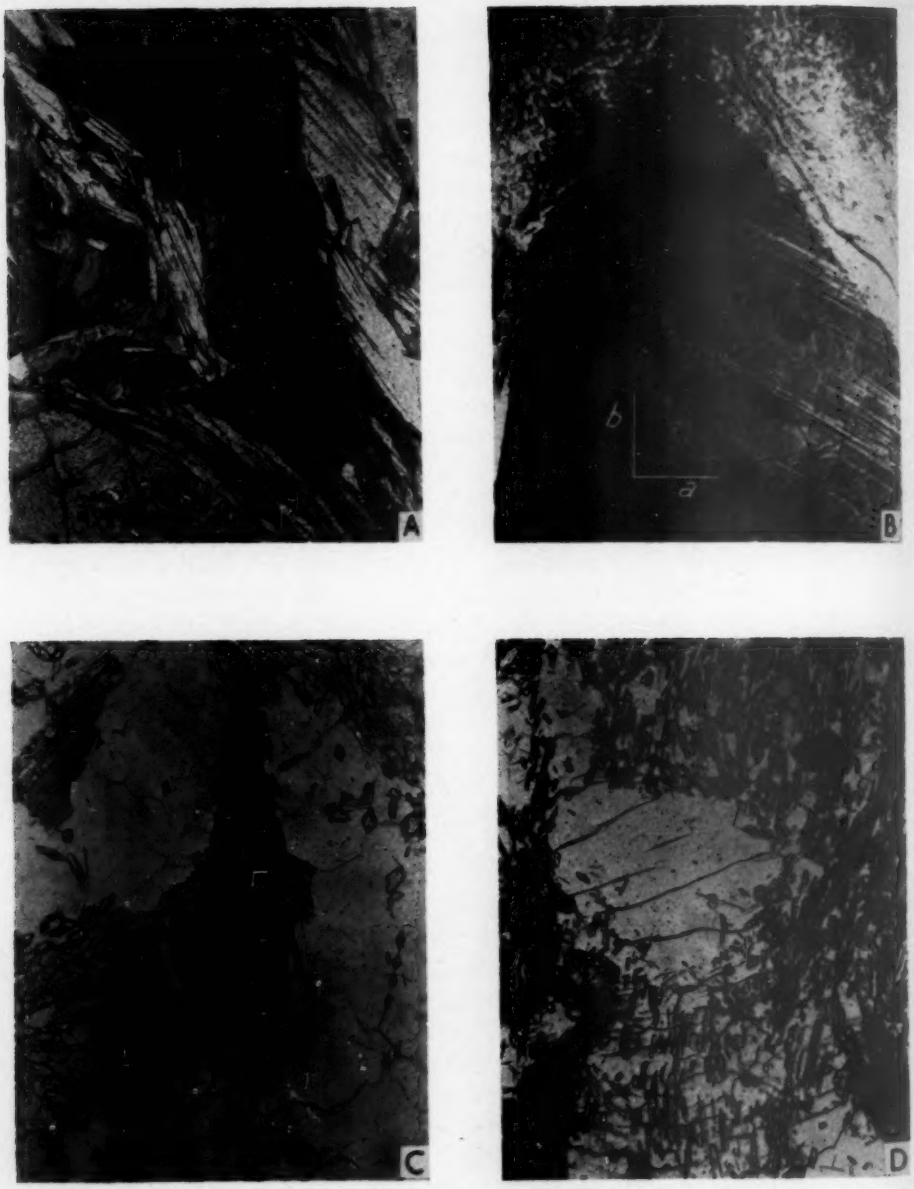

G. A. CHINNER

ACKNOWLEDGEMENTS

I am grateful to Mr. D. McKie, Dr. S. O. Agrell, Professor D. S. Coombs, and Professor C. E. Tilley for reading and discussing the manuscript.

REFERENCES

Barrow, G., 1893. On an intrusion of muscovite–biotite gneiss in the south-eastern Highlands of Scotland, and its accompanying metamorphism. *Quart. J. geol. Soc. Lond.* **49**, 330–54.

Billings, M. P., 1937. Regional metamorphism of the Littleton–Moosilauke area, New Hampshire. *Bull. geol. Soc. Amer.* **48**, 463–65.

Buckley, H. E., 1951. *Crystal growth.* New York: Wiley.

Chapman, C. A., 1952. Structure and petrology of the Sunapee Quadrangle, New Hampshire. *Bull. geol. Soc. Amer.* **63**, 381–426.

Chinner, G. A., 1960. Pelitic gneisses with varying ferrous/ferric ratios from Glen Clova, Angus, Scotland. *J. Petrol.* **1**, 178–217.

Clark, S. P., Robertson, E. G., & Birch, F., 1957. Experimental determination of kyanite–sillimanite equilibrium relations at high temperatures and pressures. *Amer. J. Sci.* **255**, 628–40.

Comeforo, J., Fischer, R., & Bradley, W., 1948. Mullitisation of kaolinite. *J. Amer. Ceram. Soc.* **31**, 254–9.

Francis, G. H., 1956. Facies boundaries in pelites at the middle grades of regional metamorphism. *Geol. Mag. Lond.* **93**, 353–68.

Fyfe, W. S., Turner, F. J., & Verhogen, J., 1958. Metamorphic reactions and metamorphic facies. *Mem. geol. Soc. Amer.* **73.**

Harry, W. T., 1958. A re-examination of Barrow's older granites in Glen Clova, Angus. *Trans. roy. Soc. Edinb.* **63**, 393–412.

Hey, J. S., & Taylor, W. H., 1931. The co-ordination number of aluminium in the aluminosilicates. *Z. Krystallogr.* **80**, 428–41.

Holser, W. T., 1956. Hydrothermal alteration of muscovite in steam gage-glasses. *Amer. Min.* **41**, 799–803.

Roy, R., & Mumpton, F. A., 1958. Weathering studies: 2. A note on the conversion of phlogopite to septechlorite. *J. Geol.* **66**, 324–6.

Tozer, C. F., 1955. Sillimanite in the Glen district, Co. Donegal. *Geol. Mag. Lond.* **92.** 310–20.

Tuttle, O. F., & Bowen, N. L., 1958. Origin of granite in the light of experimental studies in the system $NaAlSi_3O_8$–$KAlSi_3O_8$–SiO_2–H_2O. *Mem. geol. Soc. Amer.* **74.**

Watson, J., 1948. Late sillimanite in the migmatites of Sutherland. *Geol. Mag. Lond.* **85**, 149–62.

Wones, D. R., & Eugster, H. P., 1959. In Annual Report of the Director, Geophysical Laboratory for 1958–9. *Yearb. Carneg. Instn.* **58**, 127–32.

EXPLANATION OF PLATE

Fig. A. Contorted fibrolite felt intergrown with biotite. 83007, Ben Reid, ×20.

Fig. B. Basal plate of biotite showing sillimanite fibres oriented parallel to the pressure-figure directions. The crystallographic directions *a* and *b* (= [010]) are indicated on the figure. Dark circular areas are haloes about radioactive inclusions. 83007, Ben Reid, ×100.

Fig. C. Recrystallized sillimanite prisms included in biotite and quartz. 83156, Craig Rennet, ×60.

Fig. D. Sillimanite prisms recrystallized with mosaics of quartz. In the centre of the figure a quartz grain remains almost inclusion-free. 83156, Craig Rennet, ×30.

Compositions and Structural States of Anhydrous Mg–Cordierites: A Re-investigation of the Central Part of the System $MgO–Al_2O_3–SiO_2$

by W. SCHREYER *and* J. F. SCHAIRER

Geophysical Laboratory, Carnegie Institution of Washington, Washington, D.C., U.S.A.

ABSTRACT

The central portion of the system $MgO–Al_2O_3–SiO_2$ has been studied with the aim of determining the range of solid solution, as well as the stability limits of the various structural states of the ternary compound cordierite. The previously suggested limited solid solution between cordierite of the composition $2MgO \cdot 2Al_2O_3 \cdot 5SiO_2$ (2:2:5) and SiO_2 is now believed to exist only metastably. Between 800° and 1,300° C the composition of cordierite was found to be invariably $2MgO \cdot 2Al_2O_3 \cdot 5SiO_2$. Above 1,300° C, however, there is evidence for the existence of limited solid solution in cordierite (2:2:5) toward a theoretical compound 'Mg–beryl' (3:1:6). The existence of cordierite solid solution at liquidus temperatures has an important bearing on the melting relations of many compositions within the system. Because of this solid solution the courses of crystallization of melts consisting of normative cordierite (2:2:5) and small amounts of $MgSiO_3$, for example, have to follow parts of the boundary curve between the cordierite and spinel fields with these two phases coprecipitating over a limited range of temperatures. The dividing line between compositions which complete their crystallization at the ternary eutectic forsterite+protoenstatite+cordierite+liquid, 1,364° ±3° C, and those which complete their crystallization at the ternary eutectic protoenstatite +cordierite+tridymite+liquid, 1,355° ±3° C was formerly considered to be the join $MgSiO_3$–cordierite (2:2:5). Because of solid solution in cordierite coexisting with liquid this dividing line is displaced slightly in the direction toward more siliceous bulk compositions. Furthermore, the temperature maximum along the boundary curve cordierite+protoenstatite+liquid cannot lie at the intersection of this boundary curve with the join $MgSiO_3$–2:2:5, but with the tie line $MgSiO_3$–cordierite$_{ss}$. The position of this temperature maximum thus moves closer to the ternary eutectic protoenstatite+cordierite+tridymite+liquid. Temperatures and compositions of some of the invariant points in the system have been redetermined.

On the basis of Miyashiro's distortion index, the structural states of the cordierites synthesized are subdivided into high-cordierite, intermediate-state cordierites, and 'low'-cordierites. High-cordierite was obtained in all compositions at any temperature as the first form of cordierite to crystallize. With continued heating at appropriate temperatures, this metastable high-cordierite was found to go over gradually through intermediate-state cordierite to the stable form 'low'-cordierite. The rate of this transition varies with bulk composition and generally increases with temperature. In contrast to this metastable behaviour are the stable relations among the polymorphs, which were found to be a function of temperature as well as total bulk composition of the cordierite-bearing mixtures. In bulk compositions with low ratios Al_2O_3/SiO_2 ($\lesssim$ 1:5) high-cordierite was not found to be a stable phase at any temperature; in bulk compositions with intermediate Al_2O_3/SiO_2 ratios high-cordierite is stable only in the presence of much liquid, whereas in those with high Al_2O_3/SiO_2 ratios ($>$ 1:2·5) a stable transition from 'low'-cordierite to high-cordierite takes place at subsolidus temperatures. This relationship is considered indirect evidence for Al/Si ordering being the principal cause of the transition from high- to 'low'-cordierite.

Owing to solid solution the transition from 'low'- to high-cordierite in the presence of liquid, for certain bulk compositions with intermediate Al_2O_3/SiO_2 ratios, takes place in a

[Journal of Petrology, Vol. 2, Part 3, pp. 324–406, 1961]

manner which cannot be described by a varying distortion index. For this reason a new variable, the intensity index, defined as $i = I_{(611+421)}/I_{(131)}$, is introduced, which is zero for high-cordierite solid solutions and 1·15–1·35 for 'low'-cordierite.

The sensitive dependence of the structural behaviour of cordierite on its chemical environment excludes the possibility of using this property as a geologic thermometer to a very large extent. Experimental investigations on cordierite-bearing synthetic 'haplobuchites', as well as on a fused shale from Bokaro coalfield in India, revealed that high-cordierite is not a stable phase for these bulk compositions at any temperature. Natural cordierites with structural states close to, or identical with high-cordierite, which have been found in rocks formed at high temperatures (buchites, &c.), are believed to be metastable products of crystallization. They are preserved because the duration of heating was not sufficient to produce the stable low-temperature form. Petrographic and X-ray studies show that there is a close relationship between the distortion index and the degree of perfection of the crystal form of cordierites in these rocks. On the basis of these results it seems possible to use the structural state of cordierites, at least in a qualitative manner, as a geologic timer for the crystallization history of the enclosing rock.

CONTENTS

page

A. INTRODUCTION 326

B. NOMENCLATURE 327

C. EXPERIMENTAL PROCEDURE 329

1. Preparation of mixtures
2. Crystallization of glasses
3. Quenching runs
4. Evaluation of results

D. THE EQUILIBRIUM DIAGRAM OF THE SYSTEM MgO–Al_2O_3–SiO_2 331

E. CRYSTALLINE PHASES 336

1. Products of metastable crystallization
2. Cristobalites
3. Tridymite
4. Mullite
5. Sapphirine
6. Spinel
7. Forsterite
8. Pyroxenes of the composition $MgSiO_3$

F. THE COMPOSITION OF THE TERNARY COMPOUND, CORDIERITE 344

1. Subsolidus investigations
   (*a*) Metastable solid solutions
   (*b*) Stable subsolidus composition of cordierite
2. Liquidus investigations

G. REFINEMENT OF THE EQUILIBRIUM DIAGRAM OF THE SYSTEM MgO–Al_2O_3–SiO_2 355

H. MELTING RELATIONS IN THE SYSTEM MgO–Al_2O_3–SiO_2 360

I. STRUCTURAL CHANGES OF THE TERNARY COMPOUND CORDIERITE 363

1. Characterization of the polymorphs encountered
2. Low-temperature transition of metastable high-cordierite
3. Stability range of high-cordierites
   (*a*) Cordierite composition 2:2:5
   (*b*) Influence of liquid on the transition
   (*c*) Compositions on the line 2:2:5–SiO_2, or very close to it
   (*d*) Compositions on the line 2:2:5–$MgSiO_3$
   (*e*) Compositions on the line 2:2:5–forsterite
   (*f*) Compositions in the triangle 2:2:5–$MgSiO_3$–SiO_2
   (*g*) Compositions on the line 2:2:5–spinel
   (*h*) Composition on the line 2:2:5–mullite
4. Influence of various rates of cooling on the structural state of cordierites
5. Nature of the structural changes in cordierite and their dependence on the total bulk composition

J. GEOLOGICAL SIGNIFICANCE OF THE STRUCTURAL STATES OF NATURAL CORDIERITES, PARTICULARLY IN BUCHITES 393

1. Difficulties in the use of the structural state of cordierite as a geologic thermometer
2. Compositions of buchites and related cordierite-bearing rocks
3. Experimental results on synthetic 'haplobuchites'
4. Experimental investigation of a fused shale from Bokaro coalfield, India
5. Petrographic and X-ray studies on cordierites in fused shales, &c.
6. The use of the structural state of cordierite as a geologic timer

A. INTRODUCTION

THE primary impetus for the present investigation was given by the recent discovery of several polymorphic forms of the mineral cordierite. The first workers in the system MgO–Al_2O_3–SiO_2, Rankin & Merwin (1918), already distinguished an unstable or μ-form and a stable or α-form of the ternary compound $2MgO \cdot 2Al_2O_3 \cdot 5SiO_2$ which exhibited different refractive indices. Karkhanavala & Hummel (1953) indicated that the μ-form had a structure similar to that of β-spodumene. These authors defined β-cordierite as the stable low-temperature phase with a cordierite structure synthesized hydrothermally by Yoder (1952), from a composition close to $2MgO \cdot 2Al_2O_3 \cdot 5SiO_2$,[1] below 830° C. This low-temperature phase had been distinguished by Yoder (1952) from what was believed to be the high-temperature or α-form synthesized above 830° C, on the basis of its higher refractive indices. One year later, in a brief note Miyashiro & Iiyama (1954), and in more detail A. Miyashiro, Iiyama, Yamasaki, & T. Miyashiro (1955), reported that on the basis of X-ray investigations both the synthetic α- and β-cordierites showed hexagonal symmetry, in contrast to the bulk of natural cordierites which are orthorhombic or, according to these authors, possibly monoclinic. The only natural material identical with the synthetic α-form was found to be a cordierite from fused sediments of the Bokaro coalfield in India previously mentioned by Fermor (1924) and described by Venkatesh (1952, 1954). Miyashiro and co-workers considered this to be a new mineral species and called it indialite. Later Miyashiro (1957) discovered that indialite is connected with orthorhombic 'perdistortional' cordierite by a series of intermediate structural states, which he named 'subdistortional' cordierites. He also confirmed the fact previously stated by Sugiura & Kuroda (1955*a*) that cordierites could be converted into indialites by heating them to temperatures close to their incongruent melting-point. Lastly, Iiyama (1958) published data which seemed to indicate that the transformation of the β- or low-temperature form into the α- or high-temperature form corresponds to a dehydration.

A great deal of the work just reported was done on natural materials containing various amounts of iron and manganese which, during the heating experiments, may have changed their oxidation states so as to result in changes of physical properties of the minerals. Furthermore, the influence of alkalis

[1] Yoder's (1952) investigations on the stability of cordierite were not done with material of the exact composition $2MgO \cdot 2Al_2O_3 \cdot 5SiO_2$ but with a composition containing 2 wt per cent forsterite and 98 per cent $2MgO \cdot 2Al_2O_3 \cdot 5SiO_2$, prepared by J. F. Schairer (Yoder, personal communication).

(Folinsbee, 1941) on the optical and X-ray properties of natural cordierites is not known well enough to neglect its role in polymorphism. In order to approach the problem of polymorphism in cordierite more systematically it seemed desirable, therefore, to go back to the simplest system, in which cordierite-like phases have been synthesized in the dry way, i.e. without any water: this is the system MgO–Al_2O_3–SiO_2.

A study of the paper by Rankin & Merwin (1918) on the system MgO–Al_2O_3–SiO_2, however, brings up a problem previously not considered in connexion with the polymorphism of cordierite. Rankin and Merwin indicated the possibility of solid solution in the α-form of their ternary compound ranging from $2MgO \cdot 2Al_2O_3 \cdot 5SiO_2$ (2:2:5) toward $MgO \cdot Al_2O_3 \cdot 3SiO_2$ (1:1:3). Hummel & Reid (1951) extended this possible solid solution in cordierite even as far as 1:1:4. Furthermore, Iiyama (1955) indicated that indialites prepared in the system MgO–Al_2O_3–SiO_2 may range in composition from 2:2:5 almost all the way to a hypothetical 'magnesium beryl' (3:1:6).

Thus the first goal of the present investigation was the determination of the range of compositional variations of the ternary compound cordierite. The second goal was to pursue its polymorphic changes and determine the temperatures of structural transitions, taking into account all the possibilities of solid solutions. A third goal which developed during this study was to determine the structural changes of cordierites when in mixture with other crystalline phases of the system, for instance $MgSiO_3$, forsterite, siiica, &c. The project also involved a restudy of the melting relations of the ternary compound cordierite and adjoining compositions, which led to a more accurate fixation of temperatures and compositions of some of the invariant points in the system MgO–Al_2O_3–SiO_2. Finally, an evaluation of the experimental results on the structural transitions of cordierite in more complex natural cordierite-bearing rocks was attempted.

This study was inaugurated by the writers at the Geophysical Laboratory early in 1958. Progress reports have been published in the Annual Reports of the Director of the Geophysical Laboratory, Carnegie Institution of Washington Year Books Nos. 57 (pp. 197–9, 1958), 58 (pp. 98–100, 1959), and 59 (pp. 85–90, 1960).

B. NOMENCLATURE

It was found, in the course of this investigation, that the experimental results on the structural changes of the ternary compound cordierite could be described more suitably by using a nomenclature different from the one introduced by Karkhanavala & Hummel (1953) and modified by Miyashiro and co-workers in later years. Hydrothermal studies on synthetic Mg-cordierites (Schreyer & Yoder, 1960) have indeed confirmed that the alleged high–low inversion of cordierite is due to a change of the water content of the mineral and is thus non-polymorphic. The prefixes 'high' and 'low', as used by Miyashiro *et al.* (1955)

in describing this relationship, are thus not justified. It was permissible, therefore, to use these prefixes for the polymorphic changes of the ternary compound cordierite which were encountered in this study and which are in many respects very similar to the structural transitions of the feldspars, for example high- and low-albite.

Although the determination of the various structural states of cordierites encountered in our work is based on the same X-ray measurement which prompted Miyashiro (1957) to distinguish between indialite, subdistortional cordierites, and perdistortional cordierites, we found it more convenient to subdivide the range of the distortion index Δ[1] as shown diagrammatically in Fig. 1.

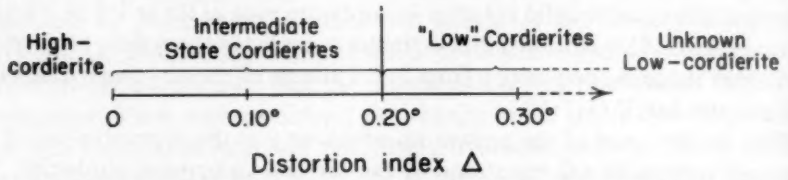

FIG. 1. Relations between the structural states of cordierite as a function of the distortion index Δ.

The hexagonal form previously named indialite ($\Delta = 0$) is for many bulk compositions the modification stable at the highest temperatures, and is therefore called *high-cordierite*. Similarly, the form with the largest Δ value, i.e. the greatest deviation from hexagonal symmetry is called *low-cordierite*. Since the greatest deviation from hexagonal symmetry, however, is still a matter of uncertainty, and since it may vary with the composition of the cordierite, a more or less artificial dividing line was drawn at a Δ value of 0·20°. Cordierites exhibiting this or a higher Δ value are defined as '*low*'-*cordierites* although they may not have reached their 'lowest' possible structural state. Cordierites with $0 < \Delta < 0{\cdot}20°$ are called *intermediate-state cordierites*. The choice of the dividing line at 0·20° is principally based on the experimental data to be reported in later sections of this paper.

The main advantage of this new nomenclature over the previously accepted one is that it retains the name cordierite as a collective term for the whole group, which had no name in Miyashiro's (1957) terminology. It is thus again possible to identify synthetic or natural material as cordierite without implication of a particular structural state, which can only be determined by detailed X-ray or optical methods and which might not have bearing on the particular problem.

[1] The distortion index was defined by Miyashiro (1957) as

$$\Delta = 2\theta_D - \frac{2\theta_A + 2\theta_B}{2},$$

where $2\theta_A$, $2\theta_B$, and $2\theta_D$ indicate the Bragg angles, in degrees, of peaks *A*, *B*, and *D*, respectively, of a cordierite powder diffraction pattern for copper $K\alpha_1$ radiation. In an independent paper, Iiyama (1956) has indexed these three peaks as follows: $A = 511$, $B = 421$, $D = 131$.

C. EXPERIMENTAL PROCEDURE

1. *Preparation of mixtures*

The compositions investigated were prepared from the following source materials: MgO (periclase) from J. T. Baker Co., lot No. 82735, containing about 0·05 per cent alkalis, ignited at 1,500° C for 1 h; Al_2O_3 (corundum), T61 (free from Fe_2O_3) from the Aluminum Company of America, ignited at 1,300° Cr of 3 h. As a source of SiO_2 specially purified quartz from Lisbon, Maryland, with total impurities of 0·02 wt per cent (after treatment with hydrofluoric and sulphuric acid) was used. It was previously heated to 1,520° C for 2 h, crushed, and dried at 1,200° C. By this means about one-half of the material was converted into low-cristobalite. It is to be stated that these starting materials are not of the ideal purity but are the best materials available. Their deviations from the ideal composition certainly represent one source of error in this work.

Well mixed powders (10 or 15 g) of the three components in the proportions calculated were melted together in air in platinum crucibles using a platinum-wound resistance furnace at temperatures between 1,500° and 1,570° C. Owing to the refractoriness of the three oxides, particularly Al_2O_3, from six to nine fusions of approximately 12 hours' duration were required to obtain liquids free from any undissolved material. The melts were quenched to glasses, the homogeneity of which was checked under the microscope by determining the uniformity of their refractive indices by means of the immersion method (accuracy $\pm 0{\cdot}003$). As a sort of 'stirring in the solid state' the partly melted charges were crushed between the fusions in a steel mortar with subsequent removal of the contaminating steel dust by means of a magnet. There is evidence from the slightly greenish-yellow colours of the glasses that the mixtures pick up small amounts of iron during their preparation, the reason being that the magnet cannot remove the steel dust quantitatively from the glass powder. Fairbairn & Schairer (1952) report an average amount of 0·15 wt per cent Fe_2O_3 contaminating the haplogranite glass, which was prepared at the Geophysical Laboratory by using the same technique. An alkali determination, kindly made by P. M. Orville with a flame photometer, on one of the compositions prepared showed a maximum of 0·05 wt per cent total alkalis (Na_2O+K_2O) with Na_2O prevailing considerably.

2. *Crystallization of glasses*

Before proceeding with quenching runs the glasses were crystallized in pot furnaces at various subsolidus temperatures for various lengths of time. This was necessary to prevent the formation of metastable assemblages during the quenching runs, but also yielded valuable information about the sequence of crystallization of the various compositions. Because of the primary formation of metastable phases, heating periods ranging from about 2 weeks to about 2 months were required. Heating of large lumps or cakes of uncrushed glass, for

example of cordierite composition, led to the formation of large single crystals of cordierite which, however, were full of inclusions of spinel, a pyroxene, and mullite, which should not have formed under equilibrium conditions. Even on longer heating these phases persisted. In order to prevent the formation of these non-equilibrium assemblages, the glasses had first to be crushed to fine powders and devitrified at low temperatures (~1,000° C). Subsequently, the temperature was raised stepwise to the optimum value of crystallization, which lies about 50° below the various solidus temperatures.

3. *Quenching runs*

To investigate melting relations and precise conditions of polymorphic changes, from 30 to 50 mg of the crystalline materials were sealed in Pt envelopes and run in quenching furnaces at a series of temperatures for various lengths of time. Three or four Pt envelopes, separated by ceramic rings, were run simultaneously. This involves a thermal gradient from the outer to the inner envelopes of less than 2° C. The temperatures were measured by means of Pt–Pt 90 Rh 10 thermocouples which were frequently calibrated at fixed points defined in degrees Centigrade as follows: the melting-point of diopside (1,391·5° C), the melting-point of pseudowollastonite (1,544° C). Temperatures were controlled automatically with motor-driven regulators motivated by the resistance of the platinum winding of the furnace. In runs of a week or more in duration, at 1,400° C and above, the EMF changes of the thermocouple (calibrated at the diopside point before and after the run) were appreciable, so that the true temperature of the furnace kept creeping up to higher values. Around 1,450° C the average rate of temperature increase was found to be from 5° to 8° during 4 weeks. Quenching was achieved by dropping the charges instantaneously into a dish of mercury (mercury quench). If this was not possible, they were pulled out of the furnace and cooled in a stream of cold air (air quench). In a few cases it was desirable to let the charges cool slowly by shutting off the power to the furnace. The cooling curve was determined by frequent temperature readings (Fig. 2).

4. *Evaluation of results*

After having recorded the consistency of the charges after the runs (loose powder, fritted or glazed cake, &c.), they were crushed and examined under the petrographic microscope. Furthermore, smear mounts were made and run for powder X-ray diffraction patterns over a range from 50° to 6° 2θ for copper $K\alpha$ radiation at a scanning speed of 1° per minute. In many cases it was only by this means that a proper identification of the crystalline phases was achieved. For distinction of the polymorphs of the ternary compound it was necessary to run several powder patterns over the critical area between 29° and 30° 2θ at a scanning speed of ¼° per minute.

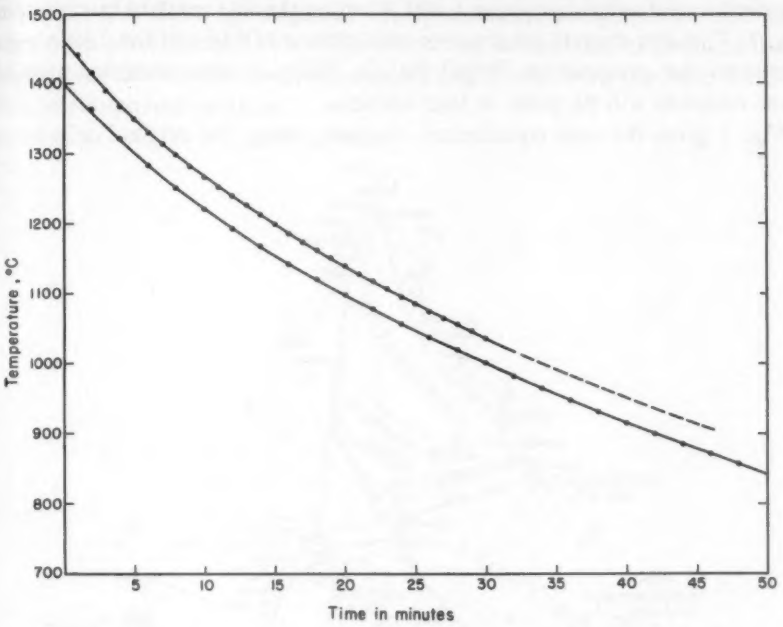

FIG. 2. Cooling rate of quenching furnace determined for two different initial temperatures.

D. THE EQUILIBRIUM DIAGRAM OF THE SYSTEM MgO–Al_2O_3–SiO_2

The original equilibrium diagram of the system MgO–Al_2O_3–SiO_2 of Rankin & Merwin (1918) was revised by Bowen & Greig (1924), who replaced the binary compound sillimanite by mullite. Greig (1927) added the two-liquid field near the SiO_2 corner, and Schairer (1942) changed the temperature of the binary eutectic mullite–cristobalite from 1,545° to 1,595°±10° C. Foster (1950 *a*, *b*) suggested tentatively, and Keith & Schairer (1952) determined precisely, the stability field of a second ternary compound, sapphirine. According to Foster (1951) the stable pyroxene at liquidus temperatures is protoenstatite.

As a result of our present study, certain refinements were made concerning compositional variations of the ternary compound cordierite, temperatures and compositions of some of the ternary invariant points and of certain temperature maxima, and the locations of some of the boundary curves. Anticipating the results of the section on the composition of the ternary compound cordierite, it was found that the composition of cordierite under equilibrium conditions below 1,300° C is $2MgO \cdot 2Al_2O_3 \cdot 5SiO_2$. There is no stable solid solution in cordierite in any direction within the system MgO–Al_2O_3–SiO_2 between 1,300° C and the lowest temperature at which the glasses could be crystallized, i.e. about 800° C. However, there are indications of metastable cordierite solid solutions in at least three directions within the diagram, as well as of stable

cordierite solid solutions above 1,300° C along the line marked by cross-bars in Fig. 3. This line depicts progressive substitution of Mg+Si for 2Al in the cordierite of the composition $2MgO \cdot 2Al_2O_3 \cdot 5SiO_2$. A more detailed analysis of these relations will be given in later sections.

Fig. 3 gives the new equilibrium diagram, using the original orientation of

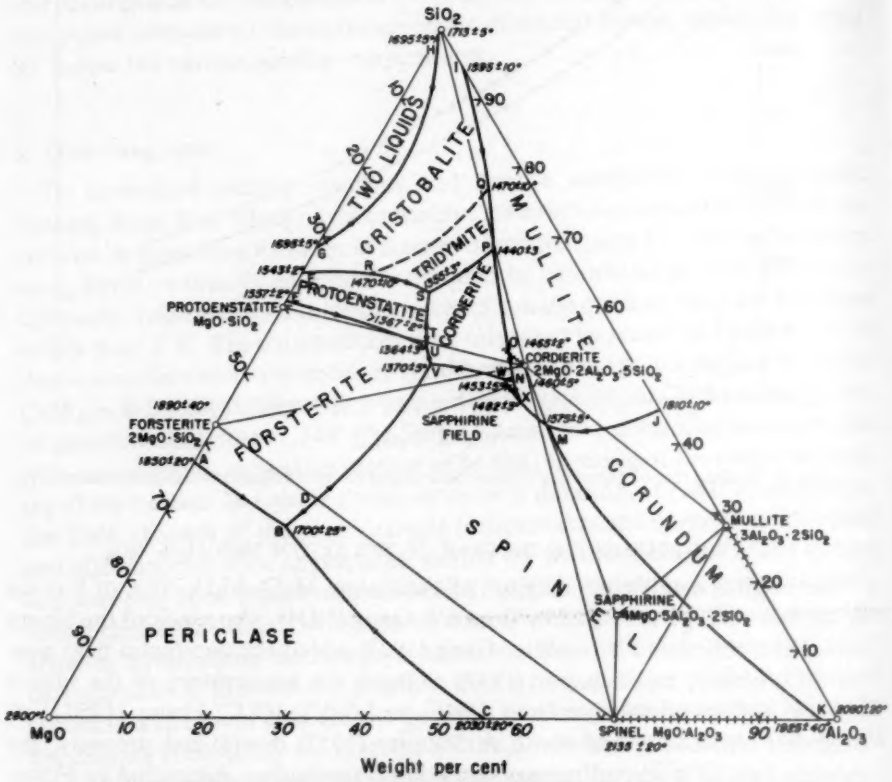

FIG. 3. Revised equilibrium diagram of the system MgO–Al_2O_3–SiO_2 based on the original work of Rankin & Merwin (1918) as modified by Bowen & Greig (1924), Greig (1927), Schairer (1942), Foster (1950 *a*, *b*; 1951), Keith & Schairer (1952), and Schreyer & Schairer (this paper). The tie lines connecting the phase cordierite with other crystalline phases are only valid in the temperature range 800°–1,300° C. Above this temperature cordierite forms binary solid solutions along the line indicated by cross bars. The effect of possible solid solutions of other compounds, on the tie lines valid for the range 800°–1,300° C, has been neglected. Maximum solid solution in mullite after Gelsdorf *et al.* (1958).

Rankin & Merwin (1918) with SiO_2 at the top. The data which led to the amendments will be discussed in detail in a later section. The relations of the cordierite polymorphs are too complex to be shown in the equilibrium diagram. Fig. 4 shows, at an enlarged scale, the part of the diagram of special interest for the present study. The heavy dots accompanied by numbers indicate the locations

of the 46 compositions investigated, whose chemical compositions and calculated modes are listed in Table 1. Their melting behaviours, as deduced from quenching experiments, are summarized in Table 2 and form the basis for discussions in subsequent sections.

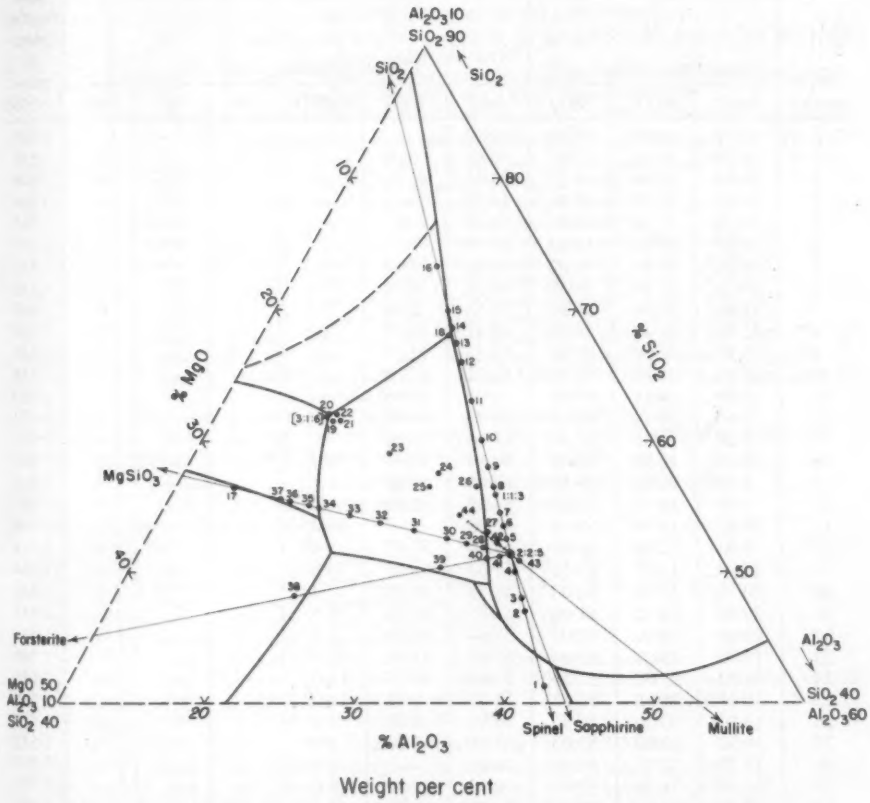

FIG. 4. Central portion of the system MgO–Al_2O_3–SiO_2 (Fig. 3) shown at an enlarged scale. Solid dots accompanied by numbers or symbols represent compositions studied in this investigation. Cross (3:1:6) indicates location of a theoretical ternary compound 'Mg–beryl,' $Mg_3AlSi_6O_{18}$.

The isofract diagram of Fig. 5 has been constructed using the measurements of the refractive indices of the 46 glasses prepared in this study. Furthermore, the refractive indices of the glasses used by Keith & Schairer (1952), and of some glasses between $MgSiO_3$ and pyrope composition ($3MgO \cdot Al_2O_3 \cdot SiO_2$) prepared by Schairer for studies with F. R. Boyd, have been determined and evaluated. Finally, the values of refractive indices of MgO–SiO_2 and Al_2O_3–SiO_2 glasses reported by Bowen & Andersen (1914), Greig (1927), and Yoder & Eugster (1955) have been taken into account.

TABLE 1

Compositions and refractive indices of 46 melts investigated

No. or symbol	*Composition (wt per cent)*			*Calculated mode (wt per cent)*						*Refractive index of glass ±0·003*
	MgO	Al_2O_3	SiO_2	*cord*	SiO_2	$MgSiO_3$	*fo*	*sp*	*mu*	
2:2:5	13·79	34·86	51·35	100·00	—	—	—	—	—	1·555
1:1:3	12·50	31·62	55·88	90·68	9·32	—	—	—	—	1·545
1	16·64	42·06	41·30	80·43	—	—	—	19·57	—	1·576
2	15·02	37·98	47·00	91·53	—	—	—	8·47	—	1·564
3	14·74	37·26	48·00	93·48	—	—	—	6·52	—	1·563
4	14·17	35·83	50·00	97·37	—	—	—	2·63	—	1·557
5	13·46	34·04	52·50	97·63	2·37	—	—	—	—	1·552
6	13·18	33·32	53·50	95·58	4·42	—	—	—	—	1·550
7	12·90	32·60	54·50	93·52	6·48	—	—	—	—	1·548
8	12·33	31·17	56·50	89·41	10·59	—	—	—	—	1·544
9	11·90	30·10	58·00	86·33	13·67	—	—	—	—	1·539
10	11·34	28·66	60·00	82·22	17·78	—	—	—	—	1·535
11	10·49	26·51	63·00	76·05	23·95	—	—	—	—	1·530
12	9·65	24·40	65·95	70·00	30·00	—	—	—	—	1·524
13	9·24	23·36	67·40	67·00	33·00	—	—	—	—	1·521
14	9·00	22·50	68·50	64·54	35·21	0·25	—	—	—	1·517
15	8·55	21·61	69·84	62·00	38·00	—	—	—	—	1·514
16	7·58	19·17	73·25	55·00	45·00	—	—	—	—	1·507
17	29·62	13·94	56·44	40·00	—	60·00	—	—	—	1·569
18	9·50	22·50	68·00	64·54	33·97	1·49	—	—	—	1·518
19	20·50	18·00	61·50	51·64	15·05	33·31	—	—	—	1·544
20	20·50	17·50	62·00	50·20	15·99	33·81	—	—	—	1·544
21	20·00	18·50	61·50	53·07	15·36	31·57	—	—	—	1·545
22	20·00	18·00	62·00	51·64	16·29	32·07	—	—	—	1·544
23	18·00	23·00	59·00	65·97	11·86	22·17	—	—	—	1·546
24	15·50	27·00	57·50	77·45	10·55	12·00	—	—	—	1·545
25	16·64	26·85	56·51	77·03	7·98	14·99	—	—	—	1·548
26	13·50	30·00	56·50	86·05	9·88	4·07	—	—	—	1·544
27	14·50	32·50	53·00	93·23	2·68	4·09	—	—	—	1·552
28	15·37	32·77	51·86	94·00	—	6·00	—	—	—	1·557
29	16·33	31·50	52·17	90·36	—	9·64	—	—	—	1·557
30	17·47	30·00	52·53	86·05	—	13·95	—	—	—	1·557
31	19·36	27·50	53·14	78·88	—	21·12	—	—	—	1·558
32	21·25	25·00	53·75	71·72	—	28·28	—	—	—	1·560
33	23·02	22·66	54·32	65·00	—	35·00	—	—	—	1·561
34	24·87	20·22	54·91	58·00	—	42·00	—	—	—	1·563
35	25·40	19·52	55·08	56·00	—	44·00	—	—	—	1·564
36	26·45	18·13	55·42	52·00	—	48·00	—	—	—	1·565
37	26·98	17·43	55·59	50·00	—	50·00	—	—	—	1·565
38	29·89	21·96	48·15	63·00	—	—	37·00	—	—	1·580
39	19·01	30·68	50·31	88·00	—	—	12·00	—	—	1·562
40	15·53	33·47	51·00	96·00	—	—	4·00	—	—	1·558
41	14·66	34·16	51·18	98·00	—	—	2·00	—	—	1·557
42	14·30	33·50	52·20	96·10	1·04	2·86	—	—	—	1·552
43	13·51	35·60	50·89	98·00	—	—	—	—	2·00	1·556
44	15·70	30·00	54·30	86·05	4·39	9·56	—	—	—	1·552

cord = cordierite (taken as $2MgO \cdot 2Al_2O_3 \cdot 5SiO_2$); *sp* = spinel; *mu* = mullite; *fo* = forsterite.

TABLE 2. *Results of quenching experiments*

No. or symbol of composition	*Results of optical and X-ray examination*		
	Primary Phase	*Liquidus temp., °C*	*Other data*
			(*a*) *Compositions on the line 2:2:5–spinel*
1	sp	1,568	mu in 1,527°; sapph in, sp out 1,475°±5°; cord in, mu out 1,460°; sp in, sapph out 1,453°
2	mu	1,540	sapph in 1,463°; cord in, mu out 1,459°; sp in, sapph out 1,453°
3	mu	1,540	cord+sapph in 1,458°; sp in, sapph out 1,453°
4	mu	1,528	cord in 1,463°; sapph in, mu out 1,460°; sp in, sapph out 1,453°
			(*b*) *Compositions on the line 2:2:5–SiO_2 or very close to it*
2:2:5	mu	1,523	cord in 1,465°; B.M. 1,445°±5°, mu out at this T
5	mu	1,523	cord in 1,462°; crist in, mu out 1,440°
6	mu	1,518	cord in 1,462°; crist in, mu out 1,440°
7	mu	1,517	cord in 1,463°; crist in, mu out 1,440°
1:1:3	mu	1,512	cord in 1,462°; crist in, mu out 1,440°; B.M. 1,430°±5°
8	mu	1,507	cord in 1,462°; crist in, mu out 1,440°; B.M. 1,430°±5°
9	mu	1,498	cord in 1,460°; crist in, mu out 1,440°; B.M. 1,430°±5°
10	mu	1,493	cord in 1,452°; crist in, mu out 1,440°; B.M. 1,430°±5°
11	mu	1,475	cord in 1,448°; crist in, mu out, 1,440°; B.M. 1,430°±5°
12	mu	1,463	cord in 1,445°; crist in, mu out 1,441°; B.M. 1,430°±5°
13	mu	1,457	cord in 1,443°; crist in, mu out 1,440°±2°; B.M. 1,430°±5°
14	mu	1,448	cord+crist in, mu out 1,438°±2°; traces of liquid between 1,355° and 1,430°
15	mu+crist	1,448	cord in, mu out 1,440°; B.M. 1,430°±5°
16	crist	1,484	mu in 1,448°; cord in, mu out 1,437°–1,440°; B.M. 1,430°±5°
18	cord+crist	1,440	traces of pyrox in 1,355°± = B.M.
			(*c*) *Compositions in the triangle 2:2:5–$MgSiO_3$–SiO_2*
19	cord	1,362	pyrox in 1,356°; SiO_2 in 1,354°
20	cord+pyrox +SiO_2	1,356	
21	cord	1,368	pyrox+SiO_2 in 1,356°; B.M. 1,350°±5°
22	cord	1,362	crist in 1,358°; pyrox in 1,355°; B.M. 1,350°±5°
23	cord	1,417	pyrox+SiO_2 in 1,357°
24	cord	1,453	crist in 1,368°; pyrox in 1,355°
25	cord	1,448	pyrox+crist in 1,356°
26	cord	1,458	crist in 1,413°; B.M. 1,355°; pyrox in 1,340°
27	mu	1,476	cord in 1,464°, mu out 1,460°; B.M. 1,355°; pyrox and SiO_2 in 1,320°
42	mu	1,481	cord in, mu out 1,465°; B.M. 1,355°; pyrox+SiO_2 in 1,320°
44	co	1,458	pyrox+SiO_2 in 1,356°
			(*d*) *Compositions along the line 2:2:5–$MgSiO_3$*
28	cord	1,463	sp in 1,435°; fo in, sp out 1,370°; pyrox in 1,365°
29	cord	1,458	sp in 1,398°; fo in, sp out 1,370°; pyrox in 1,365°
30	cord	1,455	sp in 1,375°; fo in, sp out 1,370°; pyrox in 1,365°
31	cord	1,438	fo in 1,367°; pyrox in 1,364°
32	cord	1,415	pyrox and trace fo in 1,364°
33	cord	1,393	pyrox in 1,366°; trace fo in 1,364°
34	cord+pyrox	1,367	trace fo in 1,364°
35	pyrox	1,373	cord in 1,367°; trace fo in 1,364°
36	pyrox	1,397	cord in 1,367°; trace fo in 1,364°
37	pyrox	1,401	cord in 1,365°±2°; trace fo in 1,364°
17	fo	1,438	pyrox in 1,433°; fo out 1,420°±5°; cord in 1,367°; trace fo in 1,364°
			(*e*) *Compositions along the line 2:2:5–forsterite*
38	fo	1,443	sp on 1,423°; cord in 1,370°±5°
39	cord	1,444	sp in 1,440°; fo in 1,370°±5°
40	cord	1,467	sp in 1,448°; fo in 1,370°±5°
41	mu	1,498	cord in 1,467°; mu out 1,462°; sp in 1,448°; fo in 1,370°±5°
			(*f*) *Composition along the line 2:2:5–mullite*
43	mu	1,532	cord in 1,465°; B.M. 1,450°±

B.M. = beginning of melting; *cord* = cordierite; *crist* = cristobalite; *fo* = forsterite; *mu* = mullite; *pyrox* = proto-enstatite (possibly quenched as clinoenstatite); *sapph* = sapphirine; *sp* = spinel.

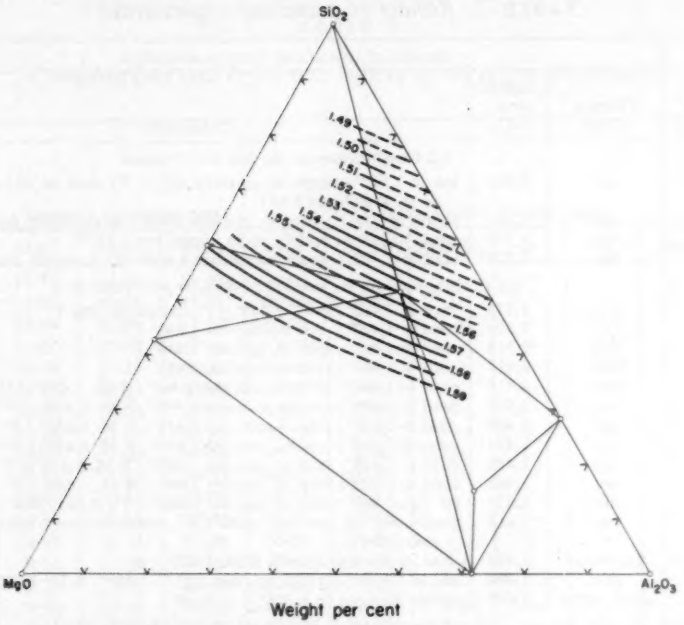

FIG. 5. Refractive indices of glasses in the system MgO–Al_2O_3–SiO_2. For references see text.

E. CRYSTALLINE PHASES

In this section a description will be given of the stable crystalline phases, other than those with a cordierite-type structure, which were encountered in the 46 compositions investigated. Data on the cordierite-type phases will be given in detail in the section on the structural changes of the ternary compound cordierite. Metastable phases appearing as early products of crystallization from glass at relatively low subsolidus temperatures are only mentioned in a cursory way. A fuller account on these very interesting phases is given in two separate papers by Schreyer & Schairer (1961 *a*, *b*).

1. *Products of metastable crystallization*

In the early stages of crystallization of glasses within the system MgO–Al_2O_3–SiO_2, metastable crystalline products play an important role. This is in accordance with Ostwald's step rule, which indicates that the phase assemblages stable at a particular pressure and temperature, i.e. those with the lowest free energies, may be arrived at stepwise through various metastable phases or phase assemblages exhibiting slightly higher degrees of free energy. This is, of course, of particular importance if the starting material used has a considerably higher degree of free energy, such as glass has in comparison with the stable crystalline assemblage.

Among the metastable phases encountered after crystallization of glasses at the relatively low subsolidus temperatures between 800° and about 1,100° C three different types may be distinguished: (1) metastable solid solutions with quartz-type structures, (2) metastable phase with an osumilite-type structure, (3) metastable phase with a petalite-type structure.

(1) The metastable solid solutions with quartz-type structures, having compositions along a considerable portion of the join SiO_2–$MgAl_2O_4$, are described in detail by Schreyer & Schairer (1961*a*). They include the so-called μ–$Mg_2Al_4Si_5O_{18}$ of Rankin & Merwin (1918) or μ-cordierite of Karkhanavala & Hummel (1953), to which the latter authors had erroneously attributed a β-spodumene structure. All these solid solutions may be considered as stuffed derivatives of quartz in analogy to β-eucryptite, $LiAlSiO_4$, in the system Li_2O–Al_2O_3–SiO_2 (Winkler, 1948).

(2) The metastable phase exhibiting a structure similar to that of osumilite (Miyashiro, 1956) also has a composition along the line SiO_2–$MgAl_2O_4$, possibly in the vicinity of the compositions Nos. 10–12 (Fig. 4). Its optical and X-ray properties, as far as they could be determined, are given in Schreyer & Schairer (1961*b*).

(3) The metastable phase with a structure similar to that of petalite, $LiAlSi_4O_{10}$, has been obtained by crystallization of glass of composition No. 20 (Fig. 4). Its composition is unknown, but presumably lies close to the MgO–SiO_2 side of the diagram. The close structural relationship of the unknown phase and also petalite with Li-disilicate, $Li_2Si_2O_5$, might suggest a composition within a fictive range of substitution with the three end members 'Mg–petalite' ($MgAl_2Si_8O_{20}$); a theoretical compound, $MgAl_2Si_3O_{10}$; and an unknown Mg–disilicate, $MgSi_2O_5$. A more detailed discussion of these questions is also given by Schreyer & Schairer (1961*b*).

The metastable phases listed above, which formed at a certain temperature of devitrification, disappear gradually at higher temperatures, or at the same temperature after continued heat treatment. They give rise to different crystalline products, which are sometimes identical but in many cases only a step closer to the final stable assemblages. The latter case is demonstrated by the ternary compound cordierite, which forms at the expense of a metastable quartz solid solution but nevertheless, in its early stages of crystallization, exhibits compositions and structural states considerably different from those stable under equilibrium conditions. These very complicated relations will be described in detail in sections F 1 and I 2. To a certain extent, metastability may also affect the appearance of the silica modifications cristobalite and tridymite as described in the following sections.

2. *Cristobalites*

In contrast to the relations shown on the equilibrium diagram, the silica phase encountered in this study was not tridymite but cristobalite, with only a few

exceptions in which both tridymite and cristobalite were present. High-cristobalite is considered to be the stable phase of SiO_2 between 1,470°±10° C and the melting-point 1,713°±5° C. When quenched to room temperature it is supposed to go through an inversion between 200° and 275° C to form low-cristobalite as a metastable phase. This phenomenon has been observed by a great many investigators (Sosman, 1927) and was also confirmed in this study for the pure SiO_2 which was used as starting material (see section C 1). In most of the ternary compositions investigated in which SiO_2 is one of the phases, however, it was found that high-cristobalite could be quenched to room temperature.

When present in moderate amounts, cristobalite forms round, fish-egg-shaped crystals with a characteristic low refractive index. The birefringence is zero in the case of high-cristobalite and very low in low-cristobalite. If cristobalite is only present in small amounts together with much cordierite, as in compositions Nos. 5–7 (Fig. 4) for example, the cristobalite forms tiny pin-points in the cordierite, which when submicroscopical, result only in a sort of granulated surface of the cordierite fragments.

In the X-ray pattern, high-cristobalite yielded peaks very close in position and analogous in intensity to those obtained by Barth & Posnjak (1932) on pure high-cristobalite at a temperature of 500° C. The displacement of peaks toward higher values of 2θ, in the high-cristobalites obtained in the present work, ranged from 0·2° to 0·4° for the area between 20° and 50°. This seems to be in accordance with the thermal contraction of the unit cell from 500° C to room temperature. As the main high-cristobalite peak at 21·8° 2θ is covered by a cordierite peak, the second strongest line at 35·7° had to be used for determinative purposes, which naturally increased the minimum amount of the phase that could be recognized.

Low-cristobalite has an X-ray pattern clearly distinct from that of high-cristobalite. In none of the compositions studied was low-cristobalite found as the only form of silica. It was always mixed with high-cristobalite±tridymite and it occurred mainly in highly siliceous compositions. Since its main peak is also covered by a cordierite peak, its recognition in assemblage with cordierite is even more difficult than for high-cristobalite, because one has to rely on minor peaks. This may be one reason why it has not been observed in compositions poorer in silica. A further difficulty of recognizing cristobalite in the X-ray pattern arises when the intensities of critical peaks are reduced by the presence of both cristobalite polymorphs simultaneously.

The reason high-cristobalite in ternary bulk compositions does not invert on cooling is not known, as yet. Barth & Posnjak (1932) have pointed out that high-cristobalite is isostructural with α-carnegieite, the high-temperature form of nepheline, $NaAlSiO_4$. α-Carnegieite can take minor amounts of excess silica into solution (Greig & Barth, 1938). It does not seem impossible, therefore, that high-cristobalite can also take minor amounts of Na+Al or, in our case, Mg+Al into solid solution. It may also be possible that these foreign ions are

able to stabilize high-cristobalite to lower temperatures than 1,470°±10° C and in part prevent its inversion to low-cristobalite during quenching.[1] It may not be without significance, therefore, that tridymite was only obtained from compositions which are the farthest away from the 'substitution-line' SiO_2–$MgAl_2O_4$. Recent studies by Roy & Roy (1959) indicate that cristobalite can indeed take up to 4 per cent $NaAlO_2$ into solid solution, whereby the temperature of its inversion to tridymite is lowered below 1,400° C. It is not impossible, however, that the assumed small amounts of Mg+Al in our cristobalites represent metastable solid solutions which would unmix upon longer heating.

3. *Tridymite*

The crystalline phase of SiO_2, tridymite, which is considered to be the stable form between 870° and 1,470° C, was encountered only in compositions Nos. 19–22 lying close to the ternary eutectic *S*, cordierite+protoenstatite+silica +liquid (Fig. 3), particularly, but not necessarily, when there was liquid present. The possible significance of this fact was already outlined in the above section on cristobalite. The phase was always quenched as low-tridymite. It was usually not the only SiO_2 phase present, however, but occurred together with variable amounts of high-cristobalite±low-cristobalite. For this reason, and because of its coexistence with a pyroxene and cordierite, it was very often not recognized optically. In favourable cases it was found as long prismatic cross-sections of thin plates with a low refractive index, very low birefringence, parallel extinction, and negative elongation. The pseudo-hexagonal outline of the plates could be confirmed only in exceptional cases.

The X-ray powder reflections of the tridymites synthesized yielded *d*-values which correspond exactly with a standard pattern run on Fenner's original material. The phase is easily recognized by its three strong peaks between 20° and 24° 2θ, only one of which is coincident with a peak of cordierite.

Recent researches of a number of investigators (Flörke, 1955*a*; Holmquist, 1958) have led to the conclusion that tridymite is not a stable phase of pure SiO_2 at 1 atm, but can only be obtained in the presence of certain fluxes, one of which may be water. If this is correct, it would mean that the tridymites obtained in

[1] Flörke (1955*b*) found that highly disordered low-cristobalites found in opals and partially devitrified glasses yield X-ray powder patterns very similar to that of high-cristobalite. Since the peak considered to be indicative of high-cristobalite in the present study was found to be very sharp in most cases, it is considered likely that there is indeed high-cristobalite present in these samples at room temperature. On the other hand, the peaks of low-cristobalite, if present, were usually more diffuse and may well indicate relatively low degrees of ordering of this phase. The drastic lowering of the inversion temperature of disordered cristobalites to 40°–60° C, as reported by Flörke (1955*b*), appears to enhance the possibility that in the presence of appropriate foreign ions the high-temperature form may indeed be encountered at room temperature with or without the low-temperature form co-existing. A differential thermal analysis of crystalline material of composition No. 16, containing the phase assumed to be high-cristobalite, did not show any peak which might be attributed to a polymorphic inversion in the whole range between 60° and 600° C. (This DTA run was kindly performed by Dr. R. A. Yund of the Geophysical Laboratory.)

our study contain small amounts of foreign ions—judging from the appearance of the phase in compositions Nos. 19–22, probably Mg.

4. *Mullite*

Mullite, $3Al_2O_3{:}2SiO_2$, was encountered as a stable phase at the liquidus of a number of compositions (Fig. 4). In short runs it was present as an irregular net of very thin long needles with parallel extinction and positive elongation. In longer runs (72 h and more), however, mullite, if present in moderate amounts, usually formed stout prisms with rather large oval voids. Owing to its association with glass of much lower index, the refractive indices of mullite could not be determined accurately, but were found to be close to 1·645. This value, as well as the position of several minor peaks in the powder pattern, makes it clearly distinct from sillimanite. Very often, however, these determinations were impossible because of the small amounts present.

In the bulk compositions studied, no evidence was found for solid solution in mullite towards SiO_2, i.e. toward sillimanite composition, or toward Al_2O_3. However, these bulk compositions are too far away from a potential range of mullite solid solution along the Al_2O_3–SiO_2 side of the ternary diagram and, therefore, cannot yield critical data concerning this problem. Gelsdorf, Müller-Hesse, & Schwiete (1958) have recently indicated that above about 1,200° C mullite can take more and more Al_2O_3 into solid solution up to a composition $2Al_2O_3 \cdot SiO_2$, which is in equilibrium with corundum between 1,700° C and 1,820° C, i.e. its incongruent melting temperature. More recently Welch (1960) presented a diagram of the system Al_2O_3–SiO_2 for 1 atm, in which the composition of mullite is not $3Al_2O_3 \cdot 2SiO_2$ at all, but is always more aluminous and may even exceed the limiting composition $2Al_2O_3 \cdot SiO_2$ indicated by Gelsdorf *et al.* (1958). Whereas all the previously mentioned authors confirmed the incongruent melting behaviour of the phase mullite as first reported by Bowen & Greig (1924), there is also a group of investigators favouring a congruent melting of this phase. A more recent contribution in this direction is that of Aramaki & Roy (1959). It appears that these conflicting results may partly be due to different experimental conditions (H. S. Yoder, personal communication, 1960). At temperatures in excess of 1,800° C, the vapour pressure of the bulk composition is appreciable and, owing to the incongruency of the vapour phase, may lead to preferential loss of silica if not contained. In the equilibium diagram of Fig. 3, incongruent melting of mullite is assumed and the maximum extent of solid solution is shown according to Gelsdorf *et al.* (1958).

5. *Sapphirine*

The ternary compound sapphirine was encountered only in the presence of liquid, in all our compositions, on the join 2:2:5-spinel, i.e. Nos. 1–4. Foster (1950 *a*, *b*) has shown that the composition of the synthetic compound is likely to be $4MgO \cdot 5Al_2O_3 \cdot 2SiO_2$. Natural sapphirines, however, tend to approach a

composition $2MgO \cdot 2Al_2O_3 \cdot SiO_2$ (Friedman, 1954; Segnit, 1957). Calculations show that a possible series of solid solutions between these end members cannot be caused by MgSi AlAl $\rightleftharpoons$ substitution, as proposed by Segnit (1957). The relations between the two compositions proposed, therefore, remain unknown.[1]

In correspondence with its small field of stability on the liquidus surface (Keith & Schairer, 1952) sapphirine was only present, in the compositions studied, over a very narrow range of temperatures. In compositions Nos. 3 and 4, sapphirine coexisted with cordierite + liquid ± mullite or spinel from 1,453° ± 5° C to 1,460° ± 5° C (Table 2 (*a*)). In composition No. 2 this range increased up to 1,463° C, where sapphirine coexisted with mullite and liquid only. Composition No. 1 should show sapphirine in coexistence with these other phases from 1,453° ± 5° C to 1,482° ± 3° C. The highest percentage of sapphirine in this composition, with a small amount of mullite, was found between 1,465° and 1,475° C. Spinel, which is in equilibrium with mullite and liquid at temperatures above 1,482° ± 3° C, that is before the sapphirine field is reached, was found to disappear as low as 1,475° ± 5° C owing to a reaction of portions of liquid and mullite with the spinel, to form sapphirine. Since spinel, however, has to appear as one of the final crystalline products, a reverse reaction, sapphirine + liquid to form spinel + cordierite, must take place at the ternary point *W* (1,453° ± 5° C, Fig. 3). The path of crystallization of composition No. 1 between 1,475° and 1,460° C thus follows the boundary curve sapphirine–mullite. The paths of other compositions, along the line 2:2:5–spinel with higher spinel contents, have to follow the boundary curve sapphirine–spinel. For a narrow range of compositions (outlined in Fig. 6), lying close to the intersection of this line 2:2:5–spinel and a straight line between the ternary reaction point *X* (spinel + mullite + sapphirine + liquid, Fig. 3) and the composition of sapphirine, the paths of crystallization would have to cross parts of the sapphirine field with only sapphirine being in equilibrium with melt over a narrow range of temperatures. From the knowledge of these particular compositions it might be possible to obtain data on the composition of the sapphirine crystallizing. These relations are shown diagrammatically in the pseudobinary section 2:2:5–spinel of Fig. 6. In accordance with the finding of the disappearance of spinel in composition No. 1 at 1,475° ± 5° C, this temperature rather than 1,482° ± 5° C (Keith & Schairer, 1952) has been used, tentatively, for the ternary reaction point *X*, which projects as a straight line in Fig. 6.

The optical properties of the sapphirines encountered in the present study were found to be identical with those given by Keith & Schairer (1952).

The X-ray pattern was compared with a standard kindly provided by Dr. W. Foster. The recognition of spinel in the presence of sapphirine by X-ray is

[1] In a recent paper Kuzel (1961) on the basis of single-crystal X-ray studies of natural and synthetic sapphirines, concluded that the formula $4MgO \cdot 5Al_2O_3 \cdot 2SiO_2$ proposed by Foster (1950 *a*, *b*) is not in agreement with the crystallographic data. Kuzel suggests that synthetic Al_2O_3-rich sapphirines are due to a limited substitution of 2Al for Mg + Si in sapphirine of the basic formula $2MgO \cdot 2Al_2O_3 \cdot SiO_2$ and may thus have a composition $7MgO \cdot 9Al_2O_3 \cdot 3SiO_2$.

difficult (Foster, 1950 *a*, *b*); however, the spinel line at 19·0° 2θ, absent in the sapphirine pattern, is diagnostic. Since this area is covered by a cordierite peak, however, this method can only be used in the absence of cordierite.

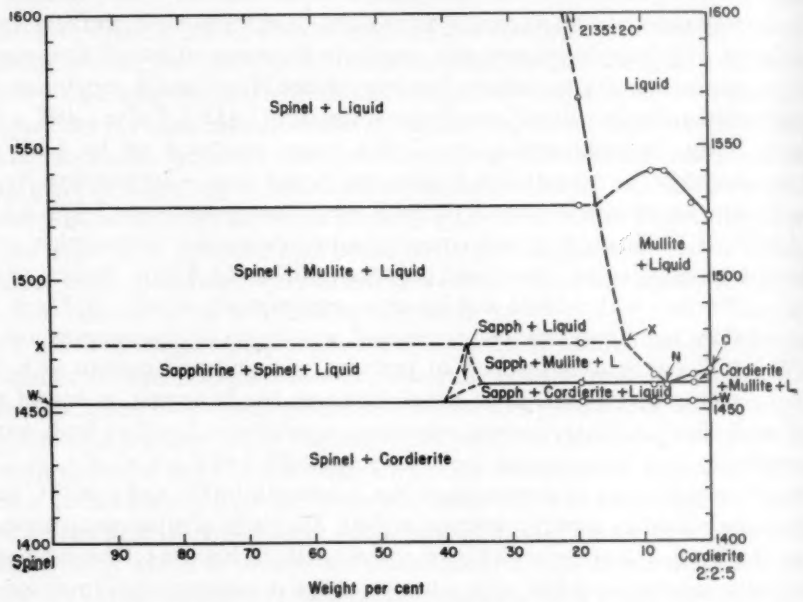

FIG. 6. Pseudobinary section cordierite (2:2:5)–spinel. Notice the presence of a narrow triangular field in which sapphirine coexists with liquid only. Assumption: no solid solution in any of the solid phases.

6. *Spinel*

At subsolidus temperatures, spinel coexists with cordierite in compositions Nos. 1–4. Even small amounts of spinel are readily recognized, optically, because of the high index of refraction. They were usually present as tiny anhedral pinpoints. Well-formed octahedra, increasing in size with the duration of the runs, grew only in the presence of liquid from the above compositions as well as Nos. 38–41 and, in small amounts, from Nos. 28–29. By powder X-ray methods, only amounts which exceeded about 5 per cent of the total material could be identified. The critical peaks in the presence of cordierite only, were at 31·3° and 44·9° 2θ; in the presence of sapphirine alone, at 19·0°. When associated with both cordierite and sapphirine, spinel could not be detected by X-ray except in large amounts. The composition of the spinels in our compositions Nos. 1–4 at subsolidus temperatures is shown to be $MgAl_2O_4$, by the absence of a third phase. No indications were found, in the compositions studied, of variable solid solution in the spinels formed at the liquidus.

7. *Forsterite*

Forsterite, Mg_2SiO_4, was found in compositions Nos. 38–41 at subsolidus temperatures; in composition No. 38, also in the presence of liquid. Furthermore, small amounts of forsterite were encountered in metastable coexistence with a pyroxene plus small amounts of high-cristobalite, during the subsolidus crystallization of almost all the glasses of compositions Nos. 17 and 28–37. Even the final crystalline materials of most of these compositions, obtained after long periods of heating above 1,300° C, contained very small amounts of forsterite. This is caused by the compositional change of the coexisting phase cordierite above 1,300° C (see section F 1 (*b*) and Fig. 7).

Forsterite forms rather small rounded, or slightly prismatic, crystals. Its distinction from pyroxenes in fine-grained mixtures was found to be very difficult, and depended entirely on the birefringence which is, in forsterite, about four times as high as in the pyroxenes.

Forsterite yields a characteristic X-ray pattern. By virtue of its strong peak at 22·9° 2θ, which is not covered by cordierite or pyroxene peaks, the minimum amount of forsterite that can be detected is relatively small.

8. *Pyroxenes of the composition* $MgSiO_3$

$MgSiO_3$ is known to occur in three different modifications—orthoenstatite, clinoenstatite, and protoenstatite. The mutual relationships between these three forms were clarified to a great extent by the high-temperature X-ray investigations of Foster (1951) and Atlas (1952). According to these authors orthoenstatite is the stable form at low temperatures. It inverts around 1,260° C (Foster, 1951) to protoenstatite, which is stable up to the incongruent melting. Protoenstatite, in turn, when quenched to room temperature inverts at various rates to clinoenstatite, which may be metastable at all temperatures. Atlas (1952), by using a lithium fluoride flux, found the inversion temperature of ortho- to protoenstatite as low as 985° C. Boyd & Schairer (1957), in a preliminary diagram of the join $MgSiO_3$–$CaMgSi_2O_6$, suggest an inversion at about 1,075° C.

In contrast to Boyd & Schairer's (1957) experience and also to Schairer and Yoder's (unpublished) results on pure $MgSiO_3$ composition, protoenstatite could, in the present work, in most cases be quenched as such with no clinoenstatite, or only minor amounts, present. Only in very few exceptional cases was clinoenstatite found to be the only pyroxene phase. This may either be due to a slower cooling or to a longer time interval between the end of the run and the X-ray investigation. It appears from these results that the presence of Al_2O_3 in the bulk compositions studied has a tendency to stabilize the phase protoenstatite. The first pyroxene crystallizing from glasses of appropriate composition at temperatures between 900° and 1,050° C was found to be a phase which is very close to, but not identical with, orthoenstatite. In comparison with the pattern of natural orthoenstatite from the Bishopville meteorite there was only one very

strong peak at $2\theta = 35{\cdot}8° \pm 0{\cdot}1°$, instead of three smaller ones at 35·5°, 36·1°, and 36·4°. Furthermore, in a number of cases peaks showed displacements, against the standard of about 0·2°, toward higher values of 2θ. It is believed that these deviations are non-equilibrium features due to the low temperatures of crystallization and may be indicative of the initial formation of a disordered type of orthoenstatite.

No particular effort has been made to determine the temperature at which the orthoenstatite-like pyroxene inverts to protoenstatite. However, the data available on the various crystallization products at subsolidus temperatures suggest that it takes place at some temperature between 1,050° and 1,250° C. The data obtained seem to indicate, also, that the rate of inversion decreases with increasing amounts of $MgSiO_3$ in the composition. Thus composition No. 17, after devitrification at 1,300° C for 16 h, showed mainly the orthoenstatite-like phase, whereas after 6 days at the same temperature protoenstatite was the only pyroxene. Compositions Nos. 35 and 37, on the other hand, after devitrification at 1,300° C for 16 h, exhibit mainly proto- and clinoenstatite with only small amounts of the orthoenstatite-like phase left. On the basis of these data, the possibility cannot be ruled out completely that the inversion is actually below 1,050° C and that the orthoenstatite-like pyroxene forms metastably above the true inversion temperature, giving way to the stable protoenstatite only very slowly at lower temperatures. The orthoenstatite-like pyroxene was found to persist at 1,050° C for at least 7 days.

Optically, the orthoenstatite-like phase forms extremely fine-grained feathers intimately intergrown with cordierite with or without a cristobalite phase. No optical constants can be given, but the mean refractive index of the intergrown mixture suggests a high value, as is common for pyroxenes. Protoenstatite forms little prismatic crystals which increase in size with increasing temperature and duration of run, especially in the presence of liquid. A characteristic feature of some of the larger prisms is their crack structure. Owing to the volume change associated with the inversion from proto- to clinoenstatite, narrow, slightly curved cracks form in a direction roughly perpendicular to the *c*-axis of the crystal. Since the inversion is only very rarely complete, one usually finds a full sequence of crystals ranging from those not affected to those slightly or much affected by this process. According to Schairer and Yoder (personal communication) this effect is very common in the pure $MgSiO_3$ composition.

The melting behaviour of the pyroxene-bearing bulk compositions studied in this investigation is in accordance with a pyroxene composition of pure $MgSiO_3$. No evidence for any solid solution could be ascertained (see also discussion of the liquidus investigations, section F 2).

F. THE COMPOSITION OF THE TERNARY COMPOUND, CORDIERITE

There are, basically, at least two independent methods of determining the composition of the ternary compound, cordierite: (1) by investigating the nature

and ratios of the crystalline compounds formed at subsolidus temperatures from compositions adjacent to the alleged cordierite composition, (2) by pursuing the paths of crystallization at the liquidus surface of compositions lying in the stability field of cordierite.

Some theoretical examples for each case may demonstrate this more clearly. If cordierite were not of the composition 2:2:5, but, for instance, 1:1:3 (see Fig. 4), the final crystalline materials of compositions Nos. 1–7, including 2:2:5, should contain spinel; those of compositions Nos. 17 and 32–37, forsterite in addition to a pyroxene; those of compositions Nos. 27, 28–31, and 42, forsterite plus spinel instead of a pyroxene; and those of compositions Nos. 38–41, spinel in addition to forsterite. If cordierite had the composition 1:1:3, its crystallization at the liquidus surface from the melts with a cordierite liquidus should follow different paths, and reach adjacent fields of other compounds at different temperatures and at different locations, than in the case of a 2:2:5 composition. If cordierite had a range of compositions owing to solid solution, it should be the only crystalline phase within this range at subsolidus temperatures. The paths of crystallization in its stability field should be curved rather than straight lines, owing to the gradual changes in composition of the cordierites crystallizing out upon cooling of the liquid. Thus the temperatures and locations at which cordierite is joined by a second crystalline phase should again be different from the cases of straight 2:2:5 or 1:1:3 compositions.

The experimental results will now be given, treating the two different methods of approach separately.

1. *Subsolidus investigations*

(*a*) *Metastable solid solutions.* The crystallization of glasses of the various compositions at low subsolidus temperatures first leads to the formation of several new metastable phases, as summarized in a previous section. It is not surprising, therefore, that the first crystals of cordierite, which form around 1,050° C at the expense of these pre-existing metastable phases, do not yet show what is believed to be the equilibrium composition of cordierite. In other words, the cordierites formed at low temperatures, which are hexagonal high-cordierites, may exhibit metastable solid solution. This fact has been established by studies of the phase assemblages in some of the compositions, as well as by the observation of definite displacements of certain peaks in the X-ray pattern of some of these high-cordierites. Since the process of unmixing, which takes place around 1,300° C, could not be reversed at the low temperature at which the cordierite solid solutions had formed first, not even in runs of 1 year's duration, it is justified to call the solid solutions metastable. It was also observed in a few cases that the unmixing does take place at medium temperatures (1,250° C) as well, only at a lower rate. At a still lower temperature (1,050° C) metastable solid solution was found to persist for as many as 248 days.

No special effort has been made to determine the actual range of metastable

solid solution in cordierite, which would not only be temperature dependent but also time dependent. It appears, however, that one direction of solid solution is along the 2:2:5–SiO_2 join from 2:2:5 at least up to our composition No. 9. The crystalline product of this composition, obtained after heating glass at 1,050° C for 4 days and then at 1,250° C for 1 day, consisted entirely of cordierite. Optically, no residual glass could be detected. All the intermediate compositions between No. 9 and 2:2:5 behaved in a similar fashion. The range thus determined exceeds that suggested by Rankin & Merwin (1918), which was given as 2:2:5 to 1:1:3. No appreciable shifts of X-ray peaks could be detected in these solid solution cordierites formed along the line 2:2:5–SiO_2. This might indicate that the excess SiO_2 does not occupy structural sites, but is possibly contained in the open channels of the cordierite structure (Byström, 1942). On the other hand, the refractive indices of the cordierites along the line 2:2:5–SiO_2 decrease with increasing amounts of SiO_2 in solid solution, as pointed out by Rankin & Merwin (1918). This seems surprising, because channel-filling of cordierite—even by H_2O—results in an increase of the refractive indices (Schreyer & Yoder, 1960). The possibility should be considered, therefore, that the excess SiO_2 is in a free state, but amorphous to X-rays, and that its physical mixture with the cordierite crystals is so intimate that it seemingly lowers the refractive indices of the apparent cordierite solid solutions.

Shifts of cordierite peaks of about 0·2° toward higher 2θ angles, in comparison with cordierite formed from 2:2:5 composition under identical conditions, were recognized in low-temperature crystalline materials of composition No. 23. Here the cordierite coexisted with a pyroxene but not with a silica phase. Composition No. 26 at 1,050° C crystallized completely to a cordierite solid solution showing similar displacements of peaks and persisting at 1,250° C for 3 days. Furthermore, solid solution was detected by X-ray data on the cordierite formed from composition No. 32 at 1,050° C, which coexisted with a pyroxene and some forsterite. These data suggest that there is metastable solid solution extending from composition 2:2:5 for a short range of composition into the phase triangle 2:2:5–$MgSiO_3$–SiO_2.

There are also indications that metastable solid solution in cordierite extends for a short range of composition from 2:2:5 toward mullite. Composition No. 43, at low devitrification temperatures (1,000°, 1,250° C), crystallizes entirely to cordierite. In addition, compositions Nos. 1–3 under the same conditions consist of a cordierite solid solution and forsterite, whereas at higher temperatures forsterite disappears and spinel forms. The metastable cordierite solid solution in composition No. 2 brought about displacements of minor peaks in the cordierite X-ray pattern of about 0·2° to *lower* 2θ angles.

In the cases just described, where solid solution is accompanied by observable changes in X-ray properties, a substitutional type of solid solution may be expected. Gossner (1928), on the basis of crystallographic and chemical data, already assumed a Mg+Si for 2Al substitution in natural cordierite of the basic

formula $Mg_2Al_4Si_5O_{18}$ (= 2:2:5). Recently Iiyama (1955), on the basis of experimental work in the system MgO–Al_2O_3–SiO_2, presented evidence for solid solution in high-cordierite almost as far as a theoretical composition $Mg_3Al_2Si_6O_{18}$, 'magnesium beryl' (= 3:1:6, Fig. 4), which is also arrived at by the above substitution proposed by Gossner (1928). The displacements of X-ray peaks, caused by this solid solution as given by Iiyama, show the same tendency toward higher 2θ angles as in the compositions Nos. 23, 26, and 32 studied in this investigation.[1] The opposite displacement of peaks to lower 2θ angles, indicated by compositions along the line 2:2:5–spinel, are suggestive of the reverse substitution $Al+Al \rightarrow Mg+Si$, which would extend from 2:2:5 approximately in the direction toward mullite.

It is to be emphasized, however, that these extensive solid solutions formed at low temperatures have to be considered as non-equilibria. Even Iiyama's (1955) runs, although at higher temperatures, were, according to the present new data, too short (1,350° ± 20° C, 10 h; 1,250° C ± 20° C, 60 h) to reach equilibrium. Furthermore, the temperature, 1,350° ± 20° C, at which he crystallized four of his six compositions was too high because the equilibrium assemblage for these compositions above 1,355° ± 3° C, i.e. the temperature of the ternary eutectic *S* (cordierite + $MgSiO_3$ + SiO_2 + liquid, Fig. 3), is cordierite + liquid without pyroxene or silica.

(*b*) *Stable subsolidus composition of cordierite.* Continued heating of the crystalline materials at elevated temperatures about 50° below the various solidus temperatures brought about a gradual unmixing and reconstitution of the solid phases. Phase equilibrium, which does not necessarily involve polymorphic equilibrium, was attained after heating periods ranging from 1 week to 1 month. It is believed that the unmixing would also take place at lower temperatures of heating, but at a much slower rate. The phase assemblages obtained upon continued heating are the following:

The composition 2:2:5 consists entirely of cordierite. Some batches contained mere traces of spinel or mullite due to slight inaccuracy of the composition caused by the presence of traces of alkalis, &c. Composition No. 4 contains, in addition to cordierite, a small amount of spinel pin-points; composition No. 43, an obvious amount of mullite needles; composition No. 41, tiny forsterite crystals; and composition No. 28, small amounts of a pyroxene.

Compositions No. 7 and 1:1:3 contain minute pin-points of cristobalite and yield a peak at 35·7° 2θ in the X-ray pattern, which is characteristic for high-cristobalite. In compositions Nos. 5 and 6 this peak was not observed. This must be due to the fact that there are only small amounts of cristobalite present, because the typical pin-points, or at least a 'granular' surface of the cordierite resulting from submicroscopic crystals of a different refractive index, was observed optically. The process resulting in the formation of the stable assemblage

[1] Low-temperature studies on the remaining compositions Nos. 24, 25, and 27, which might be of interest in this connexion, have not been undertaken.

cordierite and SiO_2 was found to be more sluggish the closer the composition was to 2:2:5, which may in part be caused by the slowness of crystallization of small amounts of free SiO_2. At temperatures between about 1,400° C and the theoretical beginning of melting of these compositions at 1,440°±3° C (*P*, Fig. 3), a gradual decrease in the amount of cristobalite was observed. It is possible that this behaviour is caused by a gradual shift of tie lines between SiO_2 and a cordierite solid solution stable at these high temperatures, as will be described later.

The final crystalline materials of compositions Nos. 19–27, 42, and 44 in the phase triangle 2:2:5–$MgSiO_3$–SiO_2 below 1,300° C, showed the three phases cordierite, a pyroxene, and a SiO_2 phase in appropriate amounts, although the normative composition of No. 27 includes only 2·7 per cent SiO_2 and 4·1 per cent $MgSiO_3$, and that of mixture No. 42 only 2·86 per cent $MgSiO_3$ and 1·04 per cent SiO_2 in addition to cordierite (2:2:5). In composition No. 42 the umixing process required heating periods of 4 days at 1,050° C, 5 days at 1,250°, and 15 days at 1,290° C. Silica was only detected optically. Single heating at 1,320° C resulted in the unmixing of some pyroxene after 7 days. The metastable solid solutions again seem to be more persistent as the bulk compositions approach $2MgO \cdot 2Al_2O_3 \cdot 5SiO_2$. In compositions Nos. 14 and 18 the very small percentage of pyroxene could not be detected in the presence of large amounts of cristobalite.

It is concluded from the results described so far that the stable composition of cordierite at subsolidus temperatures between approximately 1,300° C and about 800°, i.e. the lowest possible temperature of devitrification, is $2MgO \cdot 2Al_2O_3 \cdot 5SiO_2$, and there is no stable solid solution in this temperature range in any direction within the system MgO–Al_2O_3–SiO_2.

On the basis of cordierite composition 2:2:5 the proper equilibrium assemblages persisted up to the beginning of melting for many of the compositions studied. However, subsolidus heating of already unmixed compositions Nos. 26, 27, and 42 at temperatures around 1,340° C, i.e. 15° below the beginning of melting at *S* (Fig. 3), resulted in the sudden disappearance of all the pyroxene. In compositions Nos. 27 and 42, cristobalite disappeared also, whereas in composition No. 26 its amount had only decreased very slightly. This behaviour cannot be caused by melting over a range due to solid solutions in any of the three phases, because the temperatures involved are below that of the lowest eutectic *S* (1,355°±3° C, Fig. 3) in the system. Furthermore, no obvious amounts of liquid could be detected. Careful studies of these bulk compositions at lower temperatures indicate that pyroxene *gradually* disappears at temperatures between 1,315° and 1,325° C in compositions Nos. 27 and 42, and between 1,335° and 1,345° C in composition No. 26. These processes proved to be reversible, because materials preheated at 1,340° C exhibited pyroxene when held at 1,310° C for 7 days.

If the disappearance of phases described were due to premature formation of

undetectable amounts of liquid because of impurities (alkalis, Fe_2O_3), one would expect a similar behaviour for compositions Nos. 28, 40, and 41. However, these compositions lose the phase pyroxene or forsterite, respectively, at the appropriate temperatures given by the ternary points *U* and *V* (Fig. 3). The writers believe, therefore, that the disappearance of phases at subsolidus temperatures in compositions Nos. 26, 27, and 42 is caused by a stable solid solution in cordierite above approximately 1,300° C. The range of this solid solution at tem-

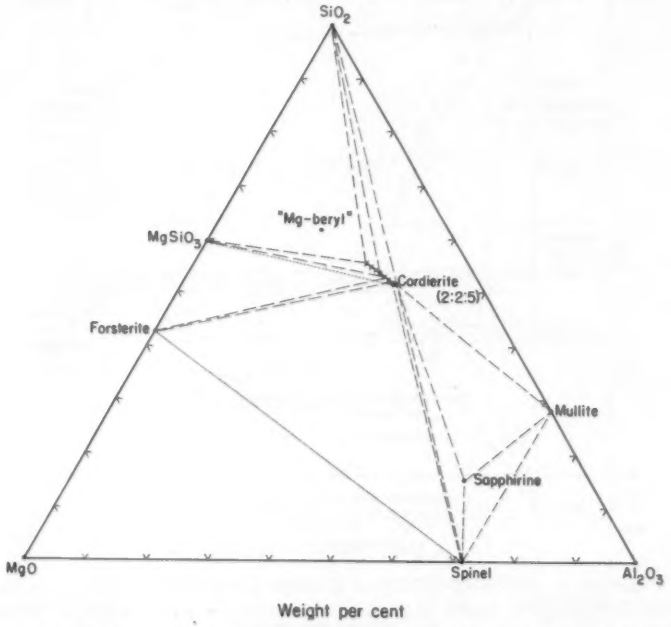

FIG. 7. Tie lines (long dashes) between cordierite solid solutions and other solid phases for a temperature just below that of the ternary eutectic *S* (1,355° ± 3° C, Fig. 3). For the sake of clarity the range of solid solution in cordierite at this subsolidus temperature has been exaggerated at a ratio of about 2:1. Short dashes indicate tie line, $MgSiO_3$–cordierite, valid for the range 800°–1,300° C. Possible solid solutions in other compounds have been omitted.

peratures between 1,325° and 1,355° C extends from 2:2:5 into the triangle 2:2:5–$MgSiO_3$–SiO_2 at least as far as composition No. 27. It appears that this solid solution is due to the substitution MgSi for 2Al in the cordierite structure, as proposed by Gossner (1928), thus extending toward the theoretical compound 'Mg-beryl' (3:1:6, Iiyama, 1955), but only over a narrow range of composition. For the temperature range 1,325°–1,355° C, solid solution terminates somewhere between compositions Nos. 27 and 44, because in the latter composition pyroxene and a silica phase persist up to the beginning of melting at *S* (1,355° C).

The bearing, on the subsolidus phase assemblages stable at about 1,350° C, of this range of solid solution in the phase cordierite is shown diagrammatically in Fig. 7. For the sake of clarity, the range of solid solution at this tem-

perature has been exaggerated by a factor of about 2. It can be seen that compositions along the line cordierite (2:2:5)–$MgSiO_3$ (short dashes) between 1,300° C and the solidus (1,364° ±3° C) should indeed contain forsterite ± spinel, or spinel only, in addition to cordierite solid solution ± $MgSiO_3$. These relations are also shown in the subsolidus portion of the pseudobinary join

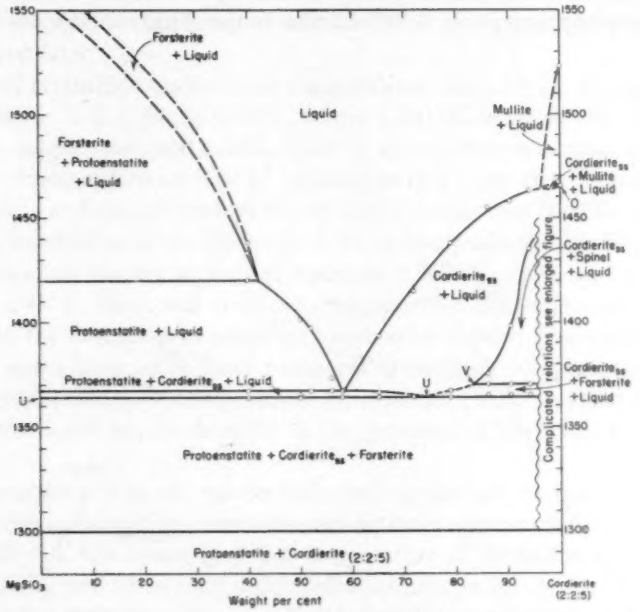

FIG. 8. Pseudobinary section cordierite (2:2:5)–$MgSiO_3$. Complicated relations on the right-hand side of the diagram, caused by solid solution in cordierite, are shown on an enlarged scale in Fig. 9.

cordierite (2:2:5)–$MgSiO_3$ given in Figs. 8 and 9. A pseudobinary section paralleling the line of substitution from cordierite (2:2:5) to 'Mg–beryl' has been constructed in Fig. 10 and will be discussed in the following section.

2. *Liquidus investigations*

Compositions Nos. 19, 21–26, 28–33, 39–40, and 44 in Fig. 4 are shown to have a cordierite liquidus. This means that at the various liquidus temperatures cordierite is the first phase to crystallize, and the paths of crystallization upon further cooling will follow lines leading away from the composition of the cordierite which is crystallizing out. If, during the course of crystallization, there were any changes in the composition of the cordierite crystallizing, the path would curve accordingly. Data on the temperature of appearance, as well as on the nature, of the second crystalline phase in the bulk compositions given previously can thus yield valuable information concerning the composition of the

cordierite crystallizing. In order to obtain these data, quenching runs were made on crystalline materials of these compositions which exhibited the subsolidus assemblages stable below 1,300° C. The results of these studies may be summarized as follows:

Cordierites crystallizing from melts Nos. 19, 21–23, 25, and 44, upon cooling

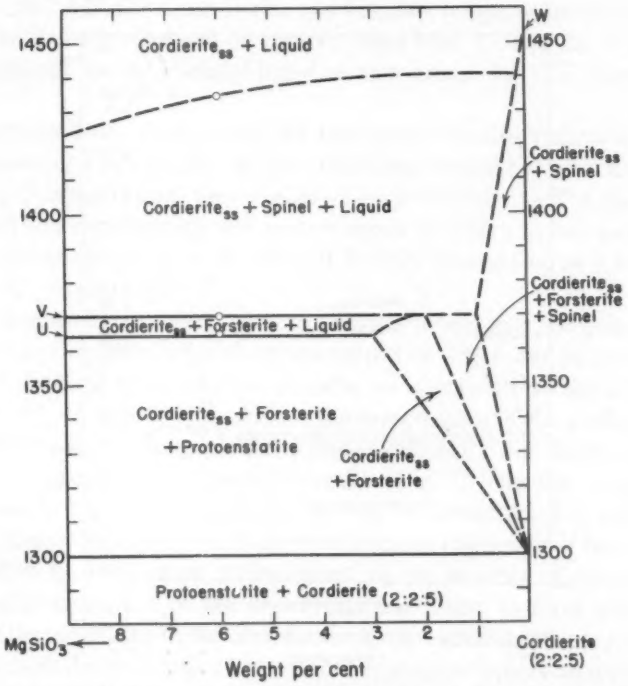

FIG. 9. Enlarged part of pseudobinary section cordierite (2:2:5)–$MgSiO_3$ shown in Fig. 8. The complicated subsolidus relations above 1,300° C can also be deduced from Fig. 7. The reader is reminded that this is a section through a ternary system. Above 1,300° C none of the phases except protoenstatite has a composition lying in the plane of this section.

from their liquidus temperatures, are joined by a pyroxene and a silica phase at approximately the same temperature (Table 2 (*c*)) which is close to the temperature of the ternary eutectic *S* determined as 1,355°±3° C (Fig. 3). Since all these compositions lie approximately on a straight line leading away from composition 2:2:5, the cordierites crystallizing out can be either of the composition 2:2:5 itself or of a composition which itself lies along this line. Compositions for the cordierite crystallizing, such as for instance 1:1:3, can thus be excluded.

Cordierite crystallizing from melt No. 24 is joined by a silica phase at about 1,368° C, while the one crystallizing from melt No. 26 is joined by a silica phase at about 1,413° C. This again indicates that the composition of cordierite in equilibrium with liquid cannot be 1:1:3 but must lie in the vicinity of 2:2:5.

Their exact composition, however, cannot be inferred from these data, because the slope of the boundary curve *SP* (cordierite+silica+liquid, Fig. 3), is not known accurately enough.

If 2:2:5 were the composition of all cordierites in equilibrium with liquid, the cordierite crystallizing from melts Nos. 28–33 should be joined by a pyroxene phase at the same temperature, which would have to be a temperature maximum

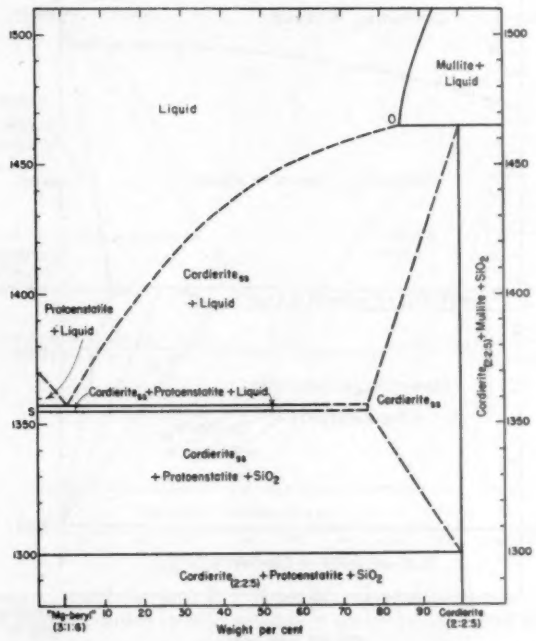

FIG. 10. Pseudobinary section going through cordierite (2:2:5) and the theoretical compound 'Mg–beryl' (3:1:6), i.e. following the line of cordierite solid solution according to the substitution of Mg+Si for 2Al. The maximum extent of the solid solution in cordierite at the various temperatures is not known very accurately.

along the boundary curve cordierite–protoenstatite. At this very temperature, pyroxenes crystallizing from melts Nos. 17 and 35–37 should be joined by cordierite, and this temperature should also be the liquidus temperature of composition No. 34, with pyroxene and cordierite crystallizing simultaneously.

The experimental results obtained show that cordierite in composition No. 28, upon cooling, is joined by small amounts of spinel at temperatures as high as 1,435° C; spinel disappears and forsterite comes in at about 1,370° C; forsterite is partially consumed and pyroxene comes in at about 1,365° C (Table 2 (*d*)). An analogous behaviour is shown by composition No. 29, with the exception that spinel does not come in until at 1,398° C. In composition No. 30 only very little spinel comes in at 1,375° C, whereas at 1,370° C forsterite appears, which

at 1,365° C largely reacts with remaining liquid to form a pyroxene. Composition No. 31, during its path of crystallization, never shows any spinel; cordierite is joined by forsterite at 1,367° C, which at 1,364° C largely disappears when pyroxene is formed. Compositions Nos. 32 and 33 do not show forsterite as the second crystalline phase but pyroxene directly, at 1,364° or 1,366° C, respectively. In compositions Nos. 17 and 35–37 protoenstatite is joined by cordierite at 1,367°±2° C, which is also the liquidus temperature of composition No. 34. The melting relations of compositions Nos. 17 and 28–37 are shown diagrammatically in the pseudobinary section along the join $MgSiO_3$–2:2:5 (Fig. 8).

Compositions Nos. 39–41 along the line 2:2:5–forsterite show a somewhat similar behaviour (Table 2 (*e*)). If the cordierites crystallizing from these melts were of 2:2:5 composition, they should all be joined by spinel at the same temperature. In the experiments, the temperatures at which spinel joins the cordierites in compositions Nos. 41, 40, and 39 were determined as 1,448°, 1,448°, and 1,440° C, respectively.

Interpretation of these data leads to the conclusion that the composition of the cordierite in equilibrium with liquid cannot be 2:2:5, but must be richer in SiO_2. Since the data obtained from liquidus investigations on the compositions Nos. 19, 21–27, 42, and 44 indicate that the composition of the cordierite cannot lie along the line 2:2:5–SiO_2, it is likely that it follows the line of $Mg+Si \rightarrow AlAl$ substitution suggested in the previous section (Fig. 7). This line of substitution is also shown in Fig. 11 as a light line marked by cross-bars. For the following discussion it is necessary to recall the fundamental relation that for equilibrium crystallization in any system, independent of the number of components involved, the composition of the first crystalline phase to form and the composition of the remaining liquid must lie along a straight line (= conjugation line) passing through the total bulk composition, as long as there is no second crystalline phase present. In the present case, the compositions of the liquids in equilibrium with cordierite for compositions Nos. 28–33 and 39–41, at temperatures infinitesimally above those of the appearance of a second crystalline phase, may be approximated from (1) the latter temperatures, (2) the nature of the second crystalline phase, and (3) the slopes of the boundary curves *VW* (cordierite+spinel+liquid), *UV* (cordierite+forsterite+liquid), and *US* (cordierite+$MgSiO_3$+liquid) (Fig. 3), which, however, are not known very accurately. Straight lines originating at these approximate liquid compositions, and passing through the requisite bulk compositions (light dashed lines of Fig. 11) at their intersection with the proposed line of cordierite solid solution, thus indicate the compositions of cordierite in equilibrium with liquid just before a second crystalline phase comes in. It can be seen from this scheme (Fig. 11) that the amount of solid solution in cordierite (2:2:5) is higher for bulk compositions farther away from 2:2:5 composition, but also that the solid solution at liquidus temperatures generally increases with decreasing temperature. On the basis of the

latter information the extension of cordierite solid solution along the pseudo-binary section cordierite (2:2:5)–'Mg–beryl' (3:1:6), as a function of temperature, has been shown tentatively in Fig. 10.

Detailed X-ray studies of the cordierites in equilibrium with liquid, taking into account their polymorphic changes, have yielded additional evidence for solid solution. The high-cordierites obtained from a number of compositions show shifts of peaks in comparison with high-cordierites of 2:2:5 composition, and

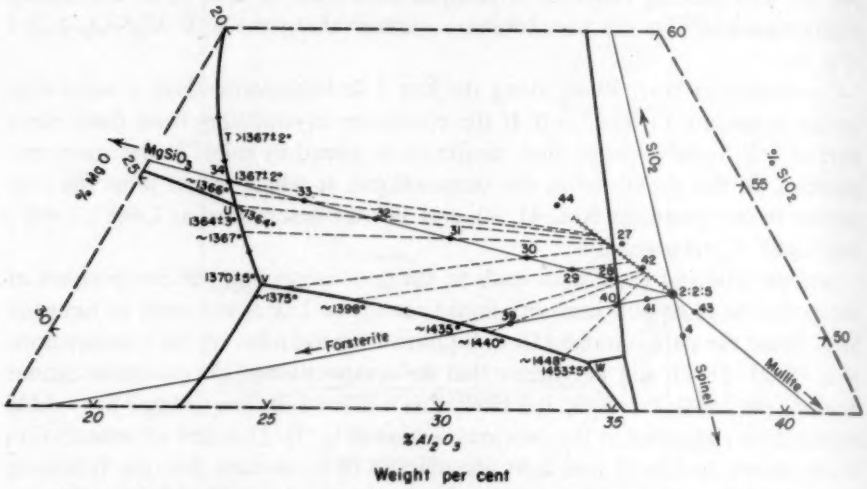

FIG. 11. Approximated conjugation lines for equilibrium crystallization of melts Nos. 28–34 and 39–40 (light dashes). The conjugation lines drawn for each melt are only valid for temperatures infinitesimally above those of the incoming of a second crystalline phase, in addition to cordierite, as determined experimentally (Table 2 and temperatures at the liquid ends of the conjugation lines in this figure). Liquid compositions at the latter temperatures have been assumed on the basis of the approximate knowledge of the slopes of the boundary curves cordierite+spinel+liquid, cordierite+forsterite+liquid, and cordierite+protoenstatite+liquid. On this basis, the intersections of the conjugation lines with the line of cordierite solid solution (solid line with cross bars) indicate the compositions of the cordierite solid solutions which crystallize from each melt just before they are joined by a second crystalline phase.

the transition from 'low'- to high-cordierite takes place in these compositions in a previously unknown fashion, for which a new variable, the intensity index *i*, is introduced. A more detailed account of these findings will be given in the section on structural changes of cordierite (I 1). It must be mentioned, however, that it was not possible to provide a quantitative basis for the determination of the composition of the cordierites, simply because these high-cordierites cannot be synthesized stably in the absence of liquid. It is possible, however, to distinguish in a qualitative way between relatively MgSi-rich high-cordierites and others closer to the composition 2:2:5. With the aid of such X-ray studies, it has been found that the most extensive solid solutions occur in high-cordierites which crystallize from melts Nos. 31–33 and 23–25 at temperatures just below their liquidus

temperatures. All the compositions closer to that of 2:2:5 seem to produce high-cordierites with a narrower range of solid solution, even at the highest temperatures. This is in agreement with the approximated conjugation lines of Fig. 11, as well as the extension of cordierite solid solution, as a function of temperature, as indicated in Fig. 10.

In conclusion, it may be stated that experimental liquidus investigations have yielded additional evidence for the existence of a largely binary solid solution in cordierite following a Mg+Si for 2Al lattice substitution.

G. REFINEMENT OF THE EQUILIBRIUM DIAGRAM OF THE SYSTEM MgO–Al_2O_3–SiO_2

The major refinement of the equilibrium diagram of the system MgO–Al_2O_3–SiO_2 worked out in this study is the variability of the composition of the ternary compound cordierite, which was discussed in the previous section. In the course of our studies new data were also obtained defining more precisely the temperatures and compositions of some of the invariant points, the precise locations of boundary curves, and the temperatures of certain temperature maxima in the system. The new data are evaluated in this section.

Rankin & Merwin (1918) gave the temperature of the ternary reaction point *P* (cordierite+mullite+silica+liquid, Fig. 3) as 1,425°±5° C, and its composition as 10·0 MgO, 23·5 Al_2O_3, 66·5 SiO_2. Schairer (1954), on the basis of data obtained in the quaternary system K_2O–MgO–Al_2O_3–SiO_2, has pointed out that this temperature must be too low, and that it should lie between 1,435°±5° C and 1,448°±5° C. In our present work there were six compositions, namely Nos. 12–16 and 18, that provided information regarding this question. The data obtained from quenching runs are given in Table 3. They indicate that the temperature of the ternary point *P* is 1,440°±3° C and its composition is 9·25 MgO, 22·50 Al_2O_3, 68·25 SiO_2. This leads to a slight enlargement of the stability field of cordierite at the expense of the silica field given in the original equilibrium diagram. At the temperature 1,440°±3° C the three crystalline phases mullite, cordierite, and cristobalite coexist with liquid. For all compositions lying along the line 2:2:5–SiO_2, no liquid should be present below this temperature. Table 2 shows that, for all six compositions, liquids form at temperatures ranging from 1,425° to 1,430° C. These liquids coexist with cordierite and cristobalite alone, and there is no mullite present, with only one exception (No. 16, 1,435° C, Table 2 (*b*)). The amounts of liquid developing are by no means small; above 1,425° C the charges were found to be well fritted. This behaviour, although not in accordance with that of a ternary invariant point, is probably the reason for the low temperature assigned by Rankin & Merwin (1918). The explanation of this phenomenon is not problematic for compositions Nos. 14 and 18, which lie slightly off the line 2:2:5–SiO_2 within the triangle 2:2:5–$MgSiO_3$–SiO_2. They should, therefore, develop liquid at a much lower temperature (1,355° ±3° C). Depending on how far off the line 2:2:5–SiO_2 the compositions lie, the amounts of liquid may increase considerably at temperatures around 1,430° C.

TABLE 3

Results of quenching experiments bearing upon temperature and composition of the ternary reaction point P

(*cordierite*+*mullite*+SiO_2+*liquid, Fig. 3*)

Composition No.	*Temp., °C*	*Time, hours*	*Results of optical and X-ray examination*
12	1,450	70	Moderate amount mullite in glass
	1,445	96	Moderate amount mullite and rare cordierite in glass
	1,442	96	Moderate amount mullite and rare cordierite in glass
	1,440	120	Moderate amount cordierite and moderate amount cristobalite in glass
	1,438	24	Lots cordierite, lots cristobalite in glass, no mullite
	1,435	120	Lots cordierite, lots cristobalite, some glass
	1,430	72	Lots cordierite, lots cristobalite, some interstitial glass
13	1,445	96	Moderate amount mullite in glass
	1,442	96	Moderate amount cordierite, moderate amount cristobalite, and rare mullite in glass
	1,440	120	Moderate amount cordierite, lots cristobalite, and rare mullite in glass
	1,440	22	Moderate amount cordierite and moderate amount cristobalite in glass, no mullite
	1,438	24	Lots cordierite, lots cristobalite in glass
	1,435	72	Lots cordierite, lots cristobalite, interstitial glass
	1,430	72	Lots cordierite, lots cristobalite, little interstitial glass
14	1,445	70	Rare mullite in glass
	1,440	72	Rare mullite in glass
	1,437	48	Moderate amount cordierite, moderate amount cristobalite in glass, no mullite
	1,437	72	Moderate amount cordierite, moderate amount cristobalite, very rare mullite in glass
	1,435	70	Moderate amount cordierite, small amount cristobalite in glass
15	1,445	72	Small amount cristobalite, small amount mullite in glass
	1,440	66	Small amount cristobalite, small amount mullite in glass
	1,440	22	Small amount cristobalite and rare cordierite in glass, no mullite
	1,435	120	Rare cristobalite and moderate amount cordierite in glass
	1,430	96	Moderate amount cordierite and moderate amount cristobalite in glass
16	1,445	22	Moderate amount cristobalite, moderate amount mullite in glass
	1,442	96	Moderate amounts cristobalite and mullite in glass
	1,440	66	Moderate amounts cristobalite, cordierite, and mullite in glass
	1,437	72	Moderate amounts cordierite, mullite, and cristobalite in glass
	1,435	72	Moderate amounts cordierite and cristobalite, and rare corroded mullite in glass
	1,430	672	Lots cordierite, lots cristobalite, interstitial glass, no mullite
18	1,445	72	All glass
	1,440	120	Small amounts cordierite and cristobalite in glass
	1,438	48	Lots cordierite, lots cristobalite in glass
	1,430	96	Lots cordierite, lots cristobalite, interstitial glass
	1,425	74	Lots cordierite, lots cristobalite, small amount interstitial glass

This explanation, however, does not hold for compositions Nos. 12–13 and 15–16, as well as for all the other compositions along the line 2:2:5–SiO_2 as given in Table 2 (*b*). Solid solution in cordierite, or even cristobalite, cannot be responsible for the low melting temperatures either, as a study of an isothermal section at about 1,430° C reveals. The explanation has to be sought in the presence of impurities, particularly alkalis, in the melts. If one assumes that all the 0·05 wt per cent alkalis found by analysis (see section on preparation of mixtures) are Na_2O, and that this is tied up completely in the mineral albite, one arrives at a normative amount of albite in the mixture of as much as about 0·4 wt per cent. Our mixture thus consists of cordierite, silica, and albite. The melting relations of this plane were given by Schairer (1957, p. 219, fig. 50). It can be seen from this diagram that the composition of the liquid, which is in equilibrium with both cordierite and a silica phase at temperatures around 1,430° C, is very close to the side line cordierite–silica of the diagram. This shows that an amount of 0·4 wt per cent albite, present in addition to cordierite and silica, may result in the formation of as much as about 10 wt per cent liquid at these temperatures. It is concluded, therefore, that the premature formation of liquid below 1,440° C, in bulk compositions lying along the line 2:2:5–SiO_2 in the ternary system MgO–Al_2O_3–SiO_2, is caused by impurities in the chemicals from which the melts were prepared and thus is not a feature of the ternary system MgO–Al_2O_3–SiO_2.

In a similar manner the temperature and composition of the ternary eutectic *S* (cordierite+protoenstatite+silica+liquid, Fig. 3) was checked by means of compositions Nos. 19–22. Table 4 gives the results of the quenching runs. The data indicate a temperature of 1,355°±3° C and a composition 20·50 MgO, 17·50 Al_2O_3, 62·00 SiO_2 for this eutectic, which differ slightly from Rankin and Merwin's values (1,345°±5° C; 20·3 MgO, 18·3 Al_2O_3, 61·4 SiO_2). Table 4 shows that there is formation of only small amounts of liquid about 5° below the temperature of the eutectic. According to the phase rule, in a ternary system three solid phases cannot be in equilibrium with a liquid and vapour over a range of temperatures. It is probable, therefore, that the premature formation of liquid is also to be explained by impurities of the chemicals, as previously mentioned.

No compositions were prepared specifically to check the temperature and location of the ternary point *U* (cordierite+protoenstatite+forsterite+liquid, Fig. 3), which was given by Rankin & Merwin (1918) as 1,360°±5° C and 25·0 MgO, 21·0 Al_2O_3, 54·0 SiO_2. Data on the melting relations of compositions Nos. 28–31 as described in the previous section, partly shown in Figs. 8 and 11 and summarized in Table 2 (*d*), seem to indicate a slightly higher temperature, which is tentatively given as 1,364°±3° C. Composition No. 34 has its liquidus point on the boundary curve cordierite–protoenstatite. Therefore, the composition of the ternary point *U* may lie very slightly closer toward the MgO–SiO_2 side of the diagram than was given by Rankin and Merwin. The liquidus temperature of composition No. 34 was determined as 1,367°±2° C. At the same temperature cordierite joins protoenstatite, in the melts Nos. 35–37 and 17, independent of

TABLE 4

Results of quenching experiments bearing upon temperature and composition of the ternary eutectic S

(*cordierite+protoenstatite+*SiO_2*+liquid, Fig. 3*)

Composition No.	*Temp., °C*	*Time, hours*	*Results of optical and X-ray examination*
19	1,360	168	Rare cordierite in glass
	1,355	168	Small amount cordierite and rare protoenstatite in glass, no silica phase
	1,354	336	Moderate amounts cordierite, pyroxene, and tridymite in glass
	1,350	120	Lots cordierite, lots pyroxene, lots tridymite, interstitial glass
20	1,360	168	All glass
	1,355	120	Moderate amounts cordierite, pyroxene, tridymite, and cristobalite in glass
	1,350	120	Lots cordierite, lots pyroxene, lots cristobalite, a little interstitial glass
21	1,360	456	Rare cordierite in glass
	1,357	120	Small amount cordierite in glass
	1,355	120	Moderate amounts cordierite, pyroxene, and tridymite plus some cristobalite in glass
	1,350	120	Lots cordierite, lots pyroxene, lots cristobalite, a little interstitial glass
22	1,360	168	Rare cordierite in glass
	1,355	74	Small amount cordierite, rare cristobalite in glass
	1,354	336	Moderate amounts cordierite, pyroxene, and tridymite in glass
	1,350	120	Lots cordierite, lots pyroxene, lots tridymite, some cristobalite, interstitial glass

the bulk composition. This fact eliminates solid solution in the phase protoenstatite. It is believed that the small temperature difference between this point (1,367°±2° C) and the ternary point *U* (1,364°±3° C) is a real one. Since all conceivable joins for $MgSiO_3$–cordierite solid solution intersect the boundary curve between the stability fields of these two phases at the liquidus, there has to be a temperature maximum along this boundary curve. According to Fig. 11 it can be predicted that the cordierite solid solution crystallizing at this maximum temperature will be very MgSi-rich. The alleged maximum *T* (Figs. 3 and 11), therefore, has to lie at a more siliceous composition than No. 34 and its temperature is presumably slightly higher than 1,367°±2° C. The slopes of the boundary curve from the inferred maximum *T* toward the two eutectics *S* and *U* (Fig. 3) are, presumably, very gentle.

The melting relations of compositions Nos. 28–30 and 38–41 (Table 2 (*e*)) indicate that the temperature of the ternary point *V* (cordierite+forsterite+spinel+liquid, Fig. 3), given as 1,370°±5° C by Rankin and Merwin, is essentially correct.

New data also give a more precise location of parts of the boundary curve cordierite–mullite. The position of the curve, drawn in Figs. 3 and 4, is based on

quenching runs on compositions Nos. 26, 28, and 40, which show a cordierite liquidus, and on compositions Nos. 27, 41, and 42, which lie in the mullite field. Since the extension of the join between mullite and cordierite intersects the boundary curve between the liquidus stability fields of these two phases, there has to be a temperature maximum also along this boundary curve. At this maximum (*O*, Fig. 3), mullite crystallizing from a melt of pure cordierite of 2:2:5

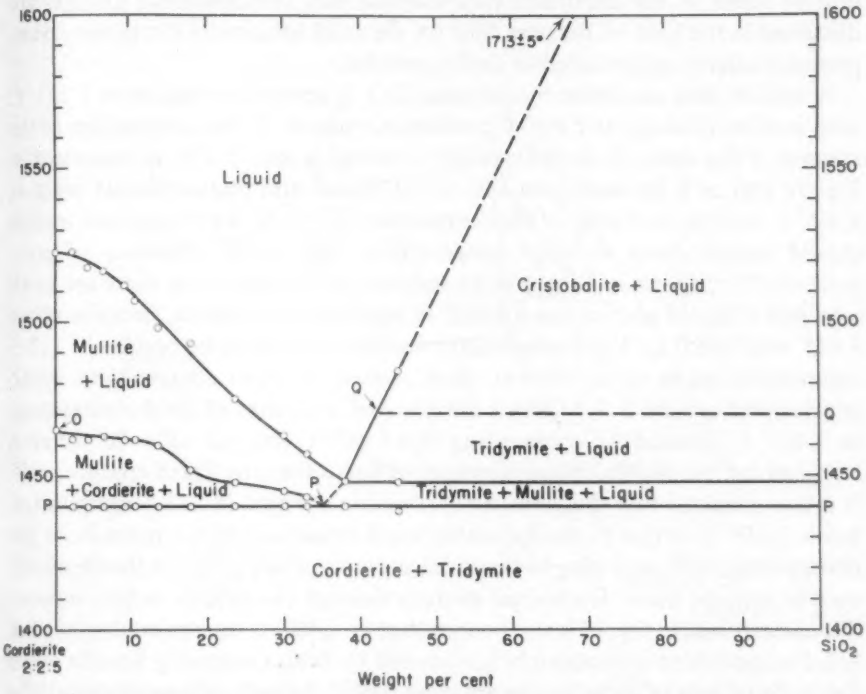

FIG. 12. Pseudobinary section cordierite (2:2:5)–SiO_2. Assumption: No solid solution in any of the solid phases.

composition is joined by cordierite. This temperature, which also applies to the incoming of cordierite in melts Nos. 27, 42, and 43, was determined as 1,465°± 2° C. It is clearly above the temperature of the ternary reaction point *N* (sapphirine+mullite+cordierite+liquid, Fig. 3), at 1,460°±5° C as determined by Keith & Schairer (1952). The slopes of the boundary curve cordierite–mullite on both sides of the maximum at *O* can be inferred from the temperatures at which mullite is joined by cordierite in melts Nos. 3–12, 1:1:3, 27, and 41–42. These temperatures apply to points which lie at the intersection of the boundary curve with straight lines (conjugation lines) leaving a mullite composition and going through the various compositions themselves. (Mullite solid solution, if any, cannot be determined from these data.) Table 2 lists these temperatures and Figs. 6 and 12 give pseudobinary diagrams for the joins 2:2:5–spinel and SiO_2–2:2:5.

It can be seen that the slopes of the boundary curve cordierite–mullite, from the maximum *O* toward the invariant points *N* and *P*, are rather gentle, with the exception of one steeper portion along *OP* (Fig. 12).

H. MELTING RELATIONS IN THE SYSTEM MgO–Al_2O_3–SiO_2

In this section the melting relations, or, conversely, the courses of crystallization of some of the important compositions and compositional groups, are discussed in the light of the new data on the solid solution in the ternary compound cordierite as described in earlier sections.

A melt of ideal cordierite composition (2:2:5) starts to crystallize at 1,523° C with mullite forming. At 1,465° C cordierite comes in. If the composition of the summit of the sheet of cordierite solid solutions is also 2:2:5, as suggested in Fig. 10 and as it appears from Fig. 11, all liquid and mullite should react at 1,465° C to form cordierite of the composition 2:2:5. Neither liquid nor mullite should remain down to lower temperatures. The actual behaviour of composition 2:2:5 (given in Table 2 (*b*)) is somewhat different in that there are small amounts of liquid and mullite present, in addition to cordierite, between about 1,445° and 1,465° C. This phenomenon was the same for three batches of 2:2:5 composition made up at different times. Among all other compositions which are clustered around 2:2:5 there is not one which remains all solid cordierite up to 1,465° C. Instead of representing the 1,465° C summit of solid solution searched for, they exhibit larger amounts of liquid than the 2:2:5 mixture itself. It is thus assumed that the premature formation of liquid in 2:2:5 composition below 1,465° C is due to the inevitable small deviations of the melts from the desired compositions, owing to the small amounts of impurities in the chemicals used to prepare them. Isothermal sections through the ternary system support this assumption. In Fig. 13 it can be seen that at 1,460° C the projection point of 2:2:5 composition is completely surrounded by fields containing liquids. Since the compositions of these liquids are close to 2:2:5 itself, only small deviations of the ideal 2:2:5 composition would result in the development of appreciable amounts of liquid. For example, a deficiency of about 0·25 wt per cent SiO_2 in the 2:2:5 bulk composition prepared could result in the development of as much as 8 wt per cent of liquid at 1,460° C. The presence of alkalis, which was discussed in a previous section, not only introduces more components into the system, but also changes the desired ratios of MgO, Al_2O_3, and SiO_2. The coexistence of mullite and cordierite with liquid in composition 2:2:5 indicates that the tendency of error is toward a composition lying closer to the Al_2O_3–SiO_2 side of the ternary diagram (Fig. 13). The fact that compositions Nos. 27–28 and 40–42 at 1,460° C consist of cordierite and liquid, without any mullite present, also supports the view that the composition of the cordierite crystallizing at this temperature lies very close to 2:2:5 (Fig. 13). The structural behaviour of the cordierite in 2:2:5 composition provides further support for this assumption (compare section I 3 (*a*)).

Bulk compositions other than 2:2:5 on the line of binary cordierite solid solution, when heated above 1,300° C, gradually lose their phases pyroxene and SiO_2, but should not develop liquid until the field marked 'cordierite$_{ss}$' in the

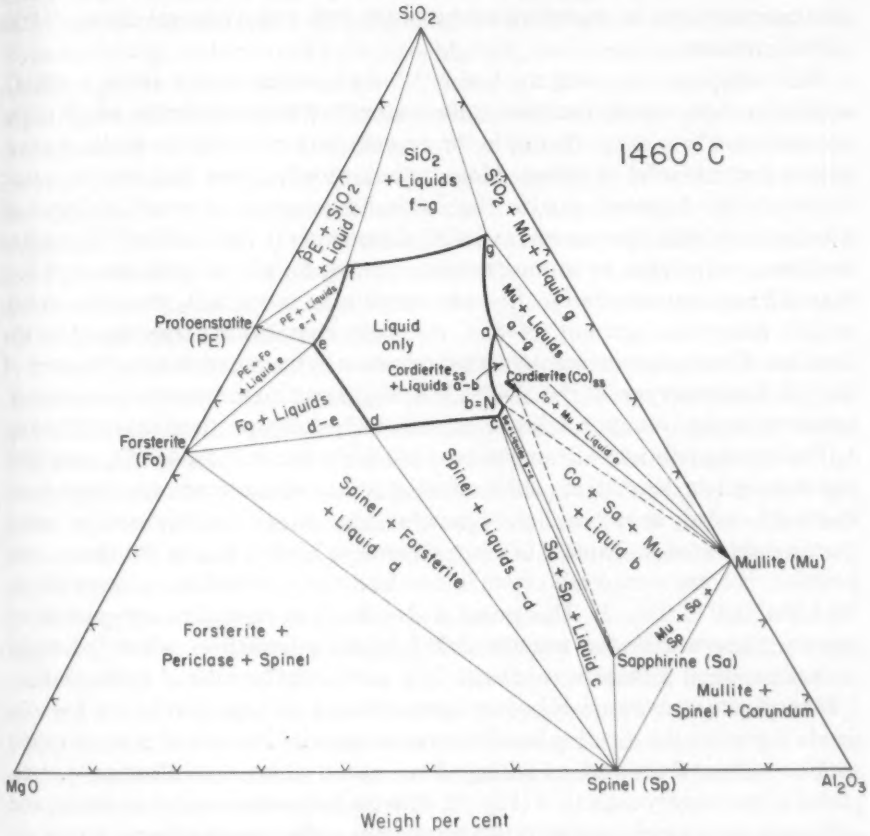

FIG. 13. Isothermal section through the system MgO–Al_2O_3–SiO_2 at 1,460° C, i.e. the temperature of the invariant point N (cordierite + sapphirine + mullite + liquid, Fig. 3). Notice the binary range of cordierite solid solution (all solid at this temperature), which is completely surrounded by two-, three-, and four-phase regions containing liquid. The dashed lines within the four-phase region cordierite + sapphirine + mullite + liquid b connect the pairs of phases involved in the reaction taking place at the invariant point N: sapphirine + cordierite $\rightleftharpoons$ mullite + liquid b. No solid solution is assumed in any of the solid phases except cordierite.

section of Fig. 10 is passed through. Composition No. 27 as well as No. 42, however, is not close enough to this line, i.e. in the plane of Fig. 10, to yield critical data. In both cases liquid develops in extremely small quantities as low as 1,355° C, but does not increase appreciably until temperatures around 1,440° C are reached.

Other compositions lying in the triangle 2:2:5–$MgSiO_3$–SiO_2 behave in a

similar fashion. Above about 1,300° C the composition of the cordierite changes gradually at the expense of small amounts of pyroxene and SiO_2, but in the absence of liquid, which does not develop until at 1,355° C, the temperature of the ternary eutectic *S* (Fig. 3). Compositions lying in the cordierite field may show curved paths of crystallization because of the compositional changes of the phase cordierite.

Bulk compositions along the line 2:2:5–SiO_2, when heated above 1,400° C, appear to show a small decrease in the amounts of free cristobalite, which might be attributed to a slight change in the composition of cordierite along the suggested line of solid solution. Liquid, theoretically, does not develop until 1,440°±3° C; however, due to the inevitable presence of small amounts of alkalis, liquid may form as low as 1,425° C (section G). At 1,440°±3° C, mullite develops and persists up to the complete melting for all compositions with less than 67 per cent total SiO_2. In melts containing more SiO_2 than this value, mullite disappears again at 1,448° C with only cristobalite persisting up to the liquidus. These relations are shown in projection in the pseudobinary diagram of Fig. 12. The ternary point *P* (1,440°±3° C, Fig. 3) is also the place where all compositions in the triangle cordierite–mullite–SiO_2 complete their crystallization.

The melting relations of compositions along the line 2:2:5–$MgSiO_3$, and their significance for determining solid solution in the phase cordierite, have been discussed already in section F 2. A pseudobinary diagram of this section, based on the data listed in Table 2 (*d*), is presented in Figs. 8 and 9. All these compositions become completely crystalline at the temperature of the ternary eutectic *U* (1,364°±3° C, Fig. 3). This point is also the final crystallization goal of all compositions within the triangle 2:2:5–$MgSiO_3$–forsterite, whose paths of crystallization, if within the cordierite field, are curved because of solid solution.

If cordierite were invariably of the composition 2:2:5, the join 2:2:5–$MgSiO_3$ would represent the dividing line between two general courses of crystallization with or without fractionation taking place: one in which crystallization is completed at the ternary eutectic *S* (Fig. 3), with the formation of a silica phase, and a second one in which crystallization terminates at the ternary eutectic *U* (Fig. 3), with the formation of forsterite in addition to cordierite and $MgSiO_3$. Because of the solid solution in cordierite at liquidus temperatures this divide is now displaced slightly toward the SiO_2 corner of the diagram, and for complete fractional crystallization coincides with a fractionation curve connecting 2:2:5 composition with the temperature maximum *T* (Fig. 3). For crystallization without fractionation, the divide is given by an equilibrium curve between 2:2:5 composition and *T*.[1] The difference between the two types of curves is that the equilibrium curve has a stronger curvature than the fractionation curve. For this

[1] Because of the incongruent melting of the phase cordierite, that portion of the fractionation, as well as the equilibrium curve lying between 2:2:5 composition and the boundary curve mullite–cordierite, is, of course, imaginary. For derivation of fractionation curves for binary solid solutions in ternary systems and their relations to the conjugation lines and equilibrium curves for equilibrium crystallization as indicated in Fig. 11, see the paper by Osborn & Schairer (1941).

reason, the displacement of the above-mentioned divide is even more pronounced under equilibrium conditions than with fractionation taking place. Under any circumstance, the courses of crystallization of certain melts, which below 1,300° C should consist of cordierite (2:2:5), $MgSiO_3$, and small amounts of SiO_2, will cross the join 2:2:5–$MgSiO_3$ and terminate at the ternary eutectic *U*, precipitating cordierite solid solution, $MgSiO_3$, and forsterite rather than SiO_2. Under equilibrium conditions a solid state reaction will take place below 1,300° C, in which, essentially, forsterite reacts with cordierite solid solution to form cordierite (2:2:5), more $MgSiO_3$, and free SiO_2. In the case of fractionation, however, in which crystals of cordierite solid solution have been effectively removed from the system, forsterite will remain among the final crystalline products, even below 1,300° C. Fractionation thus causes a depletion of these melts in normative SiO_2. For melts lying on the other side of the divide yet not too far away from it, fractionation will have the opposite effect of an enrichment of the residual liquids in normative SiO_2.

It may be of interest in this connexion that density determinations at room temperature showed that crystalline cordierite is less dense than its own glass as well as the one in equilibrium with mullite at 1,465° C (= composition No. 27); data will be given in section I 1. These relations might be reversed at high temperatures due to the almost negligible thermal expansion of cordierite. If not, it has to be concluded that cordierite would float on certain melts with which it is in equilibrium. A special type of fractionation dependent on this property would thus be achieved.

Bulk compositions along the line 2:2:5–forsterite, as well as within the triangle 2:2:5–forsterite–spinel, without fractionation complete crystallization at the ternary point *V* (1,370°±5° C, Fig. 3). A representative composition exhibiting this behaviour is the one of the Mg–garnet pyrope ($3MgO \cdot Al_2O_3 \cdot 3SiO_2$), which is not stable at atmospheric pressure (Chinner & Schairer, 1960). Curving of the paths of crystallization due to cordierite solid solution only occurs in those compositions lying relatively close to 2:2:5.

Certain compositions within the triangle 2:2:5–forsterite–spinel, as well as all those occurring in the triangle 2:2:5–spinel–mullite, contain the second ternary compound sapphirine either at subsolidus temperatures or at least over a narrow range of temperatures in the presence of liquid. The paths of crystallization of compositions along the line 2:2:5–spinel have already been discussed in the section on sapphirine and are shown in projection on the pseudobinary diagram of Fig. 6. The binary solid solution in cordierite does not have appreciable effects, if any, on the melting relations in this part of the diagram.

I. STRUCTURAL CHANGES OF THE TERNARY COMPOUND CORDIERITE

In this section the polymorphic changes of the ternary compound cordierite, that occurred during the heat treatment of the various compositions, will be discussed. Since these relations were found to be extremely complex, it may be

of help to the reader to preview some of the conclusions drawn from the experimental data.

(1) For each temperature *stable* and *metastable* structural states of cordierite have to be distinguished. High-cordierite is the first structural state to form at any temperature. With continued heating at appropriate temperatures metastable high-cordierite goes through a gradual structural transition, strictly as a function of time, toward low-cordierite which is the stable form at relatively low temperatures. In the experiments this truly stable form, low-cordierite, could not be ascertained but only closely approached. It is believed, however, that this approach was close enough to show in a general way the stable relations among the cordierite polymorphs. On this basis 'low'-cordierite, as defined in section B, is assumed to be representative for the truly stable low-temperature form, which is yet unknown.

(2) The *stable* relations among the cordierite polymorphs present in the various mixtures, which are, of course, independent of time, are not only dependent on temperature (at constant pressure), but also on the bulk composition of the particular mixture. Irrespective of the amount of solid solution present in cordierite, high-cordierite is not a stable phase at any temperature in bulk compositions with relatively low ratios of Al_2O_3/SiO_2. In bulk compositions with intermediate Al_2O_3/SiO_2 ratios, high-cordierite forms stably only in the presence of much liquid, and in those with relatively high Al_2O_3/SiO_2 ratios a stable transition from 'low'- to high-cordierite takes place even below the solidus. Furthermore, the temperatures at which the cordierite transitions take place in the two latter ranges of bulk compositions, i.e. those with intermediate and high Al_2O_3/SiO_2 ratios, are also a sensitive function of total bulk composition.

(3) The presence of cordierite solid solutions in certain bulk compositions with intermediate Al_2O_3/SiO_2 ratios, at temperatures above 1,300° C, affects the relations outlined in (2), only in such a way that the gradual transition from 'low'- to high-cordierite takes place in a manner which cannot be described by the variable distortion index Δ. For this reason a new variable, the intensity index *i*, is introduced. It is to be emphasized, however, that the use of this variable is confined to the description of structural changes of cordierites with high amounts of 'Mg–beryl' in solid solution.

In the following sections the reader will be acquainted first with the experimental data on the structural behaviour of cordierites. Seemingly conflicting results, described in different sections, should be seen in relation to their dependence on total bulk composition. Finally, in the last section (I 5), a comprehensive evaluation is attempted on the basis of a synopsis of all the results.

1. *Characterization of the polymorphs encountered*

Since the synthetic cordierites were in all cases very fine grained and mostly intimately intergrown, no optical constants could be determined to verify the polymorphic form. The most sensitive value in this respect would be the axia

angle $2V_\alpha$, which should be 0° for high-cordierite and in the vicinity of 90° for 'low'-cordierite. Even in cases where cordierite formed rather long pseudo-hexagonal hollow prisms embedded in glass, the crystals were too small for the determination of $2V$. No values of α, β, and γ could be obtained, but only a mean refractive index $n_m = (n_\alpha + n_\beta + n_\gamma)/3$, which was found to be about $1{\cdot}524 \pm 0{\cdot}003$. The birefringence was approximated by comparison with powder aggregates of material of known birefringence and similar grain size. It was found to be clearly lower than that of quartz. Rankin & Merwin (1918) report a value of 0·003–0·004. By very careful observations in immersion oils at constant temperature, a small difference in the mean index of refraction could be observed between high-cordierites and 'low'-cordierites, both of which were crystallized from the 2:2:5 composition. The value obtained for 'low'-cordierite prepared by devitrifying glass at 1,420° C for 102 hours, was 1·523; the index for high-cordierite prepared by devitrifying glass at 1,000° C for 14 days was 1·526. Intermediate states should have mean indices between these two values, both of which actually lie within the error of determination.

It is thus clear that the determination of the structural state of synthetic cordierites grown in this study is fully dependent on measurements by X-ray powder diffraction patterns. X-ray diffraction data up to 64° 2θ, of a high-cordierite of 2:2:5 composition, are given in Table 5. All the observed reflections can be indexed on the basis of a hexagonal unit cell with dimensions $a = 9{\cdot}7698$ Å and $c = 9{\cdot}3517$ Å. These values are in reasonable agreement with those given by Miyashiro *et al.* (1955) for 'α-$Mg_2Al_4Si_5O_{18}$' ($a = 9{\cdot}782$ Å, $c = 9{\cdot}365$ Å). In comparison with the X-ray data reported by these authors, seven more reflections were found in this study for the same range of 2θ, which, however, are still compatible with the space group $P6/mcc$ (D_{6h}^2). From these X-ray data the calculated density of high-cordierite was found to be 2·513 and the calculated mean refractive index, following the Gladstone–Dale relationship, 1·524. This is in good agreement with the measured value of 1·526.

Table 6 shows the powder diffraction data of a 'low'-cordierite of 2:2:5 composition with a distortion index Δ of 0·25°. This very complicated pattern is characterized by a number of peak doublets and triplets, which have developed from single peaks in hexagonal high-cordierite. The pattern was indexed on the basis of an orthorhombic cell with dimensions $a = 17{\cdot}0621$, $b = 9{\cdot}7208$, $c = 9{\cdot}3389$, space group $Cccm$ (D_{2h}^{20}). From these cell dimensions the calculated density of 'low'-cordierite was found to be 2·507 and the calculated mean refractive index, according to the Gladstone–Dale relationship, 1·523. This is in perfect agreement with the optically determined value of 1·523.

A comparison of the cell dimensions of high- and 'low'-cordierite as given above shows that for 'low'-cordierite the lattice has not only been distorted in a direction perpendicular to the c-axis, but has also slightly contracted parallel to c. This indicates that the length of the unit cell edge c or the Bragg angle 2θ of related reflections such as (004) (Iiyama, 1956) can only be used incontrovertibly

TABLE 5

Powder X-ray diffraction data of high-cordierite crystallized from glass of the composition $2MgO \cdot 2Al_2O_3 \cdot 5SiO_2$ *at 1,000° C for 16 days*

(Copper $K_{\alpha 1}$ radiation)*

hkl	2θ	I/I_0	d_{obs}	d_{calc}
100	10·43	100	8·475	8·461
110	18·14	32	4·886	4·885
002	18·96	15	4·677	4·676
102	21·70	51	4·092	4·092
112	26·35	57	3·379	3·378
202	28·42	66	3·138	3·137
211	29·48	86	3·027	3·026
212	33·93	26	2·640	2·640
220	36·79	6	2·441	2·442
302	37·22	4	2·414	2·415
004	38·47	12	2·338	2·338
311	39·57	5	2·276	2·276
104	40·00	<1	2·252	2·254
213	40·39	5	2·231	2·232
222	41·68	6	2·165	2·165
114	42·87	8	2·108	2·109
312	43·08	12	2·098	2·097
204	44·23	3	2·046	2·046
320	46·76	8	1·941	1·941
402	47·12	6	1·927	1·927
321	47·79	3	1·9014	1·9006
214	48·20	4	1·8863	1·8875
313	48·51	15	1·8750	1·8748
410	49·32	6	1·8461	1·8463
411	50·34	7	1·8111	1·8114
304	50·68	9	1·7997	1·7999
412	53·29	3	1·7179	1·7173
224	54·29	28	1·6882	1·6889
314	55·44	3	1·6559	1·6562
323	55·76	4	1·6472	1·6477
330	56·45	4	1·6286	1·6283
215	56·97	3	1·6150	1·6145
420	57·60	6	1·5988	1·5990
413	58·01	9	1·5885	1·5886
404	58·80	2	1·5690	1·5685
006	59·24	3	1·5584	1·5586
332	60·12	3	1·5377	1·5377
106	60·35	1	1·5325	1·5329
324	62·09	8	1·4935	1·4934
116	62·48	5	1·4852	1·4849
315, 206	63·56	5	1·4625	1·4625

* With the technique in use at the National Bureau of Standards (Standard X-ray Diffraction Powder Patterns, N.B.S. Circular 539) possible errors in the *d*-values caused by the failure to recognize K_{α_2} reflections at low angles 2θ are largely eliminated by the use of an internal standard also defined on the basis of K_{α_1} throughout the pattern.

TABLE 6

Powder X-ray diffraction data of 'low'-cordierite ($\Delta = 0{\cdot}25°$) crystallized from glass of the composition $2MgO \cdot 2Al_2O_3 \cdot 5SiO_2$ at 1,000° C for 3 days, then at 1,180° C for 3 days, and finally at 1,380° C for 7 days

(Copper $K_{\alpha 1}$ radiation)*

hkl	2θ	I/I_0	d_{obs}	d_{calc}
200	10·36	100	8·532	8·531
110	10·46	95	8·450	8·446
310	18·05	30	4·910	4·909
020	18·24	14	4·860	4·860
002	18·99	17	4·669	4·669
400	20·80	1	4·267	4·265
112	21·73	72	4·086	4·086
312	26·33	56	3·381	3·383
022	26·43	48	3·369	3·367
510	27·70	<1	3·217	3·220
420	27·80	1	3·206	3·206
402	28·32	40±	3·149	3·149
222	28·47	64	3·132	3·132
511	29·34	53	3·041	3·044
421	29·42	53	3·033	3·032
131	29·63	40	3·012	3·013
600	31·47	1	2·840	2·844
512	33·79	16	2·650	2·651
422	33·87	18	2·644	2·643
132	34·05	9	2·631	2·630
620	36·59	3·5	2·454	2·454
040	36·96	4·5	2·430	2·430
332	37·28	3	2·410	2·411
621	37·88	1	2·373	2·374
004	38·54	11	2·334	2·335
711	39·27	2	2·292	2·292
531	39·52	2	2·278	2·279
241	39·72	1	2·267	2·267
204	40·00	1	2·252	2·251
423	40·34	3	2·234	2·233
133	40·50	2	2·225	2·226
622	41·53	4	2·173	2·173
042	41·87	1	2·156	2·156
800	42·36	<1	2·132	2·133
712	42·88	7	2·107	2·109
532	43·05	6	2·099	2·099
242	43·22	5	2·091	2·090
333	43·30	5	2·088	2·088
224	44·28	2	2·044	2·043
820	46·44	2	1·954	1·953
730	46·58	4	1·948	1·948
802	46·80	3	1·938	1·940
150	46·98	2	1·932	1·932
442	47·20	3	1·924	1·924
821	47·52	1	1·911	1·912
151	48·05	1	1·892	1·892
424	48·15	2	1·888	1·888
314, 713	48·33	5	1·882	1·883
533	48·52	7	1·875	1·875
243	48·66	7	1·870	1·869
910	48·93	3	1·860	1·861
640	49·30	2	1·847	1·847
350	49·51	2	1·839	1·840
115	49·93	1	1·825	1·824
641	50·33	2	1·811	1·812
604, 351	50·54	5	1·804	1·804
334	50·74	6	1·798	1·797

* See footnote for Table 5.

for determination of composition of cordierites with identical structural states. It may be of interest to note that the measured values $2\theta_{(004)}$ for the high- and 'low'-cordierite of the composition $2MgO \cdot 2Al_2O_3 \cdot 5SiO_2$ synthesized in this study would, according to Iiyama's (1956) curve, indicate ratios $\frac{Fe^{+2}+Mn}{Fe^{+2}+Mn+Mg} \times 100$ of 5 and 15, respectively. Furthermore, an independent variation of the cell dimension c with solid solution within the system MgO–Al_2O_3–SiO_2 could be shown qualitatively in this study; because of structural changes occurring concomitantly, however, it was not possible to use this variation for determinative purposes.

The most pronounced differences between the powder X-ray patterns of high- and 'low'-cordierite given in Tables 5 and 6 are observed near the following values of 2θ for copper $K\alpha$ radiation: 18°, two peaks in 'low'-cordierite instead of one in high-cordierite; 28·5°, two peaks instead of one; 29·5°, three peaks instead of one; 34°, three peaks instead of one; 37°, three peaks instead of two; 48·5°, three peaks instead of one. Accompanying the development of new peaks are appreciable displacements of pre-existing reflections. The greatest changes take place at high 2θ angles, for example, between 69° and 70° (not listed in Tables 5 and 6). Since the relative intensities of these peaks, however, are low, they are not practical for the distinction of the two forms, particularly in the presence of other phases. In this respect, the most favourable part of the diffraction pattern with high relative intensities as well as angular displacements was found to be, as noted by Miyashiro (1957), the area between 29° and 30°, on which the applied nomenclature of cordierite polymorphs is based. Intermediate states between high- and 'low'-cordierite and the deviation of 'low'-cordierite from hexagonal symmetry can be characterized by the value of the distortion index Δ (Miyashiro, 1957) as shown in Fig. 1. During the transitions from one form to the other, in most cases the Δ angles change gradually from a maximum value to 0°, and vice versa, due to the gradual union or separation of the peak triplet (Fig. 14). For Δ values equal to, or higher than, 0·20° a clear distinction of the various reflections indicative of orthorhombic symmetry was usually possible, and structural transitions of these cordierites into structural states with lower Δ values could be detected readily. This was one of the reasons for choosing a Δ value of 0·20° as the dividing line between 'low'-cordierite and intermediate-state cordierites.

In a number of compositions in the system, it was observed that the structural state of high-cordierite was approached by a gradual decrease of the intensities of the (511) and (421) reflections of 'low'-cordierite without any measurable change of the Δ value. The critical peaks of a cordierite of this kind are shown in Fig. 15. All the other peaks of the pattern behave in a similar fashion. This 'anomalous' cordierite, therefore, is orthorhombic with a fixed distortion index, until the intensities of the two peaks (511) and (421) and of other related reflections become zero. Thus the transition of 'low'-cordierite into high-cordierite, as defined on

the basis of the distortion index Δ, would in these cases be abrupt rather than gradational. It is also to be emphasized that the peaks of the high-cordierite produced by this 'anomalous' transition are displaced to higher angles in com-

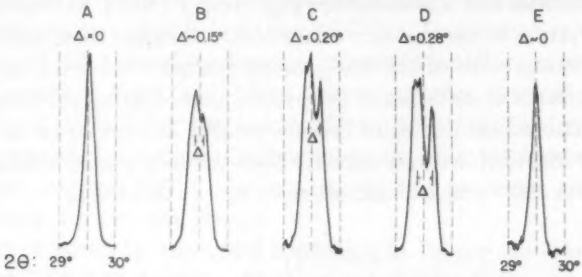

FIG. 14. X-ray powder diffraction patterns between 29° and 30° 2θ (copper $K\alpha$ radiation) for structural states of cordierite of the Δ-variable type. All cordierites were crystallized from glass of the composition $2MgO \cdot 2Al_2O_3 \cdot 5SiO_2$ under the following conditions: A, at 1,000° C for 301 days. B, at 1,000° C for 12 days, then at 1,200° for 11 days, then at 1,320° for 17 days, and finally at 1,453° for 21 h. Before this final heating a Δ value of 0·23° had been attained. C, at 1,420° C for 24 h. D, at 1,300° C for 33 h, then at 1,420° for 102 h, and finally at 1,000° for 314 days. E, at 1,050° C for 4 days, then at 1,200° for 4 days, then at 1,400° for 13 days, and finally at 1,460° for 20 h. Before this final heating, a Δ value of 0·25° had been attained.

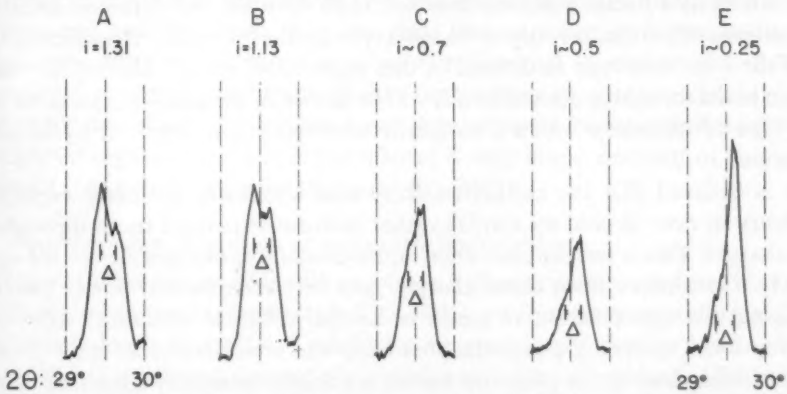

FIG. 15. X-ray powder diffraction patterns between 29° and 30° 2θ (copper $K\alpha$ radiation) for structural states of cordierite of the *i*-variable type. All cordierites were initially crystallized from glass of composition No. 32 (Table 1 and Fig. 4) at 1,050° C for 8 days and then at 1,250° for 1 day. The structural states shown in this figure were attained by subsequent heating under the following conditions: A, at 1,330° C for 11 days. B, at 1,330° C for 11 days and then at 1,360° for 6 days. C, at 1,370° C for 5 days. D, at 1,330° C for 11 days and then at 1,385° for 48 days. E, at 1,330° C for 11 days and then at 1,400° for 27 days. It can be seen from this sequence that the *i* value is decreasing with increasing temperature of the final heating, whereas the Δ values remain constantly around 0·20°.

parison with high-cordierite of 2:2:5 composition, the difference being about 0·10°–0·15° 2θ. It is concluded, therefore, that these high-cordierites are not of 2:2:5 composition, but are richer in Mg and Si due to the substitution Mg+Si → 2Al. The structural change can be described, at least in a semiquantitative way, by the ratio of one-half of the combined intensities of the (511) and (421)

reflections versus the full intensity of the (131) reflection. In synthetic 'low'-cordierite of the composition $2MgO \cdot 2Al_2O_3 \cdot 5SiO_2$ the intensities for (511) and (421) are always decidedly higher than for (131). The ratio has been measured in a number of cases and was found to range from 1·15 to 1·35. Preferred orientation of the crystals in the powder would tend to change these values. Owing to the intimate intergrowth of the fine-grained synthetic material, however, there is no such preferred orientation in the present case. During the transition of the 'anomalous' cordierites the ratios become smaller and are equal to 1 when both intensities are identical, and are zero for high-cordierite solid solutions. For the present purpose this ratio is called *intensity index i* defined as

$$i = \frac{I_{(511)} + I_{(421)}}{2I_{(131)}}.$$

Since in most cases the reflections (511) and (421) cannot be separated, only one mean intensity value for (511) and (421) is obtained, which is divided by the intensity of (131):

$$i = \frac{I_{(511+421)}}{I_{(131)}}.$$

On this basis a distinction may thus be drawn between two types of structural transitions of cordierites: the Δ-variable type as discovered by Miyashiro (1957) and the *i*-variable type as defined in this paper (also called 'anomalous' transition in the foregoing discussion). It will be shown in the following sections that the type of transition which a cordierite undergoes is determined by its composition.

It is believed that the cordierites from runs which are quenched rapidly in mercury or even in cold air display rather uniform structural states throughout the charges. This is not the case when liquid-containing charges are cooled more slowly. Cordierites from these charges give very complicated X-ray patterns showing the superposition of peaks of several different structural states (see section I 4). On these grounds the possibility was considered that the *i*-variable type of behaviour in the phase cordierite is actually caused by a gradual change in the ratios of two coexisting cordierites, a 'low'-cordierite and a high-cordierite solid solution. On account of the gradational nature of the transition from 'low'- to high-cordierite even in pure 2:2:5 composition, however, this possibility was discarded. The exact structural significance of the *i*-variable type of transition is still unknown.

With the kind assistance of Dr. B. J. Skinner of the U.S. Geological Survey, high-temperature X-ray studies were carried out on a sample of 'low'-cordierite of 2:2:5 composition with a Δ value of 0·25°. No changes in the X-ray pattern could be observed in the temperature range from 25° to 1,025° C. Even the Δ value remained constant within the limits of error. The exothermic peak occurring in DTA curves of natural as well as synthetic cordierites around 900° C (Sugiura, 1959), therefore, cannot be caused by structural changes related to the

'low'-high transition described in this paper. The significance of this exothermic peak, therefore, is yet unknown. The variations of peak locations in the X-ray pattern due to thermal expansion of the cordierite lattice for all the reflections between 5° and 50° 2θ in the whole temperature range investigated, were found to be extremely small (certainly less than 0·10° 2θ). This indicates that the thermal expansion of the mineral cordierite is extremely small, even over a range of 1,000° C. Hummel & Reid (1951) had determined this thermal expansion as approximately 20×10^{-7} for the range 25° to 1,000° C. Sugiura & Kuroda (1955*b*) even reported a very small thermal contraction of synthetic high-cordierite between 20° and 500° C. On account of this property, cordierite is an excellent material for ceramic bodies.

The density of pure Mg–cordierite according to Tröger's (1956) extrapolated curve is about 2·54. The density values computed from X-ray data given above are still lower ($\sim$ 2·51). On the other hand, the density of glass of pure 2:2:5 composition was determined at room temperature as 2·62$\pm$0·02. The liquid in equilibrium with cordierite at 1,465° C has a composition approximately identical with mixture No. 27. The density of glass of composition No. 27 at room temperature was determined as 2·63$\pm$0·02. Thus it has been shown that at room temperature crystalline Mg–cordierite is less dense than glass of its own composition and also less dense than the glass formed when cordierite melts incongruently. With regard to the extremely low thermal expansion of cystalline cordierite, however, there is some doubt whether these anomalous relations also hold at the actual liquidus temperatures. According to Hummel & Reid (1951) the thermal expansion of a 2:2:5 cordierite is only about one-half of that of a glass of 1:1:4 composition for the range 25°–700° C.

2. *Low-temperature transition of metastable high-cordierite*

The metastable compounds with quartz- as well as osumilite- and petalite-type structures mentioned earlier (section E 1), which are formed by crystallizing glass at relatively low temperatures, gradually disappear upon further heating and give way to an increasing amount of cordierite and other compounds. This initial cordierite was in all cases found to be hexagonal high-cordierite. Like the phases from which it formed, it has to be considered metastable, because upon further heating it gradually goes over through a complete series of intermediate structural states into 'low'-cordierite. For all compositions, with the exception of Nos. 1–4, 'low'-cordierite was found to be the stable polymorphic form at subsolidus temperatures.

As already mentioned in a previous section (F 1 (*a*)), the metastable high-cordierites exhibit rather extensive metastable solid solutions in several directions within the diagram. The gradual attainment of the stable 'low' form is for many compositions more or less concomitant with the gradual unmixing of these metastable solid solutions. Composition No. 8, for instance, after crystallization at 1,050° C for 2 days and 1,250° C for 3 days, consisted of high-cordierite

but showed no cristobalite. The latter could be detected optically and by X-ray only after further heating at 1,320° C for 4 days and 1,330° C for 11 days. Meanwhile 'low'-cordierite with $\Delta = 0{\cdot}20°$ had been attained. The displacive types of solid solution in composition No. 23, &c., on the other hand, show what looks like complete unmixing while there is still intermediate-state cordierite ($\Delta \approx 0{\cdot}10°$) present. A third type of behaviour is displayed by composition No. 3: After a devitrification period of 11 days at 1,050° C, 5 days at 1,250° C, and subsequently 1 more day at 1,050° C 'low'-cordierite with a Δ of 0·21° was present; however, no spinel had unmixed yet, the metastable assemblage being cordierite$_{ss}$+forsterite.

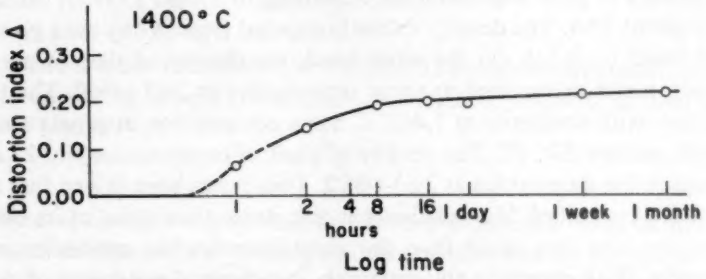

FIG. 16. Increase of the distortion index Δ of anhydrous Mg–cordierite with time of heating at 1,400° C, 1 atm. Starting material is glass of the composition $2MgO \cdot 2Al_2O_3 \cdot 5SiO_2$. The curve is dashed for very short times of heating, because Δ values below 0·10° cannot be measured very accurately.

It is thus evident that the structural transition from metastable high- to stable 'low'-cordierite in various bulk compositions at subsolidus temperatures may be, but is not necessarily, accompanied by changes in the composition of the cordierites.

The rate of transition of metastable high-cordierite of 2:2:5 composition to 'low'-cordierite at 1,400° C is represented diagrammatically in Fig. 16, using a logarithmic scale for the crystallization time. The starting material used was glass, which after 1 h had completely crystallized to a form structurally very close to high-cordierite.[1] The increase of the Δ-value with continued heating at this temperature is rather rapid, so that a 'low'-cordierite with $\Delta \approx 0{\cdot}20°$ is obtained within less than 1 day. The further increase of Δ, however, is shown to be an extremely sluggish process. This fact is also one of the reasons why $\Delta = 0{\cdot}20°$ was chosen as the dividing line between intermediate-state and 'low'-cordierites (Fig. 1). At lower temperatures of crystallization the rate of the transition is much smaller. The magnitude of the Δ value attained is thus proportional to the product of the crystallization temperature and the crystallization period, pro-

[1] This form exhibited one peak at 29·5° 2θ which, however, was slightly broader than for high-cordierite with $\Delta = 0$. The distortion index was estimated as $0{\cdot}05 < \Delta > 0{\cdot}10$.

vided that low-cordierite is indeed the stable phase for the particular composition at the temperature of crystallization.

A third variable bearing on the rate of transition is given by the bulk composition in which the cordierite occurs. As a general rule it can be stated that at constant temperature the gradual transition is the more sluggish the farther away the bulk composition lies from that of cordierite 2:2:5, i.e. the lower the percentage of cordierite 2:2:5 among the crystalline phases under equilibrium conditions. This does not seem to be true for compositions Nos. 13–16 and 18–22, lying close to, or beyond, the two ternary invariant points *P* and *S* (Fig. 3). They, at least, do not exceed, in the sluggishness of their transition, the compositions closer to 2:2:5. A probable explanation for this fact may be that these compositions do not have a stable field of high-cordierite under any conditions (see later, section I 5).

In compositions along the line 2:2:5–spinel, 'low'-cordierites were difficult to obtain. They formed in some cases at very low subsolidus temperatures below 1,100° C, but only from materials that had been preheated at higher temperatures. This peculiar behaviour is due to the fact that in these compositions structural transitions may occur at subsolidus temperatures (see section I 3 (*g*)). As the rate of transition from high- to 'low'-cordierite decreases with decreasing temperatures, it was not always possible to attain the 'low' form during the time of the experiments.

A large amount of data on the gradual transition of cordierites, in the compositions studied, has been obtained during this investigation. Table 7 lists only a small, but rather representative, selection. The Δ range of intermediate-state cordierites has been divided into three groups which seemed to represent the various steps of the transition in the best manner. In a number of cases, which are indicated by asterisks, the highest Δ values were attained only in the presence of liquid. This does not mean that, in these cases, the Δ value of the cordierite in the subsolidus assemblage has to be a lower one. On the contrary, it should be identical or even higher, but owing to the lower transition rate at subsolidus temperatures it could not be attained in the course of the experiments.

3. *Stability range of high-cordierites*

It has been shown in the previous section that 'low'-cordierite is the stable form of cordierite at least up to the beginning of melting of the various compositions, with the exception of compositions Nos. 1–4. At still higher temperatures, in the presence of liquid, these 'low'-cordierites in a number of compositions gradually go over into high-cordierite. Since this transition is reversible, high-cordierite has to be considered the stable modification under these conditions. It is to be emphasized, however, that the transition *does not take place at one particular temperature* for all cordierite-bearing mixtures, like the inversion of pure low-quartz (SiO_2) into high-quartz at 573° C at 1 atm. *Whether 'low'-cordierite goes over into high-cordierite or not, and at what temperature the*

TABLE 7. *Structural states of cordierites contained in devitrified glasses of various compositions after various periods of heating*

Composition No.	Structural state					Highest Δ value attained	Conditions
	High-cordierite	Δ = 0–0·10	Δ = 0·11–0·15	Δ = 0·16–0·19	'Low-' cordierite		
	(a) Compositions on the line 2:2:5–SiO_2 or very close to it						
2:2:5	1,000° 301 d 1,100° 56 d 1,200° 5 d 1,300° 20 h	1,000° 16 d + 1,200° 10d + 1,200° 21 d 1,400° 1 h	1,250° 5 d	1,400° 2 h	1,000° 13 d + 1,350° 6 d + 1,420° 1 d 1,300° 33 h 1,420° 102 h + 1,000° 314 d +	0·28	1,300° 33 h 1,420° 102 h + 1,000° 314 d +
1:1:3	1,300° 16 h	1,050° 6 d 1,300° 6 d +	1,050° 4 d 1,400° 20 h + 1,400° 7 d 1,050° 12 d + 1,320° 1 d + 1,310° 7 d + 1,050° 329 d	1,050° 6 d 1,300° 6 d + 1,380° 3 d + 1,415° 12 d 1,430° 7 d	1,050° 6 d + 1,300° 6 d + 1,380° 10 d +	0·21	1,050° 6 d 1,300° 6 d + 1,380° 10 d +
8	1,050° 2 d 1,250° 3 d + 1,400° 1 h	1,400° 1 d		1,050° 2 d 1,250° 4 d + 1,320° 4 d + 1,330° 7 d + 1,400° 7 d	1,050° 2 d + 1,250° 4 d + 1,320° 4 d + 1,330° 11 d + 1,400° 28 d	0·22	1,050° 2 d 1,250° 4 d + 1,320° 4 d + 1,330° 11 d + 1,405° 10 d +
12	1,000° 10 d + 1,250° 4 d +	1,000° 10 d + 1,250° 4 d + 1,300° 3 d +			1,000° 10 d + 1,250° 4 d + 1,300° 3 d + 1,400° 9 d +	0·20	1,000° 10 d + 1,250° 4 d + 1,300° 3 d + 1,400° 9 d +
14		1,300° 2 d		1,300° 10 d 1,400° 14 d +	1,300° 10 d 1,400° 22 d +	0·25*	1,300° 10 d 1,400° 25 d + 1,437° 3 d* +
15	1,050° 7 d 1,250° 1 d +			1,050° 7 d 1,250° 1 d + 1,400° 17 d +	1,050° 7 d 1,250° 1 d + 1,400° 17 d + 1,437° 3 d* +	0·21*	1,050° 7 d 1,250° 1 d + 1,400° 17 d + 1,437° 3 d* +
	(b) Compositions in the triangle $MgSiO_3$–2:2:5–SiO_2						
27				1,050° 2 d 1,200° 5 d + 1,300° 1 d +	1,050° 2 d + 1,200° 5 d + 1,300° 14 d + 1,330° 6 d +	0·25	1,050° 2 d + 1,200° 5 d + 1,300° 14 d + 1,330° 6 d +
26	1,050° 4 d	1,050° 5 d 1,250° 3 d +	1,050° 5 d 1,250° 3 d + 1,330° 4 d + 1,305° 9 d +	1,050° 5 d 1,250° 3 d + 1,330° 4 d + 1,305° 9 d + 1,330° 7 d +	Heating discontinued	0·19	1,050° 5 d 1,250° 3 d + 1,330° 4 d + 1,305° 9 d + 1,330° 7 d +
25	1,250° 6 d	1,250° 6 d 1,300° 16 d +		1,250° 6 d 1,300° 16 d + 1,330° 31 d +	Heating discontinued	0·18*	1,250° 6 d 1,300° 16 d + 1,330° 31 d + 1,375° 3 d* +
24		1,250° 2 d 1,320° 2 d + 1,300° 2 d +	1,250° 2 d 1,320° 2 d + 1,300° 18 d +	1,250° 2 d + 1,320° 2 d + 1,300° 18 d + 1,330° 11 d +	Heating discontinued	0·18*	1,250° 2 d + 1,320° 2 d + 1,300° 18 d + 1,330° 11 d + 1,375° 3 d* +

TABLE 7 (*cont.*)

Composition No.	Structural state					Highest Δ value attained	Conditions
	High-cordierite	Δ = 0–0·10	Δ = 0·11–0·15	Δ = 0·16–0·19	*'Low'-cordierite*		
22	1,050° 3 d	1,050° 3 d + 1,250° 1 d +		1,050° 3 d + 1,250° 2 d + 1,320° 20 d +	1,050° 3 d + 1,250° 2 d + 1,320° 36 d +	0·25*	1,050° 3 d + 1,250° 2 d + 1,320° 36 d + 1,354° 14 d* +
	(c) Compositions on the line 2:2:5–$MgSiO_3$						
28		1,300° 7 h		1,230° 2 d + 1,330° 1 d +	1,230° 2 d + 1,330° 5 d +	0·24	1,230° 2 d + 1,330° 5 d +
30	1,050° 4 d			1,050° 4 d + 1,250° 4 d + 1,320° 11 d +	Heating discontinued	0·20*	1,050° 4 d + 1,250° 4 d + 1,320° 11 d + 1,360° 7 d* +
32	1,050° 8 d	1,050° 8 d + 1,250° 1 d +			1,050° 8 d + 1,250° 1 d + 1,330° 11 d +	0·20	1,050° 8 d + 1,250° 1 d + 1,330° 11 d +
33		1,300° 1 d + 1,320° 6 d +	1,300° 1 d + 1,320° 6 d + 1,300° 12 d + 1,330° 16 d	1,330° 30 d	Heating discontinued	0·18	1,330° 30 d
17		1,300° 16 h	1,300° 16 h + 1,320° 13 d +	1,330° 9 d	1,330° 23 d	0·21*	1,330° 23 d + 1,360° 72 h* +
	(d) Compositions on the line 2:2:5–forsterite						
39		1,250° 5 d			1,250° 24 d + 1,320° 23 d +	0·22	1,250° 24 d + 1,320° 23 d +
38			1,250° 5 d	1,250° 5 d + 1,330° 7 d +	1,250° 5 d + 1,340° 14 d +	0·20	1,250° 5 d + 1,340° 14 d +
	(e) Compositions on the line 2:2:5–spinel						
4	1,050° 4 d				1,050° 5 d + 1,250° 6 d +	0·23	1,050° 5 d + 1,250° 6 d +
2	1,000° 3 d + 1,250° 1 h + 1,150° 8 d + 1,200° 7 d + 1,400° 1 h +	1,250° 1 d + 1,350° 8 d + 1,380° 7 d +	1,250° 28 d	1,350° 8 d + 1,380° 7 d + 1,250° 7 d + 1,150° 8 d + 1,200° 7 d +	1,350° 8 d + 1,380° 7 d + 1,250° 4 d + 1,050° 8 d +	0·20	1,350° 8 d + 1,380° 7 d + 1,250° 4 d + 1,050° 8 d +
1	1,050° 3 d	1,050° 89 d + 1,200° 1 d + 1,300° 5 d + 1,415° 20 h +	1,200° 1 d + 1,300° 5 d + (anomalous intensities) 1,200° 1 d + 1,300° 5 d + 1,330° 11 d + 1,050° 83 d + 900° 108 d + (normal intensities)	Heating discontinued		0·15	1,200° 1 d + 1,300° 5 d + 1,330° 11 d + 1,050° 83 d + 900° 108 d +

* Highest Δ value attained in presence of liquid.
d = days; *h* = hours; repeated heating is indicated by + between the figures.

transition takes place, are dependent on the total bulk composition of the particular mixture. This is the important result of this part of the study. The data on the various compositions, which lead to this conclusion, will be given in the following sections. Since it is not practical to discuss each of the compositions separately, groups of similarly behaving compositions will be established and the structural behaviour of their cordierites will be shown by the aid of various diagrams.

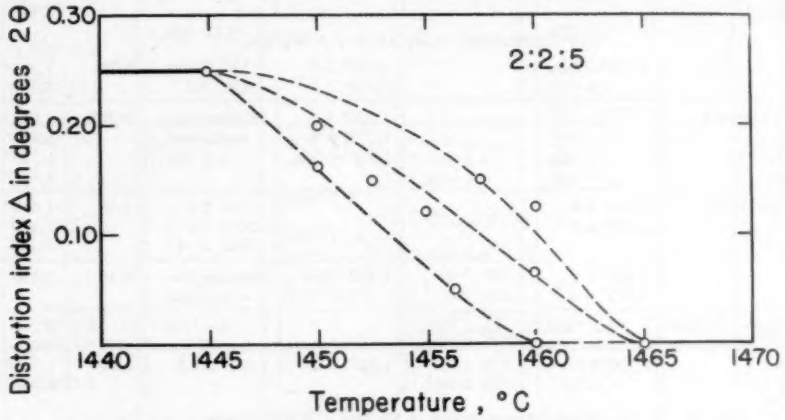

FIG. 17. Dependence of the distortion index Δ of cordierite on temperature for the bulk composition $2MgO \cdot 2Al_2O_3 \cdot 5SiO_2$ (2:2:5). Due to the scattering of points in the temperature range 1,450°–1,465° C the true slope of the curve is not known. Three possibilities are indicated by dashed lines. See discussion given in text.

(*a*) *Cordierite composition 2:2:5.* As discussed previously in section H, cordierite composition 2:2:5 shows partial incongruent melting into mullite and liquid, starting at about 1,445° C. With increasing temperature, decreasing amounts of cordierite coexist with increasing amounts of mullite and liquid until 1,465° C, where cordierite disappears. Starting out with 'low'-cordierite, a gradual decrease of the distortion index Δ of cordierite can be observed between about 1,450° and 1,460° C, so that between about 1,460° and 1,465°, or at 1,465° itself, hexagonal high-cordierite is the stable modification. These relations are shown diagrammatically in Fig. 17. The slope of the curve between 1,450° and about 1,465° C is now known very well; in Fig. 17, several possibilities are indicated. Measurements in this respect are difficult for at least three reasons: (1) The temperature in this range cannot be held exactly constant for long periods of time; changes of $\pm 2°$ may, on the other hand, have a great bearing on the Δ value. (2) Low Δ angles cannot be determined accurately. (3) There may be a quenching effect in such a way that more cordierite may crystallize from the liquid. This cordierite would always be high-cordierite (compare section I 2) and would modify the shape of the critical peak of the cordierite which is in equilibrium with liquid. Nevertheless, the measurements are believed to be

accurate enough to show the principal polymorphic behaviour of cordierites at these high temperatures.

Influences on the polymorphic transition of various starting materials, as well as of different durations of runs, have also been investigated. The data obtained on 2:2:5 composition are compiled in Table 8 (*a*). The starting materials used were (1) glass; (2) metastable high-cordierite, prepared previously by devitrifying glass at 1,000° C for 16 days; (3) 'low'-cordierite, prepared by devitrifying glass at 1,300° C for 36 h plus 1,420° C for 71 h (the distortion index Δ attained was measured as 0·22°). These materials were run at 1,460° C for 1 h, 1 day, 1 week, and 4 weeks. In long runs it was necessary to start at a temperature about 3° below the one desired because of the EMF changes of the Pt–PtRh thermocouples. The data show that the transition of 'low'- to stable high-cordierite is rather rapid. However, 24 h should be considered the minimum amount of time to reach polymorphic equilibrium. The differences of the Δ values of the 24-h and 168-h runs against the 672-h run may not be caused by the time differences but rather by temperature inaccuracy, &c., such as stated above. In other runs at 1,460° C of only 24 h duration, using the same starting materials, high-cordierites with $\Delta = 0$ were obtained.

The time studies prove that high-cordierite persists in its stability range—as it should—even after very long periods of heating. Intermediate-state cordierites, according to Fig. 17, also have a true, although not very well defined, range of stability at high temperatures. According to the experimental results, the general stability relations between low-cordierite and high-cordierite do not seem to be affected perceptibly by the fact that low-cordierite proper, exhibiting the maximum Δ value, has not been attained. So the gradual transition from 'low'-cordierite to high-cordierite was found to take place at the same temperatures, no matter whether the starting materials showed a Δ value of 0·21° or of 0·28°. This somehow justifies the term 'low'-cordierite and restricts the quotation marks around low to a reminder for the reader that the cordierite has not, or may not have, attained its lowest possible structural state.

It is of considerable interest that the temperature for the transition from 'low'- to high-cordierite given as 1,450°–1,465° C for 2:2:5 composition, was found to be the highest among all the compositions investigated. This confirms the significance of this composition as an end-member of the cordierite series of solid solution and also as the highest melting member in the plane of $cordierite_{ss}$ as shown in Fig. 10. It is possible, therefore, that for ideally pure composition 2:2:5, 'low'-cordierite would be stable up to 1,465° C, where it would invert rather abruptly to high-cordierite, and that its behaviour described above is only caused by the premature formation of liquid due to impurities in the chemicals used in the preparation of the mixture (compare section H).

(*b*) *Influence of liquid on the transition.* It appears from the data reported in the last section that the presence of large amounts of liquid is the guiding factor for the transition from 'low'- to high-cordierite. In order to test this influence

TABLE 8

Time studies on the structural states of cordierites

Starting material	*Duration of run*			
	1 hour	*24 hours*	*168 hours*	*672 hours*
	(a) 2:2:5 composition, 1,460° C			
'Low'-cordierite	$\Delta = 0{\cdot}15$	$\Delta \approx 0{\cdot}08$	$\Delta \approx 0{\cdot}06$	$\Delta = 0$
High-cordierite	$\Delta \approx 0{\cdot}05$	$\Delta \approx 0{\cdot}05$	$\Delta \approx 0{\cdot}08$	$\Delta = 0$
Glass	$\Delta = 0$	$\Delta = 0$	$\Delta = 0$	$\Delta = 0$
	(b) Composition No. 2, 1,250° C			
Intermediate-state cordierite, $\Delta = 0{\cdot}15$*	$\Delta = 0{\cdot}14$	$\Delta = 0{\cdot}15$	$\Delta = 0{\cdot}14$	$\Delta = 0{\cdot}15$
Metastable high-cordierite	$\Delta = 0$	$\Delta = 0{\cdot}15$	$\Delta = 0{\cdot}15$	$\Delta = 0{\cdot}14$
Stable high-cordierite	$\Delta = 0{\cdot}15$	$\Delta = 0{\cdot}16$	$\Delta = 0{\cdot}18$	$\Delta = 0{\cdot}18$*
Glass	$\Delta = 0$	$\Delta = 0{\cdot}10$	$\Delta = 0{\cdot}14$	$\Delta = 0{\cdot}14$
	(c) Composition No. 2, 1,400° C			
Intermediate-state cordierite: two peaks $\Delta = 0{\cdot}15$*	One slender symmetrical peak $\Delta = 0$*	One slender slightly unsymmetrical peak*	One broader unsymmetrical peak*	One broader symmetrical peak*
Metastable high-cordierite	One slender symmetrical peak $\Delta = 0$	One slender slightly unsymmetrical peak	One broader symmetrical peak	One broader unsymmetrical peak 'Δ' $\approx 0{\cdot}13$?
Stable high-cordierite	One slightly broader symmetrical peak	One slightly broader symmetrical peak	One broader unsymmetrical peak 'Δ' $\approx 0{\cdot}10$?	One broader unsymmetrical peak 'Δ' $\approx 0{\cdot}15$?
Glass	One slender symmetrical peak $\Delta = 0$	One slender unsymmetrical peak	One broader unsymmetrical peak	One broader symmetrical peak

* See also Fig. 22.

of the liquid, two particularly favourable compositions are examined here in detail: in composition No. 28, liquid develops around 1,365° C and increases in amount over a range of about 100° up to 1,463° C, constantly being in equilibrium with cordierite crystals. The other extreme is displayed by composition No. 38, in which liquid forms, theoretically, at the same temperature at which cordierite disappears. This temperature was shown to be 1,370°±5° C. Fig. 18 gives the Δ-versus-temperature curves for compositions Nos. 28 and 38, in comparison with the one for 2:2:5. It is obvious from this plot that the Δ values of the cordierites of composition No. 28 are gradually decreasing with increasing

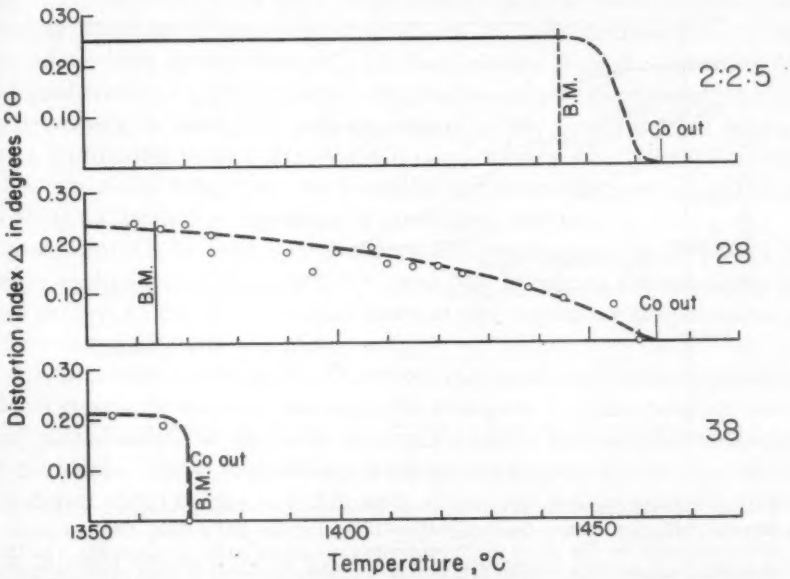

FIG. 18. Dependence of the distortion index Δ of cordierites on temperature for the bulk compositions 2:2:5 (taken from Fig. 17), and Nos. 28 and 38 (Table 1 and Fig. 4). For explanation see text. 'B.M.' indicates temperature of beginning of melting; 'Co out' indicates highest temperature at which cordierite is stable.

temperature, thus resulting in a rather smooth curve between 'low'-cordierite below 1,365° C and high-cordierite at 1,463° C. The cordierites of composition No. 38, similarly, do not show any marked decrease in their Δ values until the beginning of melting. Since melting and the disappearance of cordierite, however, take place over a very narrow range of temperature, and the last cordierites in equilibrium with liquid were found to be high-cordierites, the Δ-versus-temperature curve shows a very sudden decline from 'low'- to high-cordierite. The structural behaviour of cordierites from composition No. 38 shows further complications which, however, are not of vital importance in this connexion. They will be discussed in a subsequent section.

It is concluded from the data presented so far that the transition from

'low'-cordierite to high-cordierite may be controlled by the amounts of liquid coexisting with the cordierite. In the following sections dealing with the behaviour of the various lines of compositions, confirmation, but also exceptions to this rule, will be discussed. As it was not always possible to show the relations in the same detailed fashion as for compositions 2:2:5, No. 28, and No. 38, a more generalized way of plotting has, partly, been used.

(*c*) *Compositions on the line 2:2:5–SiO_2 or very close to it.* The polymorphic behaviour of cordierites in compositions Nos. 5–16, 18, 1:1:3, and 2:2:5 is shown in a simplified fashion in Fig. 19. The upper curve is taken from Fig. 12

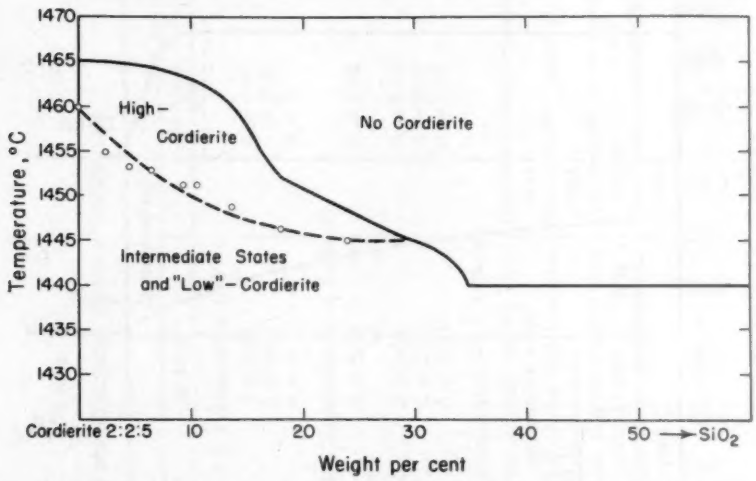

FIG. 19. Dependence of the structural states of cordierites (Δ-variable types) on temperature and bulk composition for compositions along the line 2:2:5–SiO_2. The heavy solid curve represents the line above which cordierite is no longer stable (compare Fig. 12). The dashed line separates the stability field of high-cordierite from that of other structural states stable at lower temperatures. Notice that for bulk compositions with more than 30 wt per cent normative SiO_2, high-cordierite is not a stable phase at any temperature.

and gives the temperatures above which cordierite is no longer stable. The lower dashed curve has been constructed from the transition data obtained on the various compositions. Above this curve only high-cordierites were encountered, whereas below it intermediate states and 'low'-cordierites, or only 'low'-cordierite, were obtained. Errors in the recognition of small Δ values might shift the position of the lower curve slightly but would not change the relations principally. The intersection of the dashed curve with the solid one indicates that from composition No. 12 on toward more siliceous bulk compositions, intermediate states or even 'low'-cordierites are stable up to the full disappearance of the phase cordierite, despite the presence of much liquid. In some of these compositions a tendency for decreasing Δ values with increasing temperature could be observed, but true high-cordierite was never attained. In composition

No. 14, for example, small amounts of cordierite coexisted with mullite, cristobalite, and much liquid at 1,437° C after 72 h. The cordierite was found to have a Δ of 0·25°. At 1,440° C cordierite was no longer present.

It is thus shown that for bulk compositions along the line 2:2:5–SiO_2, with more than 30 wt per cent of normative silica, high-cordierite is not a stable phase at any temperature.

(*d*) *Compositions on the line 2:2:5*–$MgSiO_3$. The polymorphic behaviour of the cordierites occurring in compositions Nos. 17 and 28–37 is complicated by solid solution. It has been shown in Fig. 11 that the cordierite solid solutions present at liquidus temperatures in these compositions become more extensive with increasing amounts of normative $MgSiO_3$ in the bulk compositions. It has, furthermore, been shown in section I 1 that in some cases the transition of a 'low'-cordierite to a high-cordierite solid solution cannot be expressed in terms of a decreasing Δ value, but only by means of the newly defined intensity index *i*. Cordierites from 2:2:5–$MgSiO_3$ compositions may follow, according to their structural behaviour, the *i*-variable or Δ-variable type of transition, depending on the bulk composition of the original mixture.

The structural behaviour of cordierites from compositions No. 28 (which has been discussed already in section I 3 (*b*)) and No. 29 follows the previously discussed pattern, in that their Δ values decrease with increasing temperatures, i.e. with increasing amounts of liquid.

Cordierites in composition No. 32, on the other hand, with increasing amounts of liquid present do not show a measurable change in Δ value; however, the intensity index *i* diminishes gradually and reaches zero when the liquidus temperature is attained. These relations are shown diagrammatically in Fig. 20. The curve drawn seems to have a rather steep slope near the temperature at which the composition begins to melt (1,364°$\pm$3° C), becoming smooth toward the actual liquidus temperature of 1,415° C. The observed decrease in the *i* value below the theoretical temperature of the beginning of melting may be due to premature formation of liquid owing to impurities. This same general behaviour is displayed by cordierites in composition No. 33, which show the decline of the *i* value over a narrower range of temperature, and also by cordierites in compositions Nos. 34–37, lying outside the cordierite field. In the latter cases this temperature range is only over about 3°, because the phase cordierite disappears at 1,367° C, i.e. only 3° above the beginning of melting (Fig. 8). Diagrams of *i* versus *T* would thus show curves similar to that in the Δ-versus-*T* plot for composition No. 38, drawn in Fig. 18.

The compositions of melts Nos. 30 and 31 lie in the border area between bulk compositions showing the *i*-variable type of structural changes just described and the Δ-variable type. It is for this reason that cordierites from these two mixtures show a structural behaviour of a composite type. In other words, these cordierites show, with increasing amounts of liquid present, a gradual decrease of both the Δ and the *i* values. This results in broad composite and inseparable

critical peaks between 29° and 30° 2θ, which are not amenable to accurate measurements, the Δ as well as the i value being of an unfavourable magnitude. High-cordierites forming at the liquidus of these two compositions show peak positions intermediate between those of high-cordierites from a melt of 2:2:5 composition and of high-cordierite solid solutions from melts Nos. 32, &c.

Cordierites in composition No. 17, also lying outside the cordierite field, behave again differently in that they do not show a transition toward high-cordierite within the melting range 1,364°–1,367° C (Fig. 8), even in the presence

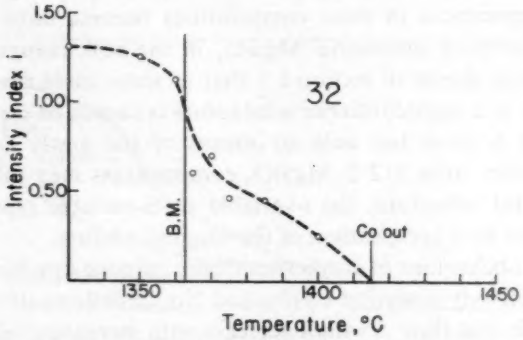

FIG. 20. Dependence of the intensity index i of cordierites on temperature for bulk composition No. 32 (Table 1 and Fig. 4). Compare also Fig. 15. For explanation of the abbreviations see legend to Fig. 18.

of much liquid. The cordierites obtained around this temperature exhibit a Δ value of about 0·22° with an i value around 1·25. The structural behaviour of cordierites in composition No. 17 thus resembles that exhibited by compositions Nos. 12–16 and 18.

If one plots the temperatures of the first appearance of high-cordierite in compositions Nos. 28–37, against composition, a curve is obtained which coincides approximately with the liquidus curve as shown in Fig. 8 for compositions Nos. 28–33. For compositions Nos. 34–37 the locus for high-cordierite would be the line at the constant temperature of 1,367° C, also shown in Fig. 8. From a $MgSiO_3$ content of about 55 wt per cent onward, however, it appears that high-cordierite would no longer form at any temperature.

(*e*) *Compositions on the line 2:2:5–forsterite.* Cordierites crystallizing from melts Nos. 38–41 are divided, with regard to their structural behaviour, into three groups similar to those discussed in the last section. Cordierites in compositions Nos. 40 and 41 show a gradual decrease in the Δ value from the beginning of melting at 1,370° $\pm$ 5° C up to 1,467° C, above which temperature cordierite is no longer present. The Δ-versus-T curves are comparable with that shown for composition No. 28 in Fig. 18. High-cordierites in composition No. 38, which are stable over a very narrow range of temperature around 1,370° C, exhibit solid solution, i.e. show displacement of peaks toward higher angles.

Thus, around 1,370° C 'low'-cordierite with normal Δ and *i* values undergoes a rather abrupt change of the *i* value to zero, which, of course, brings about an equally abrupt decline of the Δ angle. This has already been shown graphically in Fig. 18. Cordierites from composition No. 39 show, in a similar manner to those from Nos. 30 and 31, composite polymorphic behaviour, i.e. *gradual* decrease of *i* as well as Δ values with increasing amounts of liquid present.

(*f*) *Compositions in the triangle 2:2:5*–$MgSiO_3$–SiO_2. Cordierites in bulk compositions containing both $MgSiO_3$ and SiO_2 in addition to cordierite (2:2:5) show different structural behaviour according to the original ratios of these three phases. Those with only small amounts of $MgSiO_3$ and SiO_2 present (compositions Nos. 27 and 42) behave like the cordierites in composition No. 28 (Fig. 18). There is a gradual decrease of the Δ values with increasing amounts of liquid present. It is of interest, however, that in these bulk compositions no structural changes of the 'low'-cordierites were recorded in the absence of liquid, despite the change of the cordierite composition above 1,300° C. Cordierites from bulk compositions in the vicinity of No. 23 display, in essence, the *i*-variable type of structural behaviour, whereas those from compositions Nos. 24, 25, and 44 belong to the composite type with *i*- and Δ-variability. Cordierites in composition No. 26 show a more or less gradual decrease of Δ values starting around 1,355° C and ending near the liquidus around 1,450° C. No appreciable decrease of the *i* values or displacements of peaks were observed. The high-cordierites in composition No. 26 which are stable close to its liquidus temperature, therefore, cannot exhibit very extensive solid solution.

Judging from the behaviour of compositions along the lines 2:2:5–$MgSiO_3$ and 2:2:5–forsterite one would expect cordierites from compositions Nos. 19–22 to correspond in their structural behaviour with those of melts Nos. 34–38. This, however, is not the case: cordierites stable at temperatures close to that of the ternary eutectic *S* (1,355°±3° C, Fig. 3) are normal 'low'-cordierites with Δ values around 0·23 and *i* values around 1·30, despite the presence of much liquid. This condition persists even up to the various liquidus temperatures of compositions Nos. 19 and 21–22. There is an analogy, therefore, in this behaviour, with that of cordierites from compositions Nos. 12–16 and 18, which are close to the ternary reaction point *P*: the liquidus surface intersects the lower stability limits of high-cordierite, as is shown in Fig. 19.

(*g*) *Compositions on the line 2:2:5–spinel.* The structural behaviour of cordierite in assemblage with various amounts of spinel shows characteristics which are different from everything else reported so far. The main difference is that orthorhombic cordierite may gradually go over to high-cordierite without any liquid present. This is the opposite behaviour from that displayed by cordierites in melts Nos. 12–22, which do not show a transition despite the presence of much liquid. The relations of Δ versus temperature for compositions Nos. 2–4 are shown in Fig. 21. The curve for composition No. 4 shows a marked decline at temperatures about 40° below the beginning of melting. In the presence of

liquid above 1,453° C, only high-cordierite is, in essence, stable. In compositions Nos. 3 and 2, high cordierites have been obtained 20° or even 50° below the beginning of melting. This indicates that the temperatures of the transition are being lowered successively by the presence of increasing amounts of spinel. In composition No. 1, no 'low'-cordierite could be crystallized, even by holding material previously crystallized at high temperatures at 900° C for 108 days. The highest Δ value attained was 0·15° (Table 7 (*e*) and section I 2 in the text).

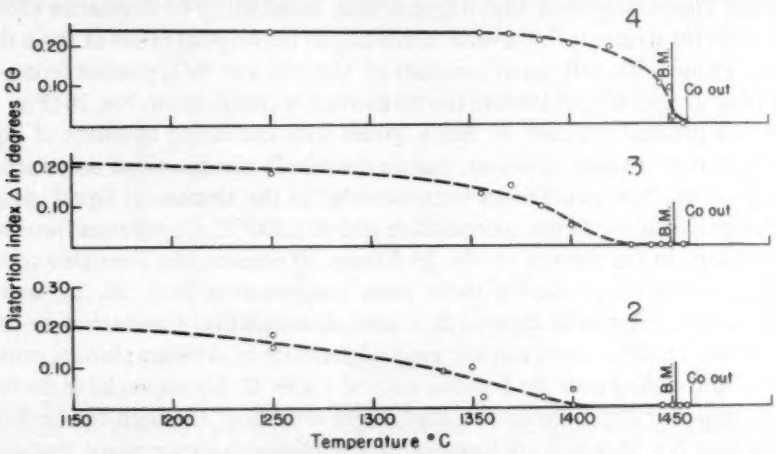

FIG. 21. Dependence of the distortion index Δ of cordierites on temperature for bulk compositions Nos. 2–4 (Table 1 and Fig. 4). For explanation of abbreviations see legend to Fig. 18.

A further complication in the structural behaviour of these aluminous compositions was discovered by a series of time studies on composition No. 2 at two different temperatures. The results are summarized in Table 8 (*b*) and (*c*). The four different starting materials used were:

(1) Intermediate-state cordierite, crystallized from glass at 1,150° C for 8 days and then at 1,200° C for 7 days. Δ was about 0·15° (Fig. 22 A).
(2) Metastable high-cordierite solid solution, crystallized from glass at 1,000° C for 3 days.
(3) Stable high-cordierite, crystallized from glass at 1,350° C for 8 days and then at 1,380° C for 7 days.
(4) All glass.

The results at 1,250° C indicate that the stable form at this temperature is an intermediate-state cordierite with Δ between 0·15° and 0·18°, which is being attained in the various starting materials after various lengths of time. At 1,400° C, in short runs up to 24 h in duration, the cordierites behaved in the fashion indicated in Fig. 21, i.e. high-cordierite was formed no matter what starting material was used. Intermediate-state cordierite inverted to high-cordierite within 1 h. In runs of 1 or 4 weeks in duration, however, definite

broadening of the high-cordierite peak was observed. The usual sequence of events, shown in Fig. 22 B–E, was a broadening starting at the base of the peak on the *low*-angle side thus producing an unsymmetrical peak, which after longer heating became symmetrical again because the broadening now affected the full intensity of the peak. In a few cases, this broadening, which might be considered to be due to subsidiary reflections, even exceeded the intensity of the primary reflection and thus produced an unsymmetrical peak with an apparent 'Δ' value. The highest apparent 'Δ' value attained lies in the vicinity of 0·15° (Fig. 22 G). There is a difference, however, from cordierites with the same Δ values

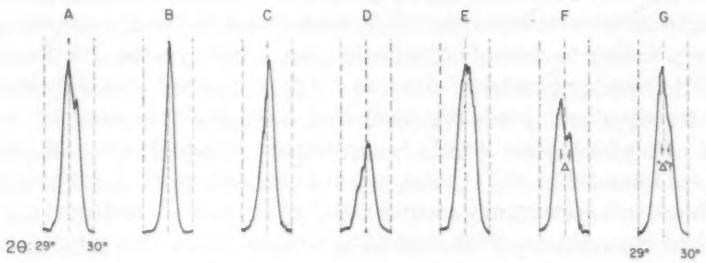

FIG. 22. X-ray powder diffraction patterns between 29° and 30° 2θ (copper $K\alpha$ radiation) of structural states of cordierites crystallized from glass of composition No. 2 under the following conditions: A, at 1,150° C for 8 days and then at 1,200° for 7 days. Structural state: intermediate-state cordierite, $\Delta = 0{\cdot}16°$. B, material A reheated at 1,400° C for 1 h. C, material A reheated at 1,400° C for 24 h. D, material A reheated at 1,400° C for 7 days. The decrease of the *total* intensity of this peak is merely caused by a smaller sample. E, material A reheated at 1,400° C for 28 days. F, at 1,350° C for 8 days, then at 1,380° for 7 days, and finally at 1,250° for 28 days; $\Delta = 0{\cdot}18°$. G, at 1,350° C for 8 days, then at 1,380° for 7 days, and finally at 1,400° for 28 days. Notice the gradual broadening of the peaks in the time sequence B through E. Notice also the difference between patterns F (exhibiting a real Δ value) and G (apparent 'Δ' value).

formed at 1,250° C from the same composition (Fig. 22 F). In the latter cases at least two peaks could easily be recognized, whereas here only 'unsymmetrical' peaks were obtained (see Table 8 (*c*) and Fig. 22).

So far there is no reasonable explanation for this strange behaviour. There is a certain similarity to the *i*-variable type of structural behaviour displayed by a number of compositions previously discussed (Fig. 15), but there are also differences: no time dependence of the *i* values, for instance, was found in those compositions. In the compositions along the line 2:2:5–spinel there is also no evidence for solid solution, cordierite and spinel always being present in the same amounts. Moreover, solid solution in cordierite along a fictive line of substitution of 2Al for Mg+Si is eliminated by the presence of invariable amounts of mullite in composition No. 43 at all temperatures.

Unless the broadening of the lines described can be attributed to influences hitherto unknown it has to be concluded from the data presented that there is a tendency for 'stable' high-cordierites, which have previously been formed from 'low'-cordierite, to reinvert gradually into a 'low' form after continued

heating at the same temperature. Thus the term 'stability' in this case would involve a time connotation, i.e. it would actually be a '*second order metastability*'. High-cordierites in these compositions, then, might not be 'truly' stable at these subsolidus temperatures. In the discussions to follow, for the sake of clarity, these incredible complications are disregarded. The stable polymorph of cordierite in the temperature range in question is considered to be the one which forms directly from a pre-existing orthorhombic polymorph ('low'-cordierite or intermediate-state).

(*h*) *Composition on the line 2:2:5–mullite.* Only one composition (No. 43), containing 2 wt per cent mullite, was prepared for studies along the join 2:2:5–mullite. The structural behaviour of the cordierite in this composition was found to be very similar to that of composition No. 4 lying on the 2:2:5–spinel join (Fig. 21): from temperatures of about 1,420° C upward, the Δ values of the cordierites decreased gradually until high-cordierite was attained at about 1,455° C. This took place largely in the absence of liquid which, theoretically, should not form until 1,465° C, but, just as in the case of the 2:2:5 composition, liquid developed prematurely around 1,450° C because of small deviations from the desired composition. With increasing amounts of mullite present, the transition temperatures are expected to decrease gradually.

4. *Influence of various rates of cooling on the structural state of cordierites*

It has been shown in previous sections that, for most of the compositions, 'low'-cordierite is the stable polymorph at all temperatures up to, or close to, the various solidus temperatures. It is thus obvious that the relatively slow cooling in Pt crucibles of the materials, which have been crystallized from glasses at subsolidus temperatures, cannot affect the structural states of the cordierites.

On the other hand, it is possible that structural changes occur when high-cordierites are quenched from their field of stability at high temperatures down to room temperature, simply because they must pass through the stability range of 'low'-cordierite. The fact, however, that truly hexagonal high-cordierite was obtained in many high-temperature runs indicates that quenching of this form can usually be achieved. The two different methods of quenching (mercury-quench and air-quench) of the small charges contained in Pt envelopes did not show consistent differences in the structural states of the quenched forms of cordierites. It is assumed, therefore, that these two methods are—certainly as a first approximation—equivalent. If there are differences they would only result in minor changes of the slopes of the Δ-versus-T curves, such as are discussed in section I 3 (*a*).

Rates of cooling slower than those of the two quenching methods, however, should, theoretically, show an increasing effect on the structural state of the cordierites, which at the high temperature had been present in the high form. Relatively slow cooling rates in our experiments were simply achieved by turning off the electric power to the furnace. The cooling curves are shown in Fig. 2.

Since high-cordierite is in many cases stable only in the presence of large amounts of liquid, the overall effect of slow cooling is opposite from what one would expect, the reason being that with slowly decreasing temperatures more and more additional cordierite crystallizes from the liquid. This cordierite, however, is metastable high-cordierite, which contributes to the amount of stable high-cordierite originally present at the high temperature. Since the amounts of secondary cordierite are usually in excess of those of primary cordierite, the composite peaks in the X-ray patterns are mainly due to metastable high-cordierite. Structural changes, which might have occurred upon cooling in the primary high-cordierite, are obscured, therefore, to a large extent.

Of particular interest is the behaviour of compositions such as Nos. 13–22 in which 'low'-cordierite, or at least intermediate-state cordierites are stable, despite the presence of much liquid up to the highest temperatures at which cordierite is present. When these compositions, run at the appropriate temperatures, were cooled slowly, single peaks in the X-ray patterns characteristic of high-cordierites were obtained in most cases. Only in favourable cases, in which the ratios of metastable high-cordierite to stable 'low'-cordierite were low enough, did the 'single' peaks exhibit broader bases, thus displaying their actual composite character.

An opportunity to study the influence of various rates of cooling on the primary cordierites alone is offered by compositions Nos. 1–3, which may contain stable high-cordierites at subsolidus temperatures. A 24-h run at 1,400° C on the four different materials of composition No. 2 used in the time studies (Table 8 (*c*) and section I 3 (*g*)) was cooled slowly according to Fig. 2 until a temperature of 790° C was reached. The structural states of the cordierites corresponded exactly to those obtained by rapid quenching, which are listed in Table 8 (*c*), second column. Stable high-cordierite previously crystallized from glass at 1,350° C for 8 days and then at 1,380° C for 7 days, when held at 1,050° C for 1 day showed a Δ value of only about 0·12°. From this information it is concluded that the transition of stable high-cordierite into 'low'-cordierite upon cooling is not at all instantaneous, but probably just as sluggish as the similar transition of metastable high-cordierite into 'low'-cordierite. Thus there is no danger of any variation of that structural state of cordierite which prevails under the conditions of the run, during the cooling procedures used in this study, unless there is liquid present.

In runs at the liquidus surface, periodical melting and subsequent recrystallization of some fraction of the cordierite should take place concomitantly with the temperature fluctuations caused by the manner of temperature regulation. The cordierites formed by recrystallization should be of the high form, independently of whether they are stable at this temperature or not. From these considerations one might deduce that the stability range of high-cordierite in the presence of liquid is only a pretended one. There are at least two reasons, however, to believe that this is not true: (1) in compositions behaving like Nos. 28, &c., there should

not be a gradual decrease of the Δ angles with increasing temperature (Fig. 18), but mixtures of 'low'-cordierite of constant Δ with high-cordierite increasing in amount with time should be encountered; (2) there should not be any compositions which contain intermediate-state or 'low'-cordierites stably up to the highest possible liquidus temperatures, as is the case in Nos. 12–22.

5. *Nature of the structural changes in cordierite and their dependence on the total bulk composition*

X-ray studies of the various forms of cordierite encountered show that the transitions take place without any drastic changes of the basic structure of cordierite. The hexagonal lattice of high-cordierite is being distorted into a lower, orthorhombic pseudohexagonal symmetry as soon as the gradual transition from high- toward 'low'-cordierite, i.e. the form with the strongest possible distortion, is initiated. The nature of this structural change, therefore, is certainly not that of a first-order transition. Miyashiro (1957) suggested that the changes are probably due to gradual ordering of the Al ions within the stacks of (pseudo-) hexagonal rings of $AlSi_5O_{18}$ composition, possibly accompanied by rearrangements of the interstitial Al^{+3}, Mg^{+2}, and Fe^{+2} ions between these rings. This would suggest that in high-cordierite the Al ions are randomly distributed (disordered) within these stacks of rings, whereas they are ordered, i.e. occupy fixed positions, in low-cordierite. The material synthesized in the experiments described in this paper was far too fine-grained to be used for single-crystal X-ray work, which alone could provide critical information concerning this suggestion. The thermal behaviour of the cordierite polymorphs is very similar to that of the feldspars, for which order–disorder relations have recently been shown by three-dimensional structure analysis (Bailey & Taylor, 1955; Ferguson *et al.*, 1958) as well as by the nuclear magnetic resonance technique (Brun *et al.*, 1960). This enhances the likelihood of Miyashiro's assumption of order–disorder in cordierite. Anorthite, in particular, displays a structural behaviour very similar to that of cordierite: its ordered modification is stable at subsolidus temperatures up to the melting-point (Laves & Goldsmith, 1955). However, metastable disordered anorthite can be obtained by crystallizing glass at subsolidus temperatures for short periods of time only (Goldsmith & Laves, 1956). No investigations are reported, however, about the polymorphic behaviour of anorthite in assemblage with adjoining phases within the system CaO–Al_2O_3–SiO_2, which might show further similarities to the polymorphic behaviour of cordierite in the system MgO–Al_2O_3–SiO_2 as described in this paper.

The variable stability conditions of high-cordierite in different bulk compositions of the melts found in this study may provide valuable information for future investigations on the actual structural processes involved in the high-'low' transition of cordierite. The behaviour of a number of bulk compositions investigated indicates that both high- and 'low'-cordierites may well be of the same composition. Certainly in the cases of the Δ-variable type, the transition

from 'low'- to stable high-cordierite does not seem to be *caused* by compositional variations of the cordierites. Influences other than compositional changes of the cordierite phase seem to be the governing factors in the transition. Fig. 23 shows the stability relations of high-cordierite within the system MgO–Al_2O_3–SiO_2. In general, there are three areas of different characteristics.

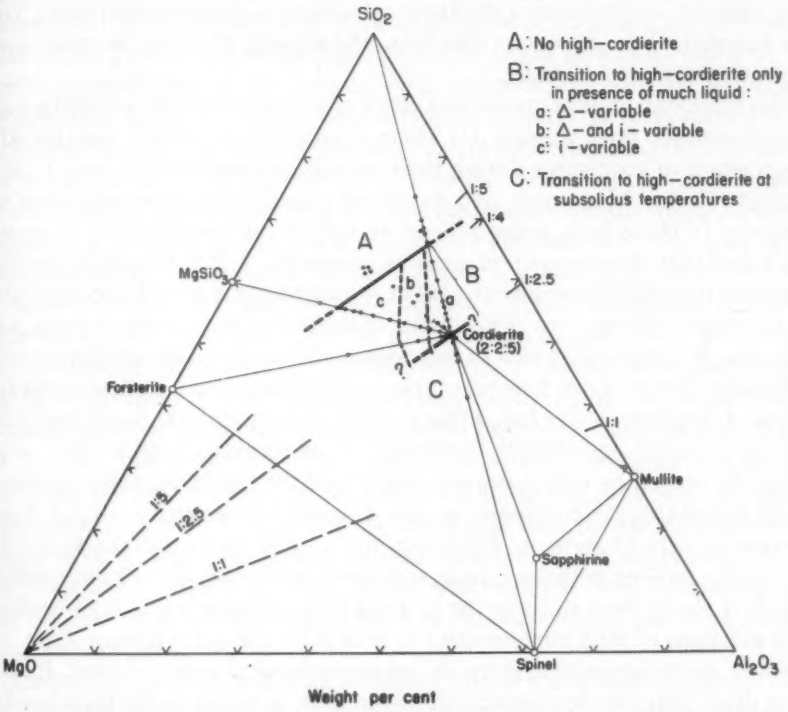

FIG. 23. Distribution of the various types of structural behaviour of the phase cordierite among bulk compositions in the system MgO–Al_2O_3–SiO_2. Solid dots indicate compositions investigated (Fig. 4). Numbers along Al_2O_3–SiO_2 side, as well as within the triangle, give the molar ratios Al_2O_3/SiO_2. For discussion of the boundaries between areas *A*, *B*, and *C*, as well as subzones *a*, *b*, and *c*, see text.

The data obtained on compositions Nos. 12–22 suggest that high-cordierite is not stable in compositions lying above a line roughly paralleling the boundary curve cordierite–silica (area A). In compositions just below this line high-cordierite is stable only in the presence of liquid. This area, *B*, is subdivided into three fields depending on whether the Δ values, the *i* values, or both vary during the transition. Area *B* has a very crudely indicated boundary against an area, *C*, of bulk compositions, in which a transition from 'low'- to high-cordierite may take place even in the absence of liquid. Although the exact boundaries between the various divisions are not known accurately, a few important conclusions

may be drawn from their distribution in relation to chemical composition. The range of bulk compositions in which no high-cordierite is stable at any temperature (area *A*) is characterized by high SiO_2 contents. However, its boundary does not parallel a constant value of SiO_2, or Al_2O_3, or MgO but moves toward lower SiO_2 contents with decreasing amounts of Al_2O_3 present. Area *B*, in which high-cordierite is stable only in the presence of liquid, shows intermediate SiO_2 values. Compositions with stable subsolidus high-cordierite (area *C*) contain less than about 50 wt per cent SiO_2, the amount probably decreasing with decreasing contents of Al_2O_3.

This threefold division cannot be a result of variable amounts of solid solution in cordierite for three reasons. (1) There is no evidence for any changes in the composition of cordierites during their *subsolidus* transitions in area *C* of the diagram. From the amount and nature of crystalline phases coexisting with cordierite in these bulk compositions at subsolidus temperatures it must be concluded that its composition remains invariably 2:2:5, despite a structural transition toward high-cordierite. (2) The second reason is given by comparison of the two types of behaviour of cordierite in the presence of liquid in areas *A* and *B*. In area *B*, structural as well as compositional changes of the cordierites stable at liquidus temperatures take place. For cordierites in bulk compositions lying in area *A*, however, it was found that a structural change to high-cordierite does not occur under equilibrium conditions. If structural changes, then, would always be caused by compositional changes of the cordierite solid solution, it would follow that the cordierites in area *A* would be consistently of 2:2:5 composition or very close to it. Therefore, for a given temperature above 1,355° $\pm 3°$ C, the tie lines between liquids and 'low'-cordierites of bulk compositions in area *A* would have to cross the tie lines between liquids and high-cordierite solid solutions of bulk compositions in area *B* for the same temperature. This, however, seems impossible from the physico-chemical point of view. It seems more likely that the 'low'-cordierites from area *A*, stable at the liquidus, have compositional variations similar to those displayed by cordierites, stable at liquidus temperatures in area *B*, which undergo structural transitions.[1] (3) In compositions Nos. 27 and 42, &c., compositional changes of 'low'-cordierites were found to take place at subsolidus temperatures without any measurable structural changes occurring simultaneously.

For these three reasons, it is believed that structural and compositional variations of cordierites are largely independent processes.

On the other hand, compositional variations of cordierites determine which

[1] Compositional variations of cordierites from bulk compositions lying in area *A* could not be demonstrated on the basis of phase assemblage studies, because the changes in the ratios of the solid phases caused by solid solution in cordierite, as well as the influence of this solid solution on the melting relations of these bulk compositions, are so small that they cannot be measured with present techniques. Attempts to confirm compositional variations by X-ray studies of the cordierites themselves have not been successful as yet, mainly because of the small quantities of cordierites coexisting with liquid, or—in the absence of liquid—because of the presence of as many as three other crystalline phases (pyroxene+cristobalite±tridymite).

type of structural transition takes place, i.e. the Δ-variable type, the *i*-variable type, or a combination of both. It is on this basis that area *B* of Fig. 23 was subdivided into three subzones—*a*, *b*, and *c*. Cordierites containing the highest amounts of 'Mg–beryl' in solid solution represent the *i*-variable type *c*, those with compositions very close to 2:2:5 the Δ-variable type *a*, and those of intermediate compositions form a subzone *b* for which both Δ and *i* vary with temperature. The direct causes of these three types of transition are differences in the lattice parameters of the high-cordierite (solid solutions) stable at the liquidus temperatures of the various bulk compositions. One might expect, therefore, that the courses of the boundary lines between the three subzones are functions of the various, so far unknown, tie lines between liquids and cordierite solid solutions. However, the amount of possible solid solution in cordierite is also a function of temperature (Fig. 10), and the temperatures at which cordierite disappears in the various bulk compositions are determined by the slope of the liquidus surface of the cordierite field of stability. It is concluded, therefore, that the boundaries between subzones *a–c* follow, approximately, the isotherms within the cordierite stability field. In the direction toward lower SiO_2 values these boundaries intersect with the field boundary, cordierite+spinel+liquid (Fig. 3). From these intersections onward they follow a different course toward the composition of spinel, and terminate when the border between areas *B* and *C* is reached. The deviation of the boundaries between subzones *a–c*, toward spinel composition, is based on the following behaviour: the first cordierites crystallizing from melts lying within the spinel field have the same compositions as those crystallizing from bulk compositions given by the intersection of the field boundary cordierite+spinel+liquid with straight lines (= conjugation lines) originating at spinel composition and passing through the compositions of the melts in the spinel field.

It has been shown above that the primary cause of a structural transition from 'low'- to high-cordierite in any bulk composition within the ternary system, no matter whether this transition is Δ- or *i*-variable, cannot lie in the variability of the composition of cordierite. The primary cause of the phase transitions in cordierite must rather be its *chemical environment*, independent of whether any atoms present in this environment enter the cordierite structure or not. The most important factor, relevant to the chemical environment influencing the phase transitions of cordierite within the ternary system $MgO–Al_2O_3–SiO_2$, is the ratio of Al_2O_3 to SiO_2: the borders between areas *A*, *B*, and *C* follow, more or less clearly, lines of constant $Al_2O_3:SiO_2$ ratios, which are indicated by light dashes in the lower left portion of Fig. 23. This observation may be interpreted in such a way that the Mg concentration has no, or only a very limited, influence on the phase transition. Thus, in compositions with molar ratios of $Al_2O_3:SiO_2$ lower than about 1:5 no high-cordierite forms stably under any conditions. Between ratios of about 1:5 and 1:2·5 high-cordierite forms only in the presence of liquid. In compositions with $Al_2O_3:SiO_2$ molar ratios in excess of about 1:2·5 no more

liquid is necessary to obtain high-cordierite, and the transitions take place with successively higher ratios at successively lower subsolidus temperatures.

Table 9 is an attempt to summarize, crudely, the structural and compositional variations of cordierites as a function of temperature and total bulk composition

TABLE 9

Structural and compositional variations of cordierites in the system $MgO–Al_2O_3–SiO_2$

			Areas of bulk compositions as defined in Fig. 23		
			A	*B*	*C*
Stable structural states of cordierites as a function of the amounts of liquid present	Liquidus (only for bulk compositions within the cordierite field)	Increasing temperature ↑	low	high	—
	Crystal+liquid region		low	high ↑ low	high
	Subsolidus		low	low	high ↑ low
Type of structural transition of cordierite			—	Δ-variable in subzone *a*; *i*-variable in subzone *c*; Δ- and *i*-variable in subzone *b*	Probably Δ-variable throughout
Solid solution in cordierite above 1,300° C following the substitution Mg+Si → 2Al			Probably variable amounts of solid solution in low-cordierites. Could not be ascertained by X-ray or other means	Increasing amounts of solid solution in subzones: $a < b < c$. Can be detected qualitatively by X-ray in high-cordierite	No evidence for solid solution of any kind

within the system $MgO–Al_2O_3–SiO_2$. The temperature as a variable is expressed only in terms of the presence or absence of a liquid phase. For further details, it is suggested that section I 3 be consulted. Metastable relations persistent only for short periods of crystallization have been omitted. The tabulation represents the relations valid for infinite time of crystallization. For this reason 'low'-cordierite is replaced by the truly stable form low-cordierite, i.e. the one with the highest Δ value to be attained. Compositions in area *C* of Fig. 23 do not have cordierites stable at their liquidus temperatures.

The structural behaviour of cordierites as a function of the Al_2O_3:SiO_2 ratio of the total bulk composition seems to support, further, the assumption that

order or disorder of Al and Si in the cordierite structure is the governing factor for the transition. The more Al in relation to Si a particular bulk composition contains, the greater the chances for the Al to find a random position within the stacks of rings of the lattice, i.e. the more likely becomes the formation of the disordered form.

J. GEOLOGICAL SIGNIFICANCE OF THE STRUCTURAL STATES OF NATURAL CORDIERITES, PARTICULARLY IN BUCHITES

1. *Difficulties in the use of the structural state of cordierite as a geologic thermometer*

In 1954 Miyashiro & Iiyama reported the finding of a new natural mineral-'indialite', polymorphic with cordierite, from fused shales of the Bokaro coalfield in India. Natural 'indialite', on the basis of its single peak at about 29·5° 2θ, is structurally close to, or identical with, the phase called high-cordierite in this paper. Sugiura & Kuroda (1955*a*), as well as Miyashiro (1957), showed that natural cordierites could be converted into 'indialite' by heating them to high temperatures. Furthermore, structurally intermediate minerals were found by Miyashiro (1957) to occur in nature, also. These discoveries seemed to enhance the possibility of using the structural state of natural cordierites as an indication of the conditions under which they were formed. More recently, Wyllie (1959) found cordierites with low distortion indices Δ in a Torridonian arkose in Soay (Hebrides), which had been fused by the intrusion of a picrite sill and converted into buchite. Wyllie strongly advocated the idea of using the distortion index Δ of cordierites occurring in buchites as a measure of the *PT* conditions during their formation.

The results of the present investigation cast serious doubts on such an application. Even in the simplest ternary system in which cordierite occurs, i.e. MgO–Al_2O_3–SiO_2, there is at constant pressure no fixed temperature for the transition of one modification into the other. Whether a transition takes place or not, and at what temperature, are dependent on the bulk composition of the mixture or, in other words, on the chemical environment in which the cordierite occurs. Natural cordierite-bearing rocks show a wide range of chemical compositions containing many more components than this simple ternary system. It is thus to be expected that the variability of the stable transition temperatures of natural cordierites with chemical composition of the host rock is increased by a large factor.[1] For a great many natural cordierite-bearing rocks there may

[1] It appears that different structural behaviour of a mineral as a function of its chemical environment may be a general property of all silicates showing order–disorder relations. Recently, Stewart (1960) has found that the structural state of albite at constant temperature, pressure, and time of heating, could be varied by adding other components. The use of the structural states of minerals of this type in geothermometry would, therefore, require additional information to ascertain temperatures of crystallization.

not be a stable field of high-cordierite under any conditions. Furthermore, there may be profound influences of confining pressure as well as of volatile components (water). Hydrothermal studies, in co-operation with H. S. Yoder, have shown that under high water pressures 'low'-cordierite is stable up to the incongruent melting temperatures of the composition $2MgO \cdot 2Al_2O_3 \cdot 5SiO_2$ (Schreyer & Yoder, 1959). This might be considered the reason why high-cordierites, or intermediate-state cordierites very close to high-cordierite, have, up to the present time, only been found in rocks like buchites, &c., which have formed at the surface or at least under conditions of low water pressure. Wyllie (1959) gives the maximum water pressure prevailing during the thermal metamorphism of the Torridonian arkose as 430 kg/cm².

With regard to the behaviour observed in the present study, however, the question arises whether the high-cordierites encountered in buchites, &c., really represent the stable modification of cordierite under the conditions of their formation, or whether initially formed metastable structural states have been preserved. In the sections to follow this problem is approached in a twofold way: (1) by an experimental investigation employing synthetic materials which approach the bulk composition of buchites, and also a natural sample from the Bokaro coalfield itself; (2) by comparison of experimental data and petrographic observations.

2. *Compositions of buchites and related cordierite-bearing rocks*

Sedimentary rocks ranging from arkoses to shales, that had been partly or totally fused owing to thermal metamorphism by shallow basic intrusions, are usually called buchites (for derivation of this name, see Tomkeieff, 1940). They are characterized by minute cordierites and orthopyroxenes or mullites in a glassy matrix. Unmelted remnants of pre-existing minerals (e.g. quartz, feldspar) may also be present in variable amounts. For rocks almost completely fused by burning coal-seams, the term paralava has been applied by Fermor (1924). Self-explanatory names such as fused shale or fused sandstone are also in common use.

The chemical composition of these rocks is in many cases identical with that of the unaltered sediment. In others, modifications of composition have taken place by contamination with igneous material (Thomas, 1922); some may result from the physical mixing of two melts (Ackermann & Walker, 1960). Only few chemical analyses of buchites and associated rocks have been reported in geologic literature. Some are shown in Table 10, which includes analyses of the buchite of the Blaue Kuppe in Germany and its parent material, as given by Ramdohr (1919) and Koritnig (1954). Unpublished analyses of cordierite-bearing fused clays and feldspathic sands from an andesite contact in northern New Mexico have kindly been made available by Roy Bailey of the U.S. Geological Survey, Washington, D.C. Furthermore, the analysis of a cordierite-bearing buchite has

TABLE 10

Selected analyses of buchites and related rocks, and their starting materials

	1	2	3	4	5	6	7
SiO_2	64·39	82·02	70·73	56·80	53·77	71·88	55·17
Al_2O_3	17·44	8·11	11·13	21·63	20·02	12·00	20·67
TiO_2	0·63	0·29		0·94	0·73	0·44	2·81
Fe_2O_3	4·87	1·28	6·88	1·58	6·60	1·19	0·27
FeO	1·29	0·14		3·80		1·87	6·23
MnO	0·07	0·02	—	—	—	0·03	0·16
MgO	3·12	0·55	1·22	2·95	3·62	0·10	5·32
CaO	0·65	0·63	0·67	0·99	1·89	1·84	2·99
BaO	0·07	0·03	—	—	—	—	0·06
K_2O	3·71	3·05	2·16	3·87	3·46	2·30	3·09
Na_2O	1·24	1·08	2·39	2·97	1·69	3·50	0·23
H_2O^+	1·63	1·93	2·48	2·38		4·00	1·64
H_2O^-	0·11	0·65	1·71	1·42	8·24*	0·25	0·37
P_2O_5	0·17	0·04	—	—		0·23	0·91
SO_3	0·35	—	—	—		—	—
F	0·07	0·01	—	—	—	—	—
Cl	—	0·01	—	—	—	—	—
CO_2	—	—	0·05	0·27	—	—	—
	99·81	99·84	99·42	99·60	100·02	99·63	99·92
Molar ratio Al_2O_3/SiO_2	1:6·26	1:17·15	1:10·78	1:4·46	1:4·56	1:10·17	1:4·53

* Ignition loss.

1. Fused clay, Arroyo de la Plaza Larga, New Mexico (Bailey, unpublished data, 1960).
2. Fused feldspathic sand, Arroyo de la Plaza Larga, New Mexico (Bailey, unpublished data, 1960).
3. Sandy clay, Blaue Kuppe, Germany (Ramdohr, 1919).
4. Glassy rock (buchite) from fusion of above sandy clay, Blaue Kuppe, Germany (Ramdohr, 1919).
5. Red clay unaltered, Blaue Kuppe, Germany (Koritnig, 1954).
6. Buchite, specimen No. 61*a*, from contact of Baksteen sill (Ackermann & Walker, 1960).
7. Fused shale, Bokaro coalfield, India. Specimen No. 23/951, Geological Survey of India. Analyst: C. O. Ingamells.

been selected from a number of new buchite analyses given by Ackermann & Walker (1960). Lastly, the first analysis to be made of the specimen of the fused shale from Bokaro coalfield, in which Miyashiro & Iiyama (1954) had discovered 'indialite' (specimen No. 23/951, Geological Survey, India), is given. This specimen was obtained through the courtesy of Dr. A. P. Subramaniam and Mr. V. Venkatesh, both of the Geological Survey of India. Table 10 lists, also, the computed molar ratios of Al_2O_3:SiO_2 of these rocks. The latter values lie within, or very close to, the range ($\lesssim$ 1:5) for which, in the ternary system MgO–Al_2O_3–SiO_2, high-cordierite was not found to be stable at any temperature (Fig. 23).

3. *Experimental results on synthetic 'haplobuchites'*

In order to study the structural behaviour of cordierites in more complex melts, runs were made at atmospheric pressure and at various temperatures on a number of compositions on the join cordierite–silica–albite, which represents a plane through the tetrahedron Na_2O–MgO–Al_2O_3–SiO_2. These compositions

had been prepared previously by Schairer (1957) for the purpose of studying the melting relations in this quaternary system. If one assumes that iron can substitute in an unlimited way as FeO for MgO, and as Fe_2O_3 for Al_2O_3, and that the presence of K_2O influences only the composition of the alkali–feldspar solid solution, but does not change the melting relations drastically, these synthetic compositions may be regarded, as a first approximation, as simplified buchites or 'haplobuchites'. The chemical compositions of the melts investigated are given in terms of wt per cents of the oxides in Table 11, which also lists their computed

TABLE 11

Compositions investigated on the join cordierite–albite–SiO_2

	Composition (wt per cent)				*Calculated mode (wt per cent)*			*Molar ratio*	*Cordierite stable up to (in °C)*
No.	Na_2O	MgO	Al_2O_3	SiO_2	*Albite*	*Cordierite (2:2:5)*	SiO_2	Al_2O_3/SiO_2	
A4	0·59	7·58	20·14	71·69	5	55	40	1:6·04	1,433
A11	1·77	7·58	22·09	68·55	15	55	30	1:5·27	1,428
A7	2·36	8·27	24·81	64·56	20	60	20	1:4·42	1,428
A26	5·20	6·34	24·59	63·87	44	46	10	1:4·40	1,388
A6	3·54	2·07	11·06	83·32	30	15	55	1:12·79	1,321
A8	7·09	2·76	18·63	71·51	60	20	20	1:6·52	1,312

molar ratio of Al_2O_3:SiO_2, as well as the temperatures up to which cordierite was found to be a stable phase. Other data, such as liquidus temperatures and the appearance of additional crystalline phases on cooling, have been omitted as not being pertinent to the present problem. It should be noted, however, that liquid forms in these compositions as low as 1,045°±10° C (Schairer, 1957). Thus cordierite is in equilibrium with liquid over a range of as much as 400° C. Despite this fact, the experimental results show that 'low'-cordierite is the stable phase throughout this entire temperature range. Similarly, as in the system MgO–Al_2O_3–SiO_2, high-cordierites are first formed metastably at all temperatures at which crystallization takes place. The rate at which they go over into the stable 'low' form increases with increasing temperature. The distortion index Δ of the cordierite was found to increase with increasing temperatures and duration of run, despite the presence of increasing amounts of liquid. The highest Δ values measured were 0·26°.

Thus the structural behaviour of the cordierites in these melts is identical with that of compositions lying in area *A* of the ternary system MgO–Al_2O_3–SiO_2 (Fig. 23). With the possible exception of compositions Nos. A7 and A26, the molar ratios Al_2O_3:SiO_2 of these more complex melts fall within the range of instability of high-cordierite in the ternary system. It is possible that with Na_2O present as a fourth component the critical Al_2O_3:SiO_2 ratio for the stable formation of high-cordierite becomes even higher, because part of the alumina is being tied up in structural units preparatory to the formation of albite.

4. *Experimental investigation of a fused shale from Bokaro coalfield, India*

The structural behaviour of cordierite in a highly complex natural melt was studied at atmospheric pressure over a range of temperatures for various lengths of time. As a typical example, specimen No. 23/951 (Geological Survey, India) of the fused shale from Bokaro was chosen, the chemical composition of which is given in Table 10. Optical and X-ray studies of the original material confirmed the finding of Miyashiro & Iiyama (1954) that most of the cordierite, which represents the main crystalline phase in this specimen, is present in a structural state very close to high-cordierite. Only minor amounts of intermediate-state cordierite were found. The other crystalline phases are ilmenite, orthopyroxene (as well as small amounts of clinopyroxene), and a little plagioclase. The rest of the bulk composition is represented by a brown glass with a refractive index of approximately 1·540.

Runs were made in air in platinum envelopes as well as in sealed platinum tubes. No appreciable differences were found in results by the two methods, even in long runs. Under these conditions the liquidus temperature of specimen No. 23/951 was determined as 1,340°±10° C. Between this temperature and 1,295°±5° C small amounts of tiny, brownish, cubic or octahedral or skeletal crystals of very high refractive index (probably perovskite or possibly brown spinel) are in equilibrium with a liquid, which can be quenched to a glass of a refractive index around 1·560. At 1,295°±5° C cordierite comes in, and this is joined by ilmenite and possibly a little magnetite at about 1,210° C. Crystallization of pyroxenes and feldspars at still lower temperatures was not pursued.

Except for the lack of volatiles the conditions of these experiments are probably not very different from those prevailing at the time when the burning of the coal-seams took place under surface conditions. The fact that cordierite starts to crystallize at 1,295°±5° C in the absence of crystalline magnetite or haematite seems to indicate that the oxidation state of iron in the rock has probably not changed drastically during the course of the experiments.

The cursory determination of the principal melting relations of the fused shale is of interest with regard to the temperatures attained in the burning coal-seams. There is petrographic evidence (see below) that a large part, if not all, of the cordierite in specimen No. 23/951 crystallized during the cooling of the melt and was not in equilibrium with the melt for a very long time. The original temperature, therefore, must have been high enough to melt most of the bulk composition. It can be estimated as being at least as high as 1,250° C, at which temperature only a small fraction of the cordierite would be in equilibrium with liquid and early accessory minerals. This temperature is of the same order of magnitude as that determined for the burning coal-seams of Coal Canyon, Arizona, by Brady & Greig (1939).

The structural behaviour of the cordierites in the fused shale was found to be as follows. The starting material contains mainly high-cordierite. In runs at

1,250° C, of only 2 h duration, no changes of the structural state were observed. After 24 h at the same temperature, however, intermediate-state cordierite with a distortion index $\Delta = 0{\cdot}17°$ had developed, and after 7 days 'low'-cordierite with $\Delta = 0{\cdot}25°$ was obtained, despite the presence of large amounts of liquid. At 1,290° C, i.e. just below the temperature at which cordierite disappears, after 7 days of heating the distortion index was found to be 0·26°, although only a very small amount of cordierite was present. On the other hand, at 1,000° C high-cordierite persisted for 19 days without any notable changes.

It can be concluded from this behaviour that the stable form of cordierite for the bulk composition of specimen No. 23/951 at 1 atm is 'low'-cordierite, up to the temperature of disappearance of cordierite. The high-cordierite originally present in the specimen must be considered a metastable phase, which is more persistent the lower the temperature and the shorter the thermal treatment. This structural behaviour is identical with that displayed by cordierites from bulk compositions lying in area *A* (Fig. 23) of the ternary system MgO–Al_2O_3–SiO_2 as well as from the 'haplobuchites' on the join cordierite–silica–albite.

5. *Petrographic and X-ray studies on cordierites in fused shales, &c.*

Venkatesh (1952), in a detailed petrographic examination of the fused shales from Bokaro coalfield, described the variable crystal development of cordierite in these rocks. To summarize briefly, he suggested that well-formed symmetrical crystals of cordierite with regular twin patterns were formed by comparatively slow growth, whereas more rapid growth led to the development of more or less imperfect, unsymmetrical, possibly skeletal crystals with irregular twin patterns. On a morphological basis he distinguished between four different types of cordierites. His statements preceded the discovery of the hexagonal form of cordierite in these rocks.

Three specimens (Geological Survey of India, Nos. 23/855, 23/951, 23/952) collected by L. L. Fermor in 1916, which display Venkatesh's (1952) four types of cordierites, were kindly made available for study by Dr. A. P. Subramaniam and Mr. V. Venkatesh, both of the Geological Survey of India. The results of petrographic and X-ray studies carried out by the present authors are:

(1) The cordierite in specimen No. 23/855 occurs in small symmetrical pseudo-hexagonal twinned prisms (type I of Venkatesh, 1952; compare his plate 1, fig. 1). X-ray investigations showed the distortion index Δ of these crystals to be 0·27°, with the peaks clearly separated. Thus these cordierites are normal 'low'-cordierites, comparable to the structural states of most other natural cordierites.

(2) Specimen No. 23/952 contains cordierites of Venkatesh's type IV showing imperfect crystals with multiple terminations and preferred growth (his plate 1, figs. 4–6). Their mean Δ value was found to be 0·18°. The shape of the X-ray peaks, however, suggests that the material is structurally inhomogeneous, thus producing composite reflections. Yet it is believed that most of the cordierites

in this sample represent intermediate structural states between high- and 'low'-cordierite.

(3) Specimen No. 23/951, which was analysed chemically in this study (Table 10) and used for the high-temperature runs described in the previous section contains cordierites of Venkatesh's types II and III, that are very imperfectly developed clusters and wreaths and which resemble certain devitrification textures known from volcanic material (Venkatesh's plate 1, fig. 3). Only a relatively small amount of the total cordierite in this specimen shows better crystal development, approaching Venkatesh's type IV. As previously mentioned, the X-ray investigation on cordierites from specimen No. 23/951 yielded mainly high-cordierite and possibly small amounts of intermediate-state cordierite.

This compilation of data shows that there is a definite relationship between crystal development and the distortion index Δ of cordierite in these rocks: the more perfect the development of the cordierite crystals is, the higher their distortion index. The chemical compositions of the three specimens, as approximated from their constituent minerals, are not so dissimilar that drastically different temperatures have to be assumed for the beginning of melting. Thus the temperatures which these vitreous rocks have endured at the time of the crystallization of cordierite cannot vary between very wide limits, although, admittedly, steep temperature gradients are possible in burning coal-seams. It is considered unlikely, therefore, that the variable crystal development of the cordierites, as well as their related different structural states, is a function of these relatively small temperature differences. It is much more likely that both of these variations are due to a difference in the time factors of crystallization. Venkatesh (1952) has expressed this variable as rate of growth. One might expect, however, that for rocks of similar bulk composition and similar environmental conditions the *rate* of growth of a crystal phase would, during their formation, be rather uniform. Based upon the experimental data obtained on cordierite-bearing systems in this study it is preferred, therefore, to introduce this variable as the *time period of heating*. During this time period a certain equilibrium amount of cordierite first grows at a rate given by the environmental conditions. If heating is continued, this fixed amount of cordierite, originally formed as high-cordierite, through rearrangements of atoms gradually approaches its stable structural state, as well as its proper crystal form.

On the basis of this concept the interpretations of the different structural states, as well as the different crystal development, of cordierites in the three above-mentioned specimens are the following:

(1) Specimen No. 23/855 had been subjected to a temperature at which all the cordierite now present was in equilibrium with liquid. This was the case for a length of time sufficient for the cordierite to attain its stable structural state ('low'-cordierite) and proper crystal form. Subsequently the rock was quenched very rapidly so that no more cordierite was able to crystallize, but glass was preserved.

(2) Two different conditions might lead to the present status of specimen No. 23/952:

(*a*) It could have been subjected to a temperature at which cordierite coexists with liquid, but not long enough to reach full polymorphic equilibrium.

(*b*) The temperature could have been high enough to melt most or all of the cordierite formed initially during a gradual temperature increase. Subsequently the temperature went gradually down through the range of coexistence of cordierite with liquid. During this time the originally crystallizing high-cordierite was not able to invert to the stable 'low' form. As the imperfections in the cordierite crystals seem to be growth rather than destruction (melting) phenomena, the second possibility is more likely.

(3) The crystal development of cordierite in specimen No. 23/951 indicates that most, if not all, of the cordierite had melted. The irregular masses of cordierite formed during the cooling of the melt, which, although slow enough for cordierite to crystallize, was not slow enough to transform the high-cordierite, formed metastably, into the stable structural state.

Specimen No. 23/951 is still the only known natural source of high-cordierite. In a search for other occurrences in rocks of similar origin eight samples were collected from the area around Gillette, Wyoming, where burning coalfields of Tertiary age have, under surface conditions, produced a series of pyrometamorphic rocks, locally named clinkers, within their adjoining shaly country rocks. The clinkers are mostly loose boulders covering the upper parts of the hills. Since they are separated from underlying horizontal coal-seams by some tens of feet of unaltered unconsolidated sediments, they are likely to have been formed through burning of stratigraphically higher coal measures, which have since been eroded. Since these clinkers are more resistant to erosion than the unfused sediments, they remained on the prevailing erosional surface. Subsequent to the Tertiary fusion of these rocks, some of their original features may have been altered.

The clinkers are very fine-grained, grey or reddish rocks, frequently with a slag-like appearance. There are all gradations, from rocks which are only fritted to others that show flow structures indicating that they crystallized from a melt. Owing to their fine grain size, the mineral contents of these rocks had to be determined mainly by powder X-ray diffraction patterns. Those rocks which are only fritted consist largely of mullite, cristobalite, and possibly a little plagioclase. These predominantly aluminous and siliceous bulk compositions, originally probably kaolinitic clays, because of their high melting-points prevented extensive fusion and did not produce cordierite. Mg–Fe-richer bulk compositions, on the other hand, which were usually fused to a larger extent, were found to contain appreciable amounts of cordierite together with plagioclase, tridymite, and a little clinopyroxene. In some cases there were also cristobalite, relic quartz,

and possibly a little mullite. Ore minerals are magnetite, ilmenite, and in some cases haematite.

Microscopic studies confirm that these rocks have an extremely fine fabric, which is only slightly coarser around certain vugs in the slag-like specimens. There, cordierite occurs as tiny but idiomorphic symmetrical prisms, which do not exceed 0·03 mm in length. In rocks with only small amounts of glass present, cordierite forms a dense felt together with the plagioclase and tridymite.

X-ray investigations of the cordierites show that they display intermediate structural states with Δ values ranging from about 0·08° to 0·18°. There is poor separation of peaks and, particularly for the low values, the reflections appear as a single but slightly broader peak. As a general rule it can be stated that the Δ values of these cordierites are lower in less extensively fused rocks. For rocks of identical bulk composition, which is, as a first approximation, the case for all cordierite-bearing clinkers, the degree of fusion is a function of the temperature attained. Thus the *lower* Δ values have to be attributed to *lower* temperatures of heating. This is exactly opposite to the original conception of Miyashiro (1957) that hexagonal cordierite is formed under the highest temperatures. These relations show clearly the type of crystallization of these cordierites, which begins with the metastable formation of high-cordierite. This high-cordierite gradually inverts toward 'low'-cordierite if the heating is sufficiently long and high to convey enough energy for ordering of the crystal lattice. The main difference between the formation of these cordierites with very low Δ and the high-cordierites of specimen No. 23/951 described previously, therefore, is that the latter formed from liquid (or glass) on *cooling*, whereas these formed from pre-existing solid material upon *heating*. However, they are both metastable products preserved because of short thermal treatments.

Partially fused clays and arkosic sands from near Espanola, New Mexico, are presently being studied in detail by Roy Bailey at the U.S. Geological Survey in Washington, D.C. Two chemical analyses of this material are listed in Table 9. In addition to pre-existing quartz and feldspars the rocks contain cordierite, pyroxene, a little mullite, and some ore minerals in a glassy matrix. Cordierite forms pseudohexagonal prisms often with symmetrical sector twinning. Bailey (personal communication) determined its Δ value as approximately 0·25°. No high-cordierite has been found. It appears that the heating was long enough for structural ordering, and no additional cordierite crystallized when the melts were quenched to glass.

In the case of the fused Torridonian arkose from the Hebrides, the idiomorphic cordierite prisms yielded a Δ value of only 0·08° (Wyllie, 1959). The bulk composition of the fused cordierite-bearing xenolith which was reported in a more recent paper by Wyllie (1961) has an Al_2O_3:SiO_2 ratio of only 1:11·04. Since this ratio is not sufficiently high to yield stable high-cordierite at any temperature, the structural state of cordierite determined by Wyllie (1959) has to be considered metastable. The temperature was obviously high enough for fusion,

but was not maintained long enough for the cordierite to attain polymorphic equilibrium. Judging from the perfect shape of the cordierite crystals it is unlikely that they formed during rapid cooling.

The distribution of temperature in the space around intrusive bodies over various lengths of time is extremely complicated, and a function of many variables such as shape and mass of the intrusion, gas content, &c. Approximations on this problem were given by Koritnig (1955) for the contact of the basalt of the Blaue Kuppe, Germany. He concluded that an intrusion temperature of 1,100° C, maintained for 2–3 days, would be enough to produce the observed contact phenomena, including fusion. From experimental evidence on the various bulk compositions studied in the present investigation it can be stated that *dry* heat treatment at 1,100° C for 2–3 days of previously non-cordierite-bearing material, independent of its composition, would not produce 'low'-cordierite (compare experiment with specimen No. 23/951, which after heating at 1,000° C for 19 days still consisted of high-cordierite). Thus it is not at all impossible that cordierites with low Δ values may persist metastably in the presence of liquid for appreciable amounts of time. This is the more so the lower the temperature of the beginning of melting of the particular bulk composition.

Cordierite in the buchites from the Blaue Kuppe, Germany, according to Ramdohr's (1919) and Koritnig's (1954) descriptions, occurs either as idiomorphic prisms surrounded by glass or as pseudomorphs after pre-existing biotite. No data on the cordierite polymorphism were reported. Through the courtesy of Dr. Koritnig of the University of Göttingen, Germany, a sample of the buchite was obtained and studied by X-rays. The distortion index Δ of the cordierite was determined as 0·18°. The separation of peaks is not very distinct. It is believed that in a *dry* environment this structural state could not have been attained at the temperature (1,100° C) and within the time (2–3 days) estimated by Koritnig (1955). The time of heating at this temperature was either longer, or crystallization took place under a moderate pressure in the presence of volatiles, as proposed by Koritnig (1955) himself.

6. *The use of the structural state of cordierite as a geologic timer*

It is quite obvious from the data presented on the synthetic as well as natural materials that the structural state of cordierite cannot be used incontrovertibly as a geologic thermometer. There is a good chance, however, that in future studies this property may find an even more interesting application as a sort of geologic *timer* for the thermal *history* of cordierite-bearing rocks. Timing in this case would be based on the gradual transition of initially crystallizing metastable high-cordierite toward low-cordierite. It presupposes that the structural states of natural cordierites—particularly of those with small distortion indices Δ—do *not* represent the form of cordierite which was stable under the conditions of rock formation but represent only more or less advanced stages on the way *toward* the stable form (low-cordierite). This presupposition is fulfilled for all rocks with

bulk compositions for which there is no stable transition to high-cordierite at any temperature; this type is represented by area *A* in Fig. 23. The bulk compositions of many, if not most, natural cordierite-bearing rocks fall, according to their Al_2O_3/SiO_2 ratios, into this category. For the other two types of bulk compositions (represented by areas *B* and *C* of Fig. 23), for which there are stable structural transitions of cordierite at liquidus or at subsolidus temperatures, respectively, the above presupposition would be fulfilled if the formation of the rock took place in a stable field of low-cordierite. Natural rocks belonging to these two types need to have highly aluminous compositions (emery deposits, &c.), which are characterized by high melting-points. The temperatures of stable cordierite transitions in these rocks, even if taking place in the absence of liquid, seem to be so high that they are not readily attained within the crust. Low-cordierite, therefore, does seem to represent the stable polymorph for most, if not all, cordierites formed under natural conditions. This also includes cordierites in deep-seated igneous and metamorphic rocks.

If the structural state of cordierites be thus used as a geologic timer the following considerations must be taken into account:

(1) The rate of transformation increases greatly with increasing temperatures of crystallization. Examples are given in Table 7. One may conclude from these data, in a semiquantitative way, that the magnitude of the structure index attained is proportional to the product of temperature and time of crystallization.

(2) The data compiled in Table 7 also show that the rate of transformation varies to a certain extent with the bulk composition in which the cordierite occurs.

(3) Studies of Schreyer and Yoder (unpublished data) indicate that high confining pressure, alone, increases the rate of transformation at a constant temperature. The presence of volatile components such as excess water vapour increases it even more.

Thus the distortion index of a cordierite is the result of a complex concurrence of all these variables. Successful timing, therefore, can only be achieved if there is independent evidence available on the magnitude of these other variables. For buchites the variables pressure, and possibly even volatile contents, can be eliminated to a very large extent. Qualitative attempts at timing the different thermal histories of these rocks have been presented in the previous section. In well-crystallized, deep-seated rocks such as plutonic and metamorphic rocks the distortion indices of the cordierites are usually closer to the stable low form than in most buchites. Nevertheless, Δ values as low as 0·12° have been reported by Miyashiro (1957) for cordierites from pegmatites. The frequent occurrence of intermediate-state cordierites in pegmatites is probably not without significance. This environment presumably results in a relatively low product of temperature and duration of heating, which causes metastable structural states to persist even in the presence of high amounts of volatile components. Recently, the authors have determined distortion indices Δ ranging from 0·12° to 0·20° on

cordierite phenocrysts from late quartz–dioritic intrusions in the Wallowa Mountains, Oregon (studied by W. H. Taubeneck). Interpretations of these low Δ values in conjunction with independent determinations of the other variables may yield valuable information about the length of time involved in the crystallization of these rocks.

ACKNOWLEDGEMENTS

The writers owe gratitude to Dr. H. S. Yoder, Jr., of the Geophysical Laboratory, who took an active part in most of the discussions during the course of this work. Dr. P. M. Orville, then also at the Geophysical Laboratory, now at Cornell University, made a flame photometer alkali analysis on one of our compositions. Thanks are due to Dr. B. J. Skinner of the U.S. Geological Survey, Washington, D.C., in whose diffractometer heating stage the high-temperature X-ray work was performed, and to Mr. Roy Bailey, also of the U.S. Geological Survey in Washington, D.C., who has made available his unpublished data on buchites from New Mexico. Mr. H. E. Swanson of the National Bureau of Standards, Washington, D.C., has helped in refining the X-ray data given in Tables 5 and 6.

We also wish to thank the following persons, who have contributed samples of various kinds for this study: Dr. W. R. Foster, Ohio State University; Dr. S. Koritnig, Universität Göttingen, Germany; Dr. J. Schlocker, U.S. Geological Survey, Menlo Park, California; Dr. A. P. Subramaniam and Mr. V. Venkatesh, both of the Geological Survey of India, in Calcutta; and Dr. W. H. Taubeneck, Oregon State College.

REFERENCES

ACKERMANN, P. B., & WALKER, F., 1960. Vitrification of arkose by dolerite near Heilbronn, Orange Free State. *Quart. J. geol. Soc. Lond.* **116**, 239–54.

ARAMAKI, S., & ROY, R., 1959. The mullite–corundum boundary in the systems MgO–Al_2O_3–SiO_2 and CaO–Al_2O_3–SiO_2. *J. Amer. ceram. Soc.* **42**, 644–5.

ATLAS, L., 1952. The polymorphism of $MgSiO_3$ and solid-state equilibria in the system $MgSiO_3$–$CaMgSi_2O_6$. *J. Geol.* **60**, 125–47.

BAILEY, S. W., & TAYLOR, W. H., 1955. The structure of a triclinic potassium feldspar. *Acta Cryst. Camb.* **8**, 621–32.

BARTH, T. F. W., & POSNJAK, E., 1932. Silicate structures of the cristobalite type. III. Structural relationship of high-cristobalite, α-carnegieite, and Na_2CaSiO_4. *Z. Kristallogr.* **81**, 376–85.

BOWEN, N. L., & ANDERSEN, O., 1914. The binary system MgO–SiO_2. *Amer. J. Sci.*, 4th ser., 37, 487–500.

—— & GREIG, J. W., 1924. The system Al_2O_3–SiO_2. *J. Amer. ceram. Soc.* 7, 238–54.

BOYD, F. R., JR., & SCHAIRER, J. F., 1957. The join $MgSiO_3$–$CaMgSi_2O_6$. *Carnegie Inst. Wash. Year Book*, **56**, 223–5.

BRADY, L. F., & GREIG, J. W., 1939. Note on the temperature attained in a burning coal seam. *Amer. J. Sci.* **237**, 116–19.

BRUN, E., HARTMANN, P., STAUB, H. H., HAFNER, ST., & LAVES, F., 1960. Magnetische Kernresonanz zur Beobachtung des Al,Si-Ordnungs/Unordnungsgrades in einigen Feldspäten. *Z. Kristallogr.* **113**, 65–76.

BYSTRÖM, A., 1942. The crystal structure of cordierite. *Ark. Kemi Min. Geol.* **15B**, No. 12.

CHINNER, G. A., & SCHAIRER, J. F., 1960. The join 'grossularite-pyrope' at atmospheric pressure, and its bearing on the system CaO–MgO–Al_2O_3–SiO_2. *Carnegie Inst. Wash. Year Book*, **59**, 72–76.

FAIRBAIRN, H. W., & SCHAIRER, J. F., 1952. A test of the accuracy of chemical analysis of silicate rocks. *Amer. Min.* **37**, 744–57.

FERGUSON, R. B., TRAILL, R. J., & TAYLOR, W. H., 1958. The crystal structures of low-temperature and high-temperature albites. *Acta Cryst. Camb.* **11**, 331–48.

FERMOR, L. L., 1924. Discussion of Tilley, C. E. Contact-metamorphism in the Comrie area of the Perthshire Highlands. *Quart. J. geol. Soc. Lond.* **80**, 70–71.

FLÖRKE, O. W., 1955*a*. Strukturanomalien bei Tridymit und Cristobalit. *Ber. Dtsch. keram. Ges.* **32**, 369–81.

—— 1955*b*. Zur Frage des 'Hoch'-Cristobalits in Opalen, Bentoniten und Gläsern. *Neues Jb. Miner., Mh.* 217–23.

FOLINSBEE, R. E., 1941. Optical properties of cordierite in relation to alkalies in the cordierite–beryl structure. *Amer. Min.* **26**, 485–500.

FOSTER, W. R., 1950*a*. Synthetic sapphirine and its stability field in the system MgO–Al_2O_3–SiO_2. *J. Geol.* **58**, 135–51.

—— 1950*b*. Synthetic sapphirine and its stability field in the system MgO–Al_2O_3–SiO_2. *J. Amer. ceram. Soc.* **33**, 73–84.

—— 1951. High-temperature X-ray diffraction study of the polymorphism of $MgSiO_3$. Ibid., **34**, 255–9.

FRIEDMAN, G. M., 1954. The spinel–silica reaction succession: a study of incompatible mineral phases. *J. Geol.* **62**, 366–74.

GELSDORF, G., MÜLLER-HESSE, H., & SCHWIETE, E.-E., 1958. Einlagerungsversuche an synthetischem Mullit und Substitutionsversuche mit Galliumoxyd und Germaniumoxid. *Arch. Eisenhüttenw.* **29**, 513–19.

GOLDSMITH, J. R., & LAVES, F., 1956. Crystallization of metastable disordered anorthite at 'low temperatures'. *Z. Kristallogr.* **107**, 396–405.

GOSSNER, B., 1928. Über strukturelle Beziehungen zwischen Beryll und Cordierit. *Centralbl. Min., Abt. A*, 204–7.

GREIG, J. W., 1927. Immiscibility in silicate melts. *Amer. J. Sci.*, 5th ser., **13**, 1–44, 133–54.

—— & BARTH, T. F. W., 1938. The system, $Na_2O \cdot Al_2O_3 \cdot 2SiO_2$ (nephelite, carnegieite)–$Na_2O \cdot Al_2O_3 \cdot 6SiO_2$ (albite). Ibid., **35–A**, 93–112.

HOLMQUIST, S. B., 1958. A note on the sluggish silica transformations. *Z. Kristallogr.* **111**, 71–76.

HUMMEL, F. A., & REID, H. W., 1951. Thermal expansion of some glasses in the system MgO–Al_2O_3–SiO_2. *J. Amer. ceram. Soc.* **34**, 319–21.

IIYAMA, T., 1955. Existence of indialite solid solutions. *Proc. imp. Acad. Japan*, **31**, 166–8.

—— 1956. Optical properties and unit cell dimensions of cordierite and indialite. *Miner. J.* **1**, 372–94.

—— 1958. Transformation des formes haute température, basse température de la cordierite. *C.R. Acad. Sci.* **246**, 795–8.

KARKHANAVALA, M. D., & HUMMEL, F. A., 1953. The polymorphism of cordierite. *J. Amer. ceram. Soc.* **36**, 389–92.

KEITH, M. L., & SCHAIRER, J. F., 1952. The stability field of sapphirine in the system MgO–Al_2O_3–SiO_2. *J. Geol.* **60**, 181–6.

KORITNIG, S., 1954. Die Vorgänge bei der Kontaktbildung im Buntsandstein durch die Basalte der Blauen Kuppe und des Alpsteins, Nordhessen. *Heidelberg. Beitr. Min.* **4**, 89–98.

—— 1955. Die Blaue Kuppe bei Eschwege mit ihren Kontakterscheinungen. Ibid. 504–21.

KUZEL, H.-J., 1961. Über Formel und Elementarzelle des Sapphirin. *Neues Jb. Miner., Mh.* 68–71.

LAVES, F., & GOLDSMITH, J. R., 1955. The effect of temperature and composition on the Al–Si distribution in anorthite. *Z. Kristallogr.* **106**, 227–35.

MIYASHIRO, A., 1956. Osumilite, a new silicate mineral, and its crystal structure. *Amer. Min.* **41**, 104–16.

—— 1957. Cordierite–indialite relations. *Amer. J. Sci.* **255**, 43–62.

—— & IIYAMA, T., 1954. A preliminary note on a new mineral, indialite, polymorphic with cordierite. *Proc. imp. Acad. Japan*, **30**, 746–51.

—— —— YAMASAKI, M., & MIYASHIRO, T., 1955. The polymorphism of cordierite and indialite. *Amer. J. Sci.* **253**, 185–208.

OSBORN, E. F., & SCHAIRER, J. F., 1941. The ternary system pseudowollastonite–akermanite–gehlenite. Ibid. **239**, 715–63.

RAMDOHR, P., 1919. Über die Blaue Kuppe bei Eschwege und benachbarte Basaltvorkommen. *Jb. Preuß. geol. Landesanst.* **40**, 284–433.

RANKIN, G. A., & MERWIN, H. E., 1918. The ternary system MgO–Al_2O_3–SiO_2. *Amer. J. Sci.*, 4th ser., **45**, 301–25.

ROY, D. M., & ROY, R., 1959. Tridymite–cristobalite relations and stable solid solutions. *Bull. geol. Soc. Amer.* **70**, 1666 (Abstract).

SCHAIRER, J. F., 1942. The system CaO–FeO–Al_2O_3–SiO_2. Part I. Results of quenching experiments on five joins. *J. Amer. ceram. Soc.* **25**, 241–74.

—— 1954. The system K_2O–MgO–Al_2O_3–SiO_2. I. Results of quenching experiments on four joins in the tetrahedron cordierite–forsterite–leucite–silica and on the join cordierite–mullite–potash feldspar. Ibid. **37**, 501–33.

—— 1957. The crystallization of rock-forming minerals from magmas and the nature of the residual liquid. *Carnegie Inst. Wash. Year Book*, **56**, 217–22.

SCHREYER, W., & SCHAIRER, J. F., 1961*a*. Metastable solid solutions with quartz-type structures on the join SiO_2–$MgAl_2O_4$. *Z. Kristallogr.* (in press).

—— —— 1961*b*. Metastable osumilite- and petalite-type phases in the system MgO–Al_2O_3–SiO_2. *Amer. Min.* (in press).

—— & YODER, H. S., JR., 1959. Cordierite–water system. *Carnegie Inst. Wash. Year Book*, **58**, 100–4.

—— —— 1960. Hydrous Mg–cordierite. Ibid., **59**, 91–94.

SEGNIT, E. R., 1957. Sapphirine-bearing rocks from MacRobertson Land, Antarctica. *Miner. Mag.* **31**, 690–7.

SOSMAN, R. B., 1927. *The properties of silica.* New York: The Chemical Catalog Company.

STEWART, D. B., 1960. Effect of $LiAlSiO_4$ and SiO_2 on the separation of the 131 and $1\bar{3}1$ X-ray diffraction lines on synthetic albite. *Bull. geol. Soc. Amer.* **71**, 1985 (Abstract).

SUGIURA, K., 1959. The water problem of cordierite. *Bull. Tokyo Inst. Tech.*, ser. B, No. 1, 1–26.

—— & KURODA, Y., 1955*a*. Thermal transformation of natural cordierite. Ibid., No. 2, 1–5.

—— —— 1955*b*. (In Japanese.) *J. ceram. Ass. Japan*, **63**, 579.

THOMAS, H. H., 1922. On certain xenolithic Tertiary minor intrusions in the island of Mull (Argyllshire). *Quart. J. geol. Soc. Lond.* **78**, 229–60.

TOMKEIEFF, S. I., 1940. The dolerite plugs of Tieveragh and Tievebulliagh near Cushendall, Co. Antrim, with a note on buchite. *Geol. Mag. Lond.* **77**, 54–64.

TRÖGER, W. E., 1956. *Optische Bestimmung der gesteinsbildenden Minerale. Teil I. Bestimmungstabellen.* Stuttgart: E. Schweizerbart.

VENKATESH, V., 1952. Development and growth of cordierite in para-lavas. *Amer. Min.* **37**, 831–48.

—— 1954. Twinning in cordierite. Ibid. **39**, 636–46.

WELCH, J. H., 1960. A new interpretation of the mullite problem. *Nature*, **186**, 545–6.

WINKLER, H. G. F., 1948. Synthese und Kristallstruktur des Eucryptits, $LiAlSiO_4$. *Acta Cryst. Camb.* **1**, 27–34.

WYLLIE, P. J., 1959. Microscopic cordierite in fused Torridonian arkose. *Amer. Min.* **44**, 1039–46.

—— 1961. Fusion of Torridonian sandstone by a picrite sill in Soay (Hebrides). *J. Petrol.* **2**, 1–37.

YODER, H. S., JR., 1952. The MgO–Al_2O_3–SiO_2–H_2O system and the related metamorphic facies. *Amer. J. Sci.*, Bowen vol., 569–627.

—— & EUGSTER, H. P., 1955. Synthetic and natural muscovites. *Geochim. et cosmoch. Acta*, **8**, 225–80.

Pumpellyite in Low-grade Metamorphism

by YÔTARÔ SEKI

Department of Earth Sciences, Saitama University, Urawa, Japan

ABSTRACT

The regional metamorphism of the Kantô Mountains in Japan produced rocks of the following facies, with rising temperature: chlorite facies, pumpellyite–chlorite facies, glaucophane–schist facies, and greenschist facies. This relationship is compared with the progressive metamorphic zones in other regions where pumpellyite has been found. Almost similar relations appear to hold in many metamorphic terrains. Pumpellyites in glaucophanitic metamorphic terrains have, generally, low Fe'''/R''' ratios. Physical and chemical conditions responsible for the formation of pumpellyite are also discussed.

INTRODUCTION

PUMPELLYITE occurs widely in some regional metamorphic terrains of Japan, New Zealand, California, Celebes, and other countries. However, the stability relations of pumpellyite in regional metamorphism have been incompletely known until recently.

In the last few years Japanese investigators have described and discussed the mode of occurrence, composition, and paragenesis of pumpellyite in the low-grade parts of the Sanbagawa metamorphic belt (Miyashiro & Banno, 1958; Miyashiro & Seki, 1958; Seki & Yokoyama,1957; Seki, 1958, 1960*b*; Seki, Aiba, & Katô, 1959, 1960). From detailed geological and petrological studies of lower-Triassic rocks in New Zealand, Fyfe *et al.* (1958) and Coombs *et al.* (1959) also discussed the stability of pumpellyite, and proposed new mineral facies called the zeolite facies and pumpellyite–prehnite facies which probably represent physical conditions intermediate between those of diagenesis and of greenschist facies.

Experience in the Japanese and New Zealand metamorphic terrains clearly shows that pumpellyite is a most useful indicator of metamorphic grade in low-temperature regional metamorphism.

In this paper, the writer intends to summarize the mineral paragenesis of pumpellyite-bearing rocks with special reference to the stability of pumpellyite in the Sanbagawa metamorphic belt of Japan. From petrological data on pumpellyite in the Sanbagawa belt and other metamorphic terrains, a tentative division of the range of physical conditions intermediate between those of diagenesis and of low-grade metamorphism of the glaucophane–schist facies and greenschist facies will also be discussed.

[Journal of Petrology, Vol. 2, Part 3, pp. 407-23, 1961]

PUMPELLYITE IN THE SANBAGAWA METAMORPHIC BELT OF JAPAN

(*a*) *Geological setting*

Pumpellyite in the Sanbagawa metamorphic terrain was first discovered by Sugi and Tsuboi (Tsuboi, 1936) from an altered dolerite intruded into low-grade metamorphic rocks of the Kantô Mountains.

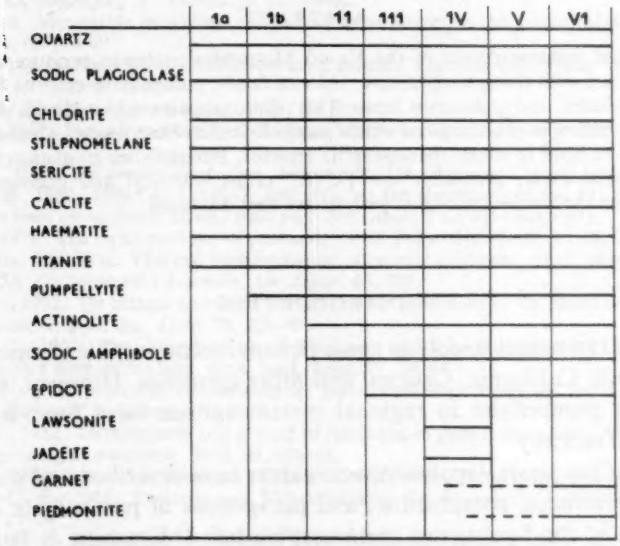

FIG. 1. Stability ranges of metamorphic minerals in the Sanbagawa metamorphic terrain of the Kantô Mountains.

During the last few years the writer has made a detailed geological and petrological study of the Sanbagawa metamorphic rocks of the Kantô Mountains. He carried out zonal mapping in terms of progressive mineralogical changes (Seki, 1958). It was found that pumpellyite is widespread in the low and middle grades, but does not occur in the higher grade. Stability ranges of metamorphic minerals in relation to metamorphic grades are shown in Fig. 1. For the geological map, see Seki (1958, fig. 2, and 1960*b*, fig. 1).

The writer formerly considered that pumpellyite does not occur in zone I. However, recent observations revealed that some of mafic pyroclastic and effusive rocks interbedded with Palaeozoic sediments in the higher-grade part of zone I have stable pumpellyite in association with sodic plagioclase, chlorite, and calcite. Thus, in Fig. 1, zone I has been divided into two parts, zone I*b* being characterized by the stable occurrence of pumpellyite. In zone I*a*, however, no pumpellyite has been found.

Thus, with reference to the stability of pumpellyite, the Sanbagawa metamorphic terrain of the Kantô Mountains may be divided into the following five areas, A, B, C, D, and E, representing zones of progressive metamorphism:

A (zone I*a*)	Chlorite is characteristic.
B (zone I*b*)	The pumpellyite–chlorite assemblage is characteristic.
C (zone II)	The pumpellyite–actinolite assemblage is characteristic.
D (zones III, IV, and V)	The pumpellyite–epidote–actinolite assemblage is characteristic.
E (zone VI)	The epidote–actinolite assemblage is characteristic and pumpellyite is not stable.

In the Sanbagawa metamorphic terrain of the Sibukawa district, central Japan, pumpellyite is also found in a relatively lower-grade part (Seki, Aiba, & Katô, 1959*a*, 1960; Seki, 1960*a*). The metamorphic terrain of Sibukawa may be divided into areas D′ and E′ in the order of increasing grade of metamorphism:

D′ Pumpellyite–epidote–actinolite assemblage is characteristic.

E′ Epidote–actinolite assemblage is characteristic and pumpellyite is not stable.

Areas D′ and E′ correspond to areas D and E of the Kantô Mountains, respectively. In the Sibukawa district, areas corresponding to A, B, and C of the Kantô Mountains are not exposed, although all five stages of metamorphism may be found in other parts of the Sanbagawa metamorphic belt.

The lawsonite–pumpellyite–epidote–glaucophane sub-facies of the glaucophane-schist facies, as defined by Miyashiro & Seki (1958), appears to represent a part of the pumpellyite–epidote–actinolite stage. Probably, high water-pressures prevailed in this sub-facies. The epidote–actinolite stage, in which pumpellyite is not stable, would belong to the greenschist facies in the ordinary sense.

Accordingly, there is a continuous series of metamorphic stages from the chlorite stage through a relatively broad intermediate stage, characterized by the presence of pumpellyite, to the stages of the greenschist and higher facies.

(*b*) *Mineral paragenesis and chemical reactions in pumpellyite-bearing rocks*

As far as we know, the lowest-grade metamorphism in the Sanbagawa belt is represented by *the chlorite stage*. In this stage, the following minerals were stably present in the Upper Palaeozoic pelitic, psammitic, calcareous, and cherty sediments, and interbedded mafic pyroclastic and effusive rocks: chlorite, sericite, stilpnomelane, calcite, quartz, sodic plagioclase, haematite, and titanite. Neither zeolite nor analcite was found in any rocks of this stage. Mafic pyroclastic and effusive rocks are almost completely altered to rocks composed of

chlorite, calcite, quartz, and sodic plagioclase with subordinate amounts of haematite and titanite, though the original textures are usually well preserved. Relics of clinopyroxene, which is often titaniferous, can be found in some effusive rocks. Calcic plagioclase and clinopyroxene were probably decomposed by the following chemical reaction:

$$2\ \text{Anorthite} + 4\ \text{clinopyroxene} + 4\ H_2O + 6\ CO_2 \rightarrow \text{chlorite} + 6\ \text{calcite} + 10\ \text{quartz} \quad (1)$$

With advancing metamorphism, the chlorite stage grades into *the pumpellyite–chlorite stage*. In mafic effusive and pyroclastic rocks of this stage, pumpellyite stably occurs in association with chlorite, calcite, sericite, stilpnomelane, quartz, sodic plagioclase, haematite, and titanite. Pumpellyite may have been formed by decomposition of clinopyroxene and calcic plagioclase by the reaction:

$$30\ \text{Anorthite} + 18\ \text{diopside} + 46\ H_2O \rightarrow 12\ \text{pumpellyite} + \text{chlorite (antigorite molecule)} + 20\ \text{quartz} \quad (2)$$

This reaction would have occurred also in the pumpellyite–actinolite and pumpellyite–epidote–actinolite stages which will be described below.

Prehnite is rarely found in altered doleritic or gabbroic rocks intruded into the metamorphic rocks of this stage. It occurs usually in veins irregularly cutting the intrusive rocks. The intrusive rocks are chiefly composed of relic augite, sodic plagioclase, chlorite, and calcite, with or without pumpellyite. It is not certain whether or not the prehnite is stably associated with the pumpellyite.

The pumpellyite–actinolite stage is characterized by the entrance of very pale-coloured actinolite in the mafic pyroclastic, effusive, and intrusive rocks, and the pelitic sediments mixed with some pyroclastic materials. Prehnite has never been found in the rocks of this stage or in those of higher grades which will be described later. Epidote was not formed under the conditions prevailing at this stage. Thus, the metamorphic minerals stably present in rocks of this stage are as follows: pumpellyite, chlorite, actinolite, calcite, sericite, stilpnomelane, quartz, sodic plagioclase, haematite, and titanite. Glaucophanitic amphibole, usually rich in the riebeckite molecule, is also found stably in the mafic effusive and pyroclastic rocks.

Pumpellyite and actinolite were probably formed from calcic plagioclase and clinopyroxene by the following chemical reaction:

$$15\ \text{Anorthite} + 11\ \text{diopside} + 22\ H_2O \rightarrow 6\ \text{pumpellyite} + \text{actinolite} + 8\ \text{quartz} \quad (3)$$

The pumpellyite–epidote–actinolite stage is characterized by the epidote–pumpellyite–actinolite assemblage. The following metamorphic minerals were stably formed at this stage: pumpellyite, actinolite, epidote, chlorite, calcite, sericite, stilpnomelane, quartz, sodic plagioclase, haematite, and titanite. Sodic amphibole rich in glaucophane and/or the riebeckite molecule has been found

commonly in mafic effusive and pyroclastic rocks. The association of pumpellyite with sodic amphibole is very rare in spite of the common occurrence of the epidote–sodic amphibole assemblage.

In some parts of the area represented by the pumpellyite–epidote–actinolite stage, jadeite and lawsonite are commonly present in stable association with epidote, pumpellyite, and sodic amphibole. These minerals jointly characterize a sub-facies (lawsonite–pumpellyite–epidote–glaucophane sub-facies) or substage.

Epidote occurs in mafic pyroclastic, effusive and intrusive rocks, as well as in pelitic, psammitic, and siliceous sediments mixed with moderate amounts of pyroclastic materials. No epidote is found in any ordinary pelitic and psammitic rocks. Manganiferous garnet and epidote have been found, though very rarely, in some siliceous metamorphic rocks.

In the passage from the pumpellyite–actinolite stage to the pumpellyite–epidote–actinolite stage, the following chemical reaction is likely to have occurred:

$$15\ \text{Anorthite} + 11\ \text{diopside} + 22\ H_2O \rightarrow 6\ \text{pumpellyite} + \text{actinolite} + 8\ \text{quartz} \quad (4)$$

In the metamorphic rocks of *the epidote–actinolite stage*, pumpellyite does not occur. Metamorphic minerals stably present at this stage are actinolite, epidote, chlorite, sericite, stilpnomelane, calcite, sodic plagioclase, garnet, haematite, magnetite, and titanite. The occurrence of sodic amphibole is very rare. It may be inferred that pumpellyite was not stable and was decomposed into the assemblage of actinolite, epidote, and calcite.

REVIEW OF OTHER PUMPELLYITE OCCURRENCES

(*a*) *California*

As is well known, glaucophanitic metamorphic rocks are widespread in California. Irving *et al.* (1932) made a detailed study of pumpellyite in glaucophane–bearing schists of this district. Afterwards, Switzer (1945, 1951), Brothers (1954), Borg (1956), Bloxam (1959), and Davis & Pabst (1960) touched upon the occurrence of pumpellyite in glaucophane schists of this district.

According to these authors, pumpellyite is stably associated with lawsonite, chlorite, epidote, glaucophane, actinolite, sodic plagioclase, and quartz. No prehnite has ever been reported to be associated with the pumpellyite. Thus, the mineral assemblages of these pumpellyite-bearing glaucophane schists appear to be similar to those of the pumpellyite–epidote–actinolite stage or lawsonite–pumpellyite–epidote–glaucophane sub-facies in the Kantô Mountains.

(*b*) *Kamuikotan belt of Hokkaidô*

In the Kamuikotan metamorphic belt of Hokkaidô, Japan, Suzuki (1938, 1959) found pumpellyite veins cutting a garnet-baring aegirinaugite–glaucophane–lawsonite schist intercalated with siliceous schist. Shidô & Seki (1959)

briefly described a common occurrence of pumpellyite in low-grade crystalline schists of the Kamuikotan belt. The pumpellyite is stably associated with jadeite, lawsonite, epidote, chlorite, quartz, sodic plagioclase, sericite, and stilpnomelane. These pumpellyite-bearing schists probably belong to the lawsonite–pumpellyite–epidote–glaucophane sub-facies.

(*c*) *Celebes and Borneo*

de Roever (1947*a*, 1947*b*, 1950, 1953, 1956) carried out petrological studies of part of Celebes and Borneo. Pumpellyite is found to occur in veins, and also as scattered grains, in some metamorphosed rocks of these islands. Pumpellyite found as a constituent of metamorphic rocks can be divided into the following three types:

(1) Pumpellyite in very weakly metamorphosed mafic effusive and intrusive rocks. These mafic rocks usually have a moderate amount of relic augite. Pumpellyite is associated with sodic plagioclase, quartz, chlorite, and calcite. Prehnite is also stably associated with pumpellyite in albite diabase of the eastern part of Borneo. Pumpellyite-bearing veins are also commonly found in these mafic metamorphic rocks.

(2) Pumpellyite in slightly metamorphosed sedimentary rocks and mafic schists. Minerals which are probably in stable association with pumpellyite in these rocks are sericite, sodic plagioclase, quartz, sodic amphiboles (glaucophane and crossite), aegirine–augite, jadeite, chlorite, lawsonite, epidote, and actinolite.

(3) Pumpellyite in (epidote–)amphibolite. This type of pumpellyite was probably formed at a retrogressive stage, after the formation of the amphibolite. In sheared amphibolite, pumpellyite is associated with sodic plagioclase, chlorite, quartz, and colourless or pale-coloured actinolite. Prehnite veins are developed within these sheared parts. Pumpellyite and sodic plagioclase occur also in veins. Crystals of green or bluish hornblende of the original amphibole, included within these veins, are usually surrounded by colourless or pale-coloured actinolite.

The first type of pumpellyite seems to belong to the pumpellyite–chlorite stage as defined in this paper. de Roever said that there may be a special facies or sub-facies characterized by the stability of pumpellyite and instability of epidote. He considered that this facies (his 'pumpellyite facies') is a part of the greenschist facies and may be representative of a lower-grade (probably lower pressure and temperature) metamorphism than the glaucophane–schist facies. According to him, the characteristic mineral assemblage of this facies is pumpellyite–sodic plagioclase–quartz–calcite. Prehnite may be stable in this sub-facies.

The second type of pumpellyite seems to belong to the pumpellyite–epidote–actinolite stage, or lawsonite–pumpellyite–epidote–glaucophane sub-facies of the glaucophane–schist facies, as defined in this paper. de Roever considered that, during progressive metamorphism, pumpellyite becomes less stable or

unstable after the first appearance of sodic amphibole and lawsonite; in other words, pumpellyite would be unstable in the glaucophane–schist facies. However, the present writer's observation shows that pumpellyite is stable at least in some sub-facies of the glaucophane–schist facies. Prehnite has never been found in the glaucophane-bearing rocks of Celebes.

(d) New Caledonia

Glaucophanite, amphibolite, and other crystalline schists occur widely in New Caledonia.

Lacroix (1942) described the mode of occurrence of pumpellyite in metamorphosed dolerite of this island. Routhier (1953) distinguished, in the Pilow district, the following two stages of mineral formation in metamorphosed dolerite:

(1) Pumpellyite–chlorite stage.
(2) Pumpellyite–lawsonite–glaucophane–chlorite stage.

The first stage appears to be almost the same as the pumpellyite–chlorite stage, while the second stage may be included in the pumpellyite–epidote–actinolite stage of the Kantô Mountains.

(e) Corsica

Glaucophanitic regional metamorphic terrain developed in the eastern part of Corsica was studied by Brouwer and Egeler (1953). They suggested a possible division of the terrain into the following four zones, representing increasing grade of metamorphism from Vezzani in the south to Cap Corse in the north:

(1) Pumpellyite zone.
(2) Glaucophane–lawsonite(–pumpellyite) zone.
(3) Garnet–lawsonite–glaucophane zone.
(4) Epidote–glaucophane zone.

In the pumpellyite zone, which represents the lowest grade in Corsica, dolerite is usually almost unchanged. In the dolerite, the only sign of metamorphism is the pumpellyitization of feldspar laths. The ophitic fabric is still completely preserved. Chlorite, leucoxene, sodic plagioclase, sericite, quartz, and calcite are associated with pumpellyite. A somewhat higher grade of transformation resulted in the formation of sodic amphibole, aegirine, and lawsonite. Pumpellyite is not found in the rocks of the garnet–lawsonite–glaucophane zone and of the higher grade. Thus, it is probable that the stability of pumpellyite in low-grade schists of Corsica is almost the same as that of pumpellyite in the Kantô Mountains.

Egeler (1948) described some mineralogical properties of pumpellyite associated with sodic plagioclase, chlorite, quartz, epidote, glaucophane, and lawsonite.

(f) New Zealand and Australia

About 20 years ago Hutton and Turner reported the occurrence of pumpellyite in the low-grade part of the chlorite zone in the Otago schists (Hutton, 1937, 1940; Turner, 1939).

Reed (1950, 1957) also described the association of pumpellyite with sodic plagioclase, epidote, chlorite, calcite, and quartz in weakly altered spilitic rocks in the lower Mesozoic formation of the Wellington district, North Island. This formation is a part of the Alpine facies deposits of the New Zealand Geosyncline. It is likely that the minerals in the spilitic rocks were formed by the pumpellyite–chlorite stage of regional metamorphism.

Regional metamorphism in south-east Nelson of the South Island has also been described by Reed (1958). On the basis of mineral paragenesis, the metamorphic terrain was divided into the following zones in the order of increasing metamorphism:

Unmetamorphosed zone
Ch 1 subzone } chlorite zone
Ch 2 subzone
Ch 3 subzone
Biotite zone
Garnet zone

Pumpellyite is stable in Ch 1 subzone. It is associated with quartz, epidote, sodic plagioclase, sericite, chlorite, prehnite, and calcite. No actinolite was found in Ch 1 subzone in spite of its common occurrence in the higher-grade zones. Pumpellyite would be a critical mineral of the lowest-grade (pumpellyite facies) part of the greenschist facies.

Coombs *et al.* made an important contribution to the stability of pumpellyite in low-grade regional metamorphism (Coombs, 1954; Coombs *et al.*, 1959). Geological and petrological studies on the rocks of the New Zealand Geosyncline show that the gap between diagenesis and the greenschist facies may be bridged by several facies or stages characterized by the assemblages involving pumpellyite, prehnite, analcite, and zeolite, as follows:

Heulandite–analcite stage } zeolite facies
Laumontite stage
Pumpellyite–prehnite stage
Greenschist facies

In the pumpellyite–prehnite stage, the following minerals are stably found in tuffs and spilitic lavas: pumpellyite, prehnite, chlorite, quartz, sodic plagioclase, adularia, calcite, and sphene. These authors also noted that the presence of the pumpellyite–actinolite assemblage in rocks of appropriate chemical composition, and the disappearance of prehnite, may represent another possible

independent facies or sub-facies between the greenschist facies and the pumpellyite–prehnite stage.

From the petrological study of diagenesis in New England, Australia, Packam and Crook (1959) also suggested the presence of the following sequence of facies starting at the surface and passing down into the deeply buried part:

Laumontite facies.
Prehnite–pumpellyite facies.
Albite–epidote facies.

The mineral assemblages of the albite–epidote facies are similar to those found in rocks of the greenschist facies in regional metamorphism.

(*g*) *Scotland*

Bloxam (1958) reported the occurrence of pumpellyite in spilitic rocks of south Ayrshire. Here, green schists are associated with spilitic lavas and mafic and ultramafic intrusives. Glaucophane schist also occurs in this district. The weakly metamorphosed spilitic rocks in which pumpellyite-bearing veins are found are chiefly composed of glass and microlitic plagioclase. The plagioclase is altered to a dense aggregate of calcite, quartz, albite, and pumpellyite. Though detailed petrography of the spilitic lavas and associated metamorphic rocks was not made, the pumpellyite-bearing rocks may represent low-grade regional metamorphism characterized by the stable appearance of pumpellyite.

(*h*) *Haiti Island*

Burbank (1927) described the mode of occurrence and some mineralogical properties of pumpellyite in weakly altered amygdule-bearing spilitic rocks of Haiti. The pumpellyite is in association with chlorite, prehnite, sodic plagioclase, and iron-rich epidote. In some spilitic lavas, sericite, prehnite, and zeolite occur commonly. Burbank considered that these mafic rocks, with or without pumpellyite, suffered very low-grade regional metamorphism in late Mesozoic time. It is probable that these rocks belong to the pumpellyite–chlorite stage as defined by the present writer.

(*i*) *Other districts*

In the above eight districts pumpellyite occurs in low-grade parts of regional metamorphic terrains. However, other modes of occurrence of this mineral are also recorded.

Soether (1942) found pumpellyite within some hydrothermally altered syenite–porphyry and dolerite intrusives of Oslo, Norway. The pumpellyite was chiefly formed by the decomposition of original plagioclase. The associated minerals are calcite, epidote, chlorite, and prehnite.

Waldmann (1934) reported the occurrence of pumpellyite in a retrogressively altered scapolite-bearing calc–silicate rock of Finnish Lapland. He also described pumpellyite found in hydrothermally altered dolerite of the same district. These

pumpellyites are in association with sodic plagioclase, epidote, chlorite, prehnite, calcite, and quartz.

Pumpellyite was described by Palache and Vassar (1925), Broderick (1929, 1931), and Klein (1939) from copper-bearing amygdaloidal lavas of the Lake Superior region, Michigan. These pumpellyites are usually associated with prehnite, sericite, quartz, sodic plagioclase, and calcite. They are believed to have been formed by low-temperature hydrothermal alteration of their host rocks. Broderick (1931) recognized several zones within altered mafic rocks of the Lake Superior region, in decreasing order of grade as follows: zeolite zone, prehnite–adularia zone, and sericite–propylite zone. In all of these zones, epidote, pumpellyite, quartz, calcite, and chlorite are present. These zones may have been formed through local upward invasion by hydrothermal solutions from the depths. Judging from the descriptions by Broderick, it is probable that the deeper part represents a higher temperature.

Quitzow (1936) found pumpellyite in altered dolerite collected from the Baikal and Altai districts in Russia. These pumpellyites are associated with chlorite, epidote, calcite, albite, sericite, and prehnite.

Some other occurrences of pumpellyite have been reported from Africa and other districts. The host rocks of these pumpellyites are mafic lavas, mafic intrusive rocks, greywacke, or tuff. Pumpellyite is usually associated with some low-temperature minerals such as chlorite, sericite, prehnite, calcite, and zeolite.

PUMPELLYITE AND TYPES OF METAMORPHISM

(*a*) *Types of metamorphism.*

Metamorphism producing pumpellyite can be divided into the following two types:

(1) Glaucophanitic type: Sanbagawa, Kamuikotan, California, Celebes, Borneo(?), New Caledonia, Corsica, and Scotland.

(2) Non-glaucophanitic type: Haiti Island, Finland, and other districts.

Eskola (1929, 1939), de Roever (1950, 1955 *a*, *b*) and Miyashiro & Banno (1958) considered that glaucophanitic metamorphism represents higher solid pressure than does the non-glaucophanitic type.

The presence of a 'crossite' core in some crystals of actinolite has already been described from low-grade mafic schists of Otago in New Zealand (Hutton, 1940). Recently, sodic amphibole and lawsonite were discovered from a Mesozoic metamorphic terrain in the northern part of Southland in New Zealand, in which pumpellyite occurs widely (personal communication from Dr. A. J. R. White, University of Otago). Hence, the Alpine and Otago schists might be considered to be closely related to the glaucophanitic type.

(*b*) Fe'''/R''' *ratio of pumpellyite, and its significance.*

Frequency curves for the refractive index β of pumpellyites in the Sanbagawa and Kamuikotan metamorphic belts of Japan are shown in Fig. 2. The range of refractive index β of pumpellyites reported from the other above-mentioned

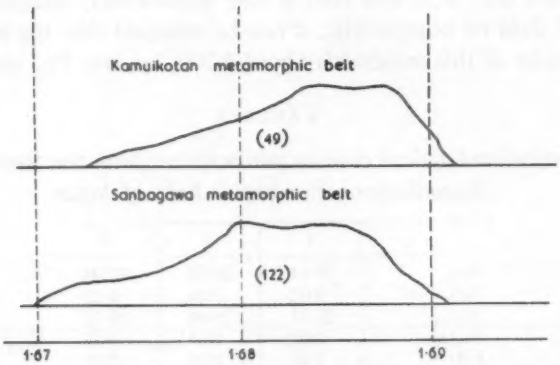

FIG. 2. Frequency curves for refractive index β of pumpellyites in metamorphic rocks of the Sanbagawa and Kamuikotan belts in Japan. The numbers of measured specimens are shown in parentheses.

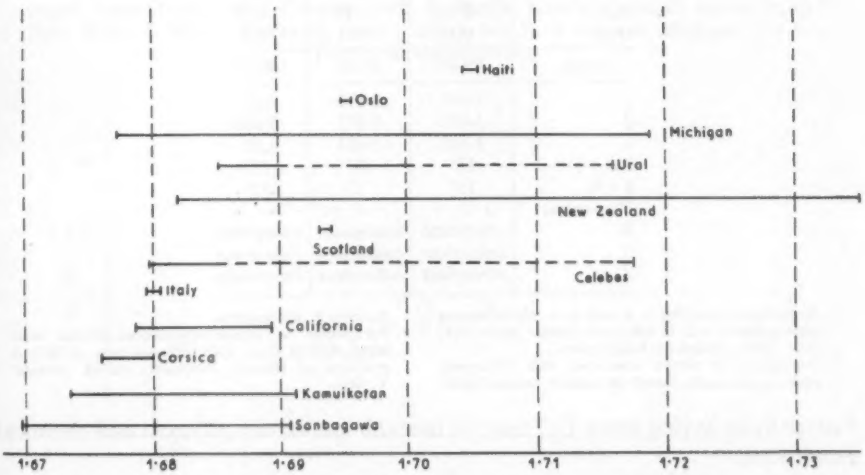

FIG. 3. Diagram showing the ranges of refractive index β of pumpellyite in various metamorphic terrains. The broken lines represent optical data of low reliability.

districts are diagramatically summarized in Fig. 3. From these diagrams, it may be considered that pumpellyite in the glaucophanitic regional metamorphic terrains has a relatively low index of refraction.

The variation of refractive index of pumpellyite was studied by de Roever

(1947*a*) and Coombs (1953). Coombs presented in his paper two figures showing that the index of refraction shows a remarkable increase with iron content.

Pumpellyite has the chemical composition of $Ca_4(Fe'', Mg, Mn)(Fe''', Al, Ti)_5 Si_6O_{23}(OH)_3 2H_2O$. Mn and Ti are generally far less abundant than (Fe″, Mg) and (Fe‴, Al), respectively. The variations of Fe''/R'' and Fe'''/R''' ratios in pumpellyite are 0·27–0·55 and 0·07–0·104, respectively. Judging from optical and chemical data on pumpellyite, it can be assumed that the highest value of the Fe'''/R''' ratio of this mineral is about 0·200, i.e. one Fe‴ ion per unit cell.

TABLE 1

New chemical and optical data on pumpellyites from the Sanbagawa and Kamuikotan metamorphic belts of Japan

	1	2	3
SiO_2	38·51	38·14	37·80
TiO_2	0·02	0·04	0·22
Al_2O_3	26·71	26·04	24·72
Fe_2O_3	0·67	0·84	3·51
FeO	1·41	0·34	2·95
MnO	0·19	tr.	0·10
MgO	2·12	3·39	2·70
CaO	22·61	24·90	22·08
Na_2O	0·19	0·06	0·09
K_2O	0·03	0·07	tr.
H_2O+	6·61	5·40	6·29
H_2O-	0·33	0·31	0·07
TOTAL	99·40	99·53	100·53
α	1·665	1·670	n.d.
β	1·670	1·672	1·693
γ	1·683	1·684	n.d.
2V(+)	15°	10°	37°
a∧X	15°	5°	32°
Dispersion	$r < v$	$r < v$	$r < v$
X	colourless	colourless	colourless
Y	colourless	colourless	pale green
Z	colourless	colourless	colourless

1. Pumpellyite occurring in a vein in a jadeite-bearing meta-gabbroic rock in Sibukawa, central Japan (Seki *et al.*, 1960). Analyst: S. Kuriyagawa.
2. Pumpellyite in albitite associated with ultra-mafic rocks of Kanasaki, Kantô Mountains, central Japan. Analyst: S. Kuriyagawa.
3. Pumpellyite in pumpellyite–epidote–chlorite semischist derived from mafic effusive rock of Mituisi, province of Hidaka, Hokkaido, Japan. Analyst: Y. Seki.

Pumpellyite having more Fe‴ may be unstable under any physical and chemical conditions.

As shown in Table 1 and Figs. 4 and 5, the increase of refractive index of pumpellyite can be correlated far more clearly with the increase in the Fe'''/R''' ratio of this mineral than with the increase in the Fe''/R'' ratio. Thus, it is very probable that pumpellyite in glaucophanitic metamorphic terrains is generally poor in Fe‴.

Coombs (1953) has already noted distinct enlargement of lattice constants as Fe‴ replaces R‴ in the pumpellyite mineral series. Pumpellyite relatively rich

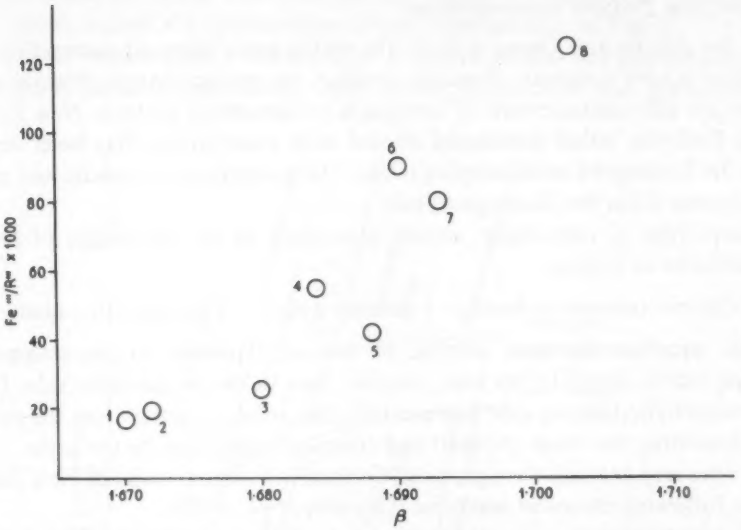

FIG. 4. Diagram showing the relationship between refractive index β and Fe'''/R''' in pumpellyites. 1. Sibukawa district, central Japan (Table 1, no. 1). 2. Kanasaki district, Kantô Mountains, central Japan (Table 1, no. 2). 3. Mill Creek, California, U.S.A. (Irving *et al.*, 1932). 4. Toba, Kantô Mountains, central Japan (Seki, 1958). 5. Asahine, Kantô Mountains, central Japan (Tsuboi, 1936; Coombs, 1953). 6. Watiba, Kantô Mountains, central Japan (Seki, 1958). 7. Mituisi, Hokkaidô, Japan (Table 1, No. 3). 8. Calumet, Michigan, U.S.A. (Palache & Vassar, 1925).

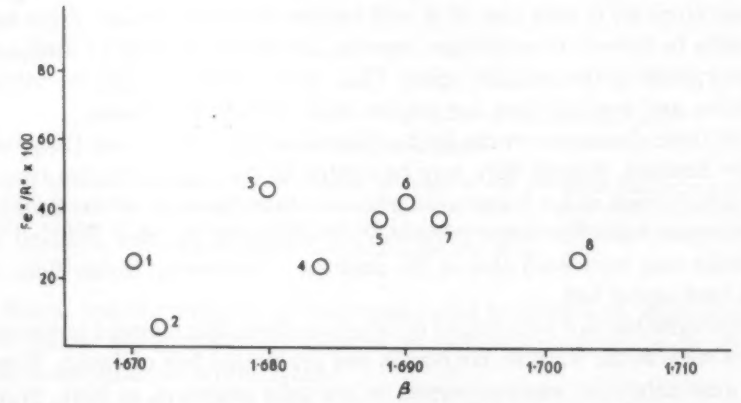

FIG. 5. Diagram showing the relationship between refractive index β and Fe''/R'' in pumpellyites. (The numbers correspond to those in Fig. 4.)

in Fe''' may be stable only when the solid pressure is low. When rocks in which the Fe'''/R''' ratio is high were metamorphosed under high solid pressure conditions, stilpnomelane, epidote, chlorite, or other minerals in which Fe''' can easily replace R''' would be formed instead of pumpellyite.

(*c*) *On New Zealand metamorphism*

In the Alpine and Otago schists, the stable association of pumpellyite with prehnite is very common. Analcite, zeolites, or zeolite-bearing mineral assemblages are also characteristic of low-grade metamorphic rocks in New Zealand.

No prehnite, either associated or not with pumpellyite, has been reported from the Sanbagawa metamorphic rocks. The occurrence of analcite and zeolites is unknown from the Sanbagawa belt.

Pumpellyite is, chemically, almost equivalent to an assemblage of prehnite and chlorite as follows:

$$\text{Chlorite (amesite molecule)} + 4\ \text{prehnite} + H_2O \rightarrow 2\ \text{pumpellyite} + \text{quartz} \quad (5)$$

In this equation the total volume of the solid phases on the pumpellyite-bearing side is about 10 per cent. smaller than those on the other side. Hence, the pumpellyite-bearing side represents higher solid pressures than the prehnite side, providing the other physical and chemical conditions be the same.

Zeolites and analcite were probably formed in volcanic rocks of New Zealand by the following chemical reactions (Coombs *et al.*, 1959):

$$\text{Anorthite} + 2\ \text{quartz} + 4\ H_2O \rightarrow \text{laumontite} \quad (6)$$

$$\text{Anorthite} + 5\ \text{quartz} + 6\ H_2O \rightarrow \text{heulandite} \quad (7)$$

$$\text{Albite} + H_2O \rightarrow \text{analcite} \quad (8)$$

The total volume of the solid phases increases remarkably during the formation of zeolites and analcite by these chemical reactions. The degree of ionic packing of these minerals is very low. It is well known that analcite and some zeolites can easily be formed in some lake deposits, unrelated in mode of formation to metamorphism in the ordinary sense. Thus, it is conceivable that the formation of zeolites and analcite does not require high-pressure conditions.

From these discussions it can be concluded that the Alpine and Otago schists in New Zealand, though they may be related to the glaucophanitic type, may have been formed under lower solid pressures than the rocks of the Sanbagawa metamorphic belt. The water pressures pertaining to the New Zealand metamorphism may have been almost the same as, or somewhat higher than, those in the Sanbagawa belt.

Pumpellyite has not been found in non-glaucophanitic regional metamorphic terrains such as the Scottish Highlands and the Ryoke belt of Japan. This may be because either low water-pressures or low solid pressures, or both, prevailed in these metamorphic terrains, or because of a possible mis-identification of this mineral as chlorite, actinolite, or other low-temperature minerals.

POSSIBLE DIVISIONS OF LOW-GRADE METAMORPHISM

It is still impossible to define, with certainty, the temperature–pressure fields of the pumpellyite-bearing facies and to show the relationship between this and

other metamorphic facies. However, the field and petrological data given in this paper would suggest the relationship shown schematically in Fig. 6.

In spite of its speculative nature, Fig. 6 illustrates that the gap between the lowest-grade metamorphic facies, such as the greenschist and glaucophane–

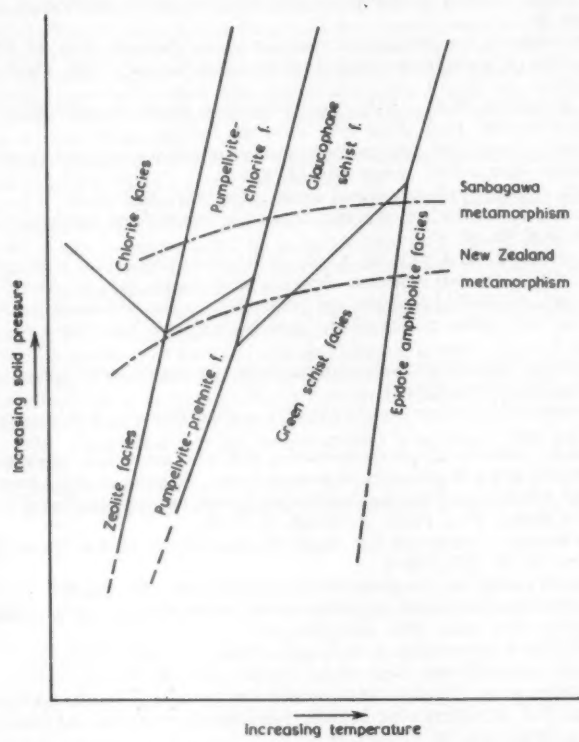

FIG. 6. Schematic representation of possible divisions of the low-grade part of regional metamorphism. Hypothetical pressure-temperature gradients for glaucophanitic regional metamorphism of the Sanbagawa belt, and for progressive regional metamorphism of the New Zealand Geosyncline, are also shown.

schist facies, and the products of diagenesis could be filled with three distinctly defined facies: the pumpellyite–chlorite or pumpellyite–prehnite facies, the chlorite facies, and the zeolite facies.

ACKNOWLEDGEMENTS

The writer wishes to express his sincere thanks to Professors Hisashi Kuno and Akiho Miyashiro, of the University of Tokyo, for their kind advice and critical reading of the manuscript. He is much obliged to Miss Sakiko Kuriyagawa, of Saitama University, for her chemical analyses of pumpellyites.

REFERENCES

BLOXAM, T. W., 1958. Pumpellyite from south Ayrshire. *Min. Mag.* **31**, 811–13.

—— 1959. Glaucophane-schists and associated rocks near Valley Ford, California. *Amer. J. Sci.* **257**, 95–112.

BORG, I., 1956. Glaucophane schists and eclogites near Healdsburg, California. *Bull. geol. Soc. Amer.* **67**, 1563–84.

BRODERICK, T. M., 1929. Zoning in Michigan copper deposits and its significance. *Econ. Geol.* **24**, 149–62 and 311–26.

—— 1931. Fissure veins and lode relations in Michigan copper deposits. Ibid. **26**, 840–56.

BROTHERS, R. N., 1954. Glaucophane-schists from the north Berkeley Hills, California. *Amer. J. Sci.* **252**, 614–26.

BROUWER, H. A., & EGELER, C. G., 1952. The glaucophane facies metamorphism in the schistes lustrés Nappe of Corsica. *Verh. Akad. Wet. Amst.* **48**, 1–71.

BURBANK, W. S., 1927. Additional data on the properties of pumpellyite, and its occurrence in the Republic of Haiti, West Indies. *Amer. Min.* **12**, 421–4.

COOMBS, D. S., 1953. The pumpellyite mineral series. *Min. Mag.* **30**, 113–35.

—— 1954. The nature and alteration of some Triassic sediments from Southland, New Zealand. *Trans. roy Soc. N.Z.* **82**, 65–109.

——, ELLIS, A. J., FYFE, W. S., & TAYLOR, A. M., 1959. The zeolite facies, with comments on the interpretation of hydrothermal syntheses. *Geochim. et Cosmoch. Acta.* **17**, 53–107.

DAVIS, G. A., & PABST, A., 1960. Lawsonite and pumpellyite in glaucophane schist, North Berkeley Hills, California, with notes on the X-ray crystallography of lawsonite. *Amer. J. Sci.* **258**, 689–704.

DE ROEVER, W. P., 1947*a*. Igneous and metamorphic rocks in eastern central Celebes. *Geol. Explorations in the Island of Celebes*, 65–173.

—— 1947*b*. Occurrence of the mineral pumpellyite in eastern Borneo. *Bull. Bur. Min. Indones.* **1**, 16–17.

—— 1950. Preliminary notes on glaucophane-bearing and other crystalline schists from south-east Celebes, and on the origin of glaucophane-bearing rocks. *Verh. Akad. Wet. Amst.* **53**, 2–12.

—— 1953. Tectonic conclusions from the distribution of the metamorphic facies in the island of Kabaena, near Celebes. *Proc. Pacif. Sci. Congr.* **2**, 71–81.

—— 1955*a*. Some remarks concerning the origin of glaucophane in the North Berkeley Hills, California. *Amer. J. Sci.* **253**, 240–4.

—— 1955*b*. Genesis of jadeite by low-grade metamorphism. Ibid. **253**, 283–98.

—— 1956. Some additional data on the crystalline schists of the Rumbia and Mendoke Mountains, south-east Celebes. *Ver. Akad. Wet. Amst.* **56**, 1–9.

EGELER, C. G., 1948. Sur la pumpellyite de Barbaggio, Corse. Ibid. **41**, 388–9.

ESKOLA, P., 1929. Om mineralfacies. *Geol. Fören. Stockh. Förh.* **51**, 157–72.

—— 1939. *Die Entstehung der Gesteine*, '*Metamorphischen Gesteine*'. Berlin: Springer Verlag.

FYFE, W. S., TURNER, F. J., & VERHOOGEN, J., 1959. Metamorphic reactions and metamorphic facies. *Mem. geol. Soc. Amer.*, no. 73.

HUTTON, C. O., 1937. An occurrence of the mineral pumpellyite in the Lake Wakatipu region, Western Otago, New Zealand. *Min. Mag.* **24**, 529–33.

—— 1940. Metamorphism in the Lake Wakatipu region, New Zealand. *Geol. Mem. N.Z.* no. 5.

IRVING, J., VONSEN, M., & GONYER, F. A., 1932. Pumpellyite from California. *Amer. Min.* **17**, 338–42.

KLEIN, I., 1939. Microcline in the copper deposits of Michigan. *Amer. Min.* **24**, 643–50.

LACROIX, A., 1942. Les Glaucophanites de la Nouvelle-Calédonié et les roches qui les accompagnent, leur composition et leur genése. *Mém. Acad. Sci. Paris*, **65**, 1–103.

MIYASHIRO, A., & BANNO, S., 1958. Nature of glaucophanitic metamorphism. *Amer. J. Sci.* **256**, 97–110.

—— & SEKI, Y., 1958. Mineral assemblages and subfacies of the glaucophane-schist facies. *Jap. J. Geol. Geogr.* **29**, 199–208.

PACKAM, G. H., & CROOK, K. A. W., 1959. The principle of diagenetic facies and some of its implications. *J. Geol.* **68**, 392–407.

PALACHE, C., & VASSAR, H. E., 1925. Some minerals of the Keweenawan copper deposits: pumpellyite, a new mineral; sericite; saponite. *Amer. Min.* **10**, 412–28.

QUITZOW, H. W., 1936. Pumpellyite, ein häufiges Hydrothermal-und Sekundärmineral in basischen Gesteinen. *Zbl. Miner. Geol. Paläont., Abt. A*, 39–46.

REED, J. J., 1950. Spilites, serpentinite and associated rocks of the Mossburn district, Southland. *Trans. roy. Soc. N.Z.* **78**, 106–26.

—— 1957. Petrology of the lower Triassic rocks of the Wellington district. *Geol. Mem. N.Z.*, no. 57.

REED, J. J., 1958. Regional metamorphism in south-east Nelson. Ibid., no. 60.
ROUTHIER, P., 1953. Étude géologique du versant occidental de la Nouvelle Calédonie. *Mém. Soc. géol. Fr.*, no. **67**, 1–266.
SEKI, Y., & YOKOYAMA, S., 1957. Pumpellyite and its distribution in the eastern part of the Kantô Mountains (in Japanese with English abstract). *J. Jap. Ass. Mineralog.* **41**, 227–35.
—— 1958. Glaucophanitic regional metamorphism in the Kantô Mountains, central Japan. *Jap. J. Geol. Geogr.* **29**, 233–58.
—— 1960*a*. Jadeite in the Sanbagawa metamorphic belt of central Japan. *Amer. J. Sci.* **258**, 705–15.
—— 1960*b*. Distribution and mineral assemblages of jadeite-bearing metamorphic rocks in Sanbagawa metamorphic terrains of central Japan. *Sci. Rep. Saitama Univ.*, ser. B, **3**, 313–20.
——, AIBA, M., & KATÔ, C., 1959*a*. Metamorphic zoning of the Sanbagawa terrain in the Sibukawa district, central Japan (in Japanese with English abstract). *J. geol. Soc. Japan*, **65**, 618–23.
—— —— —— 1959*b*. Edenite in Sanbagawa crystalline schists of the Sibukawa district, central Japan. *Jap. J. Geol. Geogr.* **30**, 233–43.
—— —— —— 1960. Jadeite and associated minerals in meta-gabbroic rocks of Sanbagawa metamorphic belt in central Japan. *Amer. Min.* **45**, 668–79.
SHIDÔ, F., & SEKI, Y., 1959. Notes on rock-forming minerals (11): Jadeite and hornblende from the Kamuikotan metamorphic belt. *J. geol. Soc. Japan*, **65**, 673–7.
SOETHER, E., 1942. Funn av pumpellyite i bergarter fra Oslofeltet. *Norsk geol. Tidsskr.* **21**, 294–5.
SUZUKI, J., 1938. On lawsonite and pumpellyite from Kamuikotan valley, Ishikari Province (in Japanese). *J. Jap. Ass. Mineralog.* **20**, 189–96.
—— & SUZUKI, Y., 1959. Petrographical study of the Kamuikotan metamorphic complex in Hokkaido, Japan. *J. Fac. Sci. Hokkaido Univ.* **10**, 349–446.
SWITZER, G., 1945. Mineralogy of the California glaucophane schists. *Amer. J. Sci.* **243**, 1–8.
—— 1951. Mineralogy of the California glaucophane schists. *Bull. Calif. Min. Bur.* **161**, 51–70.
TSUBOI, S., 1936. Petrological notes (11): Pumpellyite from Asahine, Tukikawa-mura, Titibu-gori, Saitama Prefecture. *Jap. J. Geol. Geogr.* **13**, 333.
TURNER, F. J., 1938. Progressive regional metamorphism in southern New Zealand. *Geol. Mag. Lond.* **75**, 160–74.
—— 1939. The geology of the Naseby subdivision. *Bull. Geol. Surv. N.Z.* no. 39.
WALDMANN, L., 1934. Pumpellyite aus Steiermark und Finnisch-Lappland. *Z. Min. Petr. Mitt.* **45**, 92–93.

Magmatic Differentiation in the Uwekahuna Laccolith, Kilauea Caldera, Hawaii[1]

by K. J. MURATA[2] *and* D. H. RICHTER

U.S. Geological Survey, Hawaiian Volcano Observatory, Hawaii National Park, Hawaii

ABSTRACT

Petrographic and chemical studies of a suite of rocks from the Uwekahuna laccolith of Kilauea Volcano show that the original mafic tholeiitic magma differentiated into tholeiitic picrite, tholeiitic olivine gabbro, and an aphanitic rock approaching quartz–basalt in composition. Mechanisms involved were an initial gravity settling of olivine and a final filter pressing of the residual liquid. The range of composition represented by the rocks of the laccolith is as great as that found among all hitherto analysed lavas of the volcano.

INTRODUCTION

THE differentiation of basaltic magma in Hawaii has been previously inferred almost entirely through chemical and petrographic studies of lavas. Intrusive bodies such as dikes and sills though numerous at some places (Stearns & Vasvik, 1935; Wentworth & Jones, 1940) have not been investigated in detail.

In other older volcanic centres, such as the British Hebrides and the Triassic basin of eastern United States, where intrusive bodies are exposed abundantly, the study of these rocks of deeper crystallization has provided much information about basaltic differentiation. By virtue of their slower and more orderly history of crystallization, intrusive rocks are likely to show more extensive differentiation than their correlative lavas. Such a difference between sills and flows is especially marked in the Eocene basalts of Oregon and Washington, according to Waters (1955).

As stressed in a recent paper (Eaton & Murata, 1960) the lavas of the currently active volcanoes, Kilauea and Mauna Loa, represent only a part of the tholeiitic differentiation series. Kuno and others (1957) discovered small patches of granophyric material (extreme tholeiitic differentiate) in a dike of quartz–diabase at Palolo quarry on the Island of Oahu. Thus, all indications encourage the study of intrusive rocks for establishing the nature and full range of differentiation of Hawaiian tholeiitic magma.

Daly (1911) first described the small laccolith of tholeiitic olivine gabbro that is exposed on the wall of Kilauea Caldera and named it the Uwekahuna laccolith. In his description he included chemical and modal analyses of a typical specimen of the gabbro. It has been assumed through the years that the rock of

[1] Publication authorized by the Director, U.S. Geological Survey.
[2] *Present address:* U.S. Geological Survey, Menlo Park, California.

[Journal of Petrology, Vol. 2, Part 3, pp. 424–37, 1961]

the laccolith was more or less uniform. A detailed examination of the accessible parts of the laccolith in 1959 disclosed considerable vertical differentiation at the south end of the laccolith, and samples were collected there for chemical and petrographic studies.

GEOLOGIC SETTING

The Uwekahuna laccolith is exposed in cross-section over a length of approximately 950 ft in the north-west wall of Kilauea Caldera (Fig. 1). The laccolith is composed of two elongate massive bodies that stand out in striking contrast against the thin-bedded basaltic lava flows that constitute most of the remaining section in the caldera wall. The larger southern body is 650 ft long, with a maximum thickness of about 90 ft; the smaller, northern body is 290 ft long and about 70 ft thick. Although the narrow area between the two bodies is covered by talus, the structural and mineralogical similarities of the two bodies and their equivalent stratigraphic position strongly indicate that they are, at least, of contemporaneous origin and are probably parts of a single continuous unit.

There is little question as to the intrusive origin of these two massive rock units. Although Powers (1916) and Washington (1923) believed the rock represented the filling of a large lava tube, Daly (1911) early noted its intrusive characteristics, a view which latterly has been accepted and supported, with additional evidence by Macdonald (1949). The north body is typically laccolithic in character, with a flat-lying concordant floor and a roughly symmetrical dome-shaped roof that during injection arched the overlying thinly bedded lava flows. The south body, which also is overlain by arched beds, is more irregular in cross-section, and along its base and top exhibits considerable cross-cutting relationships with the enclosing lavas. Moreover, near its south end a distinct dike-like apophysis, averaging 16 ft thick, extends upward into the overlying bedded flows. The contact between intrusive and bedded lavas is generally well defined and sharp. At the contact the host lavas exhibit variable degrees of metamorphism, but do not show any evidence of gross assimilation. Within the intrusive bodies the contact is marked by a relatively thin (1–2 ft thick) fine-grained chill zone.

Thickness of cover over the laccolith at the time of intrusion was certainly no greater than 350 ft—the present approximate height of the caldera wall above the floor of the intrusive—and no smaller than 135 ft, as evinced by the upward extent of discernible deformation in the overlying strata.

The sampled part of the south body is asymmetric in the vertical direction with respect to several features, in contrast to a symmetrical body like the Dillsburg diabase sill described by Hotz (1953). A single zone of accumulated olivine occurs in the lower half of the body. Alteration of iron-bearing minerals, particularly olivine, is more pronounced in the upper part of the body, as is apparent from the reddish colour of the rocks. Flow rocks constituting the roof of the laccolith are more intensely metamorphosed than those forming the floor.

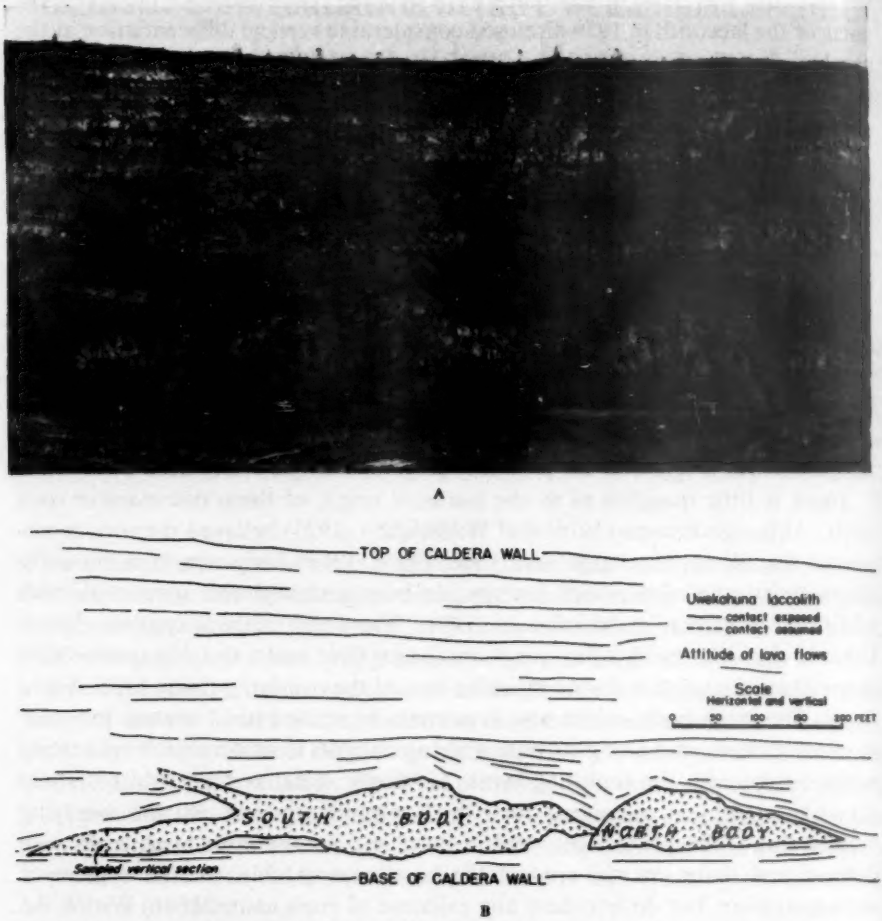

FIG. 1. A, view looking north-west from the floor of Kilauea Caldera. The two massive bodies of the Uwekahuna laccolith are exposed along the lower portion of the caldera wall. B, sketch of same area delineating the laccolith and showing the attitude of a few of the lava flows that constitute the remaining part of the section.

The origin and injection mechanism of the Uwekahuna laccolith may be analogous to the phenomenon observed in 1924 in Halemaumau (Jaggar, 1924, pp. 59–67), the crater in the floor of Kilauea Caldera and usual site of historic summit activity. During the period 1907–24 Halemaumau contained a continuously active lava lake. In early 1924 the withdrawal of the lava column and subsequent phreatic eruption, which deepened and enlarged the crater, exposed a number of fresh intrusive bodies in the new walls. Two of the largest of these bodies, between depths of 400 and 1,000 ft, remained incandescent for a month after their exposure. In historic time (since 1823) the main caldera itself has

undergone four episodes of collapse and subsequent refilling by surface accumulation of lava or by bodily uplift of the floor through subterranean intrusions. Lateral injection during a prehistoric period of refilling of the caldera may well explain the origin of the Uwekahuna laccolith.

METHODS OF STUDY

The Uwekahuna laccolith provides an opportunity to study differentiation in a relatively thin single-unit basaltic intrusive. The data presented in this paper are derived principally from a chemical and petrographic study of an easily accessible 28-ft vertical section near the south end of the south body of the laccolith (Fig. 1). Although well exposed along its entire length, much of the laccolith forms an inaccessible vertical wall and hence the nature of the rocks in the thicker portions is mainly inferred from samples collected from talus blocks below the outcrop.

Five of the eight new chemical analyses, published herein, are of rocks collected at various intervals through the sampled vertical section. Modes of these analysed rocks were determined by the point-count method, utilizing 1,000–1,500 counts per thin section. No detailed determinative mineralogy was attempted. The results of the chemical analyses and petrographic determinations are given in Table 1.

PETROGRAPHY

The principal rock of the Uwekahuna laccolith is a tholeiitic gabbro porphyry consisting of olivine phenocrysts set in a groundmass of pyroxene, plagioclase feldspar, opaque minerals, and minor glass. Megascopically, the rock is principally holocrystalline throughout, with the olivine phenocrysts commonly attaining sizes of 4 to 5 mm in diameter and the groundmass minerals up to 1 mm in diameter. Vesicles constitute approximately 10 per cent of the volume of the rock and are apparently evenly distributed from top to bottom.

The groundmass texture of the gabbro, in specimens taken from the 28-ft vertical section near the south end of the south body, is predominantly intergranular, becoming decidedly intersertal in the thin, finer-grained, chilled border zone. Thin sections of the gabbro, collected from talus blocks below thicker sections of the intrusive and probably representative of a coarser-grained phase, exhibit a hypidiomorphic-granular texture that is locally ophitic.

Most of the olivines (Fa_{15}; analysis 9, Table 1) in the gabbro are characteristically embayed and rounded by magmatic resorption, but otherwise exhibit no evidence of olivine → pyroxene reaction. In the thin, chilled border zone the olivines are conspicuously more euhedral but have about the same composition ($\beta = 1{\cdot}681$) as those in the coarser-grained rocks.

Pyroxene occurs as hypidiomorphic stubby prisms and irregular grains, averaging 0·2 mm in diameter, interspersed between the plagioclase laths in the groundmass and as scarce microphenocrysts as much as 1·5 mm in diameter. As

TABLE 1

Chemical and modal analyses of the tholeiitic gabbro from the Uwekahuna laccolith and associated basaltic rocks

	1	2	3	4	5	6	7	8	9	10
	Chemical analyses									
SiO_2	48·37	48·25	46·59	46·32	48·56	49·50	52·04	45·72	50·38	39·76
Al_2O_3	11·19	10·72	7·69	8·58	11·62	12·67	13·20	—	12·99	0·54
Fe_2O_3	3·08	2·14	2·20	1·58	2·90	4·89	2·86	—	11·63	0·11
FeO	8·65	9·50	10·46	10·98	8·56	6·36	8·55	—	1·05	14·14
MgO	15·26	16·45	21·79	21·98	14·65	11·55	5·84	—	8·76	44·85
CaO	8·94	8·79	7·41	7·11	9·36	10·05	8·83	—	9·82	0·46
Na_2O	1·76	1·61	1·33	1·28	1·74	1·99	2·79	—	2·09	—
K_2O	0·28	0·25	0·28	0·21	0·26	0·32	0·83	—	0·40	—
H_2O+	0·10	0·06	0·37	0·12	0·14	0·11	0·33	—	0·19	—
H_2O-	0·03	0·05	0·04	0·03	0·03	0·03	0·08	—	0·05	—
TiO_2	1·88	1·75	1·83	1·44	1·92	2·14	4·16	—	2·32	0·15
P_2O_5	0·16	0·16	0·11	0·11	0·14	0·18	0·49	—	0·21	—
MnO	0·17	0·17	0·18	0·17	0·16	0·16	0·16	—	0·17	0·18
CO_2	0·02	0·01	—	0·02	0·00	0·01	0·01	—	0·00	—
F	0·02	—	—	0·02	0·02	0·03	0·07	—	0·02	—
S	0·00	—	0·00	0·00	0·00	0·01	0·00	—	0·05	—
	99·91	99·91	100·53*	99·95	100·06	100·00	100·24	—	100·13	100·19
Less O	0·01	—	—	0·01	0·01	0·01	0·03	—	0·04	—
TOTAL	99·90	99·91	100·53	99·94	100·05	99·99	100·21	—	100·09	100·19
	Modal analyses									
Olivine	24	26	40	39	21	15	—	47	—	—
Clinopyroxene	31	37	31	29	39	35	—	17	—	—
Hypersthene	3	2	—	4	2	1	—	9	—	—
Plagioclase feldspar	26	26	27	25	31	34	—	23	—	—
Opaque	5	4	1·7	3	4	9	—	2	—	—
SiO_2	<1	1	—	<1	<1	<1	—	<1	—	—
Glass	11	4	—	<1	3	6	—	2	—	—
Apatite	—	Tr	0·3	—	—	Tr	—	—	—	—

* Includes Cr_2O_3, 0·13; and NiO, 0·12.

1. Tholeiitic olivine gabbro, basal chill zone, south body of laccolith. Analyst, V. C. Smith.
2. Tholeiitic olivine gabbro, 3 ft above base, south body of laccolith. Analyst, D. F. Powers.
3. Tholeiitic picrite gabbro, from unrecorded section in north body of laccolith. Analyst, G. Steiger (Daly, 1911).
4. Tholeiitic picrite gabbro, 10½ ft above base, south body of laccolith. Analyst, V. C. Smith.
5. Tholeiitic olivine gabbro, 23½ ft above base, south body of laccolith. Analyst, V. C. Smith.
6. Tholeiitic olivine gabbro, upper chill zone, south body of laccolith. Analyst, V. C. Smith.
7. Black aphanitic dikelets, ½ in. thick, in joints in north body of laccolith. Analyst, V. C. Smith.
8. Tholeiitic picrite gabbro, from extreme olivine-rich zone in north body of laccolith. Analyst, R. Okamura.
9. Metamorphosed tholeiitic basalt flow, immediately overlying north body of laccolith. Analyst, V. C. Smith.
10. Olivine separated from a sample of tholeiitic olivine gabbro from north body of laccolith. Analyst, K. J. Murata.

recently described by Muir, Tilley, & Scoon (1957) two pyroxenes, augite and hypersthene, are recognizable in the gabbro, with hypersthene generally in subordinate amounts. This paucity of hypersthene was especially noted in the 28-ft vertical section studied in detail, where its observed mode did not exceed 4 per cent and averaged considerably less. In the coarser-grained facies of the gabbro from the north body (analysis 3, Table 1), hypersthene is apparently

more abundant—or possibly more conspicuous—constituting as much as 9 per cent by volume of the rock. Some of the larger augitic pyroxenes show simple pair twins and a few exhibit exsolution lamellae of pigeonite.

Plagioclase feldspar (An_{60}) is disseminated throughout the groundmass as lath-shaped crystals as much as 2 mm long, with an average of 0·3 mm. Only very minor zoning was noted. The composition was determined optically on cleavage fragments after the method of Tsuboi (1923).

Interstitial glass, coloured dark brown to grey by an abundance of included opaque microlites, is present in minor amounts throughout the rock and is locally abundant (10–11 volume per cent) in the chilled border zone. Larger crystals of opaques, probably magnetite and ilmenite, are also uniformly distributed through the rock. Minor cristobalite and possibly a few small crystals of tridymite were observed in a thin microcrystalline lining on some of the vesicle walls.

Dikelets of dark aphanitic material (analysis 7, Table 1) as much as $\frac{1}{2}$ in. thick are fairly common as joint fillings in the north body; none were observed in the 28-ft sampled section of the south body. Under the microscope the dikelet rock is seen to consist of a dense, unoriented felty mass of feldspar, pyroxene, and opaque microlites with numerous and relatively large and irregular interspaces filled with clear glass and cristobalite. Scattered through the dense groundmass are a few small highly corroded olivine crystals, some with hypersthene reaction rims, and ragged plagioclase and clinopyroxene crystals.

Post-emplacement alteration of the Uwekahuna rocks appears to have affected only the olivine and to a minor extent some pyroxene. Throughout most of the laccolith olivine crystals commonly show an incipient yellowish-brown stain along their margins and internal fractures. Within a few feet of the upper and lower contacts these alteration halos become more intense, and particularly in the upper chilled zone develop into a dark brown, in part opaque, rind around the crystals. The alteration is evidently due to the oxidizing action of vaporized groundwater mixed with primary acidic gases that emanated from the crystallizing interior of the intrusive.

Thin sections of the metamorphosed lava flows overlying the laccolith bear a remarkable similarity to some of the 1924 phreatic ejecta of Kilauea described by Macdonald (1949) and Muir, Tilley, & Scoon (1957). The flow rocks within 1 to 2 ft of the contact display a few relict crystals of olivine set in a dense hornfelsic groundmass of plagioclase, hypersthene, clinopyroxene, and opaques. The remnant olivine phenocrysts exhibit various degrees of reaction; the larger crystals are all mantled by an intimate fine-grained mixture of hypersthene and magnetite, whereas the smaller are generally replaced entirely by these two minerals.

Elongate brown laths and needles of pseudobrookite (Muir, Tilley, & Scoon, 1957) are randomly scattered through the altered rock, and relict (?) vesicles lined with euhedral plagioclase and clinopyroxene and minor brown glass are

also common. The chemical composition (analysis 9, Table 1) corresponds to that of a typical Kilauea tholeiitic basalt, except for the greatly oxidized state of iron brought on during metamorphism. Rocks of this nature which were hurled out during the 1924 phreatic explosions were likely torn from the roof of a deep-lying sill or other intrusive.

MAGMATIC DIFFERENTIATION

Petrographic evidence

The efficacy of gravity settling and filter pressing as important mechanisms of differentiation in a relatively thin intrusive is clearly demonstrated by the chemical and modal analyses (Table 1) of the rocks in the Uwekahuna laccolith.

Fig. 2 shows the variation of the mode and SiO_2 content of 5 samples as plotted against their positions in the 28-ft vertical section. The effectiveness of the gravitative separation of olivine in varying the silica content of the rock from 46·3 to 49·5 per cent is clearly indicated. Modal olivine in this vertical section is observed to range from a low of 15 per cent in the uppermost zone to a high of 39 per cent in the olivine-enriched zone, $10\frac{1}{2}$ ft above the base, and exhibits an inverse linear relation with per cent SiO_2. Even greater concentrations of olivine are evident in the thicker sections of the laccolith; a sample of olivine-rich gabbro from the north body was found to contain 47 per cent modal olivine and only 45·7 per cent SiO_2 (analysis 8, Table 1). The basal chill zone probably closely approximates the composition of the initially intruded magma, although it is possible that some olivine was added to this zone—just as it was evidently depleted from the upper chill zone—prior to solidification.

The olivine-rich horizon, $10\frac{1}{2}$ ft above the base, corresponds to a similar horizon in the well-known Palisade diabase sill described by Walker (1940). But the settling of olivine was far from complete in the Uwekahuna laccolith. This incomplete settling of a mineral has the interesting consequence that there could be a zone some distance above the horizon of accumulation where the concentration of that mineral will be more or less the same as in the initially intruded magma. The condition of equality results not because no crystals of the mineral have left the zone, but rather because the number lost from the zone was just compensated by the number gained from above so that the original concentration was preserved. This mechanism probably explains why the composition of sample 5 of the laccolith is so similar to that of sample 1, the rock of the basal chill zone. Texturally, the two samples are quite different, this in accord with their dissimilar cooling histories.

There is no apparent systematic variation in the amount of modal pyroxene, which ranges between 33 and 41 per cent, in the 5 samples from the vertical section. The modal trend of plagioclase (25–34 volume per cent) also roughly parallels that of pyroxene, with the exception of the upper part of the section when there is evidence of minor plagioclase enrichment. Both the basal and

upper chilled border zones of the laccolith are delineated by a marked increase in modal glass and, in the upper chill zone especially, by an increase in opaque minerals. The abundance of opaque minerals in the border zones, however, does not imply an increase of magmatic haematite or magnetite, but as noted pre-

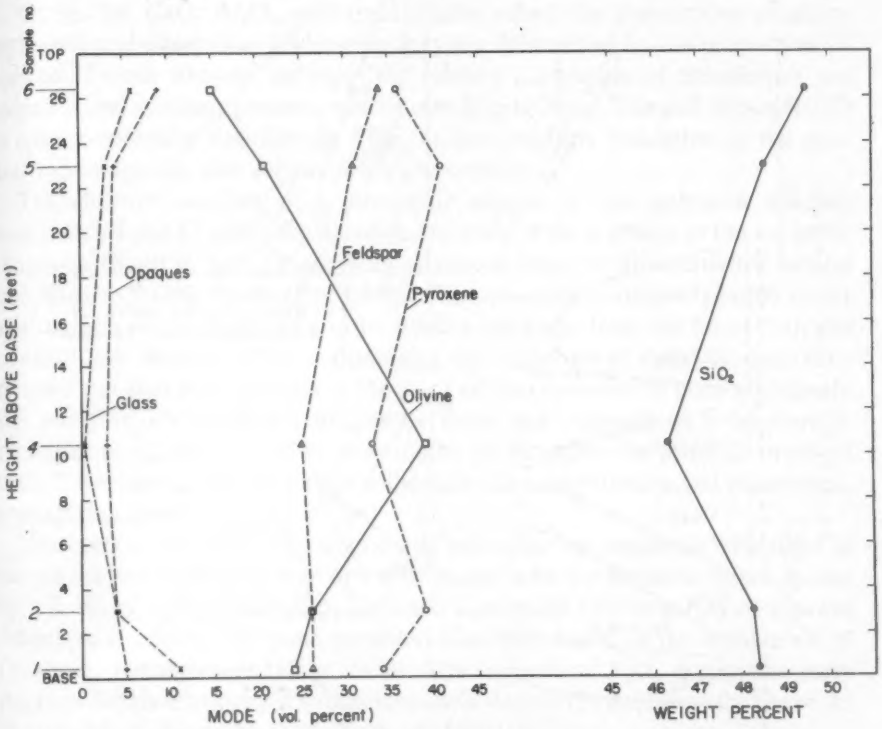

FIG. 2. Mode and silica content of five tholeiitic gabbro samples from the 28-ft vertical section through the Uwekahuna laccolith.

viously, is considered to be solely the result of alteration processes. Furthermore, total iron varies uniformly throughout the section and is not affected by the marked decrease in the $FeO:Fe_2O_3$ ratio which correlates with increase in the opaque minerals.

Chemical evidence

Chemical-variation diagrams shed additional light on the differentiation trends exhibited in the Uwekahuna laccolith. The nine curves on the left side of Fig. 3 show the per cent oxide content of the analysed rocks plotted against per cent silica. The three diagrams on the right have been obtained by plotting the weight per cent MgO, CaO, and Na_2O+K_2O against the Al_2O_3/SiO_2 weight ratio of the same rocks (Murata, 1960).

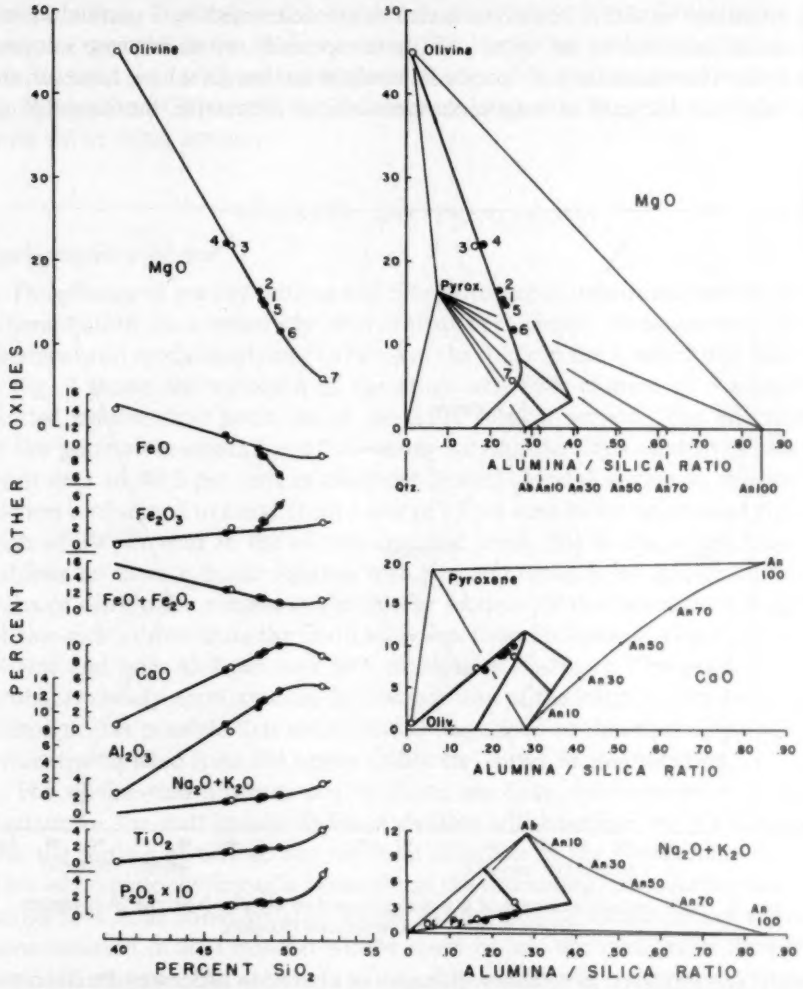

FIG. 3. Chemical variation diagrams of rocks from the Uwekahuna laccolith. Points 1 to 7 and olivine refer to the analyses in Table 1. Open and black circles designate samples from the north and south bodies, respectively.

Plots of per cent MgO versus per cent SiO_2 for the analysed samples 1 to 6 and olivine (analysis 10) lie along a straight line—the olivine control line of Powers (1955)—and demonstrate the effect of the addition or depletion of olivine in different parts of the laccolith. If point 1 (basal chill zone) is considered representative of the original intrusive magma, points 2, 3, and 4 indicate enrichment in olivine, and points 5 and 6 depletion of olivine.

Trends of ferrous and ferric iron in the silica diagram are complicated by the aforementioned deuteric oxidation of iron-bearing minerals in samples 1, 5, and

6 of the upper and lower border zones of the laccolith. In the unoxidized condition, most of the total iron of gabbroic rocks is divalent, so variations in total iron would primarily be due to variations in ferrous iron. In this sense, the curve for total iron for the rocks of the laccolith reflects the control exerted by ferroan olivine prior to deuteric alteration.

Curves for CaO, Al_2O_3, and total alkalis reflect the proportions of clinopyroxene and plagioclase feldspar as they are determined by the proportion of olivine. Titania likewise indicates the relative proportion of titaniferous ore minerals and of clinopyroxene, which according to Muir, Tilley, & Scoon (1957) is also moderately titaniferous. Phosphorous oxide is indicative of the proportion of apatite, also subject to olivine control.

The chemical analysis of a composite sample of the aphanitic dikelets (analysis 7, Table 1) within the laccolith, and plots of these results in the variation diagrams (point 7, Fig. 3), show an advanced stage of differentiation totally unrelated to simple removal of olivine. The constituent oxides, plotted either against SiO_2 or the Al_2O_3/SiO_2 ratio, deviate markedly from the linear 'olivine-control' line. Bowen (1928), in discussing the properties of variation diagrams, pointed out that such changes in the slope of variation curves generally signify the onset of crystallization of one or more new minerals in a fractionally crystallizing magma. As will be shown later in the paper, the minerals involved in the later stages of differentiation in the laccolith were pyroxene and plagioclase, crystallizing together.

The marked enrichment of titania and phosphorous pentoxide with silica in the dikelet rock is noteworthy, and is in accord with the chemical trends shown by a series of olivine-poor lavas collected during the 1955 eruption of Kilauea (Macdonald, 1955). The same trend has also been found in the diabase sill of Dillsburg, Pennsylvania (Hotz, 1953). The increase of P_2O_5 during the early stages of differentiation of a gabbroic magma was early established for the rocks of Glen More dike in Mull (Bailey *et al.*, 1924).

The trend of differentiation exhibited by the rocks of the Uwekahuna laccolith is most readily interpreted with the aid of the MgO–Al_2O_3/SiO_2 diagram (Fig. 3). This diagram has the advantage of providing compositional reference points for the major minerals of basaltic rocks, olivine, pyroxene, and plagioclase. The heavy line, on which the plots of all analysed samples fall, is the tholeiitic line of differentiation, ranging from tholeiitic picrite (oceanite) near points 3 and 4 to compositions approaching granophyre toward the abscissa axis. The straight-line portion of this line, extending from olivine to just below point 6, again represents a compositional change due only to the addition or depletion of olivine, which in the case of the Uwekahuna rocks is indicative of post-intrusive gravitational settling.

Olivine is sparse in the rocks below point 6, where the line curves to the left, and hence exerts no strong control on the composition of the more advanced differentiates. This change in trend, as suggested by pertinent phase-equilibria

diagrams, is the result of fractional syncrystallization of pyroxene and plagioclase, producing residual liquids progressively richer in silica and alkalis. The aphanitic dikelets, therefore, represent an end-stage interstitial fluid that was squeezed out (filter pressed) from the crystallizing core of the intrusive into joints and cracks in the surrounding parts that had already solidified.

Calculation of fractional crystallization

It is of much interest to calculate the amounts of the various minerals that need to be separated from the original magma (analysis 1, Table 1) to derive the residual liquid represented by the dikelet rock (analysis 7, Table 1). The compositions of three of the major minerals of the Uwekahuna gabbro are known approximately on the basis of analysis of a single sample of each mineral. That of olivine is given as analysis 10 of Table 1, and those of clinopyroxene and orthopyroxene have been published by Muir, Tilley, & Scoon (1957). The plagioclase may be assumed to approximate the optically determined composition of An_{60}.

The best fit of the data indicates that the following weight percentages of the various minerals were fractionally crystallized from the original magma to produce the particular residual liquid.

22·2	Olivine, Fa_{15}
20·1	Plagioclase, An_{60}
16·8	Clinopyroxene, $Wo_{39·5}$, $En_{49·8}$, $Fs_{10·7}$
1·6	Orthopyroxene, $Wo_{5·3}$, $En_{73·4}$, $Fs_{21·3}$
3·7	Titaniferous magnetite (10 per cent TiO_2)
2·3	Silica
66·7	

These proportions are not significantly changed if allowance is made for the incorporation of 0·25 per cent K_2O in the plagioclase, suggested by the general data of Emmons *et al.* (1953). No particular significance should be attached to the 2 per cent of silica which comes out as a residuum in the calculation. If either olivine or clinopyroxene were slightly richer in ferrous iron than the compositions assumed above, no silica would be left over in the calculation. The dikelets were apparently injected when the bulk of the original magma had been reduced to about a third by fractional crystallization. Only a small part of the residual liquid of this stage was involved in the formation of the dikelets because these constitute less than 1 per cent of the total rock of the laccolith. Most of the liquid apparently remained in the interstices of the crystallizing minerals and underwent further crystallization or formed a glassy residuum.

Thermal considerations

It might have been argued that the 28-ft sampled section, or even the thicker parts of the laccolith, are too thin and hence would have cooled too quickly to

permit any appreciable differentiation. However, rough calculations based on Jaeger's work (1957) indicate that sufficient time is available for the differentiation observed. Assuming an initial intrusive temperature of about 1,150° C, which is in keeping with measured temperatures in very similar basalt extruded from Kilauea in 1959 (Ault, Eaton, & Richter, 1961), the time required for the centre of a 30-ft thick body intruded into relatively cool rocks to become essentially crystalline (about 1,050° C) would be approximately 6 months; and for a 90-ft body about 4½ years. If the country rock at the time of the intrusion were also heated, say by an adjacent lava lake in the caldera, the time necessary for complete crystallization would be even longer. But even so—and here assuming an unrealistically high average viscosity of 30,000 poises for the cooling melt—a 6-month cooling period would allow olivine crystals, 3 mm in diameter and with a gravity contrast of 0·7, to sink as much as 50 ft (Hess, 1960, fig. 30). Fuller (1939) has noted very local instances of olivine settling in basaltic lava flows only 18 in. thick, which he interpreted to result from ponding of extremely fluid lava near the vent.

COMPARISON OF EXTENT OF DIFFERENTIATION SHOWN BY KILAUEA BASALTS AND BY ROCKS OF UWEKAHUNA LACCOLITH

The composition of the most highly differentiated material (dikelet rock) of Uwekahuna laccolith falls considerably short of the extreme differentiation shown by the granophyric patches found in the quartz diabase of Palolo quarry (Kuno *et al.*, 1957). However, the primitive nature of the starting material (tholeiitic–olivine–basalt–magma) in the laccolith makes the attainment of such a composition very unlikely. Yet, the dikelet material of the laccolith closely represents as advanced a stage of differentiation of Kilauean magma as any rock heretofore analysed. In this connexion it is instructive to compare the extremes of composition found among basalts of Kilauea with those established for the rocks of the laccolith. Table 2 contains the pertinent data.

Analyses A and B of Table 2 are extremes of composition which have been found among a total of 43 samples of Kilauea flows studied by many persons during the past several decades. Analysis C is that of a segregation vein in an augite–olivine basalt flow from Kilauea. The extreme compositions of the rock of the Uwekahuna laccolith (analyses D and E) equal or even slightly exceed those of the flow rocks and very closely approach the composition of the segregation vein. It is most interesting that a single small intrusive body in a volcano should reveal as much about the range of differentiation of tholeiitic magmas as several dozen samples of widely scattered lava flows, and this fact makes Hawaiian intrusive rocks very attractive subjects for future studies. The present results suggest that the Uwekahuna laccolith itself merits closer sampling and more detailed chemical and mineralogical study.

TABLE 2

Comparison of extremes of composition found among 43 samples of Kilauea basalts and among 7 samples of Uwekahuna laccolith

	Kilauea basalts			*Uwekahuna laccolith*	
	A	B	C	D	E
	Most mafic flow	*Least mafic flow*	*Least mafic segregate*	*Most mafic*	*Least mafic*
SiO_2	46·50	51·24	52·36	46·32	52·04
Al_2O_3	9·37	13·60	12·34	8·58	13·20
Fe_2O_3	2·47	1·87	2·81	1·58	2·86
FeO	10·79	11·19	13·59	10·98	8·55
MgO	21·00	5·12	2·87	21·98	5·84
CaO	6·25	9·03	7·54	7·11	8·83
Na_2O	1·52	2·81	2·99	1·28	2·79
K_2O	0·22	0·83	0·80	0·21	0·83
H_2O+	0·14	0·03	0·77	0·12	0·33
H_2O-	0·03	0·00	0·12	0·03	0·08
TiO_2	1·70	3·74	2·95	1·44	4·16
P_2O_5	0·10	0·41	0·76	0·11	0·49
MnO	0·11	0·18	0·22	0·17	0·16
CO_2	—	0·01	—	0·02	0·01
Cl	—	0·01	—	—	—
F	—	0·06	—	0·02	0·07
S	—	0·01	—	0·00	0·00
	100·20	100·14	100·12	99·95	100·24
Less O	—	0·03	—	0·01	0·03
TOTAL	100·20	100·11	100·12	99·94	100·21

A. Picritic basalt, west of Kamakaia Hills, Kau Desert. Analyst, H. S. Washington. Washington (1923).
B. Basalt, Keahialaka flow, erupted 28 Feb. 1955, east Puna. Analyst, M. Balazs. Macdonald (1955).
C. Segregation vein in augite–olivine basalt flow, Kilauea Caldera. Analyst, T. Katsura. Kuno *et al.* (1957).
D. Analysis 4 of Table 1.
E. Analysis 7 of Table 1.

ACKNOWLEDGEMENTS

The generous help received from our colleagues, J. P. Eaton, R. T. Okamura, V. C. Smith, and D. F. Powers, during the course of this study is gratefully acknowledged.

REFERENCES

AULT, W. U., EATON, J. P., & RICHTER, D. H., 1961. Lava temperatures in the 1959 Kilauea eruption and cooling lake. *Bull. geol. Soc. Amer.* **72**, 791–4.

BAILEY, E. B., *et al.*, 1924. Tertiary and post-Tertiary geology of Mull, Loch Aline, and Oban. *Mem. geol. Surv. U.K.* 1–445.

BOWEN, N. L., 1928. *The evolution of the igneous rocks.* Princeton, N.J.: Princeton Univ. Press.

DALY, R. A., 1911. Magmatic differentiation in Hawaii. *J. Geol.* **19**, 289–316.

EATON, J. P., & MURATA, K. J., 1960. How volcanoes grow. *Science*, **132**, 925–38.

EMMONS, R. C., *et al.*, 1953. Selected petrogenic relationships of plagioclase. *Mem. geol. Soc. Amer.* **52**, 11–22.

FULLER, R. E., 1939. Gravitational accumulation of olivine during the advance of basaltic flows. *J. Geol.* **47**, 303–13.

HESS, H. H., 1960. Stillwater igneous complex, Montana. *Mem. geol. Soc. Amer.* **80**, 1–230.

HOTZ, P. E., 1953. Petrology of granophyre in diabase near Dillsburg, Pennsylvania. *Bull. geol. Soc. Amer.* **64**, 675–704.

JAEGER, J. C., 1957. The temperature in the neighbourhood of a cooling intrusive sheet. *Amer. J. Sci.* **255**, 306–18.

JAGGAR, T. A., 1924. *Bull. Hawaii. Volcan. Obs.* **12,** 57–69.
KUNO, H., *et al.*, 1957. Differentiation of Hawaiian magmas. *Jap. J. Geol. Geogr.* **27,** 179–218.
MACDONALD, G. A., 1949. Petrography of the Island of Hawaii. *Prof. Pap. U.S. geol. Surv.* **214–D,** 51–96.
—— 1955. *Catalogue of the active volcanoes of the world. Part III. Hawaiian Islands.* Naples: Int. Volcan. Assoc. 1–37.
MUIR, I. D., TILLEY, C. E., & SCOON, J. H., 1957. Contributions to the petrology of Hawaiian basalts. I. The picrite-basalts of Kilauea. *Amer. J. Sci.* **255,** 241–53.
MURATA, K. J., 1960. A new method of plotting chemical analyses of basaltic rocks. Ibid. **258-A,** 247–52.
POWERS, H. A., 1955. Composition and origin of basaltic magma of the Hawaiian Islands. *Geochim. Acta,* **7,** 77–107.
POWERS, S., 1916. Intrusive bodies at Kilauea. *Z. Vulkanol.* **3,** 28–33.
STEARNS, H. T., & VASVIK, K. N., 1935. Geology and ground-water resources of the Island of Oahu Hawaii. *Bull. Hawaii Div. Hydrography,* No. **1,** 399–409.
TSUBOI, S., 1923. A dispersion method of determining plagioclases in cleavage-flakes. *Miner. Mag.* **20,** 108–22.
WALKER, FREDERICK, 1940. Differentiation of the Palisade diabase, New Jersey. *Bull. geol. Soc. Amer.* **51,** 1059–1106.
WASHINGTON, H. S., 1923. Petrology of the Hawaiian Islands. III. Kilauea and general petrology of Hawaii. *Amer. J. Sci.*, ser. 5, **6,** 338–67.
WATERS, A. C., 1955. Volcanic rocks and the tectonic cycle: in A. Poldervaart, ed., Crust of the earth. *Spec. Pap. geol. Soc. Amer.* **62,** 703–22.
WENTWORTH, C. K., & JONES, A. E., 1940. Intrusive rocks of the leeward slope of the Koolau Range, Oahu. *J. Geol.* **48,** 975–1006.